Investigation of chaotic mixing in laminar fluid systems by the use of Computational Fluid Dynamics.

Matthew Michael Overd

Doctor of Philosophy

University of Aston in Birmingham

September 2001

(Awarded May 2002)

University of Aston in Birmingham

Investigation of chaotic mixing in laminar fluid systems by the use of Computational Fluid Dynamics.

Matthew Michael Overd **Doctor of Philosophy** **September 2001**

Summary of thesis

This work presents significant development into chaotic mixing induced through periodic boundaries and twisting flows. Three-dimensional closed and throughput domains are shown to exhibit chaotic motion under both time periodic and time independent boundary motions. A property is developed originating from a signature of chaos, sensitive dependence to initial conditions, which successfully quantifies the degree of disorder within the mixing systems presented and enables comparisons of the disorder throughout ranges of operating parameters. This work omits physical experimental results but presents significant computational investigation into chaotic systems using commercial computational fluid dynamics techniques. Physical experiments with chaotic mixing systems are, by their very nature, difficult to extract information beyond the recognition that disorder does, does not or partially occurs. The initial aim of this work is to observe whether it is possible to accurately simulate previously published physical experimental results through using commercial CFD techniques. This is shown to be possible for simple two-dimensional systems with time periodic wall movements. From this, and subsequent macro and microscopic observations of flow regimes, a simple explanation is developed for how boundary operating parameters affect the system disorder. Consider the classic two-dimensional rectangular cavity with time periodic velocity of the upper and lower walls, causing two opposing streamline motions. The degree of disorder within the system is related to the magnitude of displacement of individual particles within these opposing streamlines. The rationale is then employed in this work to develop and investigate more complex three-dimensional mixing systems that exhibit throughputs and time independence and are therefore more realistic and a significant advance towards designing chaotic mixers for process industries. Domains inducing chaotic motion through twisting flows are also briefly considered. This work concludes by offering possible advancements to the property developed to quantify disorder and suggestions of domains and associated boundary conditions that are expected to produce chaotic mixing.

Keywords/ phrases: Periodic boundaries, viscous fluid, cavity, continuous mixing, quantification of chaotic mixing.

Dedication

To my family, thank you for you continued support and encouragement throughout my development. Without the love and patience that you have shown me I would not have been able to achieve a fraction of what I feel that that I have.

To Jo, Thank you for your patience and unconditional support. I would also like to thank you for being you, I would never want you to change that and I look forward to sharing one life forever.

Acknowledgements.

This is to acknowledge my thanks and gratitude to Dr Sotos Generalis for his continued enthusiasm and support throughout the course of research and production of this thesis.

Thanks also to Dr Alan Harries who was there at the beginning of my research to offer guidance, comment and support and who is still there, but now as a true and great friend.

Table of Contents

List of appendices.

List of figures and tables

1. Chaos, mixing and chaotic mixing

1.1 Introduction

There are many processes in a variety of industries that involve the mixing of laminar fluids, for example the blending of a polymer melt, the homogenisation of soup ingredients or the movement of broth inside a biochemical reactor. Considerable time and expense is often involved in the development of mixing processes particularly when using physical scale up methods. Often it is considered, however, that as long as the mixer mixes then there is little need for intensive investigation. This may lead to over design, inefficient power consumption or in shear sensitive processes, degradation of product

Computational Fluid Dynamics (CFD) is becoming a more popular tool for investigating mixing systems, as it enables the designer to predict and visualise flow patterns. This work uses CFD to investigate the mixing of two- and three-dimensional, time dependent and time independent, laminar fluid systems operating within highly disordered chaotic flow regimes.

This work aims to use commercial CFD to produce transferable concepts for chaotic mixing systems and to develop a method for quantifying differences in mixing quality. It must first be shown in simple systems that it is possible to simulate chaos using commercial CFD, then a property of disorder must be investigated for reliability. From this theories concerning chaotic mixing can be conceptualised and examined within more complex systems. This will lead to suggesting possible future developments into chaotic mixing. This chapter begins this process by offering a relevant introduction to the theory of chaos and mixing, followed by a review of significant previous works, which is sufficient to assure an appreciation of the investigations of chaotic mixing domains presented throughout.

1.2 What is Chaos?

Chaos has long been used to describe disorder in systems. It is said in Roman mythology [1] that the god Janus has two faces. One looking forward towards the order created by the forming of the earth, the other face looking back into the disordered matter, where the elements that made up the earth were all formless and in a chaotic state.

The literary meaning of the word would then be clear. It describes a state of great disorder. From a mathematical point of view chaos refers to the random outcomes of deterministic equations due the high sensitivity of certain non-linear equations to initial conditions and operating parameters. It is this behaviour that has intrigued scientists, mathematicians, engineers and philosophers alike and reviews of the popular concepts can be found in [2 – 4.]

Let us consider the ultimate non-linear equation. If equations were obtainable for the behaviour and relationship of every particle in the universe to all others and if it was possible

to obtain the exact position and velocity of those particles, then it would be expected to follow that it would be possible to predict every outcome of the future. The derivation and collation of the enormous scheme of equations and information required would take many lifetimes to complete. Even if one continued, undeterred, and actually completed the task, one would find that an early and quite fundamental problem occurs. The equations themselves would be of little use as a predictive tool. The large and complicated system of non-linear equations would be so sensitive to minute deviations in operating parameters and initial conditions of the modelled and actual systems that they would be unable to accurately predict the events of even the smallest measurable time increment into the future. The mathematical model for the Universe could be considered to be highly chaotic. If it were possible to model the equations deterministically the output would be sufficiently stochastic to reduce its value as a predictive tool. Such an impressive model, however, could be used to investigate the sensitivity of the Universe to initial and operating conditions and parameters, producing behavioural trends and highlighting various system characteristics. This is how many stochastically behaving deterministic systems are investigated, and is indeed the focus of the mixing studies in this work. The concern is not where an individual particle will be after some time, but how the mass of particles behave and the relationships to the associated disorder

Meteorologist Edward Lorenz found great divergence and sensitivity to initial conditions in simplified models that he used to attempt to predict weather patterns [5].

$$dx/dt = -a(x-y) \tag{1.1a}$$

$$dy/dt = -xz+rx-y \tag{1.1b}$$

$$dz/dt = xy-bz \tag{1.1c}$$

Lorenz simplified his atmospheric model to three coupled equations, two of which are non-linear, containing three variables, (equations 1.1a-c.) Even in the simplified form the equations exhibit stochastic behaviour, and have since become popular and extensively studied. They have been shown to highlight many of the signatures of chaos, and in particular the divergence of close initial positions. Figure 1.1, shows the x variable of the Lorenz system against time for a total evolution of 40 seconds. Constants a, b and c are 10, 28 and 2.67 respectively. Two points, starting at (x, y, z) = (1, 1, 1) and (1.0001, 1, 1) are shown to evolve as blue and red lines respectively. Initially both plots are of a similar trajectory. As time

evolves they begin to diverge, up to the point where their paths become significantly different and the plots bare absolutely no resemblance to each other.

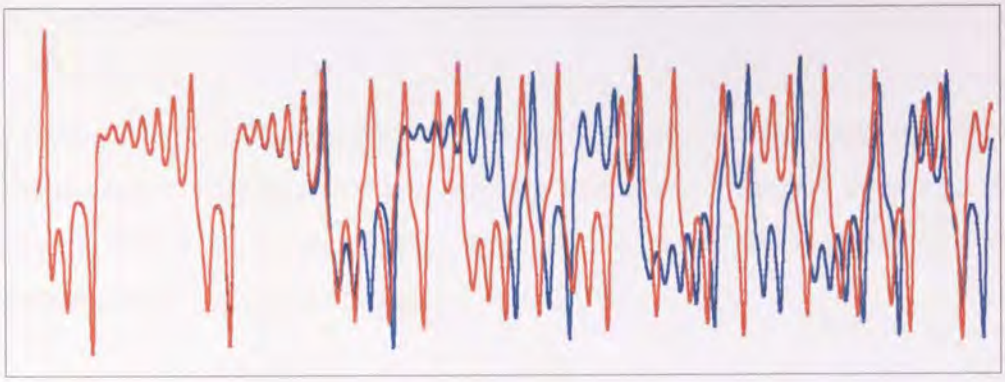

Figure 1.1. Two trajectories of the x variable against time originating at positions 0.0001 apart, within the Lorenz equations. The values for the constants a, b and c are 10, 28 and 2.67 respectively.

The sensitive dependence to initial positions indicates that the values of the constants and initial conditions places the system within a chaotic range, Now consider a chaotic mixing system. Instead of two initially close points within Lorenz's chaotic system consider two initially close particles of fluid in a chaotic mixing system. Through time the initially close particle trajectories will diverge to a point where they are no longer close thus it follows that good mixing has taken place. This is briefly the essence of this work, as such this phenomenon is discussed in more detail in later chapters.

Many continuous non-linear systems are known to oscillate either periodically or chaotically. There are specific ranges of parameters for particular systems that they must be operated within in order for chaotic conditions to exist. This has significance when considering the application of chaos to mixing as in order to achieve good mixing systems must be operated within specific ranges of certain control parameters. Transitions from order into chaos are considered in detail for the mixing systems presented in this work.

Transitions from order to chaos are not abrupt changes and often involve cascades through period doubling into chaos. Cascades in chaotic mixing systems may be observed as a result of an incremental change of operating parameters inducing an alternating streamline motion [6, 7] or properties relating to the fluid effecting the Reynolds number [8] or in flows such as the Couette-Taylor flows [9, 10]

The Rossler system of equations highlights the effect of gradually changing parameters [11]. The coupled equations (1.2a-c) are noted for being simpler than the Lorenz equations, containing only one non-linear term, yet also exhibiting chaotic motion.

$$dx/dt = -(y+z) \qquad (1.2a)$$

$$dy/dt = x + 0.2*y \quad (1.2b)$$

$$dz/dt = 0.2 + xz - cZ \quad (1.2c)$$

Equations 1.2a-c contain three co-ordinate variables and one constant parameter, c. It is the value of this parameter that changes the systems behaviour. Figure 1.2a shows the time evolution where c=2.5, it can be seen in they x, y plot that the trajectory of the plot returns to itself, in a limit cycle, after each revolution.

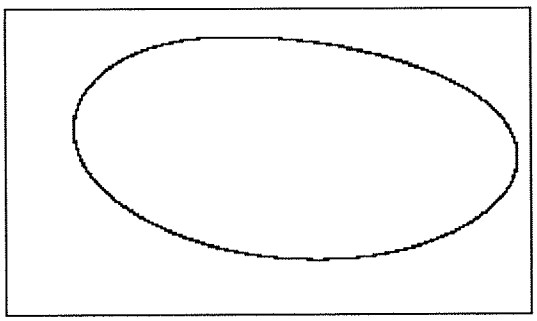

Figure 1.2a. Plot of x, y trajectory showing a limit cycle from the Rossler equations, where c=2.5

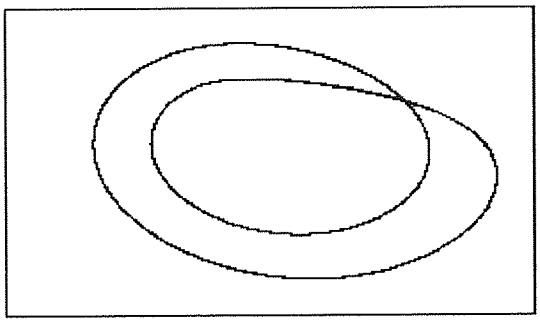

Figure 1.2b. Plot of x, y trajectory showing period doubling from the Rossler equations, where c=2.9

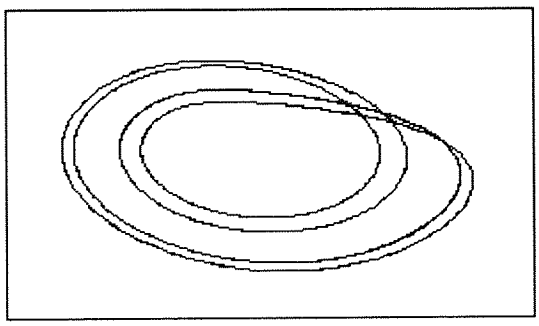

Figure 1.2c. Plot of x, y trajectory showing period quadrupling from the Rossler equations, where c=4.

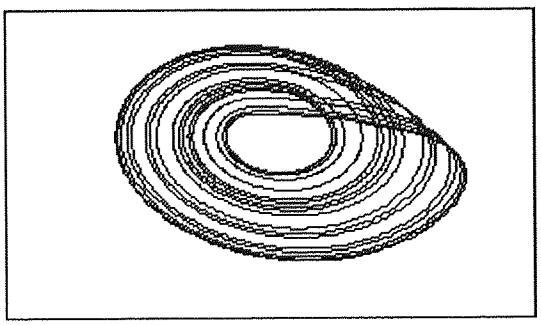

Figure 1.2d Plot of x, y trajectory exhibiting chaotic behaviour from the Rossler equations, where c=5.7

If the value of c is gradually increased to 2.9 it is possible to see in figure 1.2b that the particle path loops twice before closing. This can be termed as period doubling. Increase the value of c to 4, and it is possible to see that there are four loops before the path to returns to itself, figure 1.2c. Further increase of c continues the period doubling sequence until the system enters chaos. This can be observed in figure 1.2d where c=5.7.

This work presents cascades from ordered motion (similar to the limit cycle) in to chaotic motion for laminar fluid mixing systems. The control parameters that are varied to cause the transition are associated with the form of the boundaries. Chaotic transitions are observed

through trajectory plots, properties of the mixing and by the use of various characteristics of chaos.

1.3. Classification of chaos.

In the previous section it was noted that time dependent non-linear systems can oscillate either periodically or chaotically. It was discussed that for systems to exhibit aperiodic motion they must be operated within specific ranges of operating parameters. It is known [12] that for systems to be considered as chaotic they must exhibit either one or more of the following: aperiodic oscillatory motion, evidence of homoclinic or heteroclinic points or sensitive dependence to initial conditions.

This section briefly describes two methods originating from the above signatures of chaotic motion, for recognising chaos within a variety of systems. Poincaré maps and Lyapunov exponents are discussed in sufficient detail to enable reference to them in later discussions. For further discussions of chaotic dynamical and non-linear systems and their development and classifications the reader should consult [13-21] or similar text.

1.3.1. Poincaré maps.

Complex trajectories can be simplified by the use of maps, such as the time-T map or Poincaré map. Consider a three-dimensional flow trajectory τ. At time t_1 the trajectory τ has a position P_1, on a cross section (of two dimensions, transverse to the flow.) As the system evolves the next time trajectory τ passes through the cross section its position can be noted as P_n. If $P_1=P_2=P_3$ and the time difference $t_3-t_2 = t_2-t_1= T$ the system could then be said to be periodic with a time period of time T. Figure 1.3a shows this pictorially, it can be seen that the map of the cross section exhibits only one point.

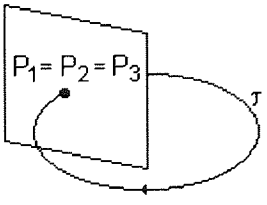

Figure 1.3a. Pictorial representation of a trajectory limit cycle crossing a cross sectional plane at position P_1 and again at P_n where $n= 0 \rightarrow \infty$.

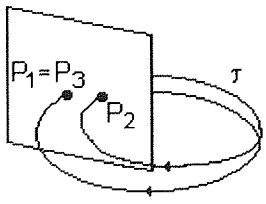

Figure 1.3b. Pictorial representation of a trajectory exhibiting period doubling where position $P_n=P_{n+2}$, where $n = 0 \rightarrow \infty$

If the trajectory τ were to be within a period doubling scheme then the associated map would show two locations, as represented in figure 1.3b, where $P_n=P_{n+2}$. The benefit of the simplified

perspective for viewing such systems becomes clear when considering a chaotic system. To view the full trajectory for a chaotic system would be confusing, and useful information would be difficult to extract.

By observing particle trajectories using Poincaré sections it is possible to observe features and signatures of chaotic systems, such as stable (elliptic) and unstable (hyperbolic) fixed points. This technique of observing disorder within fluid systems is used in Chapter 6. By observing particle trajectories using Poincaré sections, positioned at regular intervals along the flow domain, it is possible to conclude the presence of elliptic points, however hyperbolic points cannot be identified. The Poincaré sections in chapter 6 do, however, enable the conclusion that as the system's perturbation grows the invariant curves are destroyed and become engulfed in a 'chaotic sea.' In completely chaotic systems total destruction of invariant curves occurs, and trajectories travel randomly throughout the system domain.

Many authors have used Poincaré sections to observe the onset of chaotic motions as the destroyed areas grow, these will be described later in this chapter.

1.3.2. Lyapunov exponents.

As discussed previously one characteristic feature of chaos is sensitive dependence to initial conditions. This was shown using the Lorenz equations where two initially near points within the chaotic system diverge rapidly up to the point where they appear to have no relationship to each other. It is possible to characterise this divergence by the use of properties such as the Lyapunov exponent. This has been carried out for systems such as the Couette-Taylor flow [10] and the Lorenz system [22, 23]

The Lyapunov exponent is a quantitative measure of the exponential growth of deviations of initially close points. However, as the growth between the two initial points is expected to be exponential in a chaotic system, problems would occur in calculating this value due to the large number causing numerical errors and computational data overflow, and also the system domain is bounded. To overcome these problems when the divergence becomes too great, another nearby trajectory can be selected for the calculation by using a repeated rescaling process. Consider two initial conditions a distance ε_0 apart, and evolving to a separation distance ε_t after time t. This produces scaling factors, ε_1, ε_2, and so on. The value of the Lyapunov exponent (λ) can then be calculated over many segments (N) and is λ is given by:

$$\lambda = \frac{1}{N}\sum_{i=1}^{N}\frac{1}{t}\ln\left[\frac{\varepsilon_{1(i)}}{\varepsilon_{0(i)}}\right] \qquad (1.3)$$

and depicted pictorially in figure 1.4.

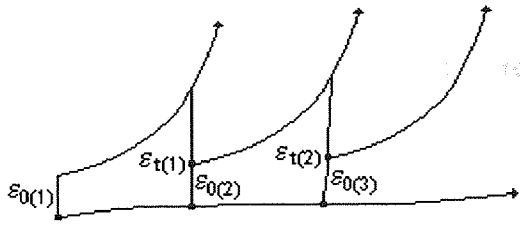

Figure 1.4. Pictorial representation of the calculation of the Lyapunov exponent through repeated rescaling of the distance between the object trajectory and reference trajectory.

By observing the sign of λ it is possible to identify the relationship between the object trajectory and the initally close trajectories. If the value is negative, due to $\varepsilon_t/\varepsilon_0 < 1$, and therefore $\varepsilon_0 > \varepsilon_t$, then the system converges and is stable. If λ is positive then the system diverges concluding the presence of chaotic evolution, and if λ is zero the system neither diverges or converges.

The Lyapunov exponent is not calculated for the systems presented in later chapters due to being unable to readily identify nearby trajectories, for use when rescaling, in the commercial fluid dynamics package used in this work. However comparisons are drawn between the Lyapunov exponent and the techniques used based on the fact that initially close trajectories diverge under chaotic conditions.

1.4. Laminar mechanisms of mixing.

There has been much work into the understanding of various mixing processes and their associated mechanisms [24-29]. This work is concerned with the mixing of laminar fluids that may be found in the food [30, 31] bio-chemical [32, 33] and polymer and plastics industry [34, 35].

The blending of a laminar fluid occurs due to the stretching, striation and segregation of elements of fluid, which does not alone, yield regions of uniform concentration gradient. This only occurs through molecular diffusion, which becomes a notable process once the elements of fluid are significantly striated and segregated. Hence diffusion terms are not included in any systems presented in this work. We take mixing in this work as the significant separation of substances, with similar properties, that begin from separate regions. Good mixing would be where like particles have separated and are distributed randomly throughout the domain. Poor mixing would show clumps and regions of like particles with defined boundaries.

Here three mechanisms of laminar fluid blending are noted, laminar shear, elongational or extensional flow and distributive mixing [36]. They will however, not be discussed in great length as they are seldom referred to later in this work.

1.4.1. Laminar shear

This can be considered as the reduced striation thickness and increased interfacial area, due to the deformation of fluid elements across streamlines. Consider the linear velocity profile formed with a Newtonian fluid between two parallel plates, of which one is moving and the other at rest. An elemental thin rectangle of fluid, initially placed perpendicular to the flow, would distort to the form of a diagonally orientated element of greater length and reduced width as shown pictorially in figure 1.5. If the same thin rectangular element were initially placed with its length in line with the fluid movement it would then evolve to elongate parallel to the walls.

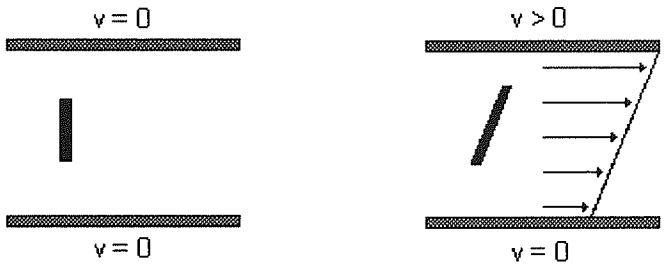

Figure 1.5. Pictorial representation of a tracer element between two parallel plates. When the top plate is in motion and the lower one stationary the velocity gradients cause a deformation of the tracer element stretching it.

Consider a steady eccentric cylindrical system with the outer wall rotating. If a small blob of tracer fluid were placed within the domain the resulting trace would evolve to create a full circle, and hence very little mixing would occur, see figure 1.6. If now we place a tracer line perpendicular to the plane of shear, but long enough so that one end of the tracer touched the inner cylinder, and the other, the outer cylinder. As time evolved we would note that tracer elongates, producing a spiral, and will continue to do so, with every revolution of the outer cylinder, until it was of infinite length and infinitely narrow, and hence appear to be completely mixed, figure 1.7.

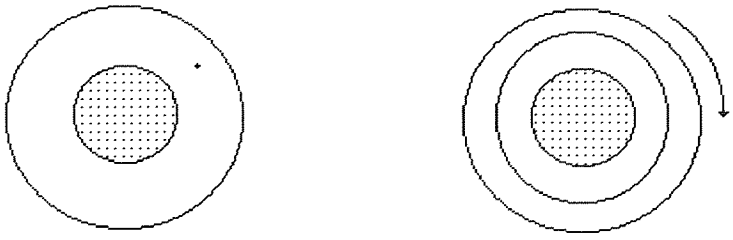

Figure 1.6. Pictorial representation of a blob of tracer between two eccentric cylinders where the outer cylinder is in motion and the inner one is at rest. After time with the cylinder in motion the blob is stretched to form a closed circular line.

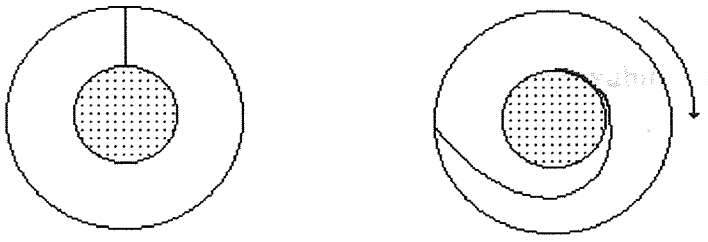

Figure 1.7 Pictorial representation of a line of tracer placed perpendicular to the shear between two eccentric cylinders where the outer cylinder is in motion and the inner one is at rest. After time with the cylinder in motion the line is deformed to produce a spiral. The tracer line will continue to stretch until infinitely thin and completely mixed.

It has been noted that the consecutive shearing in two different directions can increase the deformation of a fluid element [37].

1.4.2. Elongational flow.

This mechanism is the reduction of striation thickness due to changes in geometry and fluid acceleration. An example of this can be found when considering the tip of a blade of an internal mixer [38] or inside a screw extruder [39,40, 41]. The fluid apparently flowing into the blade will be elongating. Between the tip of the blade and the wall there will be a region of high shear. And the fluid flowing out from behind the blade will once again be elongating.

1.4.3. Distributive mixing.

This occurs with the constant splitting, rotation and recombination of fluid streams. This is a common mechanism of mixing within static mixers such as the Kenics [42, 43] or rotating partitioned pipe mixer [12]. With each splitting of the stream there is an associated increase in the fluid interfacial area, and a reduction of striation thickness.

The above mechanisms of mixing involve reduction of the striation thickness, elongation of fluid elements and increased interfacial area to produce greater segregation between fluids. Many methods have been employed for assessing the quality of mixing of laminar fluids including the segregation and concentration differences. However in this work others methods are used to suggest the degree of disorder and the quality of the mixing taking place.

1.5. Mixing in chaotic flows.

Mixing of laminar fluids, such as polymer melts, takes place by a series of stretching, folding, shearing and bending movements. A two-dimensional, where velocities are constant, will flow in a series of streamlines. It is well known that when operating a system under time dependent conditions, such that opposing streamline motions are formed, mixing takes place

more readily. It is this that many authors have used to develop chaotic mixing systems and also forms the basis for this work.

It is due to the presence of chaos yielding increased mixing within a fluid domain that this area has attracted much attention. Work, both experimental and computational has been previously carried out in the investigations of viscous fluid chaotic mixing systems. The aim of this section is to briefly present the notable works of other authors as an introduction to discussions in later chapters and should be considered as a comprehensive, but not definitive review of works relating to this subject.

The works initially considered involve two-dimensional viscous fluid chaotic mixing. First there is an introduction to the analysis of various chaotic mixing systems through a discussion of early and influential works. This is then followed by a brief overview of some applications of chaos within different configurations of fluid system and the various properties therein that the onset of chaos is observed to affect. The discussion of three-dimensional viscous fluid chaotic mixing is presented in chapter 5.

The pioneering work of Aref, 'Stirring by Chaotic Advection,' [44] is discussed first. This work presents a two-dimensional circular system, which stirs a fluid considered as inviscid and incompressible, by the use of two point vortexes. It is noted that the way in which the vortexes are operated can create a more efficient form of mixing. In essence a laminar fluid exhibiting stochastic motion is presented, or as Aref explained: 'We have a situation in which an innocuous, fully deterministic velocity field, in the Eulerian view, produces an essentially stochastic response in the Lagrangian advection characteristics of a passive tracer. It is proposed to call this situation or regime chaotic advection.'

The increased mixing in Aref's system is caused by the alternate operation of the point vortexes, which became termed the 'blinking vortex motion.'

His work presented control parameters associated with the onset of chaos. The first considered is the time period of which one vortex is operated, before switching to the other. It was noted in this work that if one vortex alone were to be operated a chaotic regime would not be formed, even if it were oscillated.

This work showed by observing the evolution of particles from strategically placed origins, that as the time period of operation was increased from a low value, the region of chaotic motion, surrounding the stirring vortexes, increases. As T was increased the region of disorder grows, up to the point where there are no visible signs of ordered motion.

At a sufficiently low time period (T) the motion of traced particles was shown to appear as a steady state system, where both vortexes are in equal operation. i.e. there appears to be no region of chaos, this was commented not necessarily to be the case, but suggests that as $T \rightarrow 0$, the size of the chaotic region also tends to zero.

To examine the increased mixing within a more 'real' application Aref introduced a 'blob' of particles near to the vortexes. Differences were presented between the steady state, and a time dependent system that has been shown to exhibit a large region of chaotic motion. For the steady system the particles originating from the blob were contained with regions close to the vortex. The particles originating within the time dependent system separated, however, to the same size as the associated region of chaotic motion. And after a short time the blob was homogenised across the whole region.

Aref commented that the greatest disorder being associated with larger time periods is not what would be initially expected. 'This result is in some ways counter-intuitive, since the more vigorous turning on and off of the two agitators might have been suspected of being the most efficient mechanism.'

Another parameter considered by Aref was the distance (B) between the two vortexes. By the crude measurement of the relative area of the chaotic region it was shown that for a particular value of B, the time period required to obtain a large chaotic region was lower than that of a smaller value of B. Although no attempt was made to suggest why either control parameter affects the disorder in such ways.

Aref concluded his observations by commenting on the presence of islands of stability within the chaotic region, although their effect and origin was not discussed.

It is known that to achieve homogenisation of laminar fluids the interfacial area between fluids must first be increased by a series of stretching, folding, shearing and bending movements. A steady state system will flow in a series of streamlines. By operating a system under time dependent conditions streamlines can be broken and mixing takes place more readily, through creation of chaotic regions. The work by Aref certainly showed that chaotic mixing of laminar fluids was possible and hence created much interest in this area.

Two significant works that are similar in appearance and hence involved some collaboration between the authors, so as not to significantly duplicate, followed Aref's paper. The works, 'Chaotic advection in Stokes flow,' [45] by Aref and Balachandar, and 'Lagrangian turbulence and spatial complexity in a Stokes flow,' by Chaiken et al, [46] are described below.

Aref noted that there was resistance to acknowledgement of the existence of laminar chaotic advection. He states that incorrect notions were that turbulence was confined to high Reynolds numbers flows or inviscid fluids, and that the presence of a high viscosity would 'smooth things out.' By the investigation of chaotic motion in Stokes flows it was hoped that this scepticism would be put to rest.

Both works [45,46] investigated eccentric dual cylindrical systems, considered of sufficient length, to make two-dimensional approximations valid. Both the inner and outer cylinders

were able to operate independently, which they do with various forms of time-dependent motion.

Both systems used Poincaré sections, at specified 'stroboscopic' or 'snapshot' time intervals. It was commented in the works that if a pattern of particles produces a smooth curve, then the motion could be considered regular. Conversely if the pattern of particles is smeared or scattered then the motion could be considered to be chaotic.

Aref and Balachander presented and compared the differences in particle trajectories for steady and various forms of time-dependent flow. They find that increasing the switching time of operation of the two boundaries produced an increase in the region of chaotic motion. They then commented on an optimum between the inefficient mixing of rapid alternation of boundary movements, and the long periods of time required for mixing to take place where longer alternation periods were used.

Chaiken et al also presented a gradual variance in disorder as a control parameter was increased. Keeping the movement of the inner cylinder constant and varying the movement of the outer (T), for systems with differing eccentricities of the cylinders, they concluded that: for the smallest T, for each eccentricity the motion is integrable. As T is increased there is a mixture of chaotic and regular motion. Although there would appear to be a range of the ratio of inner and outer cylinder movement that yields maximal chaos, as at larger values of T regular regimes predominate. They presented the above trends for both counter- and co-current motion, but indicated that co-current movement yields the greater chaotic regions.

By observations of particles originating from lines, or specific shapes within a chaotic flow domain it was shown, by Aref and Balachander that particles are 'stretched considerably more than in the steady flow case.' Whereas Chaiken et al observed and commented on the presence of whorls and tendrils within the flow domain.

Aref concluded that '...the flow is completely dominated by viscous forces. The flow is always laminar. The particle trajectories in this flow, however, can be chaotic.'

It would be possible at this point to cease the review of chaotic mixing. In essence all that is required for an appreciation of this work are the fundamental principles that are; integrable systems exhibit streamlines, particles originating on a streamline will remain unconditionally within that streamline. It is by causing a particle to switch the streamlines that chaotic regions can be produced. This can, for example, be achieved through time dependent boundaries. It should then be noted that there exist parameters that control the degree of disorder within an associated range.

Experimental work that followed and complimented Aref's work was conducted by Chein et al [47]. Their work concentrated on laminar mixing within cavities and described the equipment used to generate two-dimensional cavity flows. They presented the mixing of both

steady and periodic systems by the use of both lines and blobs of tracer. A variety of cavity configurations and boundary conditions were investigated. They also concluded that operation of the boundaries periodically increases the efficiency of the mixing over that of steady flows. They also suggested that there is a frequency of the boundary oscillation at which an optimum value for the mixing can be achieved. It was found that when operating at the optimum frequency that the initial position of the tracer is 'not critical'.

Leong and Ottino [48] continued the experimental work, investigating the two-dimensional cavity system and presented investigations of the mixing achieved for discontinuous and continuous sinusoidal boundary movement.

In this work they commented that due to the nature of chaos computational simulations cannot accurately predict the arrangement of striations of fluid, but can predict more coarse structures, such as islands and folds in the fluid. This is entirely understandable. Consider now the discussion of Lorenz's model, his values, within a chaotic system, were entered with a discrepancy of one thousandth of a unit. The result then diverged to an unrecognisable degree. It would not be possible to set the initial conditions of a physical experiment to such accuracy that the positions of particles would not diverge from those within a corresponding computer simulation. That being said the fact that chaotic systems do diverge can be used to an advantage when comparing systems that do or do not exhibit chaos throughout ranges of control parameters. This is discussed further in later chapters.

Leong and Ottino also commented that the flows involved are complex, and not completely understood, but they presented a beginning to the understanding of more realistic flows that are unable to be condensed into simple operating terms. This, as will be observed throughout this section, remains the case. The definitive universal rules for the induction of chaos remain un-stated.

Much work has taken place into the investigations of a variety of systems, observing chaos through the inclusion of various properties within the flow. What follows in this section is a brief overview of some notable works of chaotic mixing systems. The types of system domain, applications of properties within the fluid and methods of observing the presence of chaos are briefly discussed.

Time periodic boundaries have been applied to a variety of two-dimensional domain configurations. Many investigations, both experimental and computational, have taken place in simple rectangular cavities [6, 47, 48, 49, 50], others occur in dual eccentric cylindrical systems [45, 46, 51, 52-57], whilst others maintain the original blinking vortex popularised by Aref [58]

Chaos within laminar fluids has also been induced in a variety of other domains, such as the enhanced mixing simulator [59], which operates laterally perturbed Couette flows. A circular

cavity mimics the rectangular cavity, with the circles' perimeter split into four walls, of which two opposing walls are able to move.

The majority of investigations consider Newtonian fluids with uniform properties, however there are exceptions, where the effects of shear thinning fluids of chaotic motion is considered [55]. Other work observes the mixing of two similar fluids, in the presence of a third dissimilar fluid [50] whilst others investigate the stretching and break up of droplets in chaotic flow regimes [56] and two interpenetrating incompressible fluid phases [60].

Work has been carried out to investigate the effect of chaotic mixing on other processes within the system. Enhanced heat transfer [61] and mass transfer [49] has been observed when operating a system under chaotic conditions. The effects of chaotic motion on reactions occurring within chaotic flow domain have also been investigated [52, 58, 62, 63] including flow reversal in continuously stirred tank reactors [64] and bubble column reactors [65].

There are many methods for observing the presence of chaos in a system, as discussed in earlier sections of this chapter. Various methods exist to quantify the disorder or blending quality. Two such methods are described by Liu et al [66] in their work on aperiodic flows. They note that Poincare sections and periodic points are not suitable for the analysis of aperiodic systems, and therefore quantify the chaotic motion by measures of the stretching field, and spread of a tracer, by the use of a box counting technique. Many authors utilise Poincare sections to observe the degree of disorder and presence of islands of regularity [45, 46, 52, 61, 67]. Others use more topological methods, and observe the dynamics of curvature [51] and the asymptotic directionality [57]. To observe a property more related to the process of mixing some authors observe the Lyapunov exponents [59, 68], or the related stretching within the domain [55] or the derived mixing efficiency [53].

Chaotic mixing has also been noted to exist in the mixing processes of granules and powders [69, 70, 71] however this is beyond the remit of this work.

1.6. Summary

This chapter has presented background to chaotic dynamics, laminar fluid mechanisms of mixing and chaotic mixing theory sufficient to enable the reader to appreciate the research findings presented in later chapters.

Initially chaotic dynamical examples were shown to indicate features of chaotic systems relevant to this work. Those notably being sensitivity to initial conditions, and chaotic motion being present within specific operating and control parameters. The divergence of two initially close points observed by Lorenz, could be considered to be similar to two initially close particles in a fluid system modelled by a different series of equations. If the system operates with chaotic motion then, as time evolves, the trajectories of the two initially close

particles will diverge. The particles will separate to positions where they bare no resemblance to their original neighbours. If particles separate to this degree then good mixing has occurred Methods of classifying both dynamical and fluid chaos were briefly discussed, primarily the observations from Poincare sections and the calculations of Lyapunov exponents.

The introduction of three laminar mechanisms of mixing led into a review of literature that concerns chaos in mixing systems. The emphasis being placed on two-dimensional, laminar fluid, primarily time dependent domains, investigated both computationally and experimentally. It is noted that much work has taken place into observing the effects of chaos on features within the fluid.

The aspects of chaos and chaotic mixing in this chapter are not intended to be a complete survey of all things chaotic, but an introduction to the principles and previous works that are relevant and compliment the investigation presented in this work.

2. Observation and recognition of chaos using commercial CFD.

2.1 Introduction

This chapter, by the use of a commercial Computational Fluid Dynamics (CFD) package, attempts to simulate two-dimensional chaotic systems.

Commercial computational fluid dynamics is fast becoming a popular tool for engineers to investigate a variety of systems involving fluid movements, [72, 73, 74]. This is due to CFD enabling the user to model complex geometries and fluids and visualise the results in a variety of different ways.

This chapter establishes that commercial CFD can simulate chaotic flow within simple domains, later chapters then shows that it is possible to apply these techniques to the investigation a variety of more complex chaotic systems. By using this technique advancement is be made towards developing concepts and rules of thumb for use in the design of industrial process fluid mixers.

2.1.1 Introduction to the system

The system to be initially investigated is a simple rectangular cavity. It is similar in geometry and properties of the fluid to the experiments presented by Leong and Ottino [48] and [12]. The rectangular domain has an aspect ratio of A = (H/W) = (6.2/10.3) = 0.6. (Where H and W are height and width respectively, measured in cm.) The fluid simulated is glycerine, with a constant density of 0.00125 g/mm^3 and a viscosity of 0.75 poise. The fluid is assumed to be fully Newtonian, with no slip occurring at the walls of the domain. Effects of temperature, gravity and inertia are neglected.

The experimental investigation [48] shows that it is possible to induce chaos by the out of phase smooth oscillation of the upper and lower walls of the domain. This forces the system to evolve through a series of alternating streamlines, which induces the disorder. The top and bottom walls will be oscillated out of phase in the form of equations 2.1 and 2.2:

$$u_{top} = U_{top} \sin^2 (\pi t / T_{top} + \alpha) \qquad (2.1)$$

$$u_{bot} = U_{bot} \sin^2 (\pi t / T_{bot}) \qquad (2.2)$$

Here u_{top} and u_{bot} are the velocities of the top and bottom walls respectively. $U_{top} = U_{bot} = U$ are the amplitudes of oscillation, t = incident time, $T_{top}=T_{bot}=T$ are the time periods for top

and bottom walls respectively, which are identical here. The phase difference between the two walls is $\alpha=\pi/2$.

The time dependent system moves through the instantaneous streamlines of the fluid as shown, in figure 2.1a-c. (Figures generation is explained in detail later in this chapter.) The system, at the start of a period (t=0), flows as figure 2.1a, where the top wall is moving and the bottom stationary ($u_{top}=U_{top}$ and $u_{bot}=0$). Then moves through figure 2.1b, where both wall velocities are equivalent ($u_{top}=u_{bot}=\{U_{top}/2\}=\{U_{bot}/2\}$) at $t=\{T_{top}/4\}=\{T_{bot}/4\}$, to figure 2.1c at $t=\{T_{top}/2\}=\{T_{bot}/2\}$. At this point the top wall is stationary, with the bottom wall at maximum velocity ($u_{top}=0$, $u_{bot}=U_{bot}$). As time evolves to $t=¾T$ the system flows once again as figure 2.1b, then returns to figure 2.1a for the beginning of the next period, t=T. The notable difference between the flows shown in the figures, is the oscillation of the 'centre point' of rotation up and down in the domain.

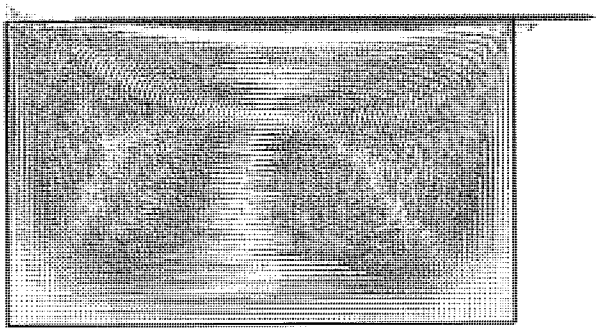

Figure 2.1a. Flow patterns showing the two-dimensional cavity with top wall moving and bottom stationary ($u_{top}=U_{top}$ and $u_{bot}=0$) at time t=0

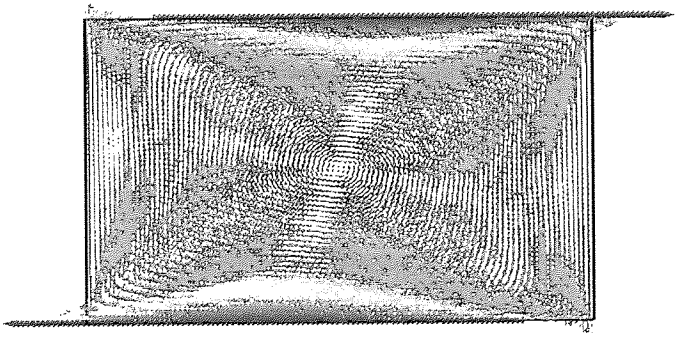

Figure 2.1b. Flow patterns showing the two-dimensional cavity with top and bottom walls moving at the same velocities ($u_{top}=u_{bot}=\{U_{top}/2\}=\{U_{bot}/2\}$) at time $t=\{T_{top}/4\}=\{T_{bot}/4\}$

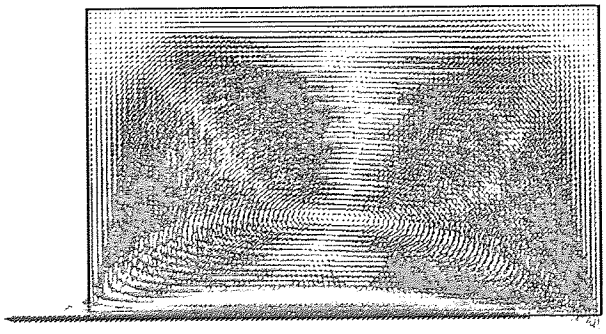

Figure 2.1c. Flow patterns showing the two-dimensional cavity with top wall stationary and the bottom wall moving ($u_{top}=0$, $u_{bot}=U_{bot}$) at time $t=¾T$.

2.2 Chaos into Commercial Computational Fluid Dynamics.

Commercial Computational Fluid Dynamics has become widely available with particular codes originating from a variety of original purposes, with a number of companies now offering this software [75-83].

The structure of all CFD software is similar requiring the user to generate a mesh, specify boundary and initial conditions, use some numerical technique to solve or approximate a solution and then view the results using some sort of graphical module. However different software packages provide different methods, modules and schemes of equations that enable problem definition, solving, viewing and post-processing for a particular area of fluid dynamics.

The commercial CFD package chosen for the simulations in this work is Polyflow [75] as it is primarily for use with laminar fluid flows, (i.e. polymers, and hence the prefix). The package contains many specialised simulations modules such as visco-elastic flows, blow moulding and fibre spinning, however, in this work the 'Mixing Module' is the capability of interest.

Polyflow's post-processing mixing module, 'Polystat,' allows the investigation of time dependent boundaries. Polystat also enables the user to approximate the movement of a boundary as its motion changes throughout time. Systems can then be investigated by the statistical analysis of various properties of mixing against evolution time. For this work the basic structure of components of Polyflow can be considered as shown in figure 2.2.

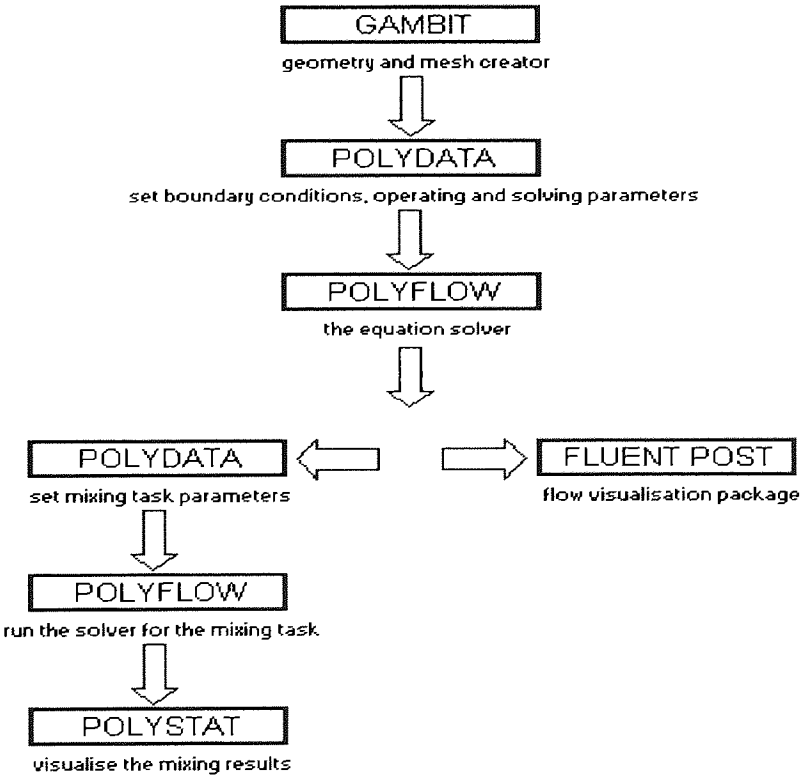

Figure 2.2. Pictorial representation of the links and orders of use of the Polyflow software relevant to the simulations in this work.

2.2.1 Mesh and optimisation

The Gambit software allows the user to generate complex geometries, using similar methods to CAD packages. It is then possible to superimpose a mesh onto the drawn structure, and hence generate a grid of nodes, with a specified density and grading. The different boundaries that are required in the simulations are highlighted as separate entities and labelled with an alphanumeric term. The type of boundary (e.g. wall, input or output) is not specified at this point. The mesh can then be exported and converted in Polydata into a Polyflow readable mesh.

The discussion here of Gambit is intentionally brief, as the meshed domains in this work are not significantly complex. Therefore it does not warrant a comprehensive discussion of the mesh generator.

Various mesh densities for the two-dimensional system were investigated and found to yield similar conclusions, therefore a detailed optimisation is not included at this stage. One node every millimetre, along the sides of approximately 60 and 100mm, was found to be of sufficient density for these initial tests.

2.2.2 Polydata and Finite Element tasks

For steady state, time independent, systems Polyflow solves the partial differential equations of fluid dynamics by the use of a finite element method. For time dependent systems, like the one being investigated here with oscillating boundaries, the solver must first solve individual steady state flow fields then analyse them consecutively in the post-processing mixing module. Therefore in order to create the sinusoidal oscillation of the boundaries, the movements are approximated into a number of steady state systems that are solved first by Polyflow and then arranged in a mixing task to calculate particle trajectories.

The velocities of the top and bottom walls during one time period of oscillation are shown in figure 2.3a. from equations 2.1 and 2.2.) The curves are approximated into forty steady state instantaneous cases for entry into the solver, as shown in figure 2.3b.

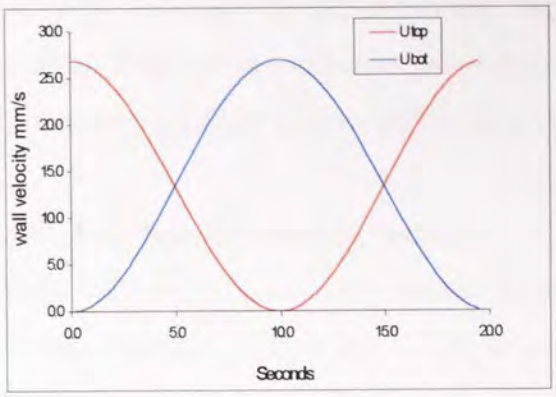

Figure 2.3a. Smooth curve representing the wall movements of the two dimensional cavity system, from equations 2.1 and 2.2

Figure 2.3b. Wall movement curve from equations 2.1 and 2.2 approximated into forty slices for entry into Polyflow mixing task.

The analysis of the time dependent boundaries is considered in section 2.2.3, this section is concerned with the methods Polyflow applies to solve the initial steady state systems. Polyflow offers a range of models for different types of viscous fluid process and rheology. As the fluid that is modelled in this work is assumed to be Newtonian and therefore have constant viscosity and density the equation of continuity (incompressibility equation) [84-87] becomes:

$$(\nabla \cdot \mathbf{v}) = 0 \qquad (2.3)$$

and the equation of motion (momentum equation) becomes:

$$\frac{\rho D\boldsymbol{v}}{Dt} = -\nabla p - [\nabla \cdot \tau] + \rho \boldsymbol{g} \qquad (2.4)$$

where:

$\frac{\rho D\boldsymbol{v}}{Dt}$ = mass per unit volume multiplied by acceleration

∇p = the pressure force per unit volume

$[\nabla \cdot \tau]$ = the viscous forces per unit volume

$\rho \boldsymbol{g}$ = the gravitational forces per unit volume (which is assumed to have no affect in this work)

Analytical solutions to the non-linear equations governing fluid motion are limited, and therefore Polyflow uses numerical methods based on the finite element method to seek approximate solutions to flow problems [72, 75, 88]

2.2.3 Polydata and mixing tasks

Polyflow is not a Lagrangian code so in order to generate trajectories of particles the post-processor mixing module has to be used. The result output files from each of the forty instantaneous velocity fields shown in figure 2.3b are entered into a Polydata mixing task to create an approximated oscillation.

When mixing tasks are solved the Polyflow mixing module generates a number of particles as labels of points in the fluid (i.e. they have no affect on the fluid motion) and tracks their trajectories as time evolves. The output data consists of the time and corresponding spatial co-ordinates of the particle. And, if desired, specific mixing related properties of the fluid can also be calculated and recorded against the corresponding time. For example the software can calculate properties such as the rate of stretching and the segregation scale. Once solved, the output data can be analysed by use of a spreadsheet or by the statistical software processor, Polystat.

To create a mixing task Polydata must again be entered, and "mixing task" must be selected. In this case "time dependent" problem must be chosen. This then allows the consecutive velocity field result files to be entered. The names of the result files, the order in which they are to operate and the time for which they are to be used are all entered. It is by the alteration of the time of operation of each velocity field, that the system boundaries can oscillate at different time periods. For example if the system containing forty instantaneous velocity fields were to operate at a time period of oscillation of ten seconds then the time of use for each segment would be 10/40 = 0.25 seconds.

It is in Polydata that the number, origin of trajectories, and time of evolution of the particles to be tracked are entered. Particles can be generated at random throughout the domain, or within regions specified by the user, for example at the inflow of an open system, or in a 'box' specified within the fluid. By using a box of specified orientation and size it is possible to accurately generate particles at the exact same origin giving consistency when considering the affect of a range of a particular parameter on a property of the mixing.

Once the mixing task data file has been created Polyflow can be run again to calculate the particle trajectories. Each particle trajectory is calculated in turn through the time integration of equation 2.5 which is an Euler explicit scheme, sufficient if we are only interested in the successive positions of material points. In chapter three the mixing efficiency is considered and which requires a much more CPU intensive numerical technique.

$$\dot{x} = v \tag{2.5}$$

The trajectory is calculated in the parent element, then integrated with the Runge-Kutta method. Polyflow's mixing module uses the algorithm, illustrated by figure 2.4.

⇓ Initialisation.
⇓ choose an initial position X in element E
⇓ find the local co-ordinates ξ of X in E
⊗ Integrate $\dot{\xi} = f(v(\xi))$ until cross boundary of element E
⇓ adapt time step to find position x on boundary of E
⇓ search neighbourhood element E*
⇓ find local co-ordinates ξ* in element E* of the current position x
⇓ return to ⊗ until lifetime of particle exceeded

Figure 2.4. The algorithm used by Polyflow mixing module to track particle trajectories.

2.2.4 Polystat

The result files, containing co-ordinate data and properties of mixing at associated times from the mixing task can be viewed by using Polystat. This statistical software provides both a pictorial view of the trajectories and a statistical analysis of any mixing properties calculated. The user is given the ability to perform simple mathematical or statistical operations on the calculated properties, to generate further property ratios or integration over time, for example. It is also possible to create slices on any property to represent the data. For example the 'rate of stretching' could be statistically analysed through a series of time or co-ordinate slices.

Trajectories can be viewed pictorially by reading the mesh and mixing result files. Polystat allows the user to view any property throughout the corresponding trajectory. Differences in property values are indicated through user defined colour variations.

Statistical data, once all required operations have been performed, can be written to file as a series of graphical plot co-ordinates. These can be viewed either by Polyflows' own plotting software, Polyplot, or by transferral into a spreadsheet software package for analysis.

Details of the various mixing properties calculable by Polyflow will be given where used later in this work.

2.3 Chaos in a two-dimensional cavity system

Before any detailed investigations can be performed on chaotic systems using Polyflow, it must be established that the tool produces results that compliment published experimental

data through exhibiting chaotic behaviour. Before progressing to more complex systems it should first be established that the commercial CFD can simulate chaos in a simple system.

2.3.1 Comparison between computational investigation and published experimental research.

Let us first look at a steady state system. The conditions are set as faithful to the experimental system [48] as possible. When both top and bottom moving boundaries are set at an equal speed in a clockwise direction it can be seen from the resulting velocity vector plot, see figure 2.1b, that streamlines, similar to those photographed and presented in [48], exist.

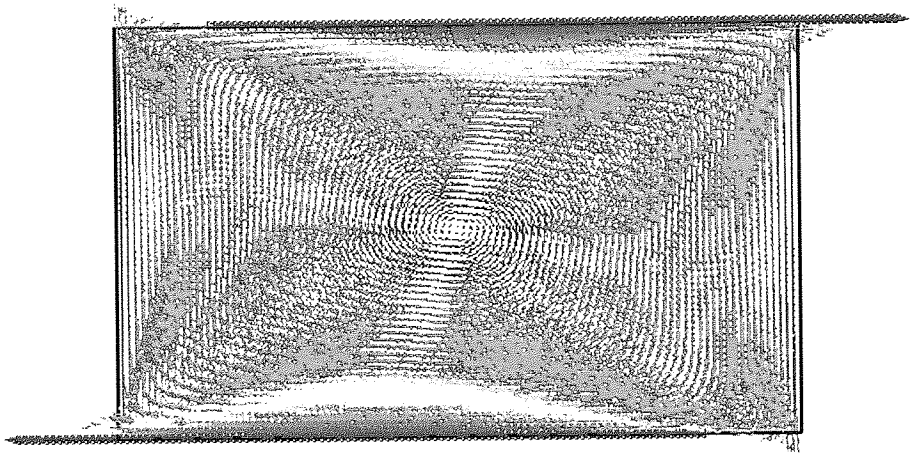

Figure 2.1b. Flow patterns showing the two-dimensional cavity with top and bottom walls moving at the same velocities ($u_{top}=u_{bot}=\{U_{top}/2\}=\{U_{bot}/2\}$) at time $t=\{T_{top}/4\}=\{T_{bot}/4\}$

It is suggested that if a blob of a tracer is placed into a streamline, the resulting trace will remain trapped in that streamline indefinitely. The computational simulation result, figure 2.5, shows a particle being generated at (x, y) = (22, 31) mm from the bottom left corner and its trajectory observed for 1000 seconds. It can be seen that the trajectory follows a streamline without deviation, thus reproducing simple time independent flows [48]. Poor mixing would be present in this system.

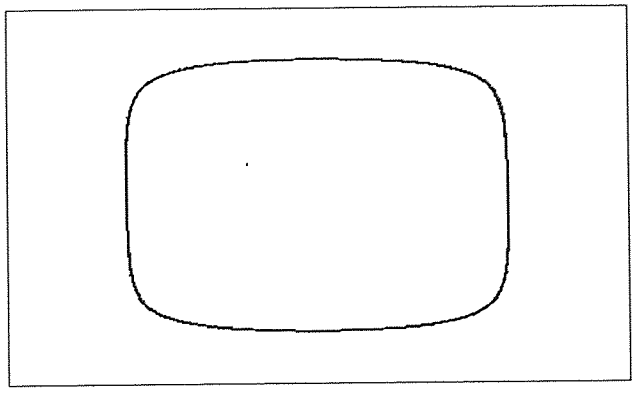

Figure 2.5. Simulation of a blob of tracer placed in the flow domain. The flow is steady and streamline, the tracer particles highlight the streamline that they were originally placed within.

When the experimental system is operated under time periodic sinusoidal boundary oscillations the mixing is improved. This is concluded from observations of a blob of tracer, that does not follow any one streamline appearing to spread randomly over the domain. Bends and folds, which are signatures of chaotic mixing, are clearly visible.

To compare the computational analysis with the published experimental data a test using the same periodic conditions as [48] is used (although here forty instantaneous segments approximate the sinusoidal motion). U = 26.9 cm/s, T=20 seconds, $\alpha = \pi/2$ and the exact dimensions of the flow domain A = (H/W) = (6.2/10.3) = 0.6.

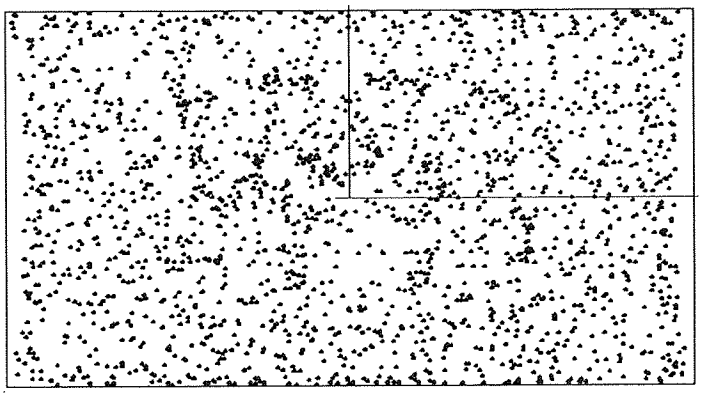

Figure 2.6. 1 second time snap shots of a particle trajectory for 3000 seconds in the two-dimensional cavity where U=26.9 mm/s, T=20 seconds. The trajectory follows a random path covering the majority of the domain.

It is found that tracer particles in the oscillating computational system obviously do not follow any singular streamline. Figure 2.6 shows one particle trajectory for 3000 seconds, where T=20 seconds. It shows the particle moving throughout the whole flow domain, thus concluding that some disorder is apparent.

The particle trajectories, however, do not look exactly as the pictures in [48], where it is suggested that chaotic motion is occurring. This can be attributed to the experiments using a blob of tracer in the flow domain and the pictures above observing the trajectory of only one particle. The experimental tracer blob would be stretched into a line that will subsequently be displaced by non-tracer particles, producing bending and folding in the tracer area. Thus the experimental tracer blob shows how well the system mixes, but is not an indication of the evolution of an individual particle, as in this computational test. Therefore a comparison between the computational and experimental results at this stage is unable to continue past the conclusion that both results show increased mixing when time periodic and a possible chaotic region. This is sufficient agreement at this stage to continue investigations.

As the computational results enable the isolation of an individual trajectory it is suggested that it may be possible to investigate chaotic motion by observing the movements of single

particles. Although one would expect that particles may behave differently depending on where in the domain they originate.

It has previously been suggested that experimental methods are limited due to the nature of chaotic motion magnifying any experimental error, hindering consistent repetition. The method of analysis with experimental data is limited to classifications of the flow. The issues of divergence in results due to minute errors or discrepancies, which is a signature of chaos, are not restricted to experimental investigations alone. The nature of chaos can also have an effect on the accuracy and reliability of computational investigations. Small differences introduced due to the way computers store data, and the various approximations when solving equations, can, under chaotic conditions, propagate into large discrepancies in results. It is expected therefore that the evolution path of a particle will be dependent on initial conditions whereas the overall state of disorder, will not be significantly affected by such minute differences. The trajectories may diverge with minute discrepancies, but whether the system enters into chaos, or not, will remain unchanged.

By the use of computational observations of trajectories, it is possible to observe a remarkable difference in fluid behaviour between order and chaos as a time period of oscillation is introduced. This enables the conclusion that there must be a point or range at which the system transforms from an ordered state to a chaotic one. And hence the possibilities of observing a cascade from order to chaos as operating parameters are varied.

2.3.2 Observing the onset of chaos as operating parameters are varied.

From the agreement of the observations above with those in [48] and the computational simulations it is suggested that analysis using commercial computational fluid dynamics for the two-dimensional flow system is viable. Therefore it is acceptable that this method should be further used to investigate the sensitivity of the system with respect to the variation of operating parameters, which will be termed control parameters when discussing their effect on the disorder of a system.

The two-dimensional system is investigated further, for the variation of control parameters, initially by two methods:

1. Observing the frequency and accuracy with which an individual particle returns to a reference point and thus showing an increase in the trajectory period, for fluid behaviour at small time periods of oscillation.
2. Observing the particle trajectory around the flow domain using pictorial methods, which is useful for investigating larger time periods up to, and past the point, where chaotic motion begins.

Cascade towards chaos, particle returning to a reference position.

In order to observe the effect of varying operating parameters on the flow behaviour the trajectory of a particle starting from an arbitrary reference point at co-ordinates (x, y) = (-29.5,0), where the origin is the centre, is observed.

In the case of the steady state system the particle returns close to the reference point after one circuit of the flow domain (as shown pictorially in figure 2.5). This system can be termed to possess a trajectory period of one.

The plots in figures 2.7 and 2.8 were achieved by generating a single particle at the reference position and recording its position at regular time intervals. The two times at which the x co-ordinate is negative and the y co-ordinate changes from negative to positive are recorded and their positions plotted. This produces a plot of pairs of points, indicating how close to the reference point the particle has passed.

It is shown here that observing the cascade by period increasing depends on the tolerance of the accuracy required of the particles returning to a reference point. For example with a large tolerance of accuracy a particle may be considered to return to the reference point every other revolution of the flow domain, and hence be pronounced as having a period of two. But the same system, subjected to a more microscopic investigation could be found to return to the reference point only once every four revolutions of the flow domain, say, and hence have a period of four.

It is shown below that it is possible to observe cascades from order towards chaotic motion, however one must indicate to what tolerance.

If the accuracy were at the first decimal, then when T=0.01, figure 2.7, could be said to also have a trajectory period of one, as, within the accuracy, after each revolution the particle returns to the reference point. However if the tolerance were to be the third decimal, then the system would have a period of eight, where the particle returns close to the reference point after eight revolutions of the flow domain.

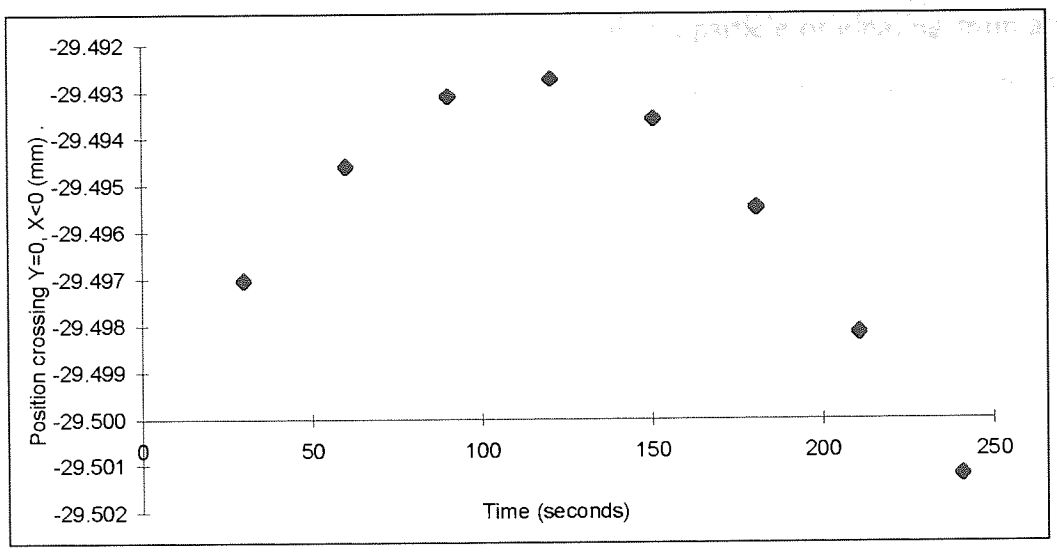

Figure 2.7. Pairs of points where a particle trajectory passing near to a reference point in the two-dimensional cavity operating equivalent to earlier tests, with a time period of 0.01 seconds.

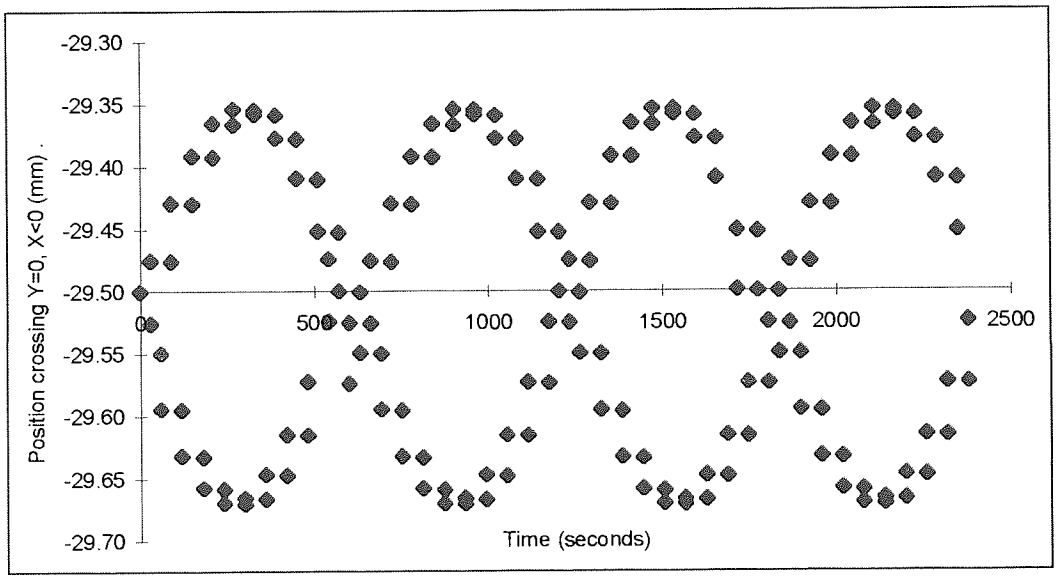

Figure 2.8. Pairs of points where a particle trajectory passing near to a reference point in the two-dimensional cavity operating equivalent to earlier tests, with a time period of 0.2 seconds.

When operating the system with a time period of oscillation of T=0.2, it is clearly visible, from figure 2.8 that the particle is oscillating around the reference point. The particle repeatedly returns, within the second decimal accuracy, to the reference point after approximately every 600 seconds. This is a notably longer period of time that for the previous system where the wall oscillation frequency was smaller. A period trajectory pattern can be found with time periods above and below T=0.2, however it is not possible to suggest how close to chaos the system is located.

To obtain the cascade, in microscopic accuracy, from steady state into chaos would require an unfeasible amount of time and would be of little practical value.

From the above investigations it can be suggested that a particle originating from a reference point within the flow domain, when operating with steady state boundary conditions, will return to the reference point in one trajectory period. Whereas a particle generated within the oscillating system takes an increased number of trajectory periods to return to the reference point. As the disturbance to the system increases, by lengthening the time period of oscillation, the time for a particle to return to a reference point will also increase. It is from the presence of a period increasing effect that the cascade into chaos could be observed. Although to obtain the whole cascade would be of little use and time consuming. From the figures shown the conclusion that can be drawn is that, the higher the time period of oscillation the more a particle oscillates around a reference point. The oscillation around this point would be expected to increase up to the point where chaos occurs.

Cascade into chaos, pictorial representation.

It was shown above that individual particle trajectories oscillate as the control parameter, time period of wall oscillation is increased. To obtain a more visual representation of this cascade for a greater range of time periods pictorial methods can be employed. Here we present particle trajectories for various time periods of the moving walls.

When the system is operating at a time period of T=1 second, as figure 2.9 it can been that the particle appears to return to itself after each revolution of the flow domain. Although from the previous section it is known that the particle is oscillating, albeit on a small scale. And hence for all time periods below T=1 the pictorial representation will appear as figure 2.9.

As the time period of oscillation is increased it is possible to observe that the particle oscillations gain amplitude. In figure 2.10, where T=5 seconds, the particle can be seen to be oscillating, but maintaining a general oval shape throughout the 3000 seconds of its life. Increase the wall oscillation time period further to T=10 seconds, figure 2.11, and it is possible to see that the particle oscillation has increased to a level where the trajectory is displaced from the general path, and no longer appears to be ordered. The particle now passes nearer to the walls and all over the centre of the flow domain. This indicates that chaotic motion is beginning as the particle is moving, apparently, without order around the domain. The particle is however, still bound by an outer limit, that suggest chaos is not fully present at these conditions.

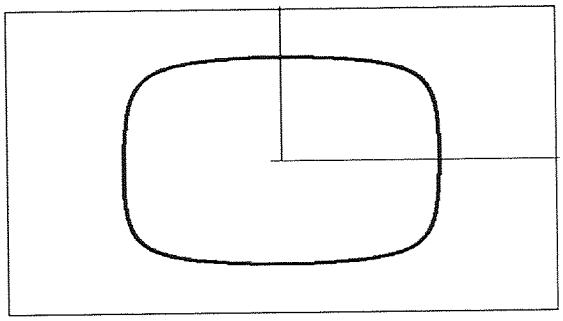

Figure 2.9. Two dimensional time periodic cavity system operating with U=26.9 mm/s and T=1 second

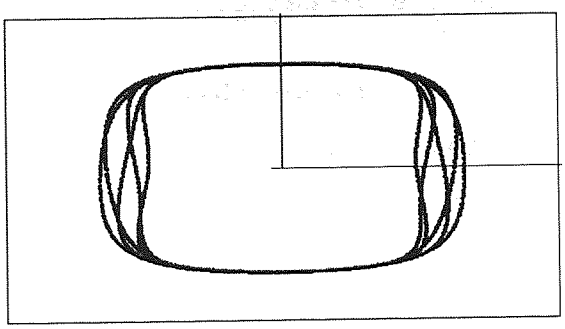

Figure 2.10. Two dimensional time periodic cavity system operating with U=26.9 mm/s and T=5 seconds

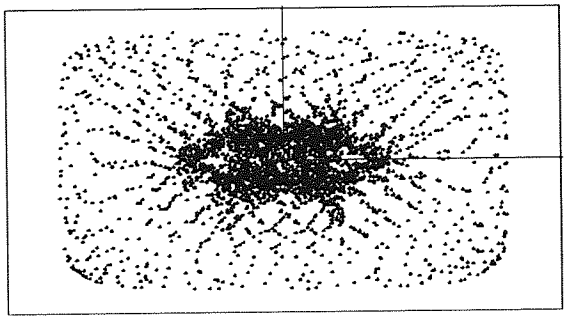

Figure 2.11. Two dimensional time periodic cavity system operating with U=26.9 mm/s and T=10 seconds

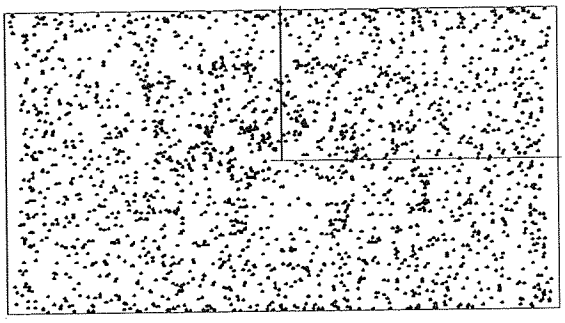

Figure 2.12. Two dimensional time periodic cavity system operating with U=26.9 mm/s and T=20 seconds

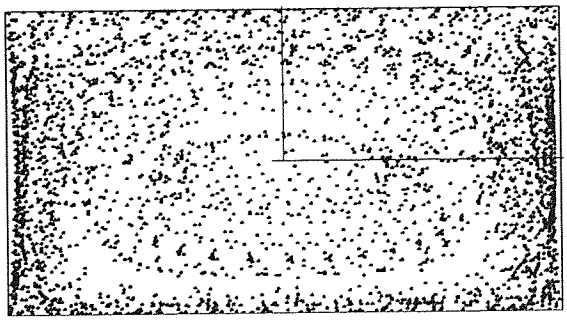

Figure 2.13. Two dimensional time periodic cavity system operating with U=26.9 mm/s and T=40 seconds

It is difficult to suggest from pictures of this kind exactly where the transition from order to chaos begins. However at a time period of T=20 seconds, figure 2.12, it is possible to see that the particle travels throughout the domain, with seemingly random movement, and is no longer bound by an outer limit. This is also apparent for a time period of T=40 seconds, figure 2.13. This system, however, also shows that the trajectory appears to gain some degree of order restoration, which can be observed by what appear to be regular patterns in the trajectory path.

Both methods described above are not without their limitations. However they both show qualitatively that a cascade from order to chaos exists for this particular system and can be observed as the control parameter, time period of oscillation, is increased from a low value.

2.4 Why varying boundary conditions effect a cascade into chaos.

Previous works have not attempted suggestions for reasons why varying boundary conditions effect cascades into chaos. The explanation, however, is conceptually simple and will form the basis of this work and will be used to predict the flow within more complex systems.

When operating at steady state conditions a particle in the two-dimensional systems will remain within the streamline within which it originated. If oscillating boundaries are introduced the streamlines vary. For the purposes of this explanation let us consider the two extremes of the smooth sinusoidal oscillation, at t=0 and at t=T/2 so the system is alternating between the flows represented by figures 2.1a and 2.1c respectively.

In the alternating system a particle will initially flow within the streamlines in figure 2.1a, as indicated by the red line, in figure 2.14a for the first time period. The instantaneous streamline motion is altered to flow as figure 2.1c for the second time period. The particle then changes direction to flow within the new flow regime, as indicated in figure 2.14b. As time evolves the particle continues to change direction for the third and fourth time periods, as in figure 2.14c and 2.14d respectively. This motion continues throughout the particle's measured life, and so the particle appears to oscillate.

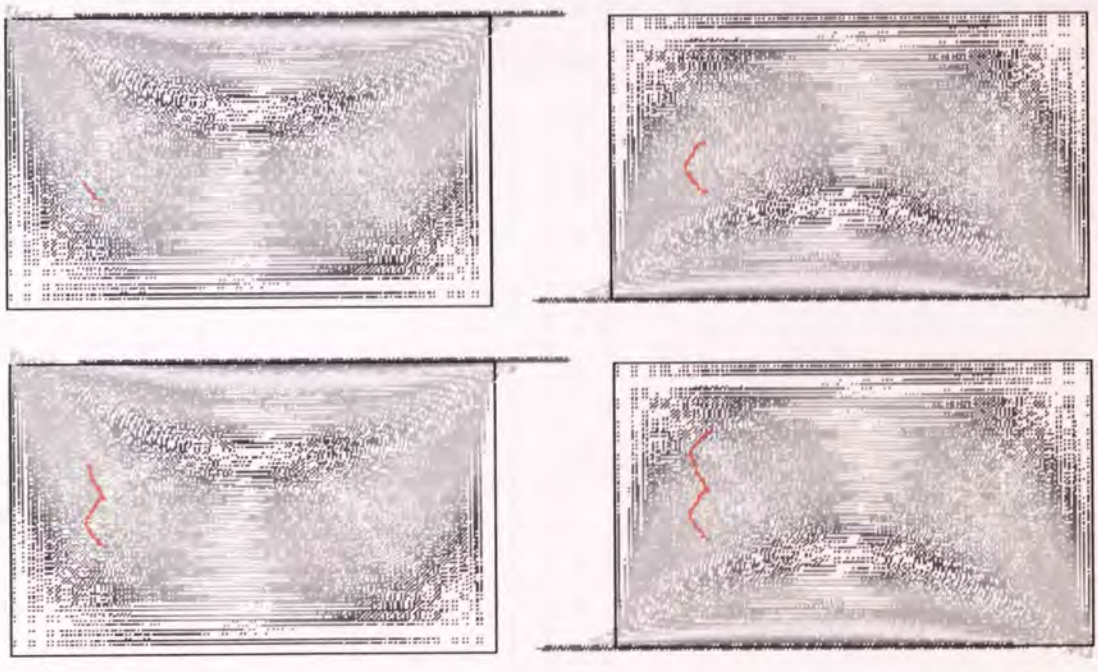

Figure 2.14 a, b, c, d. The two extremes of the oscillation of the rectangular cavity system pictorially showing the movement of particles as the streamlines alternate for four consecutive time periods of oscillation.

The distance that particles can travel in any one streamline depends on the length of time resident in that streamline, and the velocity magnitude of the particles. At a low time period a particle can only displace a small distance from one instantaneous streamline, before being

affected by another. Hence the particle oscillation is small, and on a pictorial scale would appear as steady state, as in figure 2.9.

As the time period of oscillation is increased a particle will remain in one streamline for an extended period of time. This will allow it to displace more distance along the instantaneous streamlines, and hence the particle oscillation will increase. The particle oscillation is now visible on the pictorial scale, see figure 2.10, where T=5.

There becomes a point where the displacement of the particle grows significantly that one extreme instantaneous flow pattern will not cancel out another to form a particle oscillation, and the particle begins to behave stochastically, as in figure 2.12, where T =20.

If the time period of the boundaries is increased further there appears to be some degree of order restoring. This may be due to particles remaining in one streamline for a considerable time before displacing, thus reducing the mixing effect of the oscillations. The system behaves as many consecutive steady state conditions and not as an oscillating one, shown in figure 2.13.

Figure 2.15 shows an increase in the magnitude of particle oscillation as the time period of the wall oscillation is increased. The cavity here has an aspect ratio of 1, and an area of 100mm^2. The oscillations are in the flip-flop [44] regime with a boundary amplitude of 20mm/s. One particle is generated at co-ordinates X, Y= 5, 5mm, and its' trajectory followed for various times. It can be seen that the oscillation of the particle increases, as the time period is increased, up to the point where the particle follows whole streamlines.

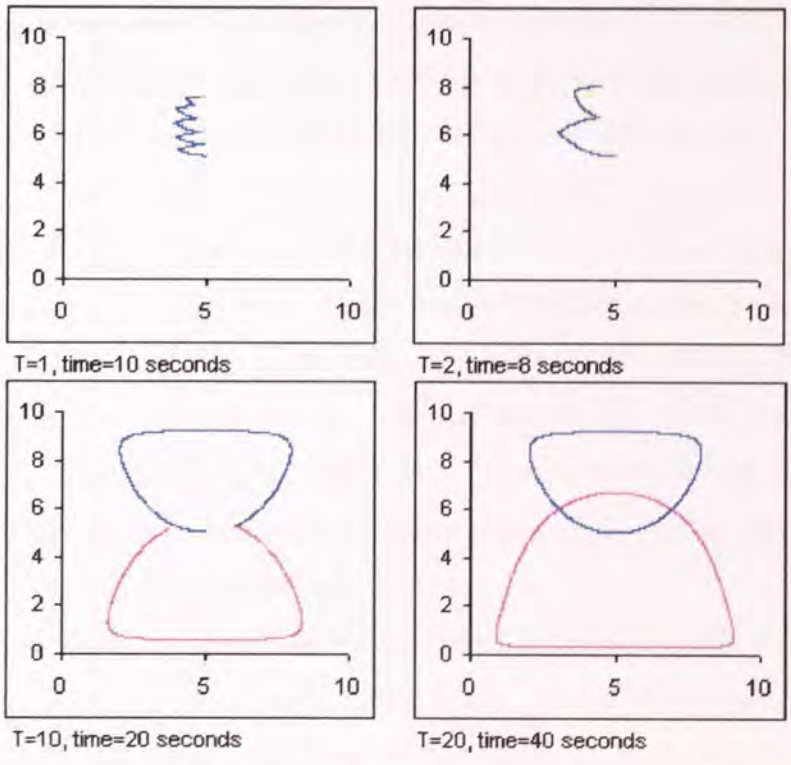

Figure 2.15 a, b, c, d. Plots of particle trajectories in the time periodic cavity system, operating with a flip-flop movement of the wall boundaries, showing the distinct direction change of particles as the streamlines alternate.

The increase in the magnitude of the boundary oscillation could be considered in a similar way. A slow moving particle will not displace within an instantaneous streamline as much as a fast moving one. As the velocity of the boundaries is increased a particle can displace more distance in the same time. The effect of this is that the particles are able to oscillate more significantly with a low time period. As it is the particle oscillation that moves the system into a cascade, then it follows that the cascade can be entered at a lower time period when the velocity amplitude is increased. This is discussed in further detail in the following chapter.

2.5 Continuation of investigation of chaotic mixing systems.

This chapter intended to introduce the concept of using commercial CFD techniques to investigate chaotic flow. The main achievement was therefore to assess whether or not it would be possible to observe chaos by this method. It has been shown that not only is it possible to replicate experimental data, but it has become evident that extensive supplementary information is potentially available through computational method which is not available experimentally.

To expand the knowledge of the characteristics of chaotic systems, and ultimately aid the design of chaotic processing equipment, further work must be undertaken. Investigation of a variety of flow domains, both two- and three-dimensional should be carried out.

The identification of a property through which chaos can be observed for a variety of operating conditions and system geometries should be attempted. It would be by utilisation of such a property that quantitative measures of chaos could be achieved leading to information concerning the optimum operating conditions for chaotic mixing systems.

2.6 Summary of observations, and conclusions.

It is shown here that it is possible to model and investigate a chaotic system successfully using commercial CFD software. This technique of analysis enables the observation of cascades from order into chaos. It has been shown that particles within a steady state system will flow in their initial streamline indefinitely. It was then shown that oscillating the movement of the top and bottom walls can induce chaos. This can be observed by the use of tracer particles, which highlight disorder in the system.

Investigation of the cavity by the use of computational methods yields a cascade from order into chaotic motion. It has been shown possible to observe a trajectory period increasing cascade as the time period of oscillation of the walls is increased. This is possible by observing a particle returning to a reference point within a sufficient accuracy. It is unfeasible,

however, to attempt to find the full trajectory cascade as the benefit does not outweigh the required hardware or time expense.

By the use of pictorial trajectory plots it is also possible to observe the cascade from order into chaos. At a low time period of wall oscillation the trajectory appears as a streamline system. The movement of the boundaries is unable to affect the particle significantly, as the instantaneous velocity field changes are too rapid. Hence the particle does not have sufficient time to be displaced from its initial streamline.

As the time period of oscillation is increased particles receive greater displacement from their initial streamlines, and begin large oscillations. Further increase of the time period causes greater oscillations up to the point where chaos overwhelms.

3. Investigation of two-dimensional oscillating boundary flow domains.

3.1 Introduction

In the previous chapter it was shown that it is possible to observe the presence of chaos from observations of individual particles, from a microscopic and macroscopic viewpoint. It was also shown that a cascade from order into chaos existed, and was affected by changing the motion of boundary oscillation.

It was shown previously that chaos can only be induced when systems are operated within a certain range of operating and boundary conditions. The change in the degree of disorder in chaotic systems, as operating conditions vary, has been noted by many authors, and was as discussed in chapter one. There is, however, seldom an attempt to offer an explanation for the apparent variations in the mixing quality over a range of conditions. This chapter using the rectangular cavity and an eccentric cylindrical system attempts to demonstrate the theory presented in the previous chapter explaining why a laminar oscillating system is sensitive to changes in boundary conditions and exhibits chaotic motion only over a certain range of conditions.

To enable a comparison, and further investigation, between systems with differing operating parameters a property of the system must be observed to give some degree of quantification. The property of mixing efficiency [12, 75] is chosen here for that purpose in this chapter. The mixing efficiency has successfully been applied to mixing systems [6, 41, 43, 45], and can be used to provide some quantification of the quality of the mixing within the fluid domain.

Two two-dimensional systems are presented in this chapter. First the rectangular cavity system, from chapter 2, and second an eccentric cylindrical system. Both of these systems contain two moving boundaries, oscillating in the approximated sinusoidal motion described in the previous chapter (see equations 2.1 and 2.2.)

3.2 The property mixing efficiency.

It has been shown that a cascade from order to aperiodic motion (with increasing time period of oscillation of moving boundaries) can be observed by the use of commercial computational fluid dynamics. In this chapter this work is extended. The same cascade will be observed by the use of the instantaneous mixing efficiency calculated from an optimum number of particle trajectories. The trajectories are generated at representative positions in the flow domain with the property calculated at uniform slices of time.

Instantaneous mixing efficiency e_λ is given by:

$$e_\lambda = \frac{\dot{\lambda}/\lambda}{D} \tag{3.1}$$

where λ is the length stretch (and $\dot{\lambda}$ is the time derivative) given by:

$$\lambda\,(X, \mathbf{M}, t) = \frac{|dx|}{|dX|} \tag{3.2}$$

where dX is the infinitesimal material length with orientation **M**, and time, t=0, and dx is material length at orientation **m** where t>0.

D is the rate of dissipation, given by:

$$D = \sqrt{(\mathrm{tr}\,\mathbf{D}^2)} \tag{3.3}$$

where **D** is the deformation tensor.

Letting $e_{\lambda m}$ denote the mean of the mixing efficiency we take:

$$M = \int_0^t e^2_{\lambda m}\,dt \tag{3.4}$$

As the parameter, rate of stretching, and therefore, mixing efficiency, is often negative, in order to maintain an absolute orientation of material length and therefore account for large negative values of mixing efficiency $e_{\lambda m}^2$ is taken as the integrand in equation 3.4.

This enables the results in the form of a single integral for each variation in operating parameters, which can be quantitatively analysed with respect to other tests with different values for the same control parameters.

3.2.1 Optimisation and agreement of mixing efficiency property.

There are many variables and assumptions involved in the production of a test result (mean value of mixing efficiency) such as the node density of the mesh, time step, duration of evolution, and the number of particles employed to gain mean values of the mixing efficiency. Therefore the system has been subjected to optimisation and tested for consistency and agreement of conclusions.

The instantaneous mixing efficiency is calculated at specific time 'slices' for each of the particles as they evolve in the simulation. The variables associated with this are, the lifetime of the particles, how often to calculate $e_{\lambda m}$ and the number of trajectories used to calculate the mean value. The parameters for the generation of the property were considered to be

optimised if the consistency of the conclusion being observed was achieved but not necessarily the numerical accuracy.

The optimisation results presented here are for the two-dimensional eccentric cylindrical system. Similar tests were conducted for the rectangular cavity system, however there is no need to include these here also.

To be able to set all but one of the variables constant, when observing the effect of only one, it is necessary to make some assumptions. It is possible to estimate values for the variables that will yield consistent conclusions. These will be used in the optimisation tests and confirmed to be adequate when isolated.

The first variable investigation presented is the lifetime of the particles trajectories. This test begins by assuming that 400 particle trajectories, storing the value of the property every one second, is sufficient. The mixing efficiency value is calculated for varying evolution times over a range of time periods of wall oscillation. It is possible to observe in figure 3.1, where M has been time averaged, that as the lifetime of the particles increases the conclusions become more consistent. As the form of the plots are similar at 300 and 399 seconds, both exhibiting a peak at T=16 seconds, and at this stage we are only interested in consistency of conclusions, we can take an optimised value for evolution time as 300 seconds. One may expect that as the time of evolution is increased further the optimised value may become closer. However to conserve computational time 300 seconds will suffice for the following tests.

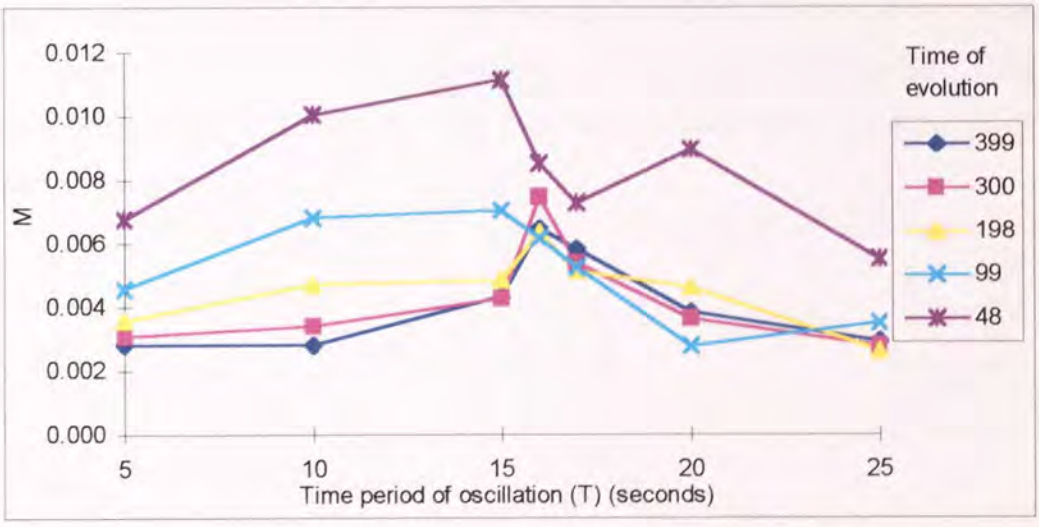

Figure 3.1. Time-averaged value of the mean mixing efficiency against time period of wall oscillation for the eccentric cylindrical system, for five different values of evolution time, where a time slice is taken every second for 400 particles.

From the above test we take the lifetime of the particle to be three hundred seconds and again assume the number of particles to generate as four hundred. In this optimisation test the

frequency at which the value of mixing efficiency is recorded is investigated. Figure 3.2 shows the property M against the time period of boundary oscillation, averaged for the number of slices, as M is cumulative. It is possible to observe that the characteristic peak is again observable here, and is located at the same point within the cascade irrespective of the number of slices taken, and once again the shape of the plot is consistent.

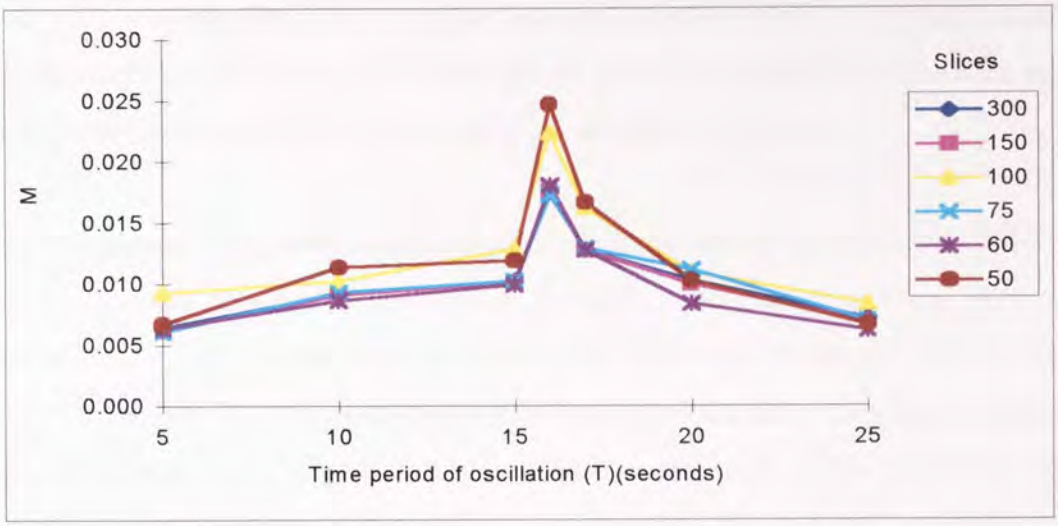

Figure 3.2. The mean mixing efficiency per time slice against time period of wall oscillation for the eccentric cylindrical system, for six different numbers of time slices taken over 300 seconds for 400 particles. (300 and 50 slices correspond to a slice every second, and six seconds respectively)

Finally in this group of variables to be optimised, the number of particle trajectories generated is investigated. The slice size and number of slices are both held constant at 1 slice per second for 300 seconds. From figure 3.3 it is possible to observe that the number of trajectories investigated has no significant affect on the form of the characteristic plot, all plots peak at approximately 16 seconds.

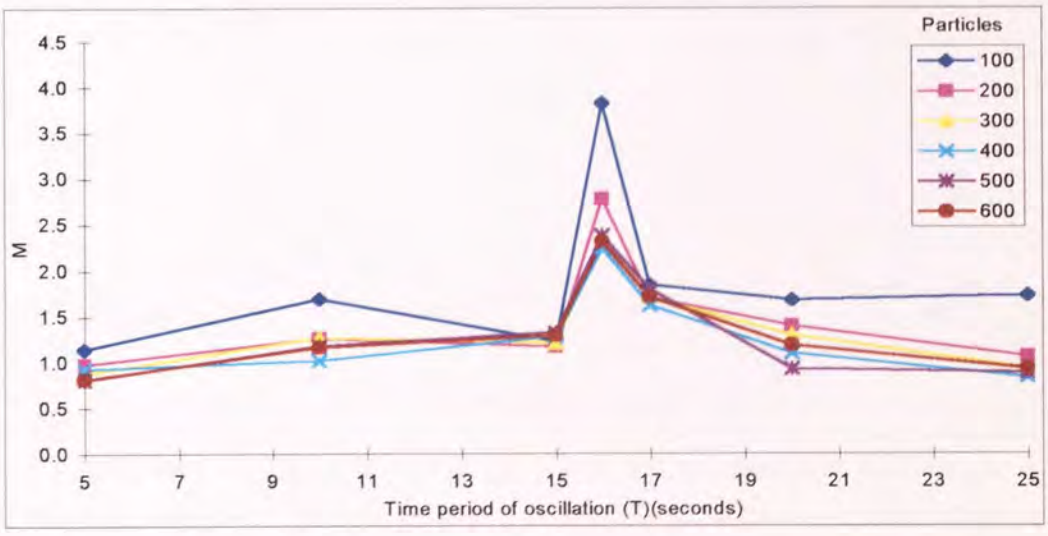

Figure 3.3. The time-averaged mean mixing efficiency against time period of wall oscillation for the eccentric cylindrical system, for six different numbers of particles with a time slice taken every second for 300 seconds.

The above optimisation of the variables used to generate the mixing efficiency property highlighted a characteristic peak. It should be noted that the value of the mixing efficiency property should not be taken as a qualitative measure of disorder. The interest of this work, at this stage, is the movement of various systems through the cascade. The peak is suggested to represent a significant point within a cascade. The work in this chapter is concerned with the movement of the peak. Therefore for the purposes of this work the optimisation results obtained above show that values of 300 seconds for particle evolution, 400 particles generated and one slice per second of sufficient accuracy for use in investigations.

3.3 Investigation of the two-dimensional rectangular cavity system.

The two-dimensional rectangular cavity flow domain is an ideal beginning point for any investigation of the effects of chaos on a particular property. Concepts derived from this simple system can then be developed towards utilisation within more complex systems.

The geometry, operating conditions and physical properties used in this system are identical to the initial system presented in the previous chapter. The form of wall oscillation and the entry of the boundary conditions and physical properties into Polyflow are also unchanged.

Using the instantaneous mixing efficiency to investigate the effect on disorder of varying the time period of oscillation yields significant information that could prove useful to the design of a chaotic mixer. The cavity system is operated with, U=26.9 mm/s, $\alpha=\pi/2$ over a range of increasing time periods from a low value. Figure 3.4 shows the mixing efficiency against time period of boundary oscillation. It can be seen that as the time period increases, the value of mixing efficiency rises to a peak suggesting maximum disorder, figure 3.4.

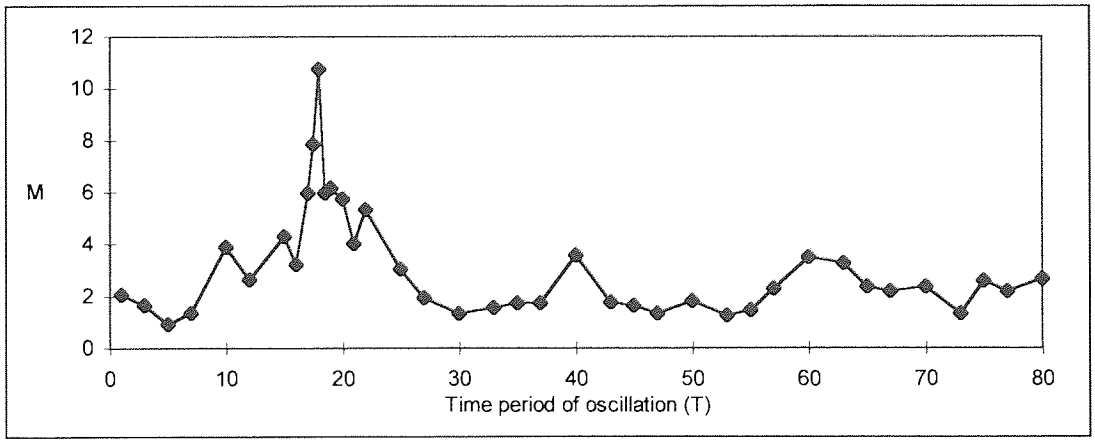

Figure 3.4. The instantaneous mixing efficiency for the two-dimensional rectangular cavity system at different values of time period of boundary oscillation, where the amplitude is 26.9 mm/s and phase difference between the upper and lower boundaries is $\pi/2$.

It can also be seen that after the peak the mixing efficiency falls rapidly as the time period increases further. Which may contradict instinct, as one would expect that once in chaos the system would remain in chaos, and hence the mixing would not significantly change.
Bryden and Brenner [52] also present a peak, corresponding to maximum disorder for their eccentric cylindrical system. They are unable to conclude a reason for the reduction due to uncertainty exhibited from observing Poincaré sections.
From the discussion in the previous chapter it may be possible to attempt an explanation for the changes in the degree of disorder throughout the time period range. The transition point at which order becomes chaos could be suggested to occur at the peak of maximum disorder in figure 3.4. One would expect, however, there to be an associated range of disorder around the peak that corresponds to the chaotic transition. The reduction in the degree of disorder past the peak, as T is increased further, may be due to particles remaining in one streamline for a considerable time before being displaced. This could have the effect of reducing the stochastic effect of the oscillations. The system may be considered to be behaving as many consecutive steady state conditions and not as an oscillating one.
In order to be able to design effective chaotic mixers, there must first be more relationships and theories developed for correlating chaos with operating conditions. It is by the detailed analysis of elementary geometries and systems that fluid behaviour within chaotic cascades and chaotic flow regimes can be more fully understood.

3.3.1 Effect of system properties on the cascade into chaos.

It has been shown above that it is possible to observe the cascade into chaos by the use of mixing efficiencies. The plot in figure 3.4 exhibits a characteristic peak within the transition into chaos. It is from observing this characteristic peak in similar plots, for differing conditions, that conclusions can be drawn as to the effect of varying system properties on chaos.

Amplitude of oscillation of the moving boundaries.

A cascade into chaos for this system can be caused by increasing the time period of oscillation, thus allowing particles more time to be displaced from their initial streamline. The effect of increasing the velocity amplitude on the chaotic cascade can be explained in a similar way to increasing the time period.
When the velocity amplitude is increased particles can move more distance in less time, and therefore do not require such a long time period to displace them from their initial streamlines. Thus the effect of increasing the velocity amplitude of the moving boundaries is to reduce the time period required to cause the transition into chaos. The point at which the

transition from order to chaos occurs is displaced to a lower time period as the velocity amplitude is increased. This can be observed from the mixing efficiency plots for varying velocity amplitudes, (figures 3.5).

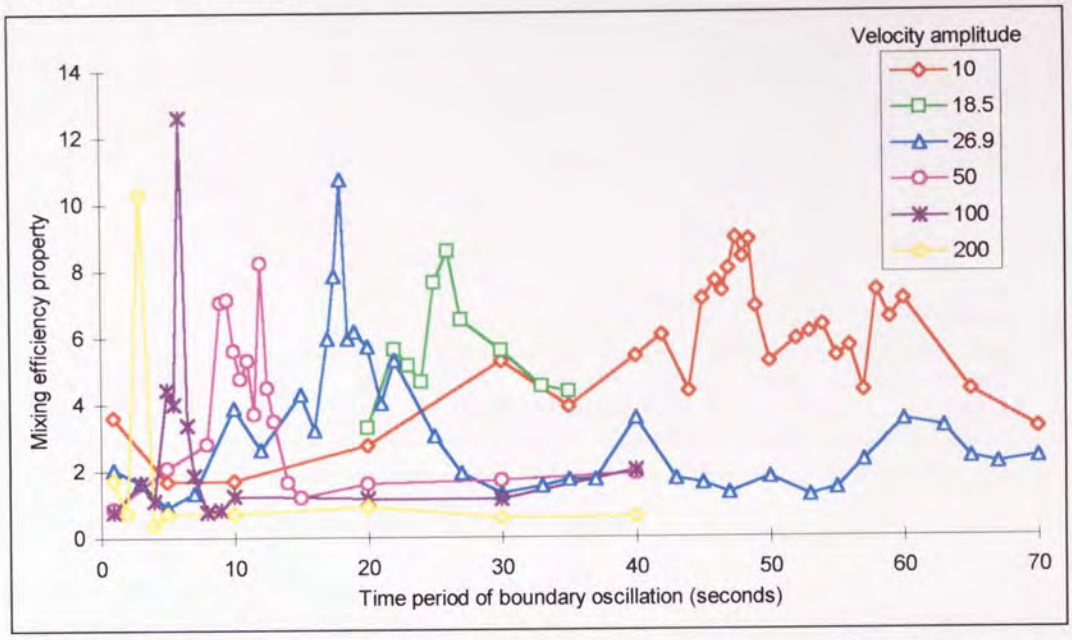

Figure 3.5. The instantaneous mixing efficiency for the two-dimensional rectangular cavity system at different values of time period of boundary oscillation, for six different values of boundary velocity amplitude, where phase difference between the upper and lower boundaries is $\pi/2$.

If the time period, at which the mixing efficiency property peaks is plotted against its associated velocity amplitude then the relationship between the time period and the velocity amplitude can be observed (figure 3.6). It can be seen that as the velocity amplitude increases the time period required to initiate chaos is reduced. As the velocity becomes sufficiently high the particles within the oscillating system travel sufficiently fast, that only a small oscillation of the boundaries is required to induce chaotic motion in the flow domain.

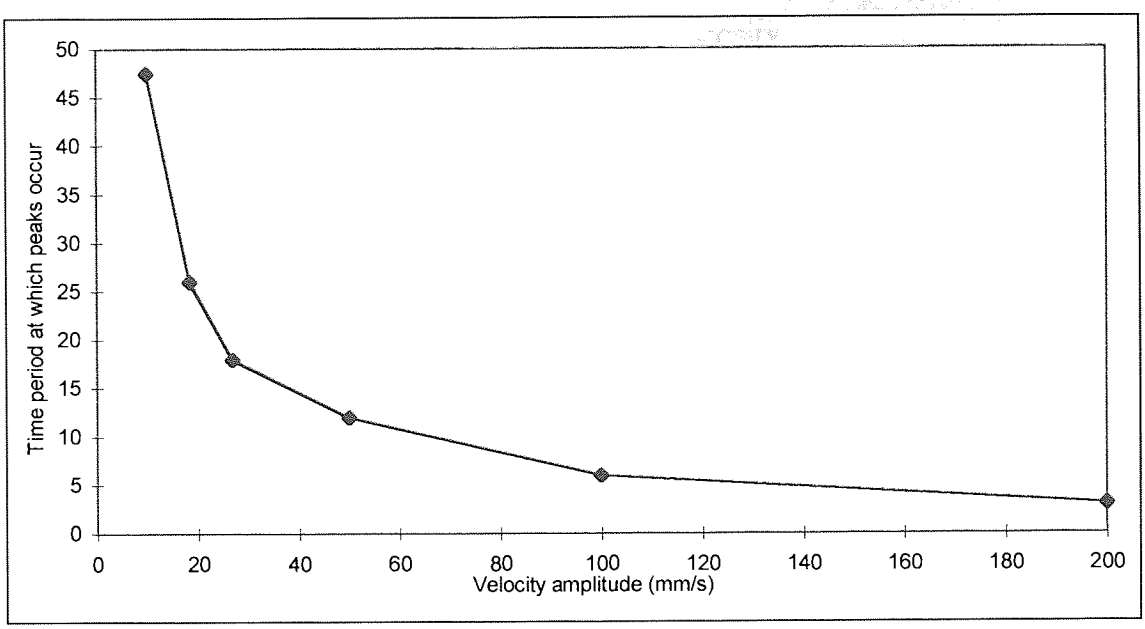

Figure 3.6. The relationship between the time period at which the characteristic peaks of the plots in figure 3.5 occur to the corresponding velocity amplitude of the boundaries.

As the curve in figure 3.6 is constructed from the mixing efficiency peaks then operating the system at a point on the curve would result in the optimum mixing efficiency. If the system is operated with boundary conditions above the curve then it will exhibit chaos although may contain some re-ordered behaviour. Boundary conditions under the curve will give oscillating or streamline motion. A plot of this nature would be useful for suggesting operating conditions for industrial equipment. It does not, however, suggest how stable the mixing efficiency value is likely to be at any point on the curve.

It can be seen, from figure 3.5 that as the velocity amplitude increases the base width of the peaks are reduced. This suggests that the band of high mixing efficiency, and therefore disorder, surrounding the transition is greater at lower velocity amplitudes. This has significance where a high mixing efficiency is required in a real processing system. The mixing efficiency would deviate less significantly from the optimum, if disturbed, when operating at low velocity amplitude. At high velocity amplitudes the peaks are sharp and a small deviation in the value of the time period would displace the system into low mixing efficiency regimes.

3.4 Investigation of the two-dimensional eccentric cylindrical system

3.4.1 System arrangement

The two dimensional eccentric circular system represents two cylinders, one, of radius r_i, inside another of radius r_o, with the centre of the inside cylinder being a distance e from the that of the outside one as shown in figure 3.7. The cylinders co-rotate with the fluid between

them assumed to be incompressible and have constant viscosity.

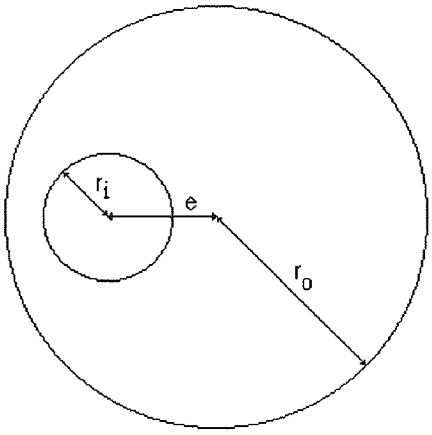

Figure 3.7. Pictorial representation of the two-dimensional eccentric cylindrical system, showing the radius of the inner and outer cylinders r_i and r_o respectively, and the value of eccentricity e between the two cylinders.

As with the rectangular cavity system the boundary velocity oscillation is made up of forty instantaneous flow simulations, in the from of equations 3.5 and 3.6.

$$u_{out} = U_{out} \sin^2 (\pi t / T_{out} + \alpha) \qquad (3.5)$$

$$u_{in} = U_{in} \sin^2 (\pi t / T_{in}) \qquad (3.6)$$

where u_{out} and u_{in} are the velocities of the outer and inner cylinders respectively, $U_{out} = U_{in} = U$ are the amplitudes of oscillation, $T_{out} = T_{in}$ are the time periods for outer and inner cylinders respectively, and α is the phase difference between the two cylinders, with $\alpha=\pi/2$.

3.4.2 Investigation of the two-dimensional eccentric cylindrical system.

In this section the observations and conclusions from the rectangular cavity are investigated and replicated for the eccentric cylindrical system.

It was shown previously that there are a range of conditions, that a system must be operated within, in order to induce stochastic motion. One such condition, investigated here, is the eccentricity of the two cylinders. In order to achieve chaos the particles in a laminar flow system must continue to be displaced from the instantaneous streamlines in which they reside. If the two cylinders are concentric, and co-rotating, then the resulting particle path for one cylinder rotating will be the same as for the other or both rotating. Although the distance travelled by the particle may alter. This is due to the instantaneous velocity vectors throughout the oscillation changing only in magnitude and not in direction. The effect being that the particles speed oscillates along the trajectory without it being able to leave its initial streamline, resulting in a similar trajectory plot as the steady state system, as can be seen in

figures 3.8 and 3.9.

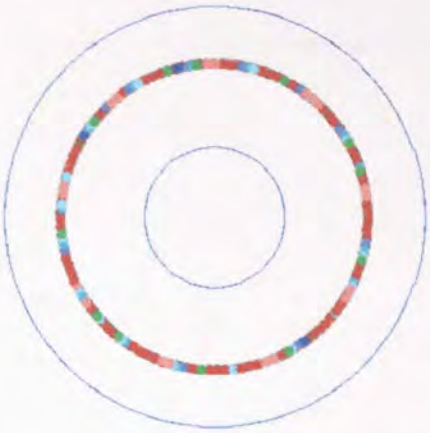

Figure 3.8

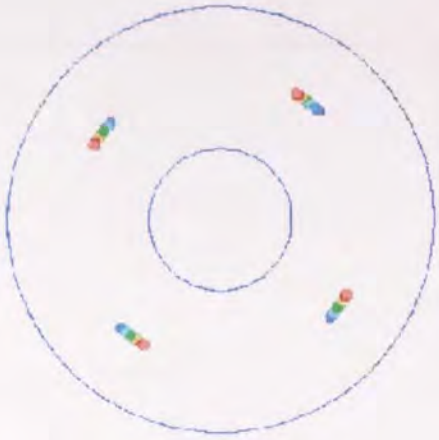

Figure 3.9

Particle trajectory generated from a time shot every one second for 500 seconds within a concentric cylindrical system, with r_i=50, r_o=150, showing that in the steady state case, figure 3.8, particles flow within one streamline. This result is comparable with the oscillating boundary case, figure 3.9, where U=π, α=π/2, T=20, which are conditions at which chaos occurs for eccentric conditions.

If the value of the eccentricity is increased it is possible to see that the instantaneous flow patterns change dramatically throughout one time period, (figures 3.10 a, b and c) the particles in the system are forced to leave their initial streamlines and chaos can then be induced.

Figure 3.10a

Figure 3.10b

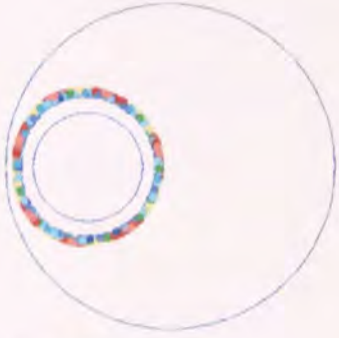

Figure 3.10c

Figure 3.10a-c. Particle trajectory for 500 seconds in the co-rotating cylindrical system where r_i=50, r_o=150, e=75, U=, α=π/2, where figure 3.10a highlights an instantaneous streamline corresponding to t=0, figure 3.10b corresponds to t=T/4=3T/4, and figure 3.10c corresponds to t=T/2.

Figure 3.11 shows the effect on disorder of varying the time period of oscillation when the co-current cylindrical system is operated with r_o=150, r_i=50, U=π, α=π/2, e=75. By use of the mixing efficiency property, M, it is possible to observe that its value rises to a peak indicating maximum disorder, as the time period increases, then fall rapidly as the time period increases

further. This compliments the observations from the rectangular cavity system, where a similar characteristic plot was achieved.

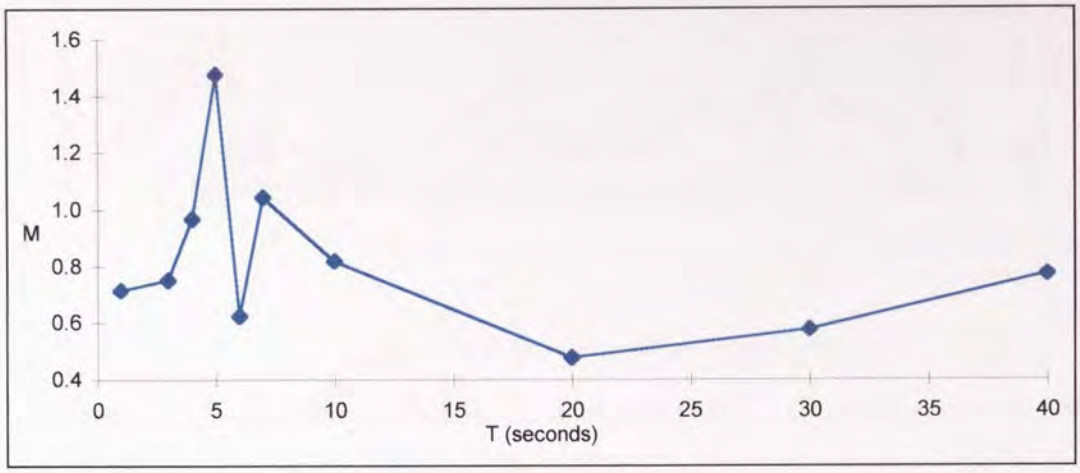

Figure 3.11. Mixing efficiency property (M) against the time period (T) for a co-rotating cylindrical system, where $U=\pi$, $\alpha=\pi/2$, $r_i=50$, $r_o=150$, $e=75$.

The characteristic plot can be confirmed by observations of particle trajectories. Figure 3.12a shows a single trajectory plot for 500 seconds of the eccentric circular system for a low time period. It can been seen that a particle placed at a point within the flow domain appears to return to that point, trapped within an apparently ordered streamline. If the time period is slightly increased, as in figure 3.12b, it is possible to see that the particle is beginning to oscillate back and forth between streamlines.

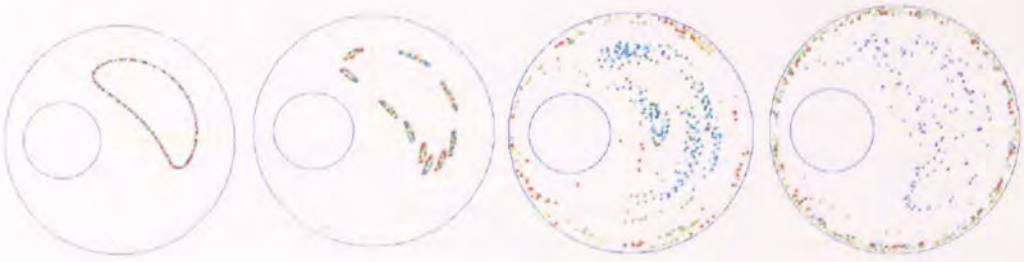

a b c d

Figure 3.12 a-d. Particle trajectory tracings for 500 seconds, with a time snap of one second, for a co-rotating cylindrical system, where $U=\pi$, $\alpha=\pi/2$, $r_i=50$, $r_o=150$, $e=75$. T is increasing, from T=0.2, T=2, T=5, T=20 respectively.

As the time period increases further the oscillations of the particle also increase, towards the point where the displacements of the particle are no longer able to 'cancel' each other out as an oscillation. In figure 3.12c, where the oscillations are significant the system appears to have gone through a transition to exhibit complete disorder, chaos.

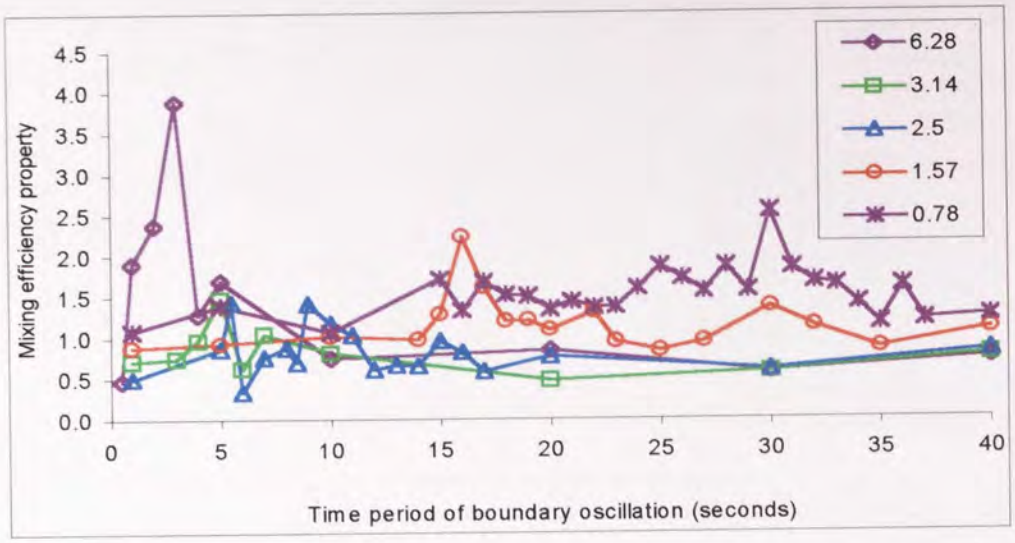

Figure 3.13. Mixing efficiency property (M) against the time period (T) for a co-rotating cylindrical system, where $\alpha=\pi/2$, $r_i=50$, $r_o=150$, $e=75$, for varying velocity amplitudes U, where U=6.28, 3.14, 2.50, 1.57, 0.78 mm/s.

Comparisons are evident between the effect of varying the boundary velocity amplitude for the rectangular cavity system and the velocity of the rotation for the cylindrical system. Again, as shown in figure 3.13, as the velocity amplitude is increased the time period required to enter chaos reduces.

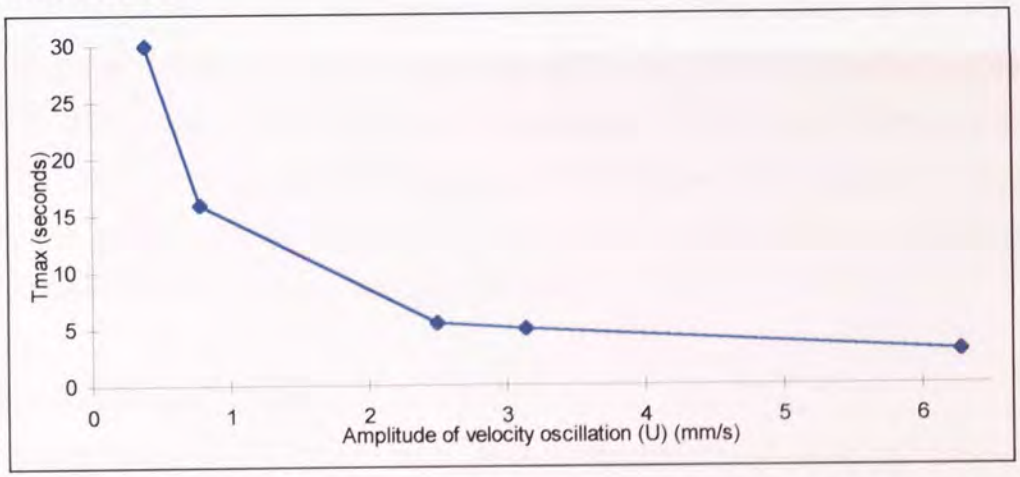

Figure 3.14. Time period at which M first peaks for a co-rotating cylindrical system, where, $\alpha=\pi/2$, $r_i=50$, $r_o=150$, $e=75$, against U, the velocity oscillation amplitude.

Figure 3.14 shows that it is possible to observe the same relationship between the time period at which the peak occurs, in figure 3.13, and the velocity amplitude of the boundaries, for the eccentric cylindrical system, as for the rectangular cavity (shown in figure 3.6.)

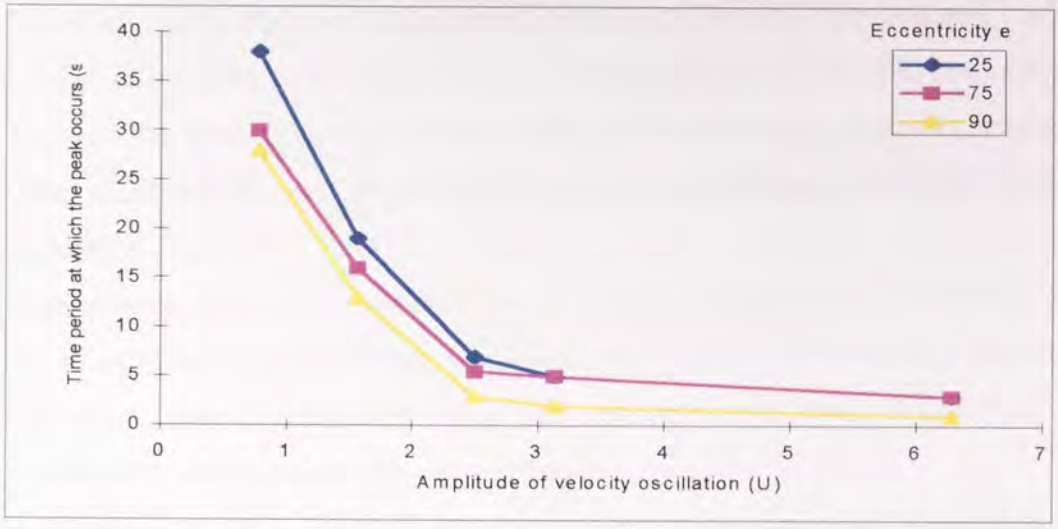

Figure 3.15. Time period at which peaks occur against the corresponding boundary velocity amplitude, for the co-rotating cylindrical system, where, $\alpha=\pi/2$, $r_i=50$, $r_o=150$, against U, for three differing values of e.(25,75, 90).

Figure 3.15 shows a comparison of the peaks of the mixing efficiency property to the velocity amplitudes over a range of eccentricities. Although only a small sample is investigated it is possible to observe that as the eccentricity is increased, the time period at which the transition occurs is reduced. A similar result is presented in [52] in which the transport enhancement, when operating within a chaotic regime, is shown to generally increase as the eccentricity is increased. The reduction in the time period required to produce chaos as the eccentricity increases can be explained in much the same way as for the effect of velocity amplitude and time period. The larger the eccentricity the greater the difference between the two instantaneous extremes of oscillation. The greater the difference between extreme streamlines the greater the ease of displacing particles from their initial streamlines, resulting in a reduction of the time period required to induce chaos.

3.5 Discussion and conclusions.

The work presented in this chapter is advancement into the investigation of chaotic mixing systems, which ultimately is seeking the development of innovative designs for effective process equipment. It is by the investigation of various boundary and operating conditions that concepts, theories and rules of thumb can be developed for equipment design and operating parameters.

Previous work has shown, both experimentally and numerically, that it is possible to induce chaotic motion into a laminar system by superimposing oscillating boundaries within a specific range. It has also been shown that there is a visible cascade from order into chaos as the time period of oscillation of the boundaries is increased. This chapter successfully observes the effects of varying system properties on the cascade by the use of the mixing efficiency property.

When observing both, the two dimensional rectangular cavity and eccentric cylindrical system, it can be seen that as the time period increases, through a cascade, the characteristic plot is formed. The plot appears to show the transition from order to chaos as indicated by a peak of the maximum value of the mixing efficiency property followed by what appears to be order restoring.

Both systems were found to be sensitive to the velocity amplitude of oscillation, with the transition point of the cascade moving to a lower time period as the velocity was increased. This leads to another characteristic curve that correlates the peak of maximum mixing efficiency property with varying velocity amplitude.

If curves similar to those in figures 3.6 and 3.14, were to be generated for industrial chaotic process equipment then the optimum blending within the system could be suggested through a simple correlation of operating parameter. This may be of importance if a fluid to be mixed is to have limited shear, for example, and therefore an enforced restriction on velocity, the corresponding time period for the boundaries to achieve optimum blending could be easily suggested.

In the eccentric cylindrical system it is found that if the extent of the difference in the extreme instantaneous flow patterns of oscillation is increased, by increasing the eccentricity of the cylinders, the time period required to induce chaos decreases. This is due to the increase in the severity of the variance in flow patterns during one time period, enhancing the displacement of particles from their initial streamline.

The results presented in this chapter are by no means definitive and at this stage should be taken as an indication of the flow behaviour within a chaotic cascade. It should be recognised that the use of the mixing efficiency property value for comparison between different chaotic systems is limited. This is due to the many approximations surrounding its generation limiting the use of the magnitude of mixing efficiency attained.

However the trends achieved from the mixing efficiency property have been shown to be transferable from one two-dimensional system to another. It is considered, though, that the property may not be universal for any other result than showing a qualitative characteristic peak within a cascade.

From particle trajectories generated after the peak it is possible to observe that disorder still remains. Instinctively one would suggest that systems cannot continue a cascade out of disorder, and it is suggested that the low value of mixing efficiency is due to the system acting as many consecutive steady state systems and not an oscillating one. A property that indicates the level of disorder past the transition into chaos should be sought.

The generation of a singular number for comparison with other systems in a range of operating parameters involves a large number of cumbersome assumptions and variables.

Access to how these assumptions are treated is not always available in commercial CFD. Also the property mixing efficiency is instantaneous. For mixing purposes it would be desirable to observe a property that would provide more information about the evolution of the mixing in a system. This would enable suggestions to be made surrounding residence times, and geometries of mixers.

In order extend our studies to be able to compare completely differing geometries and systems for their degree of disorder, a fully quantifiable property of the flow, which can be visualised throughout various cascades, must be developed and employed. Further chapters in this work consider the possibilities of a more universal property.

The generation of the mixing efficiency property relies on the commercial CFD post-processing and statistical tools. Certain information about exactly how the programmes interpret data, use models and make assumptions that is known only to the code creators. As a result, in the following chapters, the author presents properties of the mixing derived directly from the co-ordinates of the trajectories that are produced through specially designed codes.

Chapter 4. Using the separation of initially close particles to observe and quantify chaotic mixing .

4.1 Introduction.

The previous chapter showed that it was possible to observe a cascade towards chaos and the effect of various properties by the use of a parameter specific to the system. The trends presented were shown to be obtainable for two different two-dimensional domains. It is suggested here that a more universal property that lends itself more readily to comparisons for any range of operating or system parameters should be sought.

Earlier in this work the divergence of two initially close points in chaotic systems was discussed. The initial discovery of chaotic behaviour in non-linear systems by Edward Lorenz [5] was due to the observation of a divergence of solutions from two very similar positions. Sensitive dependence to initial conditions is noted to be one of the signatures of chaos [12].

It is with the divergence of initially close particles within a mixing domain that this chapter is concerned. The feasibility and consistency of using the divergence of initially close points with CFD techniques, as a measure of chaos, is investigated.

Recall that the two plots in figure 1.1 begin with a difference in initial conditions of 0.01%. Their initial positions diverge significantly so that they have completely no knowledge of each other whatsoever. We now consider that those two initial positions are two initially close particles in a fluid system. If, when operated under chaotic conditions, they diverge to a similar degree of disassociation then it follows that good mixing occurs. It is from this feature, of significant divergence, that a property of divergence can be developed.

There are assumptions and variable parameters that are required to be set for generating particle trajectories. The effect of these, on the observation and classification of the existence of chaos is considered, but the exact replication of trajectory co-ordinates is not necessary.

The emphasis away from the calculation of established dynamical tools, is partly due to limitations surrounding the software, but more significantly, the increased information available from considering the particle separation, and therefore the evolution of mixing. Unlike instantaneous properties, averaged over the range of the domain, observing the temporal evolution of distance of divergence of the particles as time evolves makes it is possible to suggest times for which satisfactory mixing takes place. Complete mixing can be suggested to be when the movements of particles, that where originally neighbours, bear absolutely no resemblance to each other.

This chapter investigates the divergence of the distance between samples of particles by calculating the distance between them at increments of time. The earlier sections are

concerned with the divergence of only two particles. The latter sections observe a more representative range of a number of particles originating from within a small area of generation.

This chapter develops a property relating to the divergence of the distance between originally close particles. The effect of the parameters and assumptions required to generate the property are investigated and optimised for consistency of conclusions. The property developed is then applied to more complex systems in the following chapters.

4.2 System configuration

The system used for these investigations is a two-dimensional cavity, with aspect ratio of unity, and sides of length 10mm. The top and bottom walls translate, in opposite directions, with an oscillation in a flip-flop motion. The two vertical walls are stationary. The moving walls have velocity amplitudes of 20 mm/s. The time period of oscillation is used as the parameter that initially controls the onset of chaos. The fluid and system properties are identical to those in the previous two chapters.

Two particles are generated at specified points close to each other within the flow domain, and their trajectory co-ordinates recorded at specific increments of time as the system evolves. Treatment of the data achieved yields values for the divergence of the distance between the two particles.

4.3 Observation of divergence of two initially close particles.

Edward Lorenz [5] first noticed the effects of chaos in computational analysis in his non-linear meteorological equations. He found that when repeating a test, with similar, but not identical initial conditions, dramatic differences in the results occurred. At first both results were similar, however, after a short evolution of time they began to diverge until they bore absolutely no resemblance to each other. This led to the conclusion of chaos present in non-linear equations and that a small difference in initial conditions can make a large difference in the solutions.

Divergence of initial conditions is a signature of chaos. Instead of observing two initially close points in a non-linear atmospheric system, here will observe two initially close particles in a non-linear mixing system.

The cavity system when operated with a time period of T=20 seconds and a velocity amplitude of 20mm/s, exhibits chaotic motion. It is possible to observe large divergences between two initially close particles. Figures 4.1a and 4.1b show two particles generated at points in the flow domain 0.001mm apart. When their trajectories are followed for the first

100 seconds it is possible to see that the two trajectories are similar, with the two particles remaining close.

Soon after, as shown in figures 4.2a and 4.2b the particle trajectories begin to diverge significantly. After 200 seconds it is possible to see that the two particles have began to follow different paths and are in different positions within the flow domain.

After particle lives of 1000 seconds it is possible to see in figures 4.3a and 4.3b that the two particles have indeed followed very different trajectory paths.

If two particles starting only 0.001 mm apart can evolve through significantly different trajectory paths, and separate to such an extent, then it must be concluded that this system is operating under chaotic conditions, and hence exhibits good mixing.

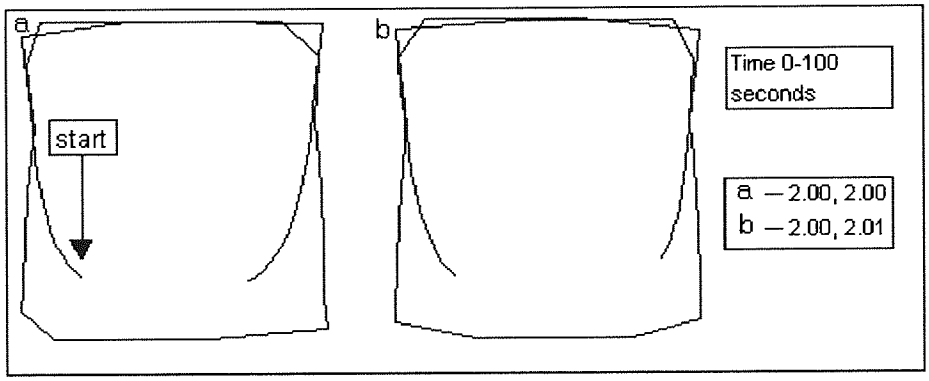

Figure 4.1. The two-dimensional square cavity, where the upper and lower walls translate with oscillating velocities in opposite directions. The time period of oscillation is 20 seconds with an amplitude of 20mm/s and out of phase by $\pi/2$. The two particles in figure 4.1a and b begin at a distance of 0.001mm apart. It can be seen that after 100 seconds that the particles have followed very similar trajectories.

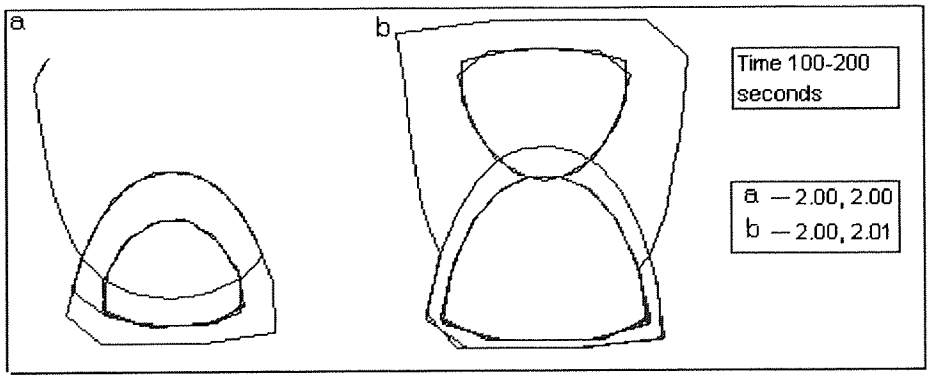

Figure 4.2. The trajectories of the same two particles as shown in figure 4.1a and b, between 100 and 200 seconds. It can now be seen that the distance between the particle is beginning to diverge as indicated by the significantly different trajectories shown.

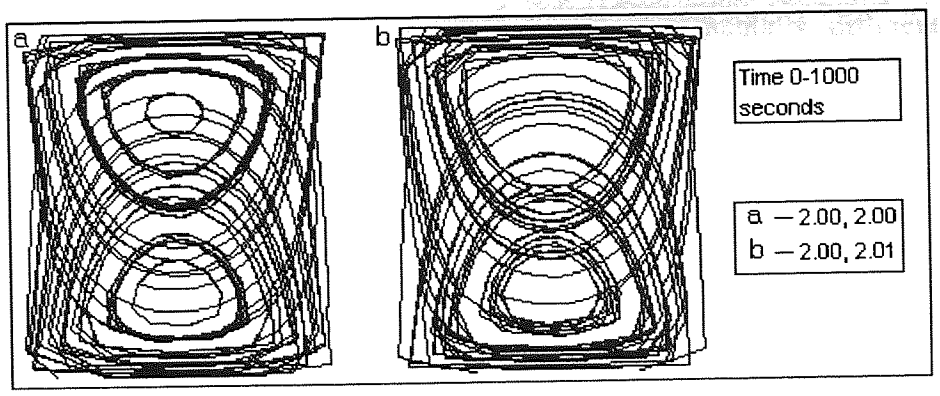

Figure 4.3. The complete trajectories for 1000 seconds of the same two particles as shown in figure 4.1a and b. It can clearly be seen that the particles have led completely unrelated lives, and their coming close together now is completely incidental. It should be noted though that both of the trajectories cover significant amounts of available domain space.

4.4 The investigation of the divergence of two particles generated at initially close positions in a fluid domain.

4.4.1 Generation of the trajectories and calculation of the distance between particles.

The trajectories of the particles are calculated by Polyflow as a mixing task, as described in chapter 2. This section will highlight and discuss the relevant parameters required by Polyflow for the calculation.

Parameters for the generation and evolution of the particles can be specified in the Polydata mixing task session. Particles can be generated at any specific point within the flow domain, they then evolve until the predetermined lifetime has been exceeded. The trajectory is stored by recording the particle position at regular intervals of time.

Two particles can then be generated initially close to each other, and their lives followed, recorded and investigated for the divergence of distance between them, thus enabling comparisons with systems operating under different boundary conditions.

Once two initially close particle trajectories have been generated, the distance between them can be calculated for each time interval by the use of the equation:

$$Z = ((x_1-x_2)^2 + (y_1-y_2)^2)^{½}$$

where Z is the distance between the two particles, x_1 and y_1 and x_2 and y_2 are the two-dimensional co-ordinates of the particles 1 and 2 respectively.

The value Z can then be plotted against time to enable an observation the distance between the two particles as time evolves. The plots of divergence between the particles can then be

used for comparison within a range of systems with incrementally different boundary conditions.

In the following section the divergence of the distance between two particles is used to investigate the cascade from order into chaos as the time period of oscillation is increased. The robustness of the property of divergence is then investigated and discussed.

4.4.2 Investigation of the cascade into chaos through a range of time periods of oscillation.

It is through observing the divergence of the distance between two particles that the variation of the degree of disorder throughout a chaotic cascade can be observed.

The rectangular cavity system, when oscillating with a low time period, as discussed in chapter two would appear, on a macroscopic scale, to act as a steady state system. This can be observed here. Figure 4.4 shows the distance between two particles originating 0.01 mm apart for a steady state system and in figure 4.5 for a time period of 1 second.

It is observed in both figures that the distance between the two particles oscillates. This corresponds to the particles moving apart as they flow around the 'corners' of their respective streamlines and being separated as they move around in an oval 'racetrack' fashion. The particles do appear to separate, although not to a considerable degree, as highlighted by the overall gradient of the plot. This small divergence can be accounted to laminar shear, and the velocity gradient reducing towards the centre of the domain.

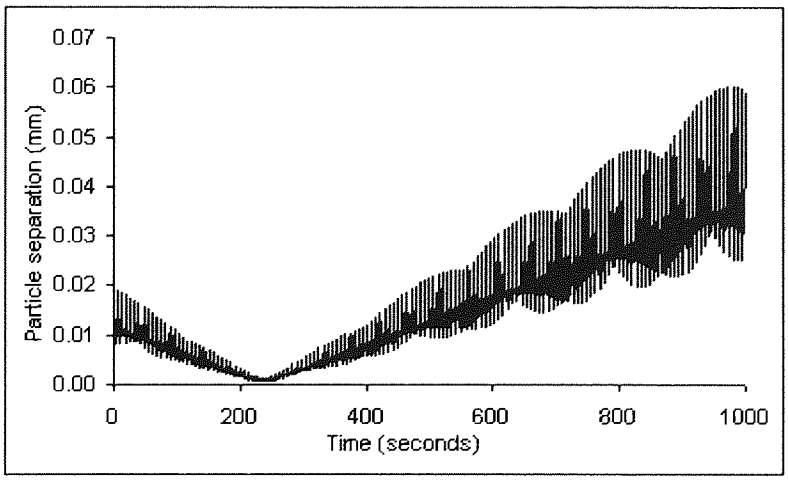

Figure 4.4. The divergence of the distance between two particles originating 0.01mm apart in the two dimensional square system, where the upper and lower walls are translating steadily in opposite directions with a velocity of 20mm/s.

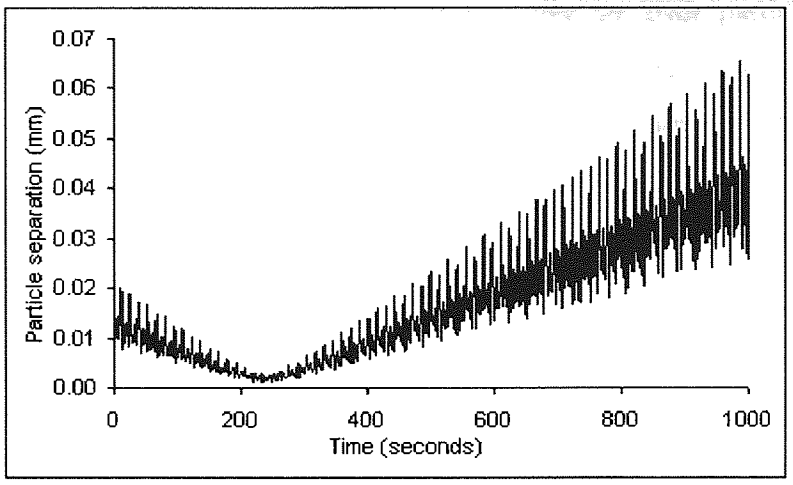

Figure 4.5. Two particles originating at the same positions in the same system as figure 4.4, except now both of the moving the walls velocities are oscillating with a time period of 1 second and an amplitude of 20mm/s.

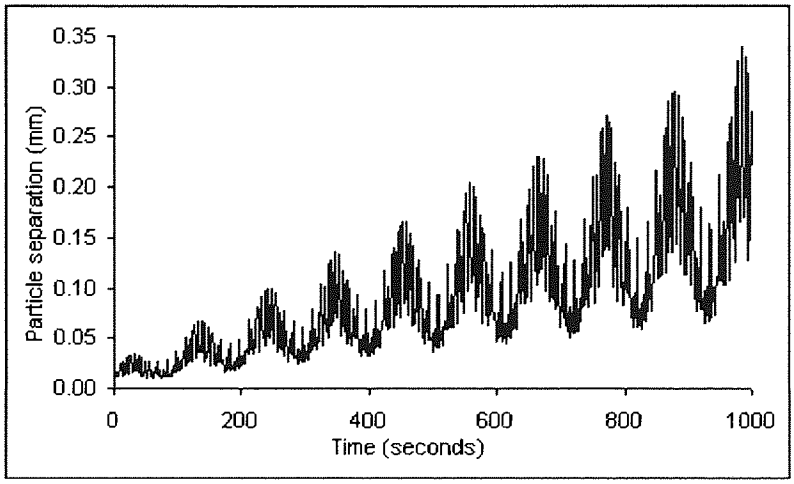

Figure 4.6. Exactly the same system configuration and placing of particles as the system in figure 4.5, except the time period of wall velocity oscillation in set at 3 seconds.

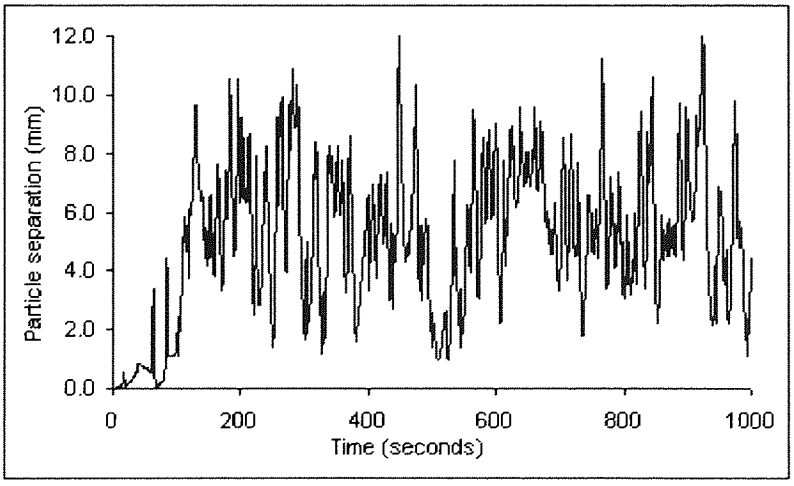

Figure 4.7. Exactly the same system configuration and placing of particles as the system in figure 4.5, except the time period of wall velocity oscillation in set at 20 seconds.

If we now increase the time period of oscillation, and hence move nearer to a chaotic regime it is possible to observe, in figure 4.6, where T=3, that the distance between the particles is

beginning to deviate from the steady state. This is due to both particles beginning to independently oscillate as they travel around the flow domain. The distance between the two particles after 1000 seconds is greater than for the lower time periods, but remains insignificant with respect to the magnitude of the flow domain.

Rapid growth of the distance between the two particles can be observed when the system is operating with a time period of T=20 seconds. Figure 4.7 shows that as time evolves the distance between the two particles becomes significantly large to suggest that the trajectories no longer bare any resemblance to their initial respective positions. The divergence of the distance between the particles to a point where the behaviour of the trajectories are no longer related can be concluded due to the rapid aperiodic alternations in the plot after the initial growth stage. The particles are now moving independently, the alternations correspond to the two particles happening to move closer or further apart as they continue their apparently unrelated evolutions.

As the plots of distance between particles against time rapidly alternate in chaotic regions there may be confusion when attempting to draw comparisons between systems with differing operating parameters. It is suggested that observing the maximum distance obtained between the two particles would provide an indication to the degree of disorder within a system. Figure 4.8 shows the maximum separation of two particles, originating within 0.01mm of each other, for a range of time periods of wall oscillation. The plot achieved is of a similar nature to those presented in chapter 3, for the mixing efficiency property. Here, however, the property lends itself, more naturally, to becoming a parameter to be used for comparisons. It can be seen in the figure that those systems that diverge do so to a similar degree. Once again there is an obvious transition between the ordered, and chaotic systems. However indications here show that once a system's time period cascade is such that it is sufficient to enter chaos it remains chaotic thereafter.

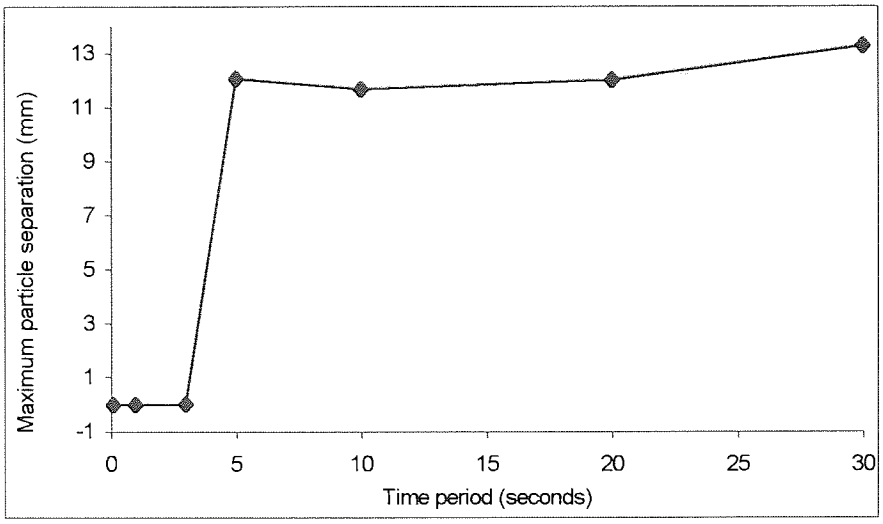

Figure 4.8. The maximum distance achieved between two particles originating 0.01mm apart in 1000 seconds within the two-dimensional square cavity with walls oscillating with amplitude of 20mm/s and varying time periods.

4.4.3 Investigation of assumptions and variables.

If the divergence of the distance between two particles were to be used for the quantification of mixing systems it would be essential to investigate how robust, with respect to the assumptions and parameters relating to its generation, the quantity is. Here the effects of the initial distance between the two particles, the position of particles within the domain and mesh density are investigated for a range of values. Each parameter is investigated in turn, whilst all others remain constant. Parameters not investigated are as described earlier.

Initial distance between the two particles (Z_0)

Until now this work has investigated two particles originating from two near positions within the domain at $(X_1, Y_1) = (2,2)$ and $(X_2, Y_2) = (2, 2.001)$, where the origin is the lower left corner, resulting in $Z=0.001$ mm at time $t=0$. This section investigates the effect that varying Z_0 has on the characteristic maximum value of separation presented in the previous section.

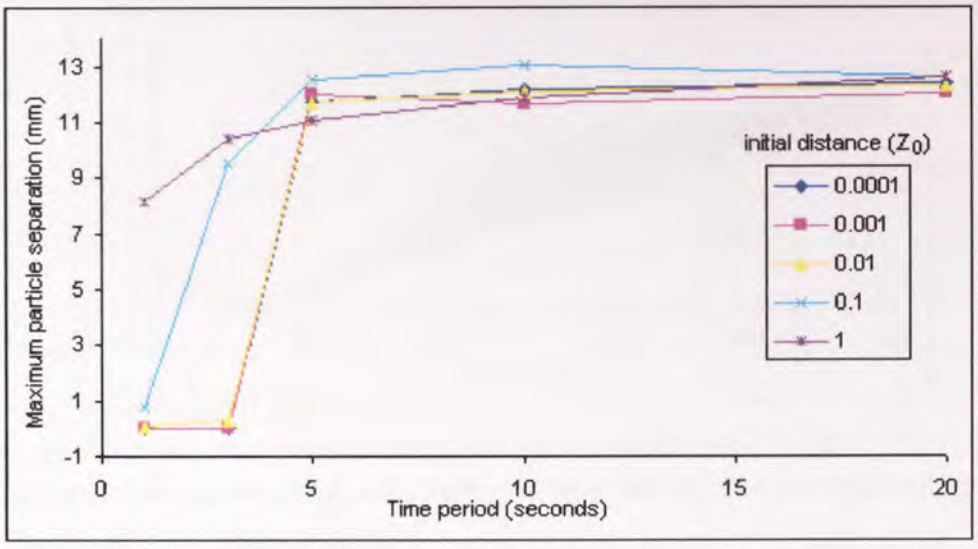

Figure 4.9. The maximum distances achieved between two particles over 1000 seconds within the two-dimensional square cavity with walls oscillating, with amplitude of 20mm/s, and varying time periods for 5 different values of Z_0.

Figure 4.9 shows the maximum separation against time period for five different values of Z_0, where co-ordinates for the two particles, from the lower left corner of the box, are (X_1, Y_1) = (2, 2) and (X_2, Y_2) = (2.0000, 2.0001) (2.000, 2.001), (2.00, 2.01), (2.0, 2.1) and (2, 3). From the figure it is possible to observe that systems that diverge do so to a similar value, this we might expect, as the domain is bounded, there is therefore a limit to the distance the particles can separate.

It can be seen that for initial distances of 0.01mm and below the form of the plot is similar. For larger initial distances it can be seen that the lower time period systems exhibit significant separation. It is suggested that this occurs due to the particles oscillating and originating sufficiently apart so that they unrelated from the outset. Figure 4.10 and 4.11 show the separation against time for two particles with an initial distance between then of 1mm, where time period is 1 and 20 seconds respectively.

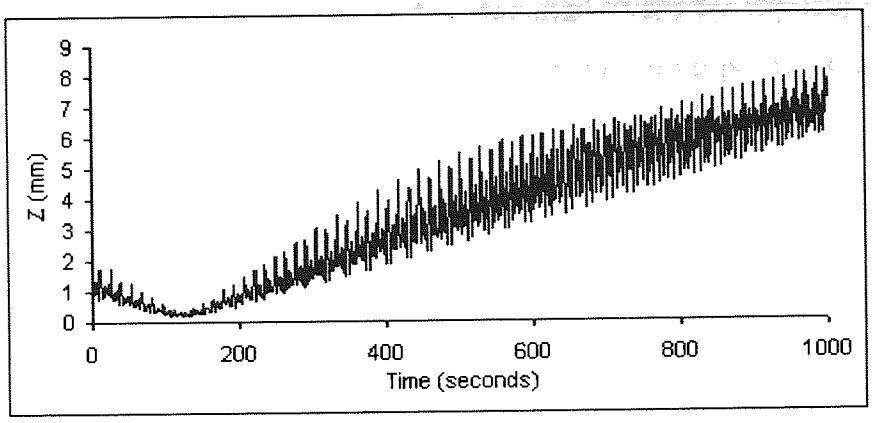

Figure 4.10. The divergence of the distance between two particles originating 1mm apart in the two-dimensional square system, where the upper and lower walls are translating in opposite directions with oscillating velocity of amplitude 20mm/s and a time period of 1 second.

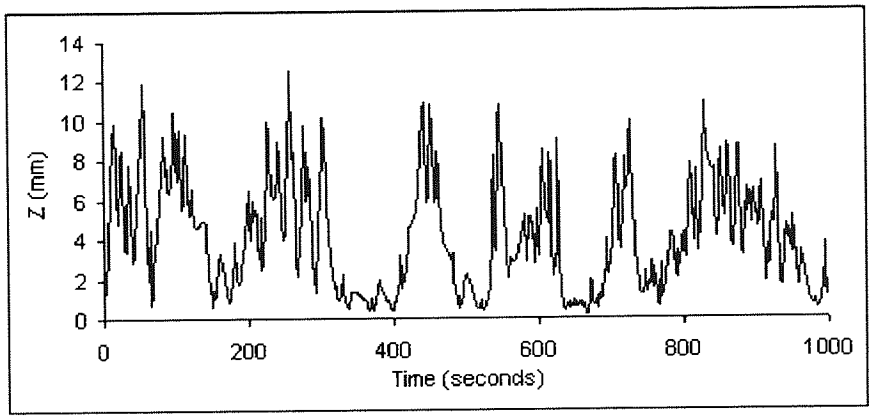

Figure 4.11. The divergence of the distance between two particles originating 1mm apart in the two-dimensional square system, where the upper and lower walls are translating in opposite directions with oscillating velocity of amplitude 20mm/s and a time period of 20 seconds.

Figure 4.9 suggests that where Z_0 = 1 mm, and T =1 second, the distance between the two particles diverges significantly which, by using the plot alone, could be mistaken as divergence due to chaotic motion. This is shown not to be true in figure 4.10. The distance between the particles does significantly increase, but the form of the relationship between the two particles does not appear to be chaotic. Whereas for Z_0 = 1 mm, T =20 seconds, shown figure 4.11, the relationship between the particles here is clearly aperiodic.

Two particles within systems exhibiting chaos will diverge to a large separation irrespective of their initial distance apart. The initial distance between particles within systems that do not exhibit chaotic motion must be very small if the divergence of the distance between particles is to be used to compare the form of the systems behaviour and disorder.

Careful selection of the initial distance is therefore required if one wishes to contrast systems of low disorder with chaotic ones.

Position of particle generation within the flow domain.

This section discusses and presents two particles originating from positions 0.001 mm apart from various positions within the flow domain. It is essential to have knowledge on whether the position that the object particles are being generated within has an affect on their divergence when considering the robustness of this method of investigation.

Figures 4.12 shows the maximum separation of two particles, throughout a time period cascade, generated from co-ordinates where (x_1, y_1) (x_2, y_2), are (1, 1) (1, 1.001), (2, 2) (2, 2.001), (3, 3) (3, 3.001), (4, 4) (4, 4.001) and (5, 5) (5, 5.001).

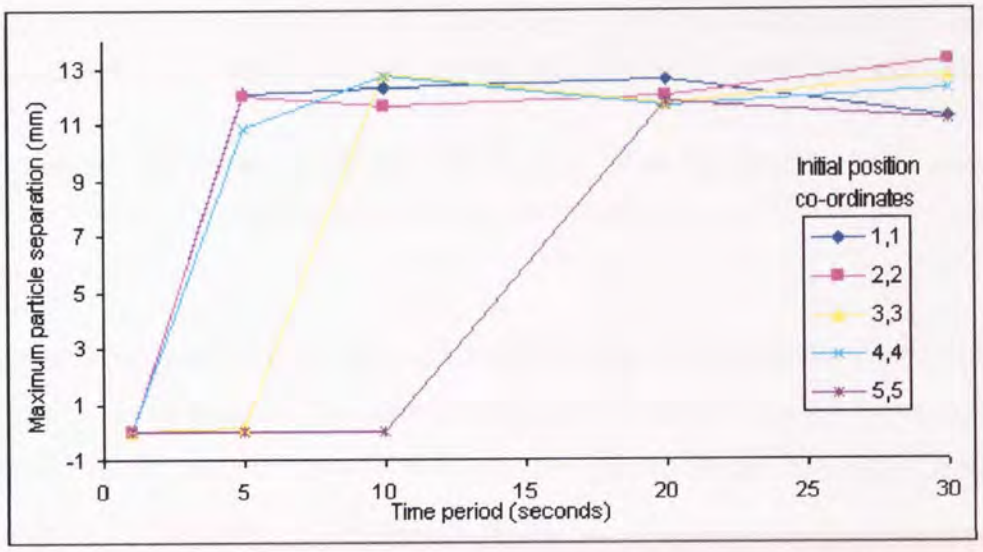

Figure 4.12. The maximum distances achieved between two particles, originating 0.001mm apart, over 1000 seconds within the two-dimensional square cavity with walls oscillating, with amplitude of 20mm/s, and varying time periods for six different initial positions within the domain.

Again it can be seen that there is a distinct difference between diverging and non-diverging systems. It can be seen that the plots relating to the different initial positions in figure 4.12 are significantly different. Not all pairs of particles show divergence at T=5 and 10 seconds. These results highlight a feature of chaotic systems. Regular regions are often present within a disordered flow regime.

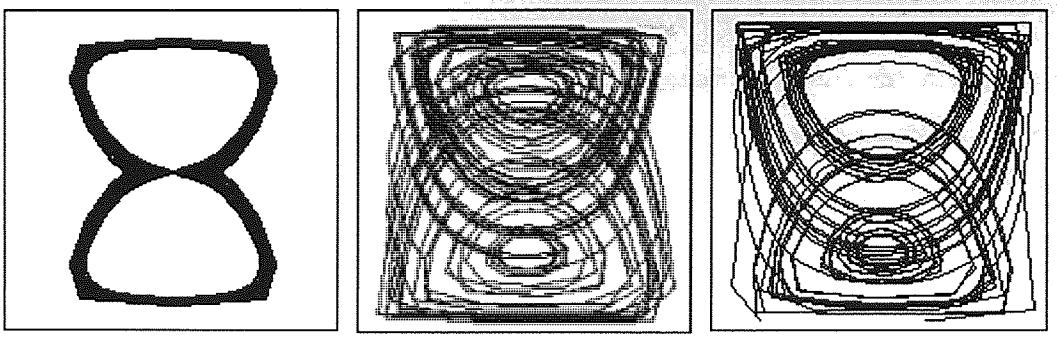

Figure 4.13. Trajectory plot of one particle for 1000 seconds, within the two-dimensional square cavity, originating in the centre at co-ordinates (5, 5) where velocity of wall oscillation is 20 mm/s and the time period oscillation is 10 seconds.

Figure 4.14. Trajectory plot of one particle for 1000 seconds, within the two-dimensional square cavity, originating at co-ordinates (4, 4) where velocity of wall oscillation is 20 mm/s and the time period oscillation is 10 seconds.

Figure 4.15. Trajectory plot of one particle for 1000 seconds, within the two-dimensional square cavity, originating at co-ordinates (5, 5) where velocity of wall oscillation is 20 mm/s and the time period oscillation is 20 seconds.

Figure 4.13 shows the trajectory for the particle originating at co-ordinates (x, y) =(5, 5), for the system where T= 10 seconds. The particle trajectory is clearly trapped within an ordered region of the flow. The system however is highly disordered, as can be seen in figure 4.14, where a particle is generated at co-ordinates (4, 4).

It was discussed in chapter one that there are regions of order in many chaotic systems, and that as the perturbations responsible for the disorder are increased more of the regular islands are destroyed and swamped by growing disordered regions. Figure 4.15 shows a particle trajectory originating at the same positions as the particles in figure 4.13, with a time period of oscillation of 20mm/s. The flow is all over the domain, and the presence of regular regions has been reduced. It could be suggested that the systems will eventuality exhibit divergence within the cascade, irrespective of the generation position of the particles, as the regular regions are destroyed. This can be seen in figure 4.12 where at T=20 all positions exhibit divergence

It can be suggested that he divergence of two particles is dependent on their initial position within the domain, but does not necessarily relate to the overall disorder of a system. Two particles separating can give an indication of the disorder within a system, but should not be used to generate conclusions alone. Careful selection of the position within a domain for the generation of particles is clearly important. Once a system cascade has entered 'full chaos' (i.e. no ordered regions) the origin of the trajectories is irrelevant.

Mesh density

As the method for quantifying the disorder in this chapter observes the distances between trajectory plots produced through CFD methods, it is could be considered important to examine the effect of the domain mesh density on the consistency of results. This section considers the divergence of the distance between two initially close particles, for a range of time periods, throughout a chaotic cascade for a range of mesh densities.

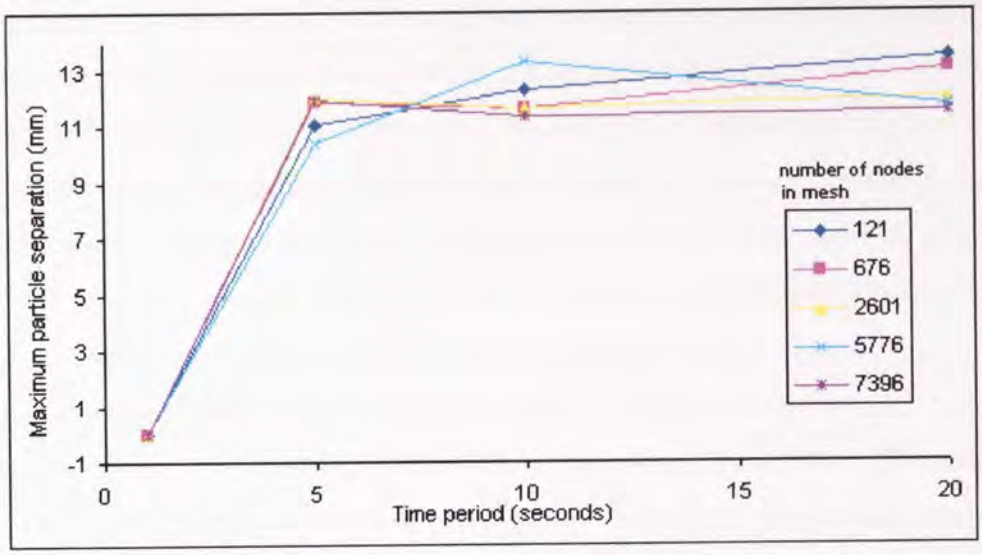

Figure 4.16. The maximum distances achieved between two particles, originating 0.001mm apart, over 1000 seconds within the two-dimensional square cavity with walls oscillating, with amplitude of 20mm/s, and varying time periods for five different domain mesh densities.

Figure 4.16 shows the maximum distance between two particles originating 0.001mm apart for a range of time periods, with each plot being generated from a domain of differing node density. The plots exhibit consistency, highlight the same features and have comparable magnitude, throughout the cascades. The systems operating with a low time period of 1 second do not diverge. Whereas systems with increased values of time period diverge significantly.

Figure 4.16 shows that within the apparently chaotic systems (T≥5 seconds) the maximum separations achieved are similar, but there is no exact convergence or consistency of values. This might be expected due to the nature of chaos. Small differences in the positions of particles will manifest into large divergences as time evolves. Altering the mesh density would change the number of calculations required to produce particle trajectories. One would therefore expect that within a chaotic regime, the identical replication of a trajectory would be impossible. A particle instead following the random path A, would now follow random path B. Both paths A and B are as random as each other, but pass through different co-ordinates. It would then follow that, as the maximum separation is derived from two random particles it

too would be random, and therefore subject to discrepancies, that do not alter the conclusion that chaotic motion exists. Also the systems that do not diverge significantly, where T= 1 second, show remarkable consistency in the maximum separation. The minute difference in co-ordinate data is not magnified significantly within the more ordered systems.

Overall the mesh density could be suggested to be of little consequence, although it would be intuitively thought that the more dense the mesh the more robust the solution.

4.5 Investigation of divergence of the distance between two particles –conclusion.

The above investigation and discussion of two particles shows that it is possible to investigate various characteristics of the flow through observing the separation of two particles. Observing the maximum separation of two particles over a set time can create characteristic plots that indicate the disorder of a system, throughout a cascade from order to chaos. These plots have been shown to produce visible contrasts between ordered and disordered regimes, especially when the initial distance between the two particles is small.

Particle pairs generated inside regular regions within disordered systems may not separate significantly, and hence yield a false indication of the systems disorder. However for all generation positions investigated, at some time period throughout the cascade, the particles pairs diverged.

The mesh density of the domain was found not to significantly affect the conclusions, from the plots obtained, throughout the cascade. It is noted however, that the separation of the particles, within disordered systems, is, due to the nature of chaos, likely to contain a random element. Although this is not expected to affect the conclusions or form of the cascade plots it does reduce the capability of making a comparison based on the magnitude of maximum separation.

It is suggested that the divergence of particles is a suitable method for investigating domains entering a cascade into chaos. Further development of this method attempts to reduce the effect of the particles random behaviour through observing a more representative sample.

4.6 Observing samples of particles originating from specified zones within the flow domain.

4.6.1 Introduce more sample particles.

By expanding the investigation of the divergence of two particles to a larger sample of particles, it is possible to achieve a more representative view of how a small 'block' or 'tracer blob' of particles will evolve under differing operating conditions throughout a cascade into

chaos. Particles are generated in a small zone within the flow domain and their positions recorded at set time intervals. Initially this section is concerned with four hundred particles, generated over a length of 0.2 mm, within the two-dimensional 'flip-flop' domain, described above.

Figures 4.17 a-d show the cascade from order into chaos by the spread of the particles originating from the small length, as time evolves. At a low time period, figure 4.17a, it can be seen that the blob stretches a little, but does not significantly deform. As the time period is increased, figure 4.17b, the particles begin to separate, and the line of particles, which can be termed a lamella, begins to bend. Within chaotic motion, figure 4.17c, it is possible to observe characteristic bending and folding of the line of particles, which has long been noted as a feature of chaos, by the presence of horseshoes in the flow [12].

In disordered systems the length of the particle lines increase more significantly as time evolves, than those in ordered systems. In this section the measurement of this length is developed into a quantifiable property the disorder.

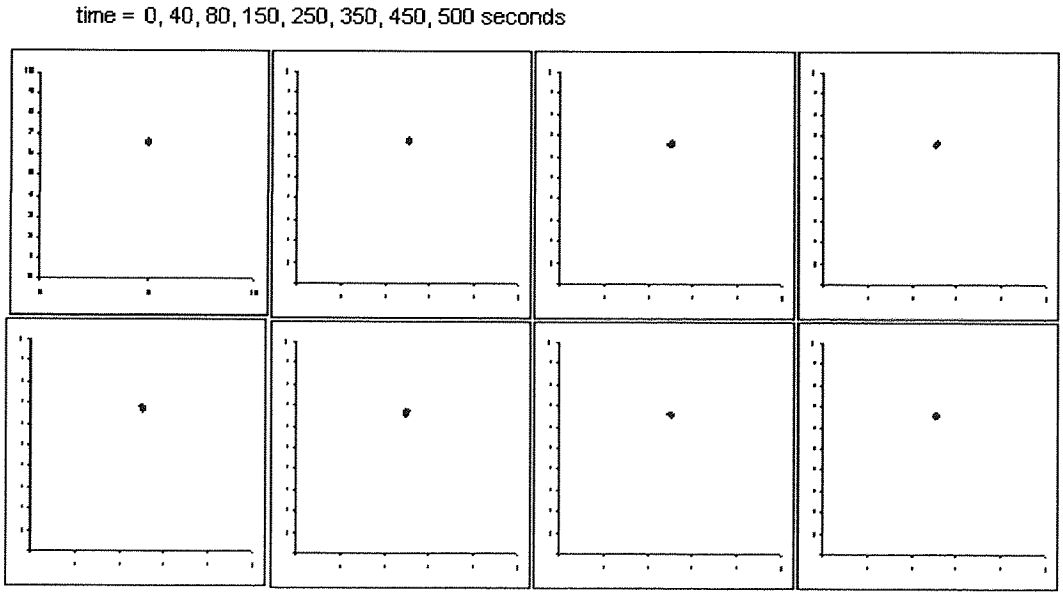

Figure 4.17a. Time snap-shots of 400 particles originating from a length of 0.2mm in the two-dimensional square cavity, with boundary velocity oscillating with a flip-flop motion with an amplitude of 20mm/s and a time period of 0.1 seconds.

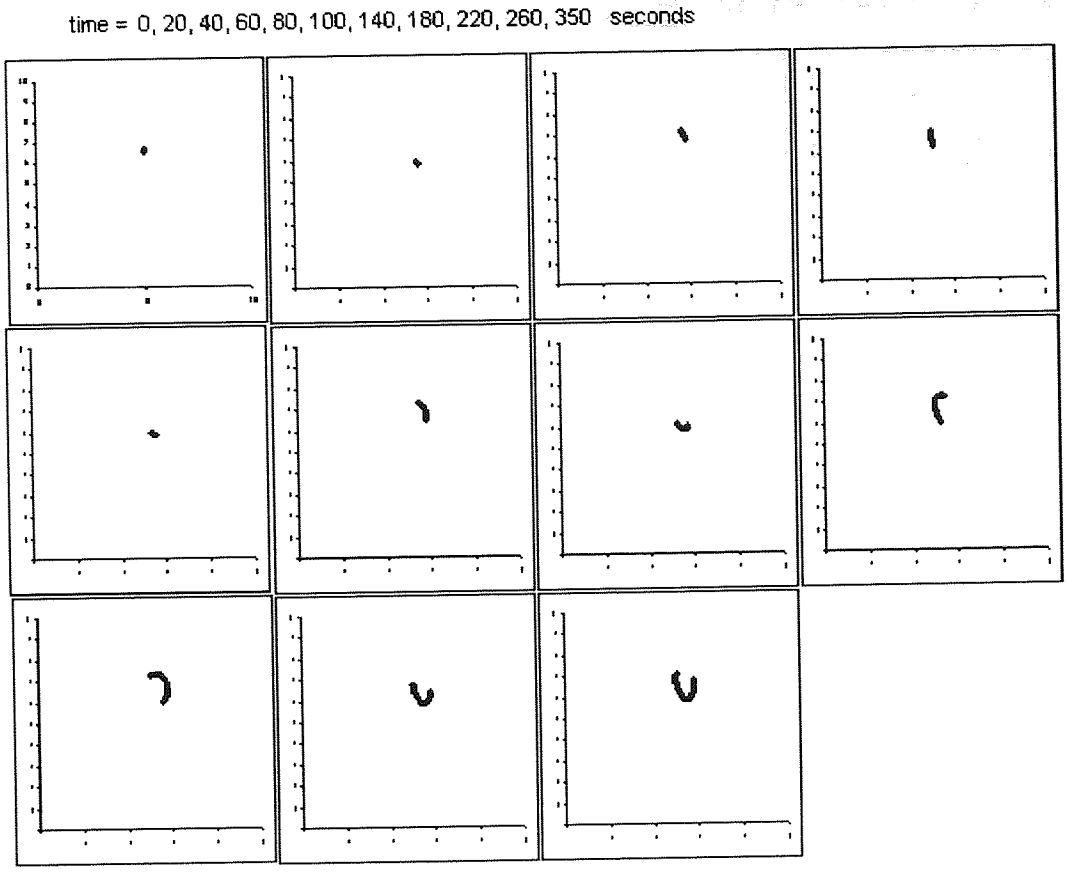

Figure 4.17b. Time snap-shots of 400 particles originating from a length of 0.2mm in the two-dimensional square cavity, with boundary velocity oscillating with a flip-flop motion with an amplitude of 20mm/s and a time period of 1 second.

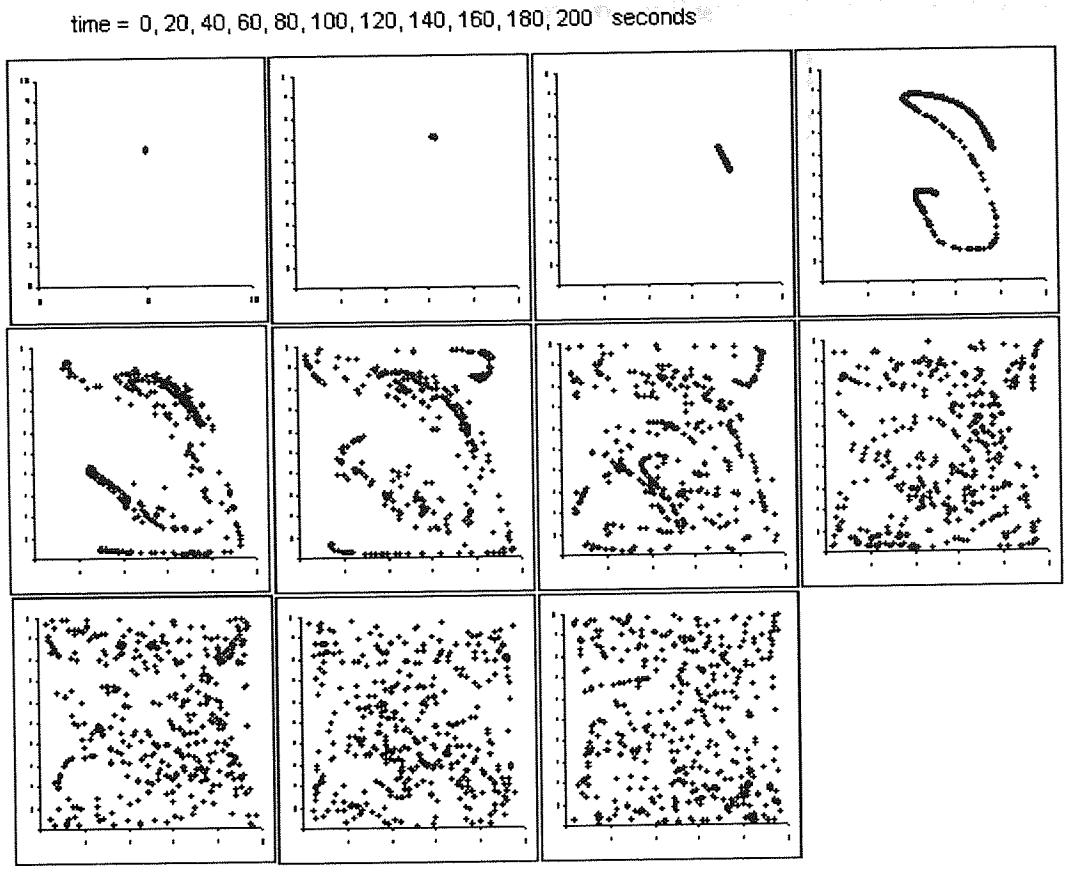

Figure 4.17c. Time snap-shots of 400 particles originating from a length of 0.2mm in the two-dimensional square cavity, with boundary velocity oscillating with a flip-flop motion with an amplitude of 20mm/s and a time period of 5 seconds.

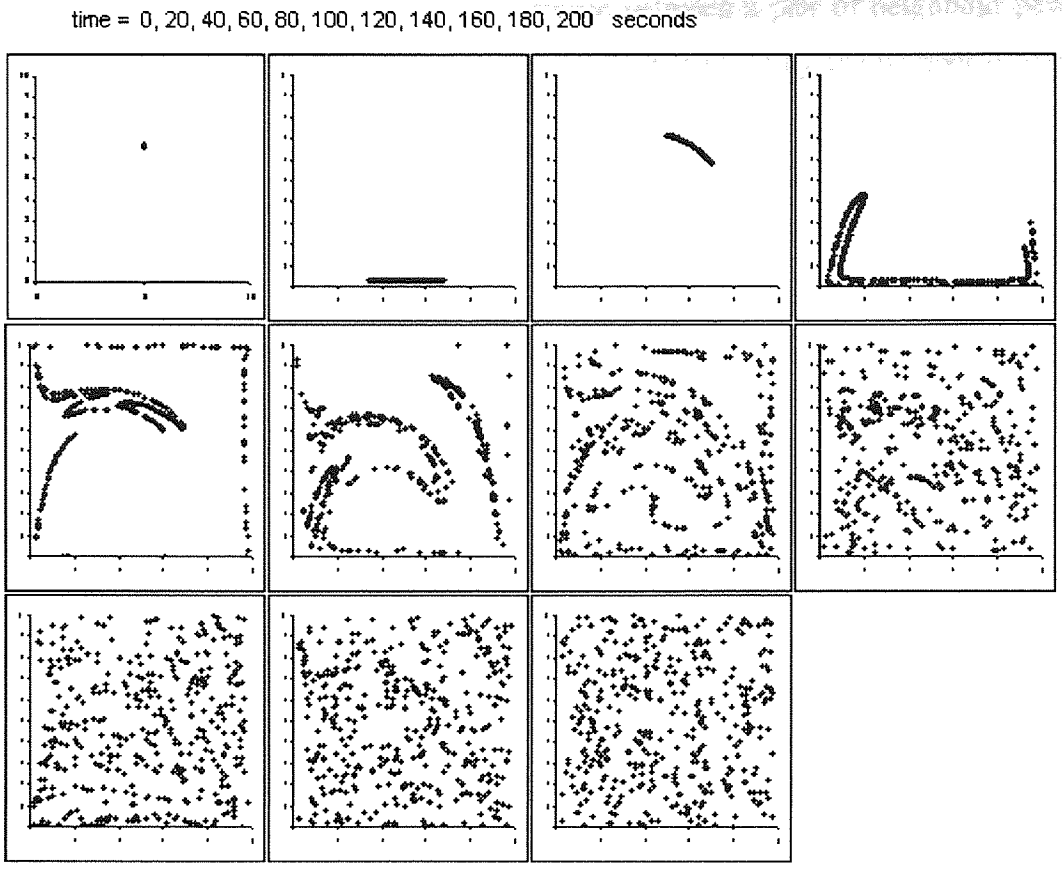

Figure 4.17d. Time snap-shots of 400 particles originating from a length of 0.2mm in the two-dimensional square cavity, with boundary velocity oscillating with a flip-flop motion with an amplitude of 20mm/s and a time period of 10 seconds.

4.6.2 Calculation of the Lamella Length.

To calculate the length of a lamella within the system we observe the divergence the distance between the sample of particles generated along a small line within the flow domain. By following this set of particles and recalculating the lamella length as time evolves it is hoped that quantitative information about the disorder within the system can be obtained.

The lamella length is the sum of the distances between each pair of originally neighbouring particles along the generation length. Many particles are randomly created on the original generation length (at time =0) and are sorted into order of position on the generation line. Each particle is assigned its two nearest adjacent particles as neighbour particles, except the two at the extremities of the generation length, that are only assigned one neighbour particle each. The distance between each particle and its neighbour particles is calculated, and summed to provide the length of the line of particles, represented by the equation:

$$\sum_{1}^{p-1} dp$$

where p is the particle number and dp is the distance between a pair of neighbour particles. From this property A can be defined as the lamella length divided by the number of particles (i.e. the average distance between all particle pairs)

Particle trajectories are generated by the use of a Polyflow mixing task. The corresponding co-ordinates for each particle tracked are tracked and processed to produce values for property A at each time increment. Property A against time is generated from the co-ordinate data by the use of the FORTRAN code presented, in annotated form, in appendix A.

4.6.3 Observing a cascade by the use of property A.

In this section the variations in disorder within the two-dimensional time periodic 'flip-flop' system, presented in the above sections is qualified by the use of property A. Figure 4.18 shows the plots of property A as time evolves, for various time periods throughout the cascade.

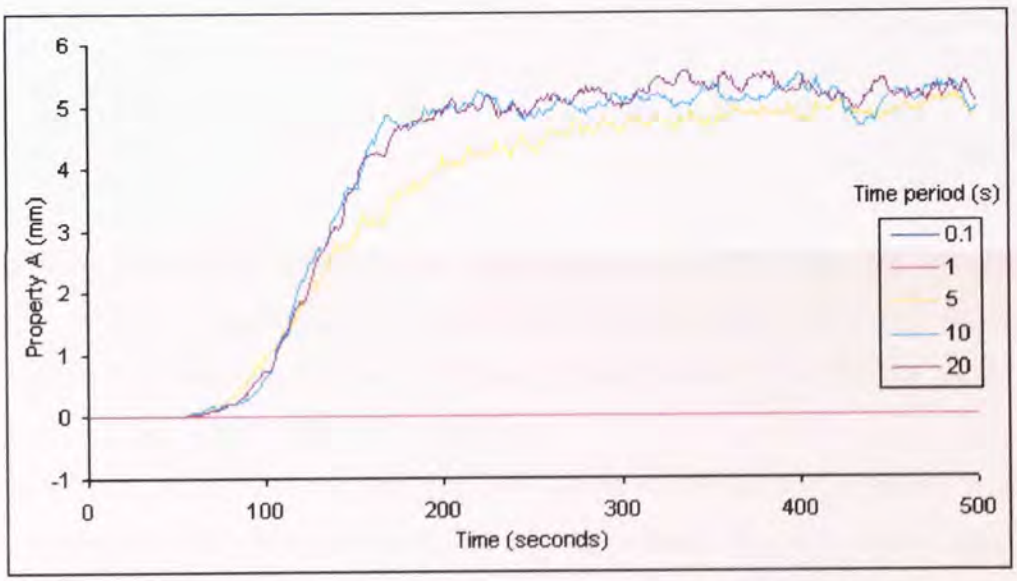

Figure 4.18. Property A against time for the two dimensional square cavity with boundary velocity oscillating in a flip-flop motion with an amplitude of 20mm/s and various time periods. 400 particles, initially generated over a length of 0.2mm, were used to create property A.

It is possible once again to observe that the divergence of the distance between particles increases as the time period of oscillation is increased, towards a chaotic regime, and that growth of the lamella length for a low disorder system is shown to be insignificant compared to the chaotic systems.

The value of property A for chaotic systems is initially low. This is followed by rapid divergence, to a levelling off point. From figure 4.17 d it can be seen that initially the lamella stretches, followed by folding movements. It is the continued folding and stretching within

the flow domain that induces exponential growth. The levelling off of the plot shows that the particles are now moving randomly and have no association to their initial neighbours.

The moving together of a pair of initially neighbouring particles is now a chance occurrence and has the same probability of happening as another pair of particles moving apart. Therefore the amount of separation viewed through property A levels off. At this point the property A can no longer be considered as a derivative of the length of a lamella, as the particles have become completely disassociated. Property A becomes the sum of the linear distances between many pairs of particles, which were once close.

The particles in the cavity separate to a bounded value, which one would expect to occur in a closed domain. This, however, leads one to consider what is the maximum, theoretical divergence obtainable.

In order to suggest such a value a slightly different method for calculating the average distance between particles is employed. Here the overall average distance between each particle and every other particle is calculated, and averaged for all particles, using:

$$\frac{1}{P}\left(\sum_{1}^{P}\left(\frac{1}{P-1}\left(\sum_{1}^{P-1} d_p\right)\right)\right) \qquad (4.1)$$

In considering methods for finding the maximum theoretical value for average particle separation, one could suggest that by calculating the average distance for a set of particles for every possible combination of particle positions would eventually reveal the maximum. This would, however, be exceedingly time consuming.

Therefore it is suggested that the uniform distribution of particles in a system would be the most homogeneous case, and undoubtedly, would certainly be well mixed. Although the uniform distribution does not yield the maximum value of the average distance between particles, as this occurs when groups of particles cluster in opposite corners. However this occurrence is unrealistic and therefore the uniform distribution of particles, as the most homogeneous, will be used for comparisons throughout this work.

Figure 4.19, using equation 4.1, shows how the uniform average distance between all particles varies for different numbers of particles within the two-dimensional system discussed above.

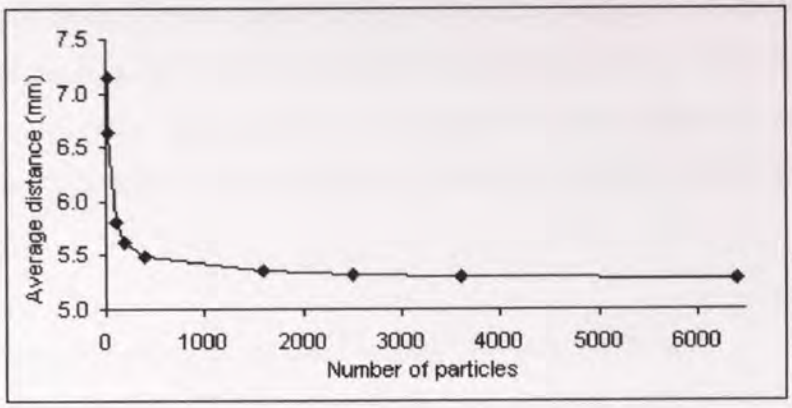

Figure 4.19. The average distance between particles against the number of particles in the calculation, for the two-dimensional square cavity of side length 10mm.

By comparing the maximum average distance between particles obtained through property A with the uniform average distance between particles, it would be possible to suggest the quality of the mixing that has taken place with respect to the size of the domain available for mixing.

4.6.4 Consistency and optimisation of conclusions from property A.

As with the investigations of the behaviour of two particles, the laminar length calculations involve many variables, this section considers the effect of such variables.

Based on the previous two particle investigations it is possible to suggest that as mesh density was found not have significant affect on the form of a trajectory for two particles, then there would be little reason why it should affect a larger number of particles.

The frequency at which property A is calculated as time evolves is not expected to have an effect of the value of the property. A system that exhibits disorder will do so whether it is observed once or a thousand times over the range evolution time. However if the system is observed more frequently then more information will be received about the rate of mixing throughout the systems operation.

A system that exhibits full chaos will diverge to a limiting value of average length, corresponding to the point at which the particles completely separate and begin to travel randomly all over the domain. The particles will diverge to this value irrespective of their initial spread, and the position within the domain of the generation zone. However, it was shown when considering just two particles that a large initial separation of particles makes it difficult to recognise whether systems are operating chaotically or not. It is recommended that a small initial separation between the particles be used to ensure that what is being observed is separation due to sensitive dependence of initial conditions.

Particles originating from a small generation zone in one position of a low disorder system may yield different divergence levels to particles from other positions. This is attributed to the presence of regions of order, throughout the domain, as noted in chapter 1 and section 4.4.3. Although particles will travel throughout all available domain within systems that are completely chaotic.

The number of particles of particles used to generate property A.

A variable in the generation of the property A that requires examining is the number of particles used in its generation. Figure 4.20 and 4.21 show property A generated from 20 and 400 particles respectively in the two-dimensional square cavity, where the upper and lower boundaries are oscillating in a flip-flop motion, with amplitude 20mm/s for a range of time periods.

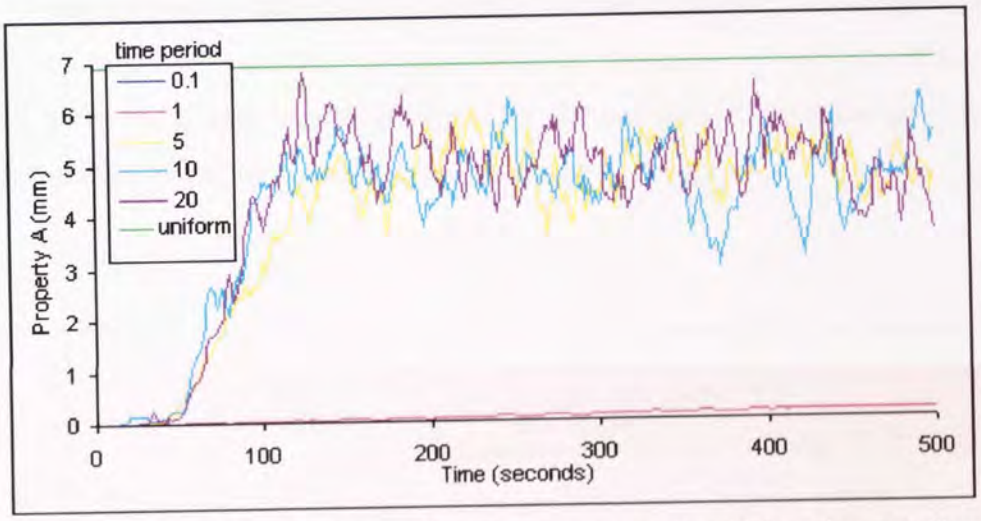

Figure 4.20. Property A against time for the two dimensional square cavity with boundary velocity oscillating in a flip-flop motion with an amplitude of 20mm/s and various time periods. 20 particles, initially generated over a length of 0.2mm, were used to generate property A.

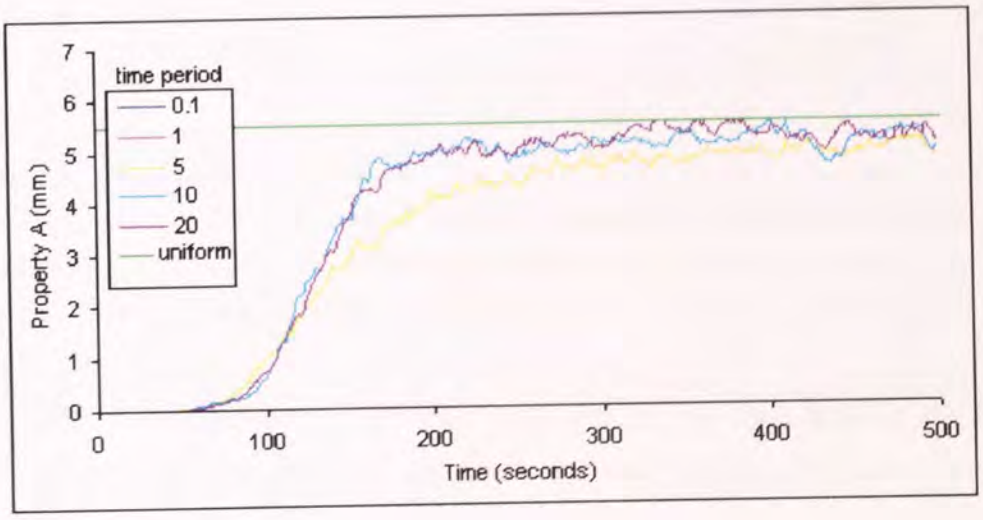

Figure 4.21. Property A against time for the two dimensional square cavity with boundary velocity oscillating in a flip-flop motion with an amplitude of 20mm/s and various time periods. 400 particles, initially generated over a length of 0.2mm, were used to generate property A.

It can be seen that both sets of plots exhibit similar behaviour. The systems that could be concluded to be chaotic by the plots in figure 4.21 could also be suggested to be chaotic based on the plots in figure 4.22. The significant differences between the two figures are, firstly that the magnitude of the maximum separation is greater where there is only twenty particles. This is expected as there is more space per particle in the system. The second significant difference between the plots is the degree of alternation of the plots in both the exponential growth and levelling off stages. The more particles that are present the smoother the curve, due to achieving a more representative view of the whole system.

Figure 4.22 uses the maximum value of property A to compare the cascade into chaos as the time period of boundary oscillation is increased for the same system containing different amounts of particles. It can clearly be seen that the number of particles used to generate property A does not affect the conclusion of chaotic or not chaotic.

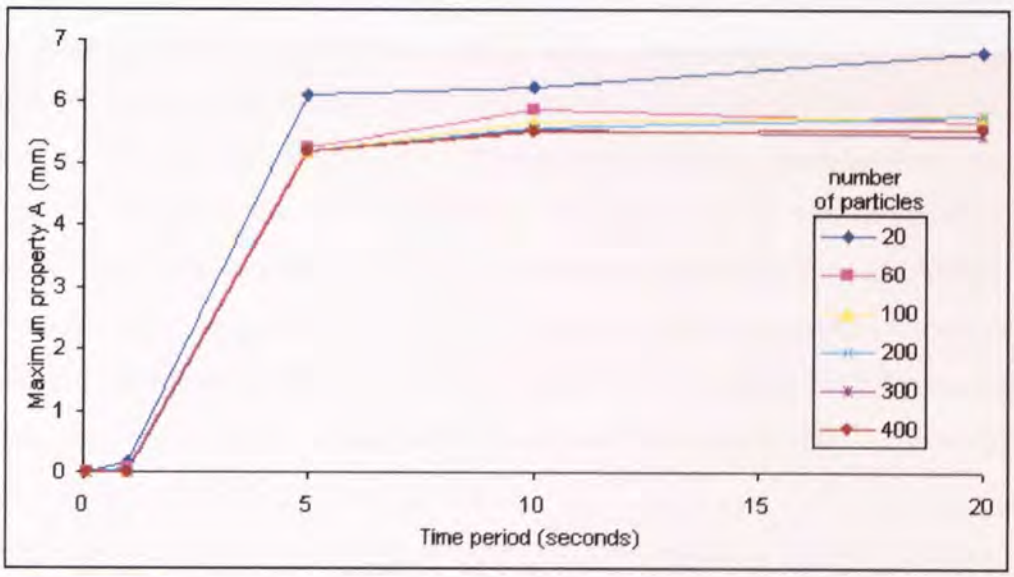

Figure 4.22. The maximum value of property A achieved, generated from six different amounts of particles originating over a 0.02mm length, over 500 seconds within the two-dimensional square cavity with walls oscillating, with amplitude of 20mm/s, and varying time periods.

It is suggested that the generation of property A, and its use for assessing the degree of disorder is robust when considering the variables associated with its generation. However the following will be observed where the property is used for the continuation of this work. The mesh of the system will be as dense a computationally possible. The generation length will be

small and of consistent length throughout ranges of control parameters. The position of the generation length will be situated in the middle of the upper half of the flow. The frequency of calculation of the property will be 1 second, so as to yield an informative plot. The number of particles used to calculate property A will be in the order of hundreds.

4.7 Discussion and conclusion.

This chapter has presented a method for quantifying the divergence of distance between particles, based on the fact that chaotic systems have sensitive dependence to initial conditions. Points that are initially close will diverge within a chaotic system. This phenomena was first investigated here though observations of two particles.

Cascades from order to chaos, similar to those presented in chapters two and three, where disorder in systems is induced through boundaries with oscillating velocities, were investigated using the separation of particles. Cascades from order into chaos have previously been shown to occur as the time period of oscillation is increased. The changes in the systems disorder can be observed by measuring the distance between two initially close particles as time evolves. The maximum distance obtained between two particles in a system, with particular operating parameters, can be compared with the same value from other systems within that parameter range to produce easy to view trends of a systems disorder throughout a cascade, although limited in the main to a conclusion of chaotic or not.

The reliability and robustness of using the divergence of the distance between two particles for quantitative analysis was investigated. It was found that the particles were required to originate sufficiently close if a contrast between order and disorder was to be achieved. The position of the two particles within the domain was found not to affect to conclusion of chaos in highly chaotic systems. However some of the particles were generated in areas of regular motion, and did not separate whilst other pairs of particles originating in different areas of the domain did. The density of the domain mesh used in the calculations did not affect being able to draw the conclusion of chaotic or not chaotic.

As the investigation of the separation of two particles appeared to yield meaningful and consistent results it was decided to investigate a more representative sample of particles originating from within a small generation area. Initially four hundred particles were considered.

Through plotting the positions of each of the 400 particles, at regular time snaps, it is possible to observe the disorder and form of motion within the systems. If the same is done for a range of time periods of boundary oscillation then it is possible to observe how the movements of particles differ throughout the cascade into chaos. At low time periods the particles remain close together. In a system where time period is increased the small 'blob' of particles begins

to stretch as time evolves. The stretched line of particles was termed a lamella. The lamella is then subjected to bending, folding and further stretching. The lamella will elongate and bend until it is so thin that it covers the majority of the domain, and can no longer be viewed as a lamella, but as many particles moving randomly.

Property A is defined as the average distance between initially neighbouring particles along the lamella. As time evolves and the lamella stretches the value of property A increases. The value reaches a levelling off point where the particles have completely separated, and no longer have a relationship with their original neighbours.

As with the investigations using two particles property A can be used to suggest whether as system is within chaotic conditions, or not. It can also be compared to the theoretical homogenised separation of particles, which is the average distance between each particle, with respect to every other particle, when the particles are uniformly distributed throughout the domain. This comparison enables a judgement on whether a system with chaotic motion is effective at mixing, or does it exhibit significant areas of order.

The number of particles used to generate property A was investigated and it was found that the conclusion of chaotic or not was not altered. However it would be desirable to use as many particles as computational hardware allows, to achieve a representative sample and to smooth the plots of property A against time

In the present chapter the disorder in a chaotic system has been classified by the divergence of many particles that originate from a small section of the flow domain. Whereas in chapter three the observations throughout the cascade were conducted by a property derived from the instantaneous mixing efficiency. Both properties allow us to suggest that at low time periods of boundary oscillation the disorder in the system is low and that as time period is increased chaos occurs. The mixing efficiency property, however, would indicate that order restoring exists after chaos initially occurs, whereas the property of divergence would suggest continued high levels of disorder. Plots of particles evolving in the region of the discrepancy would suggest order restoring does not occur, and as the divergence of initial points is a feature of chaos, one would be inclined to rely on property A more.

The differences can be accounted for if we consider that the instantaneous mixing efficiency is derived from the rate of stretching. Systems with high degrees of disorder and rapid bending would produce high rates of stretching. This is what is observed as a system enters chaos at the lowest time period possible (possibly corresponding to the peak.) As the time period increases the systems remain in one streamline for increased periods of time. For the majority of the time they exist as steady state systems, and steady state streamline flows exhibit low stretching, therefore the instantaneous time-averaged values are also low.

Property A measures the evolution of the particles, and their behaviour with respect to their initial orientation.

As the concern of mixing is separation and homogenisation of particles the divergence of particles, as measured by property A will be used further to quantify the mixing in the investigations of more complex systems in further chapters. Property A has been shown to produce reliable and robust conclusions concerning the disorder of systems, but care must be taken in selecting the initial conditions and positions of particles and the parameters for it generation.

Chapter 5. Chaotic mixing in a four different three-dimensional domains

5.1 Introduction.

The previous chapter discussed the generation of property A as a measure of the disorder within a system through quantifying the divergence of the distance between a sample of initially close trajectories. This chapter considers the implications of amending property A for investigating three-dimensional systems and then uses this property to examine four different chaotic systems.

The first system presented is a closed cubic domain exhibiting two walls with boundary movements that are time periodic and perpendicular to each other. The three other systems have a throughput of fluid with wall movements perpendicular to the flow, where the cascades into chaotic motion rely on the periodicity of boundary movements, wall configuration or geometry. For each of these four systems it is possible to observe a cascade from order towards chaotic motion as control and other parameters are varied.

5.2 Three-dimensional chaotic mixing

Investigations of chaotic systems in this work have so far been limited to two-dimensional domains. There is less accepted work concerned with three-dimensional chaos, and only a few of these are concerned with time periodic domains. One such work is Anderson et al [89] their work discussed the extension of methods for locating and classifying periodic points within three-dimensional cavity flows. Kusch and Ottino also presented three-dimensional time dependent boundary systems [90]. Their experimental results, with supporting computational analysis, showed an eccentric helical annular mixer, where both the inner and outer walls are time dependent. They presented similar analysis for the partitioned pipe mixer. Khakar et al [91] also considered the partitioned pipe mixer, work that motivated investigations into the comparisons of Poincare maps and residence time distributions in a similar system by Mezic et al [92]. Investigations by the use of commercial CFD into the Kenics mixer have been carried out by Avalosse, [43] and with an accompanying discussion on chaotic flow by Hobbs and Muzzio [93]. There is interest in other mixing devices that also contain no moving parts. Jones et al [94] present chaotic motion within laminar flow in a twisted pipe. By the use of Poincare maps, stretching of material lines and disassociation of tracer blobs they show how differing degree of disorder can be induced by alterations in the geometry of the twisted pipe alone. The increased stirring does not require additional energy, and is noted to be fundamentally different to the transition from laminar to turbulent regimes, as it is a kinematical effect. This work was later extended [95] with the inclusion of diffusive tracers.

Dombre et al [96] presented a three-dimensional system operating chaotically within specific parameters of the ABC (Arnold, Beltrami, Childress) flows. They opened their paper with the comment 'Three-dimensional steady flows with simple Eulerian representation can have a chaotic Lagrangian structure. By this we mean that infinitesimally close fluid particles following the streamlines may separate exponentially in time, while remaining in a bounded domain, and that individual streamlines may appear to fill entire regions of space.' They showed how this occurs due to the presence of 'principle' vortices, and observe regions chaotic motion and islands of stability by the use of a number of Poincare sections, spread equidistantly throughout the domain, recording intersections with streamlines. Another work showing regular and chaotic regions is that of Fountain et al [97]. They presented experimental and supporting computational results for a cylindrical rotating mixer containing an angled impeller that creates a secondary flow. Whilst Cartwright et al presented biaxial unsteady spherical Couette flow in an incompressible fluid [98].

Ottino et al [99] provided a review of chaotic mixing processes and discuss issues surrounding both two- and three-dimensional flows. They included a brief discussion of duct flows [100] with the addition of spatial periodicity, examples being the partitioned pipe and Kenics mixers. They also discussed the improvement of cavity throughput flows by the use of a fixed corrugated baffle that alters the geometry available for flow. This was then likened to the construction of a single screw extruder device. They concluded by encouraging engineers to 'adapt and modify what is already available or to develop new concepts and ideas.' And indeed other authors have also found the potential for chaotic mixing in existing process equipment. Kim and Kwon [40, 41] used chaos in traditional polymer industry equipment to develop the 'chaos screw.'

Investigations containing the third dimension are becoming increasingly feasible with the advent of more powerful computational hardware and more sophisticated software. Many of the concepts developed in simple two-dimensional geometries are transferable to simple three-dimensional geometries. Research into chaotic mixing appears to be fast becoming more practical, with real applications for industry being considered.

Previous authors work, discussed above, show that chaos can be induced into three-dimensional time periodic, or steady systems. The steady systems can involve no moving parts (twisted pipe and Kenics mixer,) steady boundaries (ABC flows) or spatial boundaries within duct flows (partitioned pipe mixer, chaos screw.)

5.3 Introduction to the three-dimensional investigation.

Cascades into chaos occur due to varying control parameters associated with alternating streamlines. Until this point the control parameter has been time dependent. The alternating

streamline motion is caused due to either a smooth oscillation or flip-flop of the movement of two boundaries. In this chapter both time dependent and independent motion is considered. The first of the four systems presented is a closed domain, whilst the other three include a throughput of material, with boundary motion perpendicular to the flow.

The closed system is a time dependent cubic system with two opposing walls that translate perpendicularly in an oscillating 'flip-flop' manner. The flow generated is then three-dimensional. The time period of the walls is considered as the main control parameter, although the velocity amplitude is also considered. The first of the three throughput domains exhibits time periodic top and bottom boundaries and can be considered to be as many two-dimensional cavities, as described in earlier chapters, placed back to back. The throughput is perpendicular to the boundary movement. The moving boundaries in the following two throughput systems are time independent. One initiates the onset of chaos by the use of spatial periodicity, and the other, by what will be termed here for differentiation between systems, as geometric periodicity. As fluid moves through the domains it is subjected to differing cross-sectional streamline motions. The spatial and geometric periodic systems could be considered as many two dimensional systems within periodic cells where half of each cell is rotated by 180^{o} or offset respectively.

5.4 Three-dimensional chaotic systems, issues.

The generation of the particle trajectory plot data within three-dimensional systems is much the same as for the two-dimensional systems described in earlier chapters. The code for the calculation of property A require amending to include the z co-ordinates (annotated in appendix B.)

The inclusion of the third dimension severely increases the number of nodes required in a domain mesh, and therefore hardware limits the maximum number available, thus resulting in a low mesh node density. As a result particle trajectories that come too near to a wall boundary often stagnate. This, if undetected, could have the affect of producing misleading results for the property of divergence of the distance between the particles. Property A is generated by the calculation of the overall average distance between consecutive pairs of object particles. If some particles stagnate at walls their co-ordinates will remain constant for the duration of the time evolution, this could produce a false and large value for divergence. Conversely if many particles stagnate before they have had sufficient time to diverge, then a small value of divergence would be observed. Therefore if stagnated particles are present in the calculation of property A the result achieved could be anywhere between the two extremes. Therefore it is imperative that the effect of stagnating particles be removed from calculations. In this work two methods are used to achieve this.

The first is available both within Polyflow and the code for the generation of the property of divergence. Parameters can be set to detect when a particle has stagnated. If this occurs and is recognised within the trajectory calculation in Polyflow then after the stored trajectory data a zero is recorded. When the code for calculating property A reads the zero the trajectory is automatically removed. There also exists within the code a tolerance on successive co-ordinate data. If the co-ordinate of one particle is sufficiently close to that of one ten time steps previous then the trajectory is rejected (this is explained further in appendix B.) This does however mean that if a specific number of particles are required throughout a series of investigations then the regeneration of particles to replace those that have stagnated will incur more computational time. It would however be suggested that if a high percentage of particles stagnate then the value of property A achieved is not a representative sample of all particles. In chaotic systems particles are encouraged to travel around the whole domain, and this includes regions near the walls. It is likely then that many particles will stagnate, thus leaving only the particles that did not travel near to the walls for use in the property of divergence calculation. The property will therefore be representative only of particles that did not travel near to a wall. It would then be recommended that this method of investigation be used only where small numbers of stagnating particles are concerned.

The second method for removing stagnating particles, from calculations is to grade the mesh to create smaller volumes near to the wall boundaries. It is found that altering the mesh grade does not affect the conclusions that can be drawn through observing property A throughout a cascade.

As it is inevitable that stagnation of particles will occur it is important to not the view the property of divergence alone. The validity of the resulting divergence value can be suggested after observing the plots of the particles positions as they move throughout the domains. By observing a sample of individual trajectories one can suggest the reliability of conclusions and account for any spurious results.

The systems in this section will not be subjected to optimisation for consistency of the property of divergence, as in the previous chapter. It is suggested that the optimisation conducted for two-dimensions showed that the property is not significantly sensitive to parameters surrounding its generation.

5.5 Three-dimensional closed domain with time periodic boundaries.

The three-dimensional closed domain could be considered as a cube with a pair of opposite walls translating perpendicularly with a flip-flop periodic motion. Each edge is of side length 10mm, the moving walls are indicated by shading in figure 5.1. Wall 1 translates in the

positive X direction, whilst wall 2 translates in the positive Z direction. The wall movements in turn cause rotations in the flow that induce a three dimensional flow of the particles.

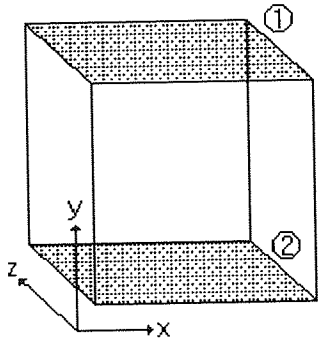

Figure 5.1. The three-dimensional closed cubic domain. The shaded numbered surfaces indicate the two walls that translate perpendicularly to each other with a flip-flop motion.

The control parameter here is considered to be the time period of operation of the moving walls. The effect of the wall velocity amplitude is also considered.

Two methods of analysis are used to observe the system to indicate the disorder throughout cascades into chaotic motion. The first, presented here for only one velocity amplitude, observes the spread of particles from a small generation zone as time evolves. Whilst the second method quantifies the spread of initially close particles by the use of property A.

5.5.1 Separation of particles in the time periodic closed mixing domain, pictorial.

It was discussed in the previous chapter that one signature of chaos is the presence of sensitivity dependence to initial conditions. In this section the evolution of 200 initially close trajectories is observed. Figure 5.2 shows the initial the particles which are generated at random within a zone of length of 0.2mm. The position of each particle is subsequently recorded at intervals of time and shown, in figures 5.3-5.5, for the system with a wall velocity of 2mm/s at values of time period of wall oscillation of 0.5, 5 and 20 seconds respectively.

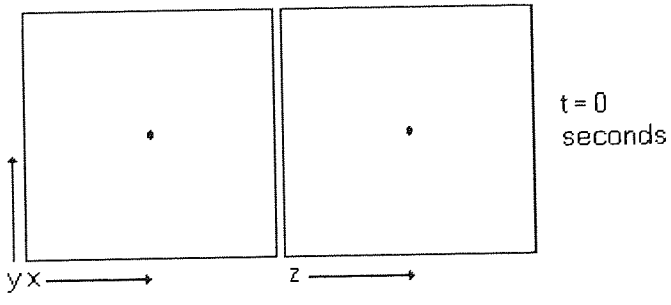

Figure 5.2. Cross sections of the initial positions of 200 particle trajectories within a small generation zone in the closed three-dimensional time periodic domain.

It can be seen that the system, for all time periods, given sufficient time exhibits significant separation of the two hundred initially close particles. Although it should be noted that for the small time periods the separation occurs after a considerable amount of time.

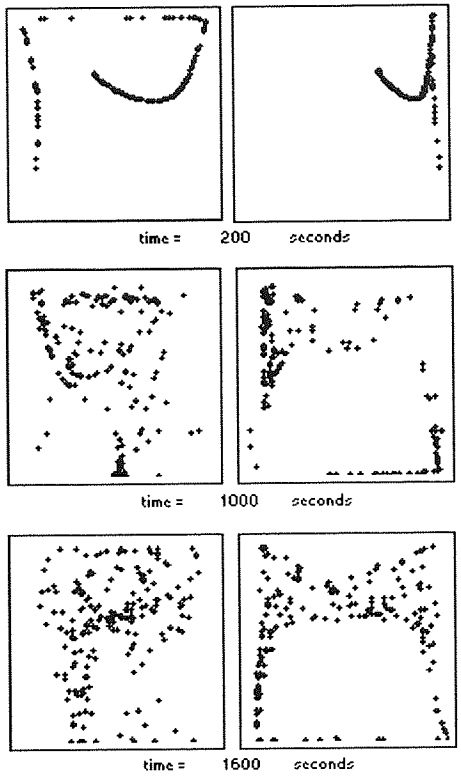

Figure 5.3, xy and yz views showing the positions of 200 originally near particle trajectories in the closed three-dimensional time periodic domain, at various times where the wall velocity amplitude is 2 mm/s, and the time period is 0.5 seconds.

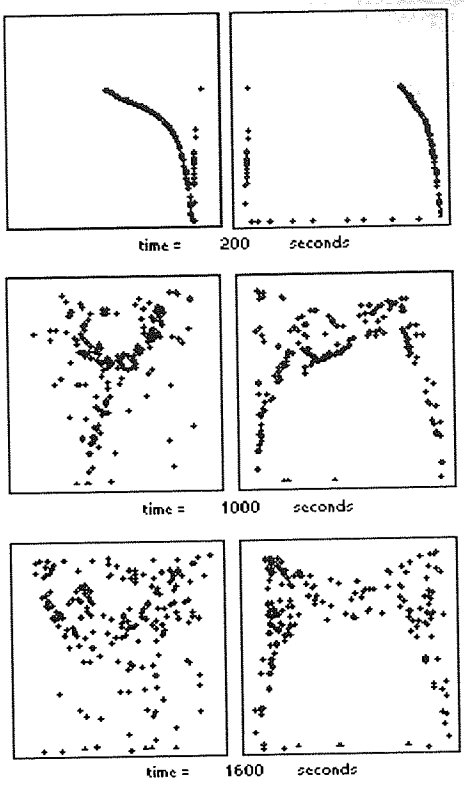

Figure 5.4, xy and yz views showing the positions of 200 originally near particle trajectories in the closed three-dimensional time periodic domain, at various times where the wall velocity amplitude is 2 mm/s, and the time period is 5 seconds.

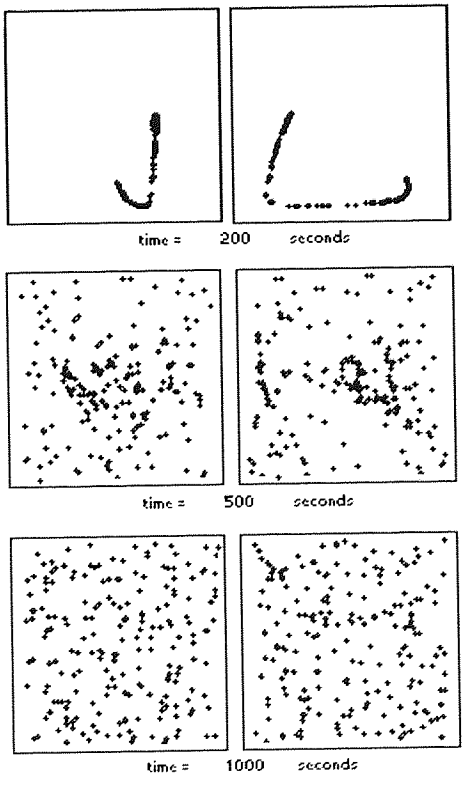

Figure 5.5, xy and yz views showing the positions of 200 originally near particle trajectories in the closed three-dimensional time periodic domain, at various times where the wall velocity amplitude is 2 mm/s, and the time period is 20 seconds.

The above figures suggest that if the three-dimensional system is operated time dependently, with perpendicular alternating streamlines, then separation between particles will occur irrespective of the time period of wall oscillation. Increasing the time period does not change the form of particle movement as significantly as observed for the two dimensional systems. All systems, even the low time period ones, appear to exhibit some disorder, however there are some regions of no flow. As with the two-dimensional investigations there appears to be a point within a range of time periods that a particular system will exhibit full chaotic motions. However, unlike the two-dimensional cases low time periods do not appear to exhibit near-ordered system behaviour.

5.5.2 Separation of particles in the time periodic closed mixing domain, property of divergence.

By the use of property A the above observation of particle separation can be quantified. Figures 5.6- 5.8 show the system with various time periods where the wall velocity amplitude is 1, 2 and 5 mm/s respectively.

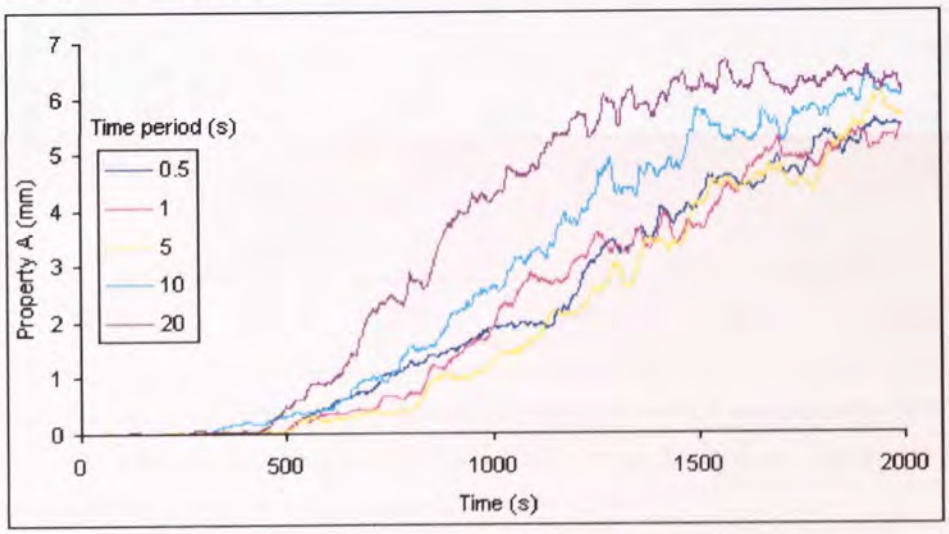

Figure 5.6. Property A against time for the three-dimensional cubic system with the oscillation of two faces operating in a flip-flop motion with an amplitude of 1mm/s and various time periods. 200 particles, initially generated over a length of 0.2mm, were used to create property A.

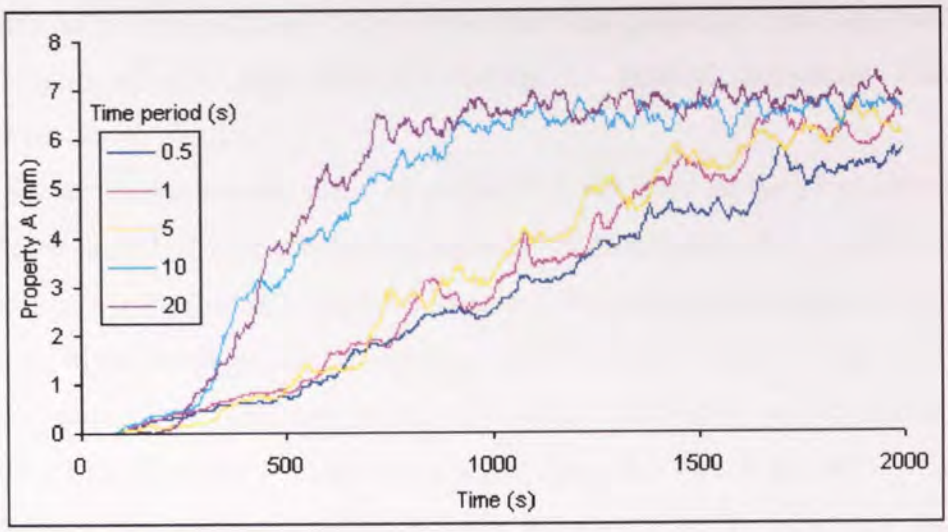

Figure 5.7.Property A against time for the three-dimensional cubic system with the oscillation of two faces operating in a flip-flop motion with an amplitude of 2mm/s and various time periods. 200 particles, initially generated over a length of 0.2mm, were used to create property A.

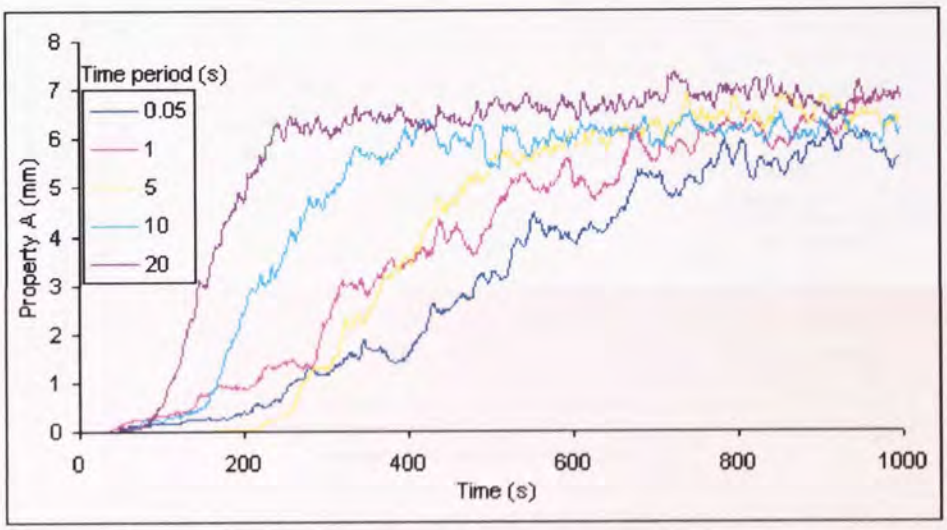

Figure 5.8.Property A against time for the three-dimensional cubic system with the oscillation of two faces operating in a flip-flop motion with an amplitude of 5 mm/s and various time periods. 200 particles, initially generated over a length of 0.2mm, were used to create property A.

It can be seen in figures 5.6 to 5.8 that all system operating parameters appear to yield some separation after sufficient time, which is indicated by the large values of property A. Three of the plots in figure 5.7 correspond to the systems presented in figures 5.3 to 5.5. It can be seen that the plots for property A against time for the systems with time periods of 0.5 and 5 seconds are similar, with both suggesting a gradual separation of particles. The system with a time period of 20 seconds however, shows that separation is achieved much earlier, with the plot suggesting rapid divergence followed by a levelling off period. This plot is similar to the property A plots in the two-dimensional cavity systems operating within chaotic regimes presented in chapter 4.

There appears to be two plots produced from observing property A as time evolves in the three-dimensional system, one that corresponds to gradual separation and one that corresponds to chaotic motion.

Figure 5.9 shows the maximum value of property A achieved in the time allowed, plotted against the time period of wall oscillation, for velocity amplitudes of 1, 2 and 5 mm/s. It can be seen that maximum value of property A irrespective of operating parameter is comparable, as the particles in the lower amplitude and time period systems would be expected to separate further given more time. This may appear confusing when using property A to assess the mixing within a system. One should also consider the form of the property A against time plot, and not just the maximum value attained, before making a judgement on whether a system is chaotic or not. For further information about the disorder one should observe the positions of the particles within the domain a various points in time.

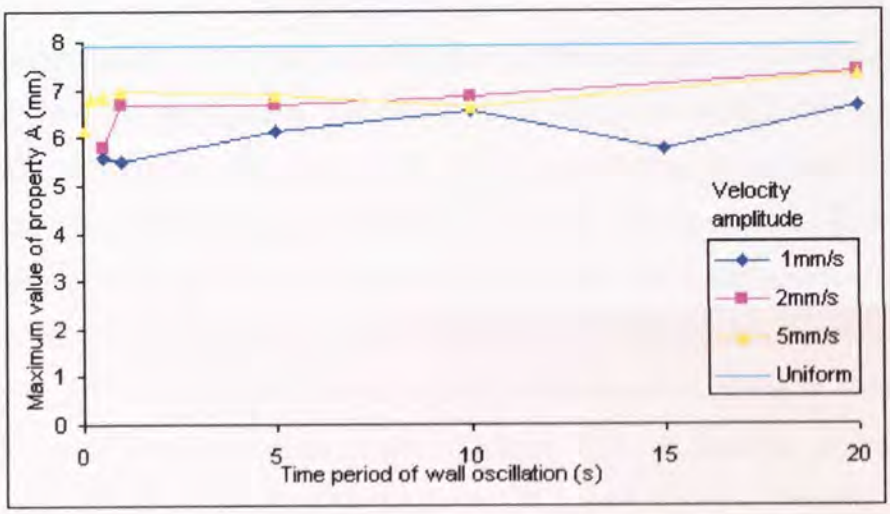

Figure 5.9. The maximum value of property A achieved, generated from 200 particles originating over a 0.02mm length, over 2000 seconds within the three-dimensional cubic system with walls oscillating, with three different amplitudes, and over a range of time periods. Also indicated is the distance between particles from a uniform distribution.

This observation is significantly different, and may initially appear contradictory, to the earlier observations of a cascade towards chaos from the two dimensional cavity, where a distinct difference between low disorder and chaos was visible. The difference between the two- and three-dimensional systems can be accounted by the opposing boundary motions being co-planar and perpendicular respectively. In the two dimensional cavity, as shown in chapter 2, and again in figure 5.10, when the system operates at a low time period the opposite streamlines, effectively, cancel out the particle movements into the form of an oscillation. The two streamlines have reflective symmetry, which cause particles to oscillate.

It is not until particles are displaced within any one streamline significantly that the opposing streamline cannot return the particle as an oscillation, and chaotic motion occurs.

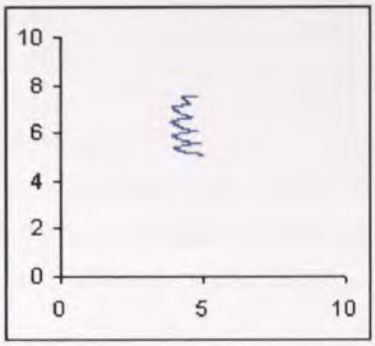

Figure 5.10 Particle trajectory in the two-dimensional time periodic cavity system, operating with a flip-flop movement of the upper and lower wall boundaries, showing the oscillation of the particle back and forth as the streamline regimes alternate. Time period of oscillation is one second for 10 time periods.

In the three-dimensional system the two differing streamline regimes are perpendicular, and possess both reflective and rotational symmetry. A particle originating in one streamline form will move within that for the first time period. As the second time period begins the particle is subjected to the other streamline, and will be moved perpendicularly away from the original. Figure 5.11 shows the trajectory of a particle within the three-dimensional cubic system operating with velocity amplitude of 1 mm/s, time period of 10 seconds for five time periods. For the first time period the particle moves within, what is considered here, for simplicity, as a two-dimensional streamline motion in the xy plane. For the duration of the second time period to particle movement is within the yz plane.

In the three-dimensional system the particle is not returned through the original streamline by an oscillation. At a low time period and amplitude of wall oscillation the particle may only move a small distance from its original streamline, but will not be returned. A cluster of particles will separate as the streamlines alternate, and will become further apart as time evolves. It would be expected that at higher velocity amplitudes and greater time periods the particles are able to separate significantly more quickly.

Figure 5.11. Particle trajectory in the three-dimensional cubic time periodic system, operating with a flip-flop movement of two wall boundaries, showing the perpendicular movements of the particle as the streamline regimes alternate. Time period of oscillation is ten seconds for five time periods.

The above investigations show that the cascade observed for the two-dimensional cavity system by the use of property A is not readily observable in the three-dimensional cubic system due to the differences between co-planar and perpendicular, alternating flow regimes. However property A does indicate the rapid mixing and does appear to exhibit two different forms of plot when considered against time. The system operating parameters that are known to produce poor mixing, identifiable through areas of no flow, yield plots that gradually increase. Whereas systems that are considered to be chaotic, as particles spread randomly throughout the domain produce a plot that exhibits a rapid rise followed by a levelling off period, which was recognised to relate to chaotic systems in chapter four.

The use of property A in three-dimensional time period systems, such as the cube with flip-flop walls, in a perpendicular motion, is suggested to be limited. One should not rely of the property alone and should consider other methods to support the conclusion of chaos, such as observing the separation of particle trajectories numerically.

Once a system's operating parameters are thought to place it in chaos the property A against time plots could be used to suggest residence times for mixing or to consider the most efficient mixing available.

5.6 Throughput chaotic systems.

Inclusion of the third dimension enables the generation of systems that are more realistic, which boast, to great advantage, the ability to model wall movement perpendicular to the general fluid motion. This is utilised in this section for the modelling of flow throughput rectangular cavities, with top and bottom walls moving perpendicular to the flow [101].

As with the closed domain stagnating particles must be avoided in calculations, especially as the effect of a throughput would be to magnify the uncertainties. If a small number of particles stagnate near to the inflow boundary and all others continue towards the exit, then the distance between the moving particles and those left behind will be considerably large.

Particles in a closed domain all evolve to the same predetermined evolution time. Particles being tracked in a throughput domain can leave, and hence cease to exist, after differing times. This is especially notable where high disorder exists and particles take highly different routes to the exit. Particles that move nearer to the walls, where the affect of the throughput rate is reduced, due to wall drag, would take more time to emerge from the exit boundary than a particle that spirals through the centre for example.

When particles reach the exit boundaries their trajectory tracking stops. This has serious implications when calculating the property of divergence as the co-ordinate values recorded become x, y, z =0, 0, 0. Consider that the origin is near to the inflow boundary, then if zero co-ordinates are compared with existing particles the divergence value will significantly increase.

Two methods for removing this effect are suggested here. The first is to remove particles from calculations as soon as they leave the domain. This would result in the divergence property being calculated from a reducing number of particles. It is therefore not be possible to compare different systems by use of the divergence property due to as a the smaller the number of particles the larger the average distance between them is likely to be.

The second, and more favourable, method used here is to cease the calculations as the first particle reaches the exit boundary. However this may be may be relatively early compared to the majority of the particles under investigation, and hence the investigation will have to make use of low throughput rates or long mixers in order to allow significant blending to take place before the test stops.

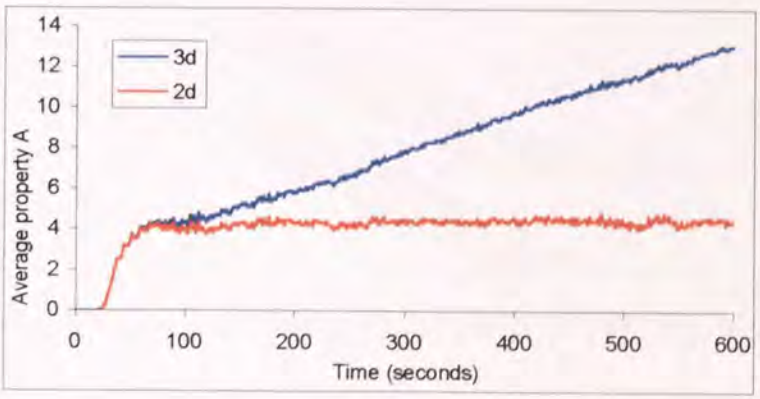

Figure 5.12. Average distance between particles calculated using both two- and three-dimensions for the same three-dimensional throughput domain operating under chaotic conditions.

Although the systems investigated here are three-dimensional it is considered that more useful information will be obtained if the divergence property is calculated over the two-dimensional cross sectional area perpendicular to the throughput flow. Figure 5.12 shows property A calculated for two- and three-dimensions for the same set of particle trajectories within a time periodic throughput domain that is within a chaotic regime. It can be seen that the two-

dimensional property A, as time evolves, appears to level off corresponding to the particles significantly separating from each other, which is was also observed in chapter 4. This however is not the case with the three-dimensional divergence plot of the same system. The average distance between the particles continues to increase, up to the point where the calculation ceases as the first particle exits. This is due to the laminar shear promoting a longitudinal spread of the particles as they travel through the domain. The inclusion of the third dimension when calculating the average distance between particles in continuous open domains makes it difficult to suggest when the particles have distributed themselves randomly. It is therefore difficult to compare the mixing to others in the series as it may be possible to achieve a large average distance between particles within a long domain predominantly due to laminar shear where the actual cross-sectional mixing is poor.

5.6.1 Chaos induced within a three-dimensional time periodic throughput flow.

The fluid modelled in all of the throughput systems has a constant density and viscosity. The throughput domain cross section has an aspect ratio of 1 and an area of $100mm^2$. The system could be considered as many two-dimensional oscillating cavity systems placed back-to-back with the throughput perpendicular to the boundary motion. The shaded boundaries in figure 5.13 oscillate with a flip-flop scheme between the top wall moving and the bottom wall stationary, and vice-versa. The fluid as it travels through the domain is therefore subjected to time periodic alternating streamline motion.

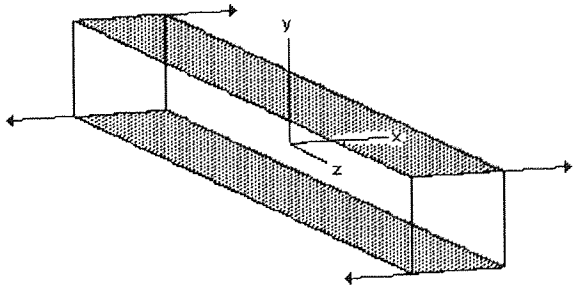

Figure 5.13. Three-dimensional throughput, time periodic domain. The shaded walls translate in the directions shown with a flip-flop motion.

The throughput used initially in these tests is low to ensure that particles within disordered systems are supplied sufficient time to diverge and hence mix to a significant degree.

The control parameter for the induction of chaos considered here is the time period of the oscillating boundaries, in a similar way to previous chapters. It would again be expected that the affect of increased amplitude of the wall oscillation would be to reduce the value of time period required to induce chaos.

Figures 5.14 – 5.16 show the instantaneous positions of 200 sample particles, that originated from a small zone of generation, of length 0.2mm, near the inflow, at intervals of time, for differing time periods of oscillation throughout a cascade. The throughput is set at $10mm^3/s$ and the velocity amplitude of the walls is 10mm/s. It is possible to observe that as the time period of oscillation increases the degree of disorder also increases. If no movement of the boundaries were applied then all particles would travel through the domain in a straight-line flow. When the time periodic disturbance is applied the particles begin to oscillate, and hence separate, as they travel throughout the domain, as can be seen in figure 5.14, where the time period is 1 second. Increase the time period and the oscillation grows and the disorder increases, as in figure 5.15, where T=2 seconds. Continue to increase the time period and chaos occurs. Figure 5.16 shows the system where the time period is 10 seconds. The particles diverge rapidly, to what appears to be a random distribution over the cross section. Bending and folding of the lamella can be observed and as the disorder increases the longitudinal spread also increases.

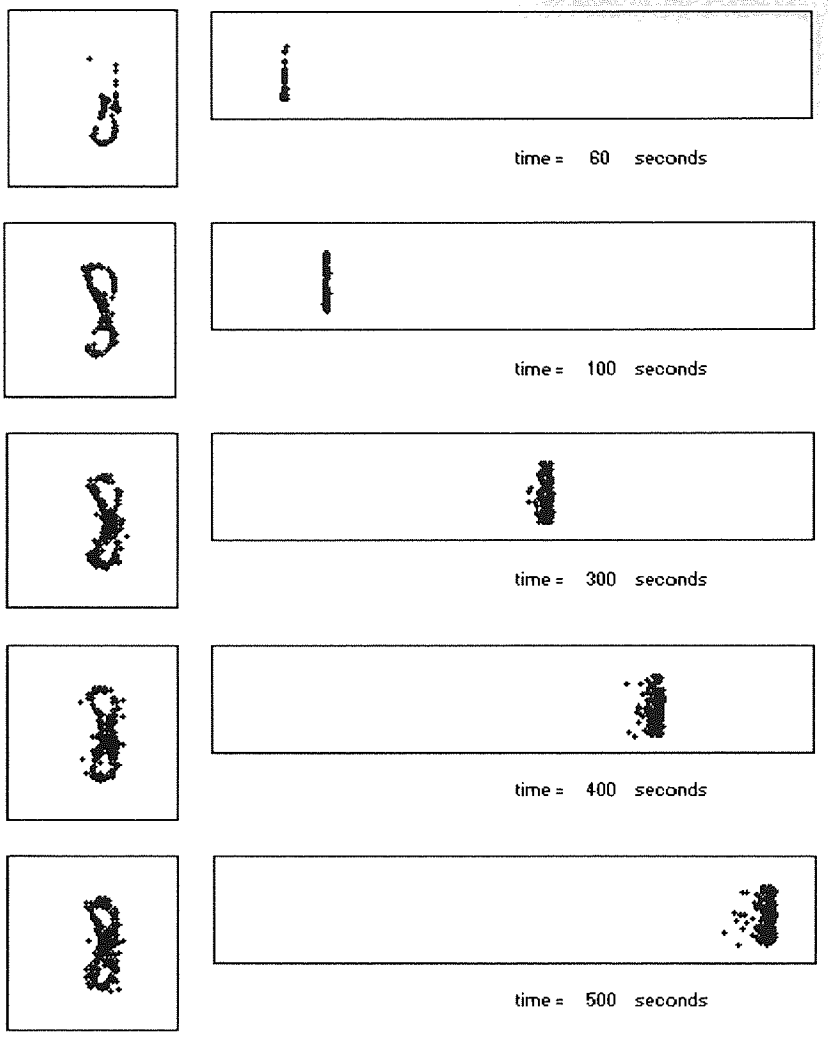

Figure 5.14. The positions of 200 particles that originate from a small generation zone near the inflow of the time periodic throughput domain at five different times. The through put of the system is $10mm^3/s$, the velocity amplitude of the upper and lower walls is 10mm/s and the time period for boundary oscillation is 1 second.

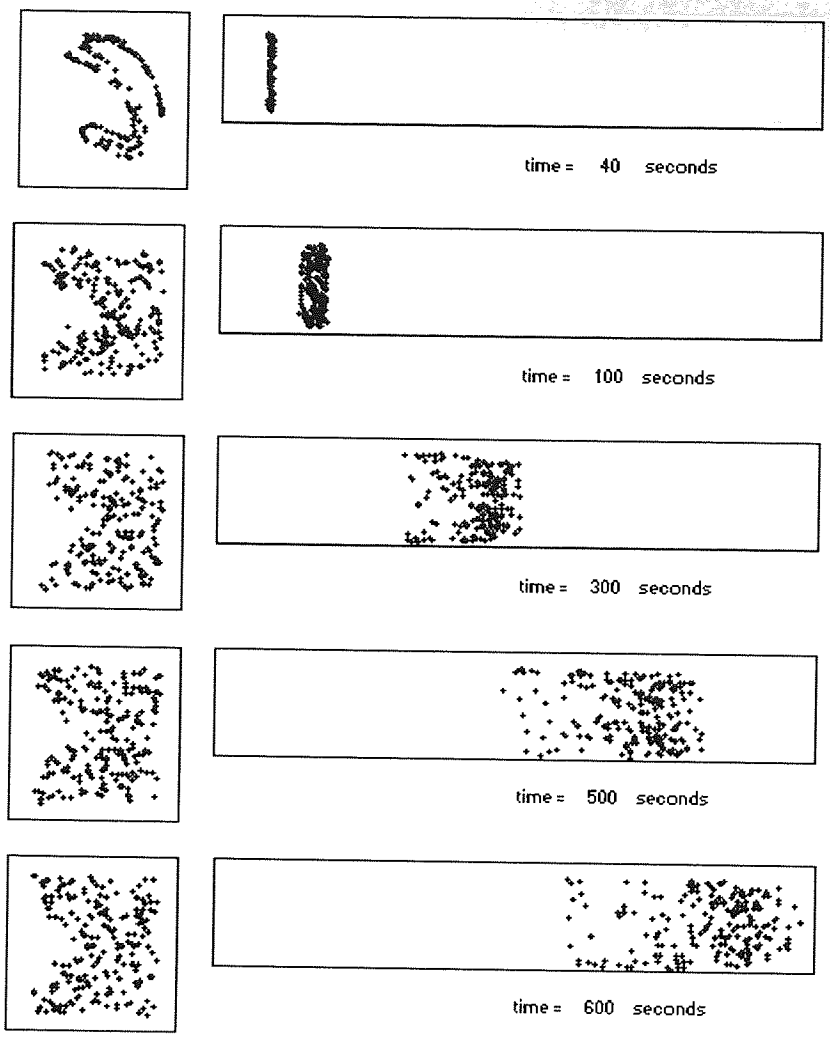

Figure 5.15. The positions of 200 particles that originate from a small generation zone near the inflow of the time periodic throughput domain at five different times. The through put of the system is $10mm^3/s$, the velocity amplitude of the upper and lower walls is 10mm/s and the time period for boundary oscillation is 2 seconds.

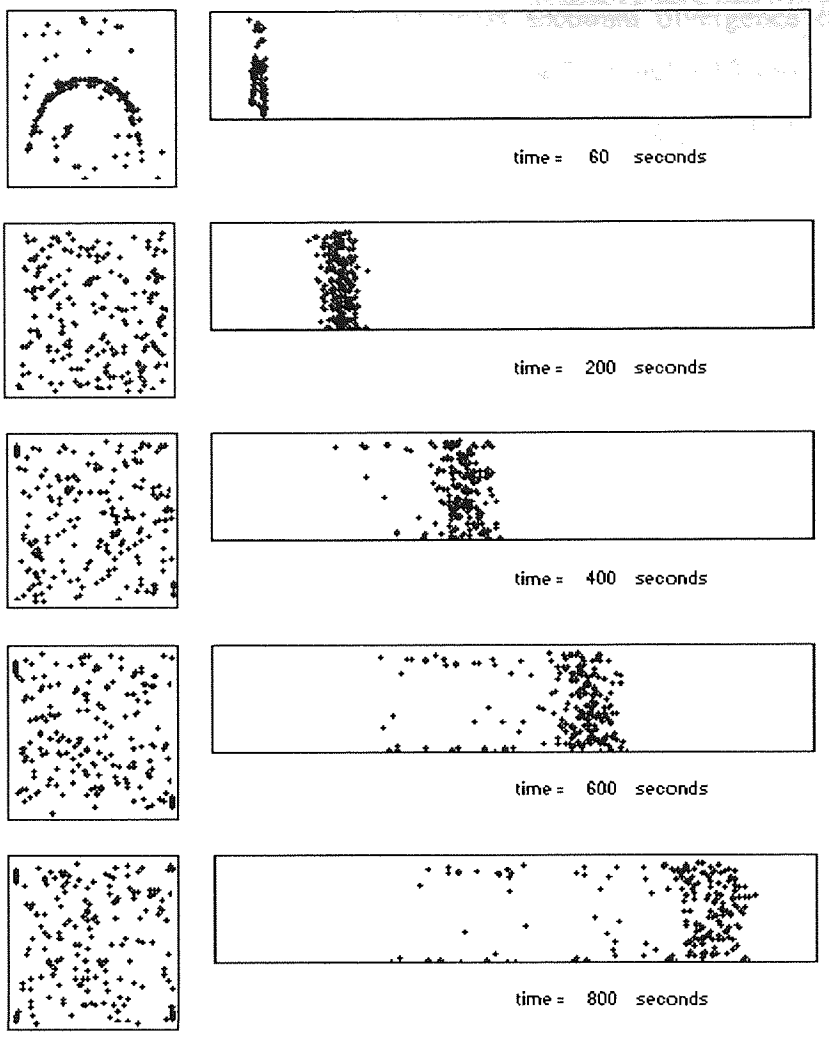

Figure 5.16. The positions of 200 particles that originate from a small generation zone near the inflow of the time periodic throughput domain at five different times. The through put of the system is $10mm^3/s$, the velocity amplitude of the upper and lower walls is 10mm/s and the time period for boundary oscillation is 10 seconds.

If we now consider the quantification of the cross sectional divergence of the distance between the two hundred particles shown above. Figures 5.17 and 5.18 show the divergence of particles throughout cascades within the system with a throughput of 10 mm^3/s and wall velocity amplitudes of 5 and 10 mm/s respectively. As with some of the chaotic systems previously discussed it is possible to observe characteristic plots of property A against time. Systems that do not significantly diverge, remain at low value, and those in chaos exhibit rapid growth, up to the point where particles have separated and the plot levels off. Figure 5.19 shows the maximum values of property A achieved for a variety of time periods, for the velocity amplitudes in figures 5.17 and 5.18, compared to the average distance obtained from the uniform distribution of two hundred particles throughout the cross sectional area of $100mm^2$. It can be seen that as with other time periodic systems the effect of increasing the wall velocity amplitude is to reduce the time period required for chaos to occur. Also notable are those systems within chaos exhibiting good mixing with the maximum value of property A being nearly comparable to that of the uniformly distributed case.

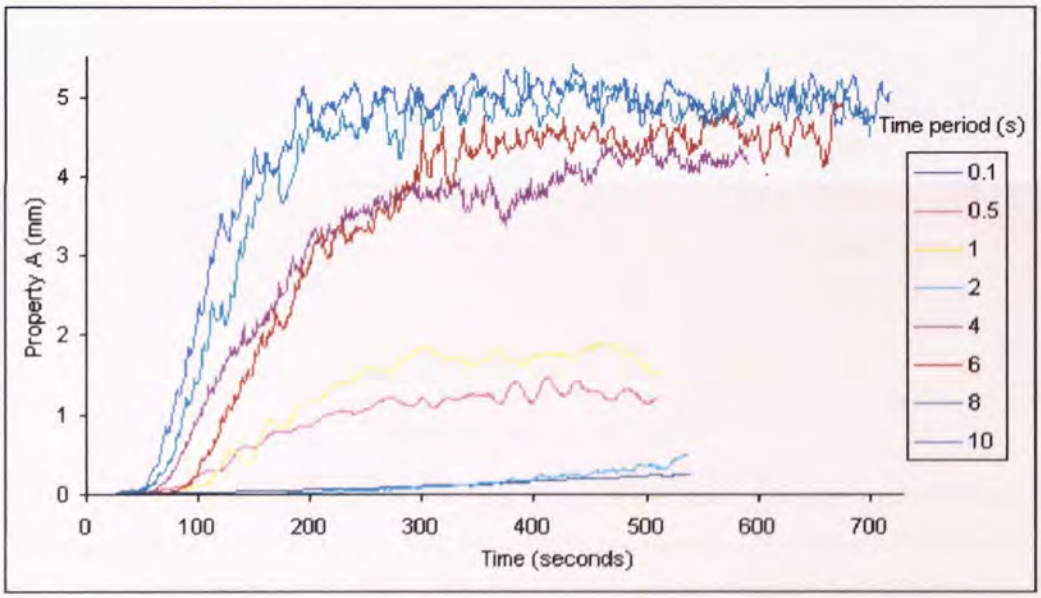

Figure 5.17. Property A against time generated from 200 particles originating over a 0.02mm length, within the three-dimensional, time periodic, throughput system. The velocity of the upper and lower walls oscillating with amplitude of 5mm/s, over a range of time periods where the throughput rate is $10mm^3/s$.

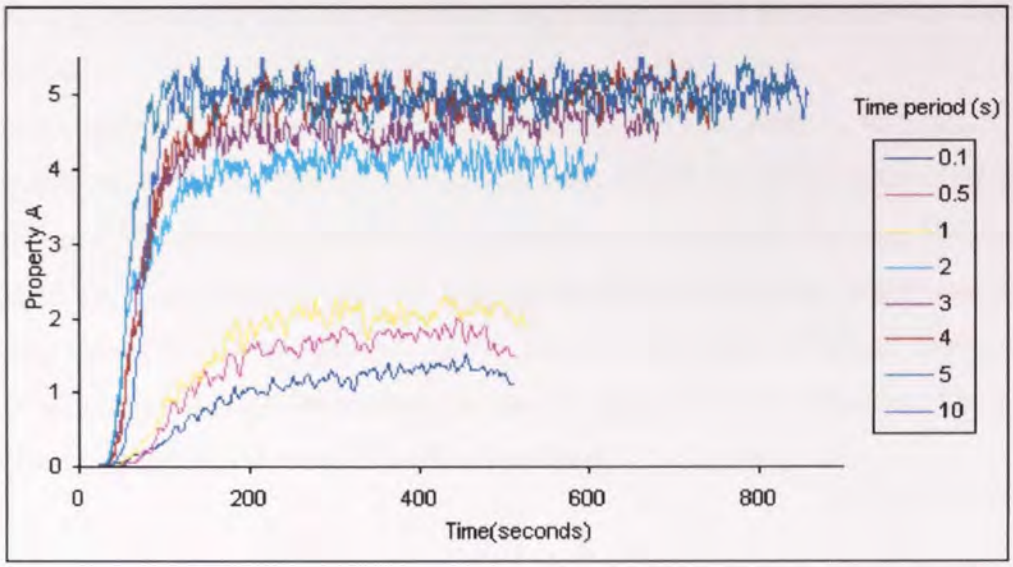

Figure 5.18. Property A against time generated from 200 particles originating over a 0.02mm length, within the three-dimensional, time periodic, throughput system. The velocity of the upper and lower walls oscillating with amplitude of 10mm/s, over a range of time periods where the throughput rate is $10mm^3/s$.

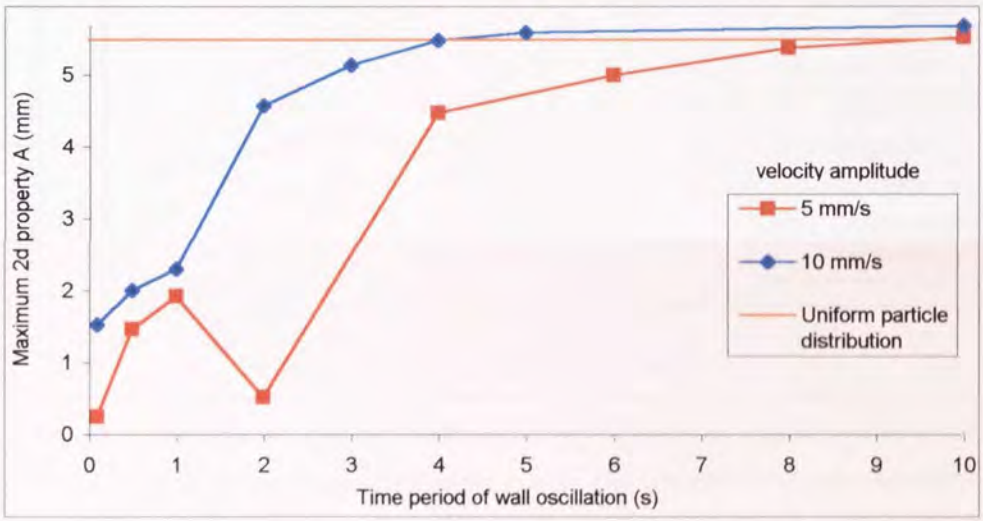

Figure 5.19. The maximum value of property A achieved, from 200 particles originating over a 0.02mm length, within the three-dimensional, time periodic, throughput system. The velocity of the upper and lower walls oscillating, with two different amplitudes, and over a range of time periods where the throughput rate is $10mm^3/s$ Also indicated is the distance between particles from a uniform distribution.

Figure 5.20 shows the maximum value for property A against, time period of wall oscillation, for three different throughput rates of 20, 35 and 50 mm^3 /s where the velocity amplitude is 20mm/s. It can be seen that the systems behave similarly, with a peak within the cascade at the same time period for each of the three throughputs. The differences in the magnitudes of the maximum property A achieved are probably related to the particles not having sufficient time to separate whilst in the domain as the throughput is increased.

The throughput does not effect the disorder of the system, only the degree of separation that the particles achieve whilst within the domian. Particles become incident to differing

streamline regimes due to the wall velocities oscillating in time irrespective of their position in the domain.

Tests on throughput mixing systems could use the plots of property A to observe residence times to achieve sufficient mixing. Ideally the fluid would be in the mixer long enough to completely mix, which is associated with the levelling off point of the plot. An optimisation of the variables, such as time period and magnitude of wall oscillation, length and throughput rate of the mixer could be carried out to identify the most efficient mixer. Costs of constructing and operating a real industrial chaotic mixer could be considered as part of the optimisation to generate the most cost-effective mixer.

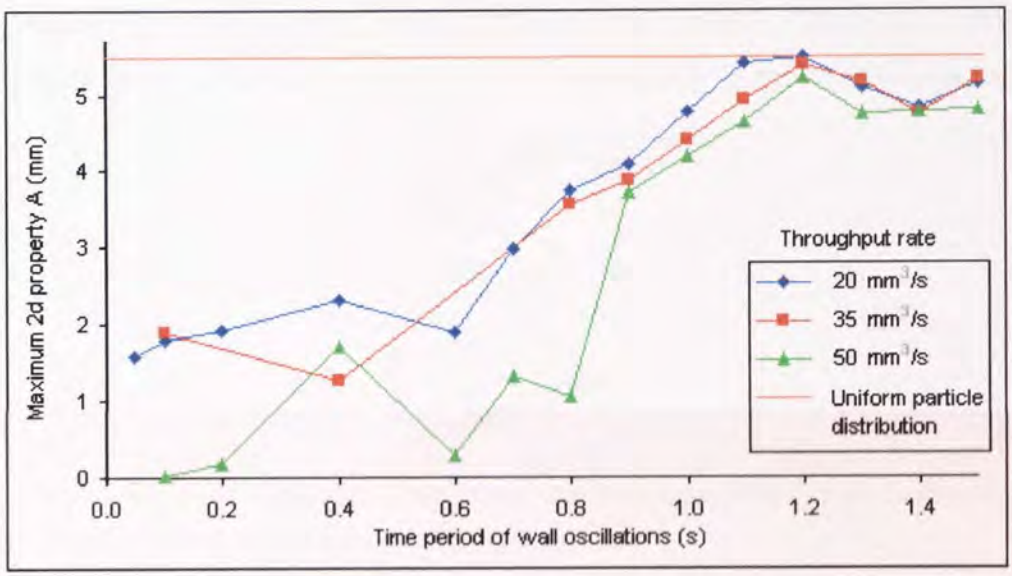

Figure 5.20, The maximum value of property A achieved, from 200 particles originating over a 0.02mm length, within the three-dimensional, time periodic, throughput system. The velocity of the upper and lower walls oscillating, over a range of time periods for three different throughput rates with a velocity amplitude of 20mm/s. Also indicated is the distance between particles from a uniform distribution.

It has been shown in this section that it is possible to observe similar behaviour with respect to control parameters, within a two-dimensional time periodic closed cavity domain and a three-dimensional time periodic throughput domain.

5.6.2 Chaos induced within a three-dimensional spatially periodic throughput flow.

Particles within chaotic regimes described up to this point become incident to differing instantaneous streamlines time periodically. If the system were not time dependent, and instead the particles became incident to cells of differing streamlines as they flowed through the domain, then the affect of the volumetric throughput would be equivalent to that of the oscillation frequency of time periodic systems. At high throughputs particles would travel

through each spatial streamline cell quickly, thus deviating from straight line through flow only minutely. Reduce the throughput rate, and at a specific value particles will displace significantly and chaos will occur. The wall velocity would be expected to have similar effect on the disorder of a time independent system of this nature as it does on a time period one.

The above conjecture is proved by the use of a spatially periodic domain with exact geometrical size and simulation fluid properties to that in the previous section. The domain could be considered as being made up of ten adjacent cells of 10mm length, each containing two opposing pairs of alternate moving and stationary walls as shown in figure 5.21. The control parameters for the induction of chaos considered here are the throughput and the translation velocity of the wall boundaries. The continuous moving boundaries in this system translate perpendicular to the throughput flow so to ensure that particles become incident to varying streamline regimes as they progress through the domain. These are shown as the shaded walls in figure 5.21, which are set moving continuously in the directions indicated.

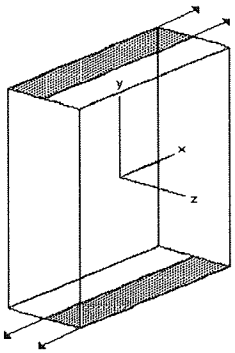

Figure 5.21. Representation of one cell of the three-dimensional throughput, spatially periodic domain. The shaded walls translate in the directions shown with a steady motion.

Figures 5.22 – 5.24 show the separation of two hundred particles as time evolves for systems with an inflow of 10 mm^3/s and constant wall velocities of 0.2, 1 and 10 mm/s respectively. Expectedly, we see very little particle disorder where a low wall velocity is used. Particles travel without separation through the domain. Increase the wall velocity and the particles begin to oscillate as they flow through the domain, and exhibit some separation. Continue to increase the control parameter, wall velocity, and arrive within a region of increased disorder. As with previous systems the spatially periodic domain exhibits a cascade into chaos in a similar way, which too can be quantified by the use of the cross sectional property A.

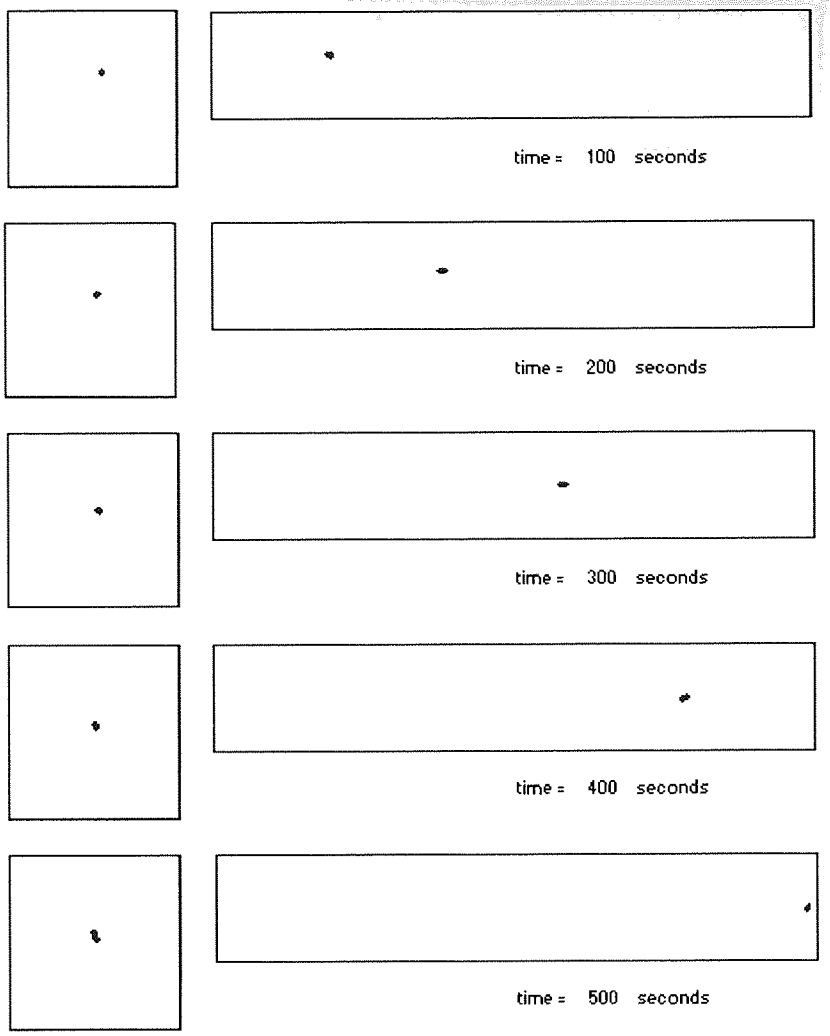

Figure 5.22. The positions of 200 particles that originate from a small generation zone near the inflow of the spatially periodic throughput domain at five different times. The through put of the system is $10mm^3/s$, the translation velocity of the upper and lower walls is 0.2mm/s.

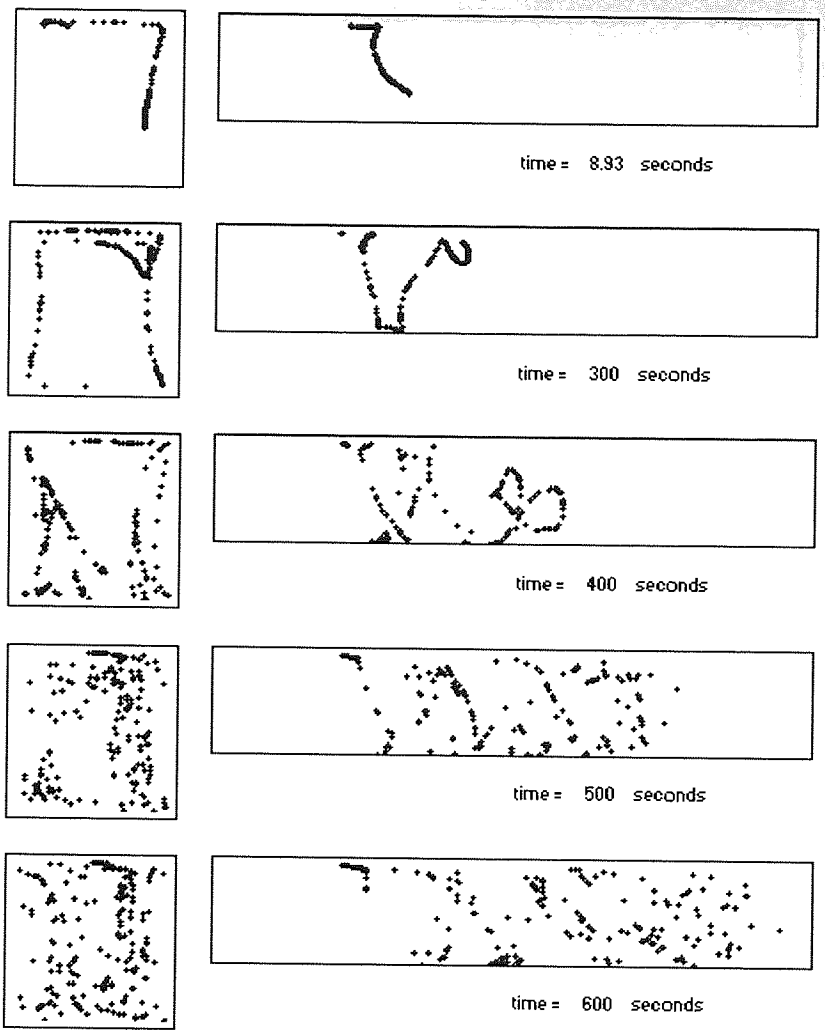

Figure 5.23. The positions of 200 particles that originate from a small generation zone near the inflow of the spatially periodic throughput domain at five different times. The through put of the system is $10mm^3/s$, the translation velocity of the upper and lower walls is 1 mm/s.

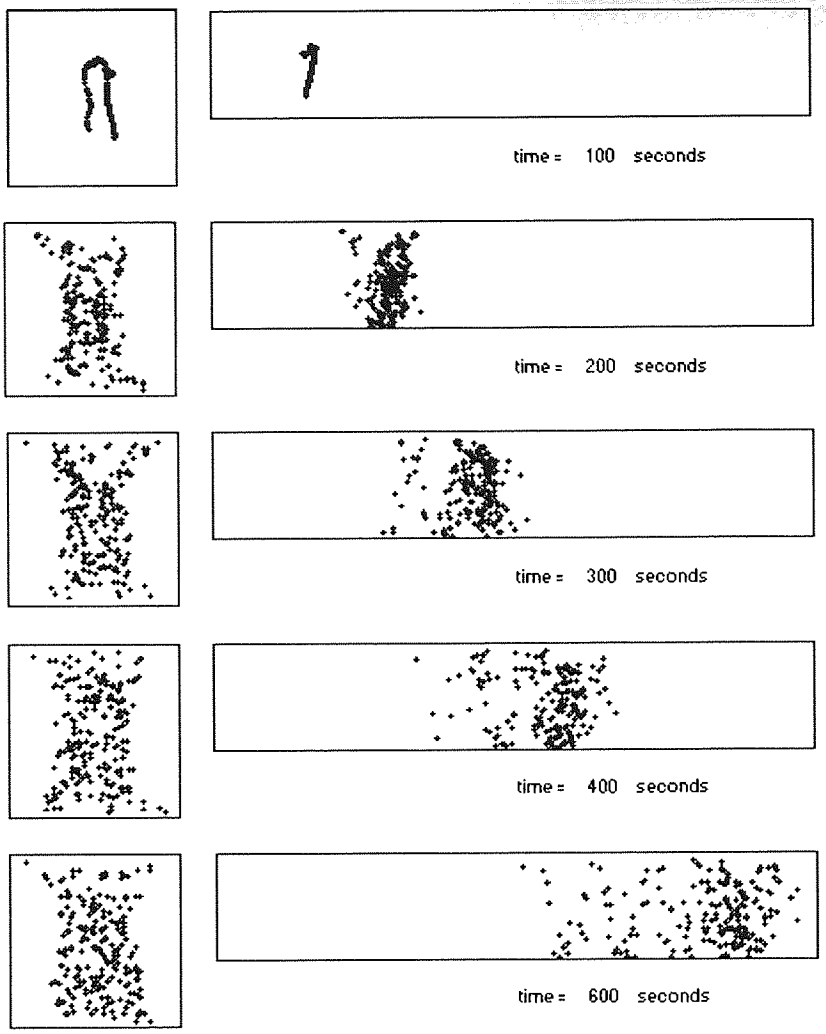

Figure 5.24. The positions of 200 particles that originate from a small generation zone near the inflow of the spatially periodic throughput domain at five different times. The through put of the system is 10mm^3/s, the translation velocity of the upper and lower walls is 10 mm/s.

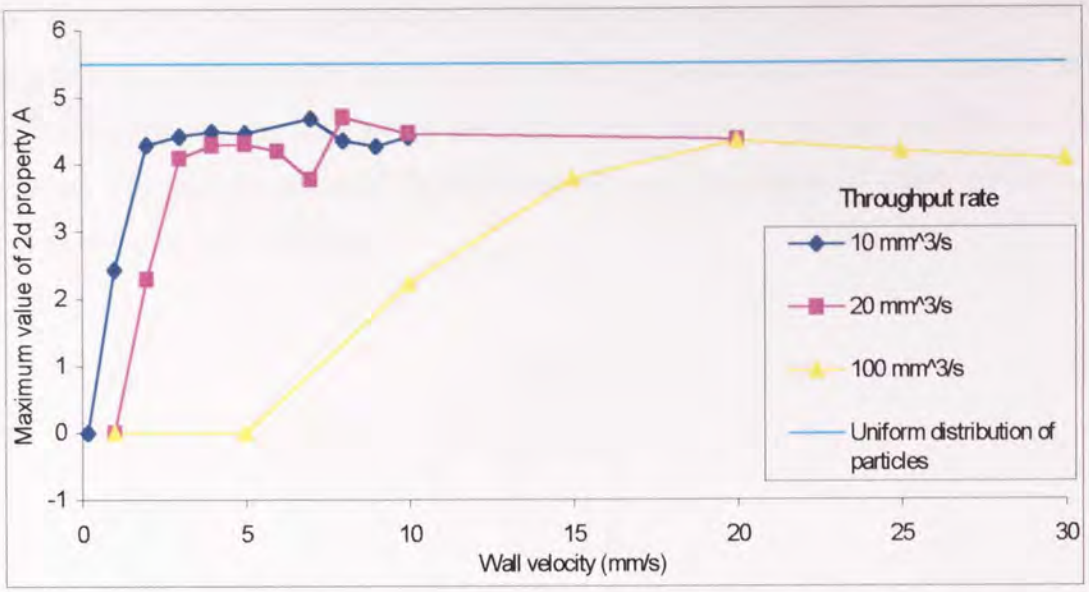

Figure 5.25. The maximum value of property A achieved, from 200 particles originating over a 0.02mm length, within the three-dimensional, spatially periodic, throughput system against the velocity of the upper and lower walls, for three different throughput rates. Also indicated is the average distance between particles from a uniform distribution.

Figure 5.25 shows the maximum values obtained by the cross sectional divergence property A plotted against the wall velocity, for all throughputs. It can clearly be seen that all three cascades attain similar levels of particle separation. The wall velocity at which the systems exhibit chaos is seen to increase as the throughput rate is increased. This supports the theory that it is the displacement within streamlines that controls the chaotic cascade. As the throughput becomes faster the higher the wall velocity has to be in order to induce the same degree of displacement perpendicular to the flow of the particles before they enter the next streamline cell. The separation of a set of particles in the system here is associated with their position and amount of displacement that they achieve in any one streamline as they pass through the mixer. As with the time periodic throughput mixer one could use the property A to suggest a residence time, mixer length and wall velocity to achieve an efficient and cost effective industrial mixer.

5.6.3 Chaos induced within a three-dimensional geometrically periodic throughput flow.

The third throughput system to be investigated in this work is termed here as geometrically periodic, and is conceptually similar to the spatially periodic system. The domain could again be considered as being constructed from ten, 10mm long cells, except here it is the

geometrical displacement of the second half of the cell that breaks the streamlines and induces increased mixing. The influence on the fluid is not, as in the spatial domain, to alter the form of the streamlines. Here the oscillation is of the centre points of the rotation caused by the upper and lower walls translating perpendicularly to the throughput flow as shown shaded in figure 5.26. Initially the control parameter is considered to be the velocity of the wall translation, although the effect of throughput variations and degree of offset within a cell are also considered to have an effect.

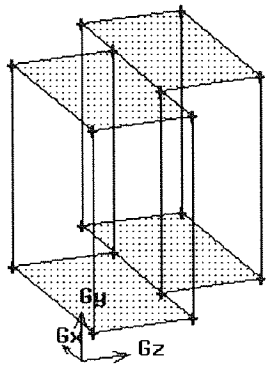

Figure 5.26. One cell of the three-dimensional throughput, geometrically periodic domain. The shaded walls translate causing a steady rotaion within the fluid in the xy palne.

Figures 5.27 –5.29 show the plots of two hundred particles as time evolves for a domain with an offset of geometric cells of 4mm, throughput of $10mm^3/s$ and wall velocities of 0.5, 3 and 20 mm/s respectively. It can be seen that increasing the wall velocity causes an increase in the disorder in the system and hence the separation of the particles, up to the point where chaos occurs. Once again the separation of these particles can be quantified by the divergence property A.

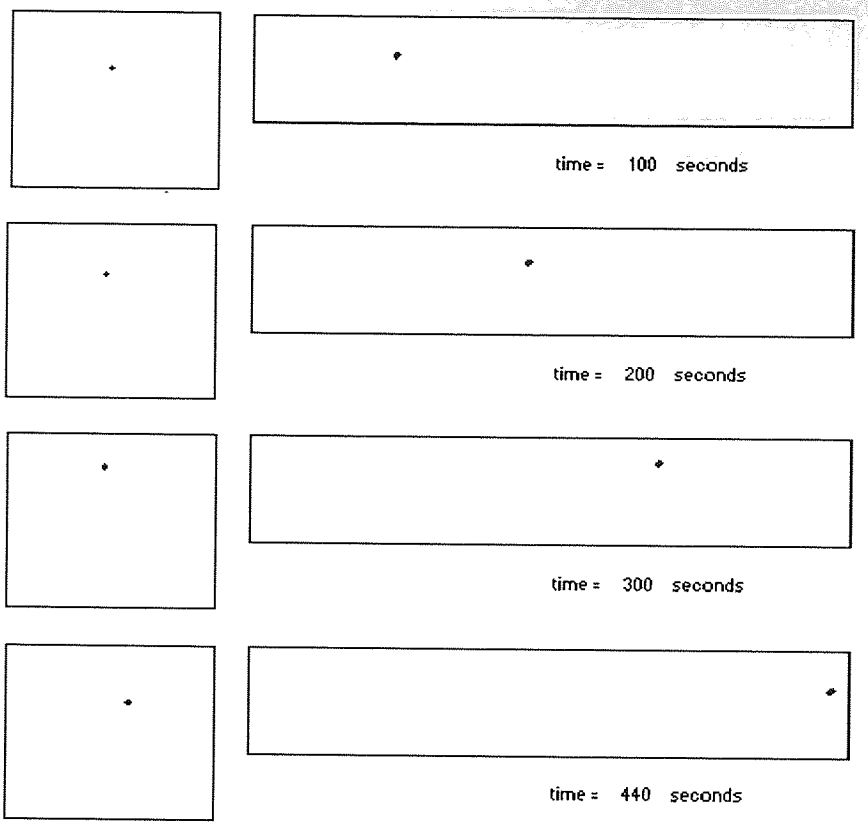

Figure 5.27. The positions of 200 particles that originate from a small generation zone near the inflow of the geometrically periodic throughput domain, with an offset of 4mm, at five different times. The through put of the system is $10mm^3/s$, the translation velocity of the upper and lower walls is 0.5 mm/s.

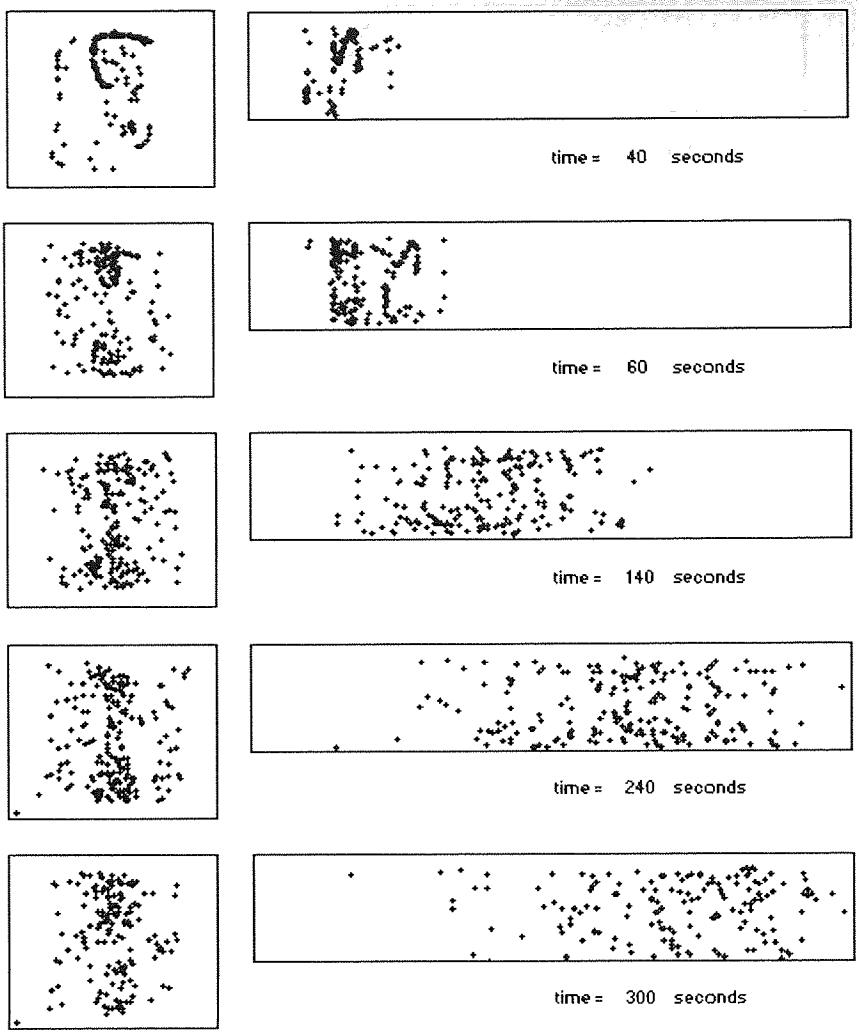

Figure 5.28. The positions of 200 particles that originate from a small generation zone near the inflow of the geometrically periodic throughput domain, with an offset of 4mm, at five different times. The through put of the system is $10mm^3/s$, the translation velocity of the upper and lower walls is 3 mm/s.

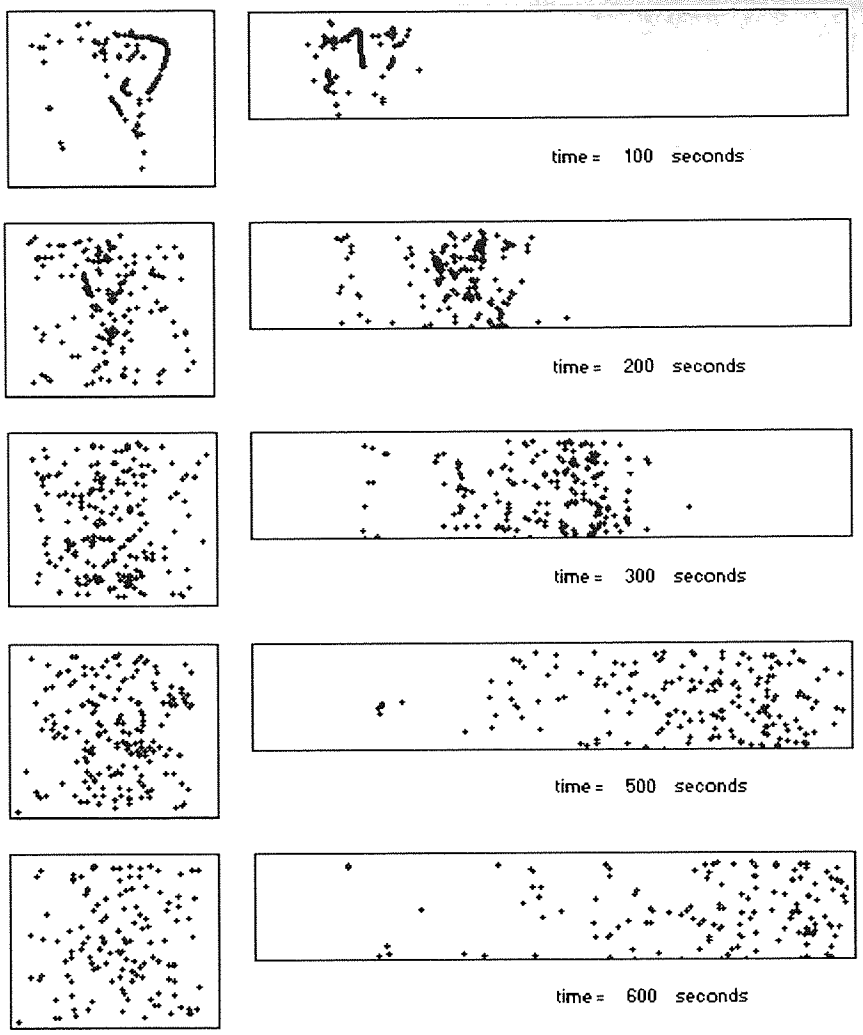

Figure 5.29. The positions of 200 particles that originate from a small generation zone near the inflow of the geometrically periodic throughput domain, with an offset of 4mm, at five different times. The through put of the system is 10mm^3/s, the translation velocity of the upper and lower walls is 20 mm/s.

Figures 5.30 – 5.35 show the separation of two hundred particles in the geometrically periodic domain, for three different wall velocities, for two further offsets of 2 and 6 mm. Once again it can be seen that as the control parameter increases the disorder within both systems also increases. However the domain with the smallest offset of 2mm does not achieve significant separation, even with a large wall velocity, particles are not randomly distributing throughout the domain, instead they appear to be flowing through the middle of the domain, and not entering the offset blocks. However the small region that the particles do occupy does appear to be chaotic, indicated by the random spread of particles within the disordered area and the longitudinal separation, associated previously with chaos. Where the offset of the cells is 6 mm, the particles do flow within the offset blocks, and the resulting separation of particles is high. The longitudinal separation is large with some particles being held in the offset blocks, resulting in particles taking longer to move through the mixer.

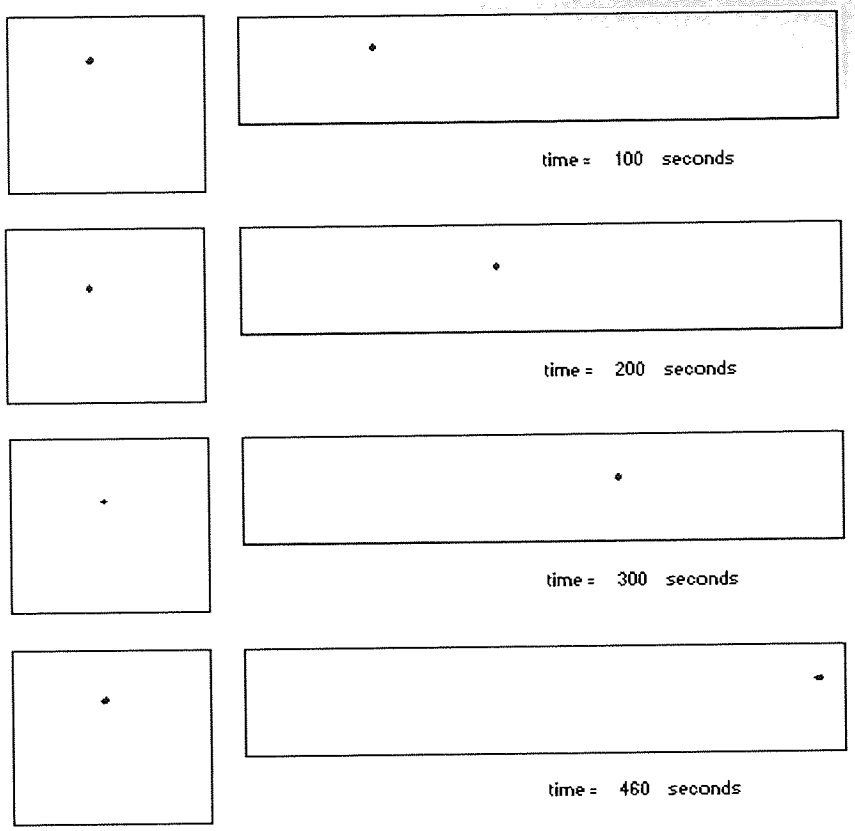

Figure 5.30. The positions of 200 particles that originate from a small generation zone near the inflow of the geometrically periodic throughput domain, with an offset of 2mm, at five different times. The throughput of the system is $10mm^3/s$, the translation velocity of the upper and lower walls is 0.1 mm/s.

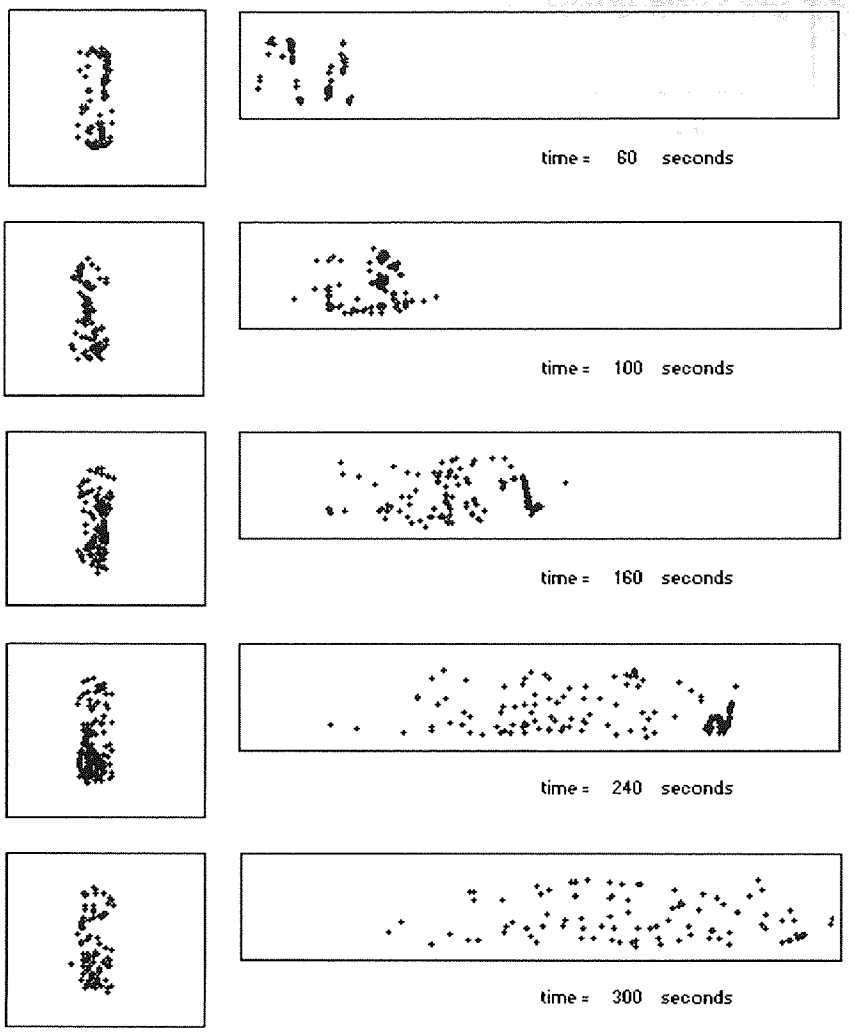

Figure 5.31. The positions of 200 particles that originate from a small generation zone near the inflow of the geometrically periodic throughput domain, with an offset of 2mm, at five different times. The throughput of the system is $10mm^3/s$, the translation velocity of the upper and lower walls is 10 mm/s.

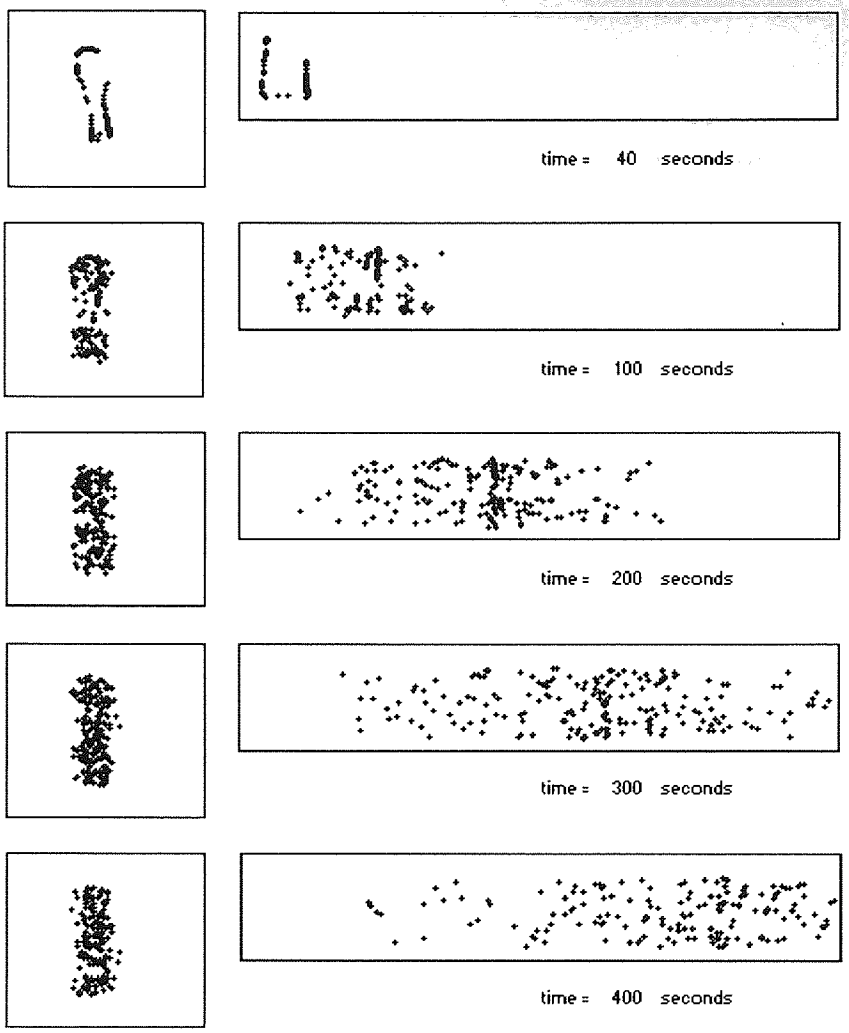

Figure 5.32. The positions of 200 particles that originate from a small generation zone near the inflow of the geometrically periodic throughput domain, with an offset of 2mm, at five different times. The throughput of the system is $10mm^3/s$, the translation velocity of the upper and lower walls is 20 mm/s.

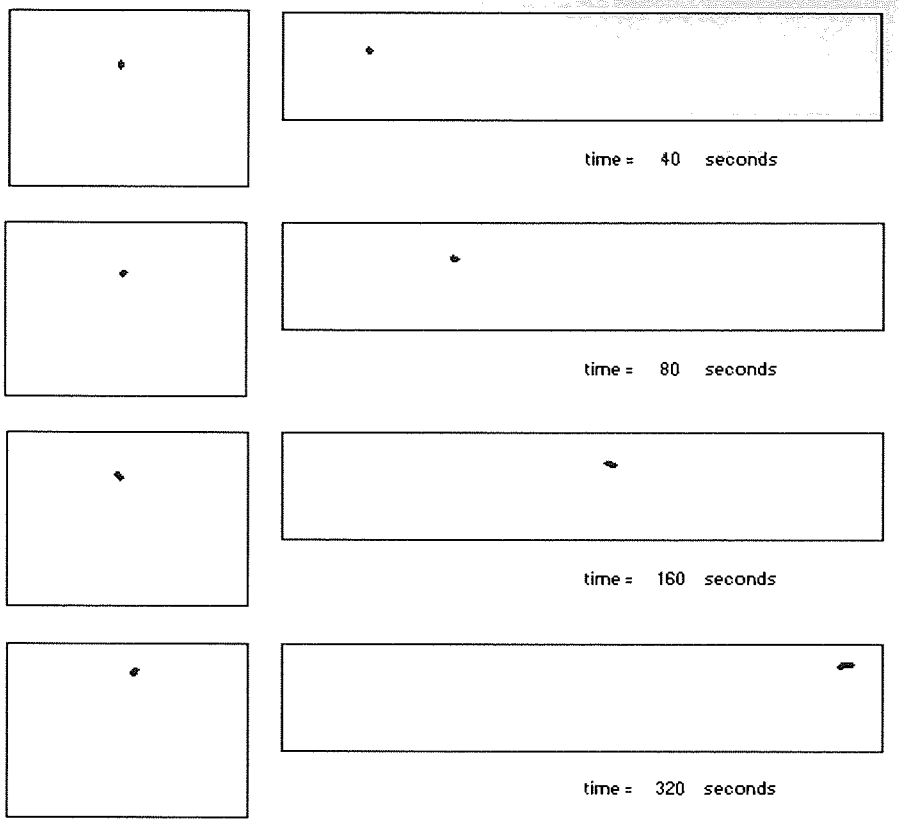

Figure 5.33. The positions of 200 particles that originate from a small generation zone near the inflow of the geometrically periodic throughput domain, with an offset of 6mm, at five different times. The throughput of the system is $10mm^3/s$, the translation velocity of the upper and lower walls is 0.1 mm/s.

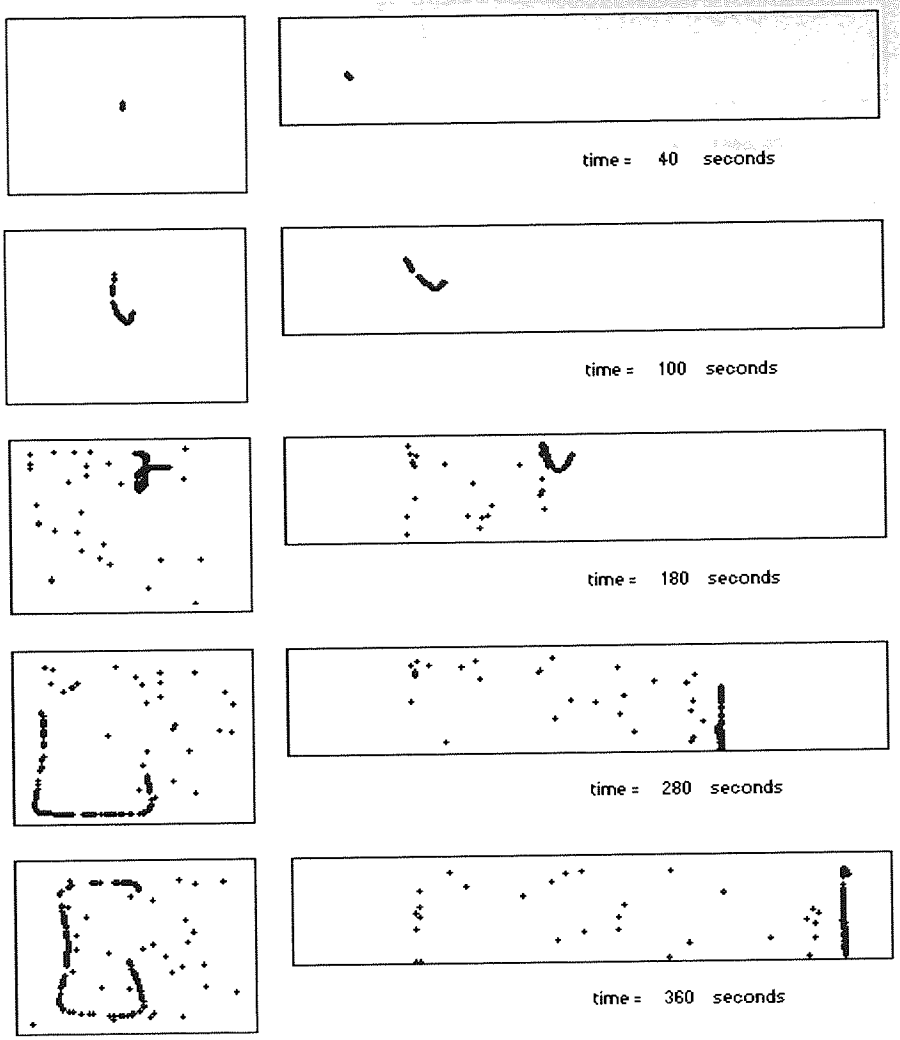

Figure 5.34. The positions of 200 particles that originate from a small generation zone near the inflow of the geometrically periodic throughput domain, with an offset of 6mm, at five different times. The throughput of the system is $10mm^3/s$, the translation velocity of the upper and lower walls is 10 mm/s.

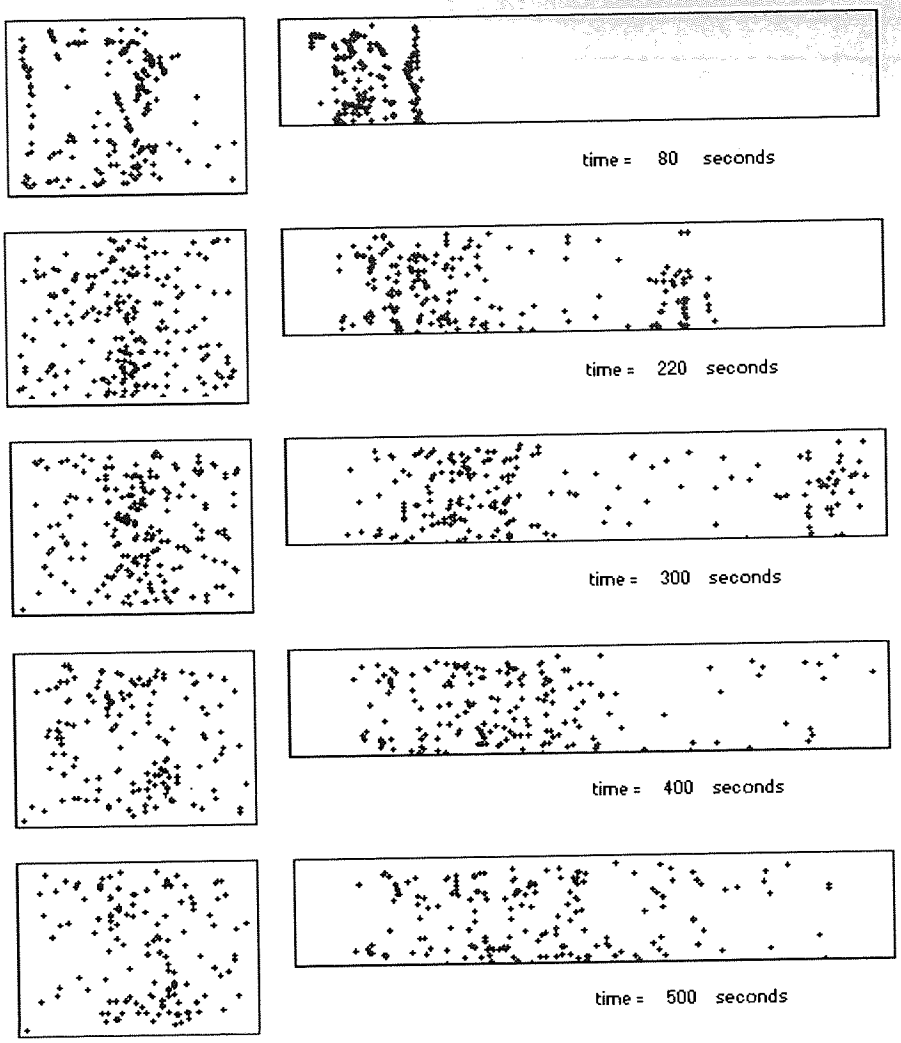

Figure 5.35. The positions of 200 particles that originate from a small generation zone near the inflow of the geometrically periodic throughput domain, with an offset of 6mm, at five different times. The throughput of the system is $10mm^3/s$, the translation velocity of the upper and lower walls is 20 mm/s.

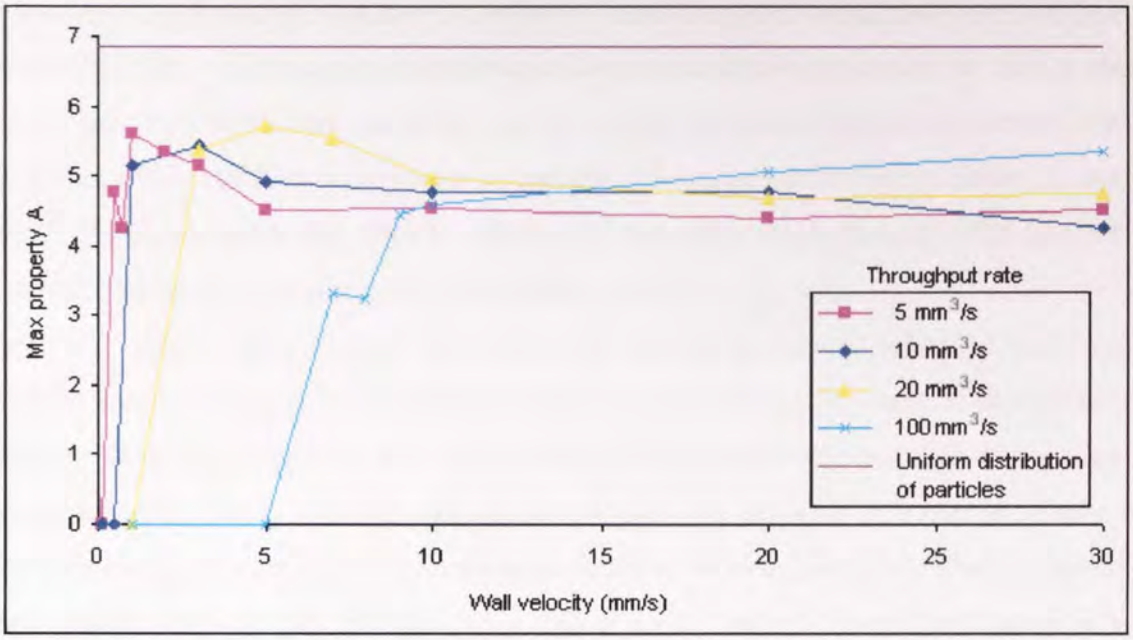

Figure 5.36. The maximum value of property A achieved, from 200 particles originating over a 0.02mm length, within the three-dimensional, geometrically periodic, throughput system, with an offset of 4mm against the velocity of the upper and lower walls, for four different throughput rates. Also indicated is the average distance between particles from a uniform distribution.

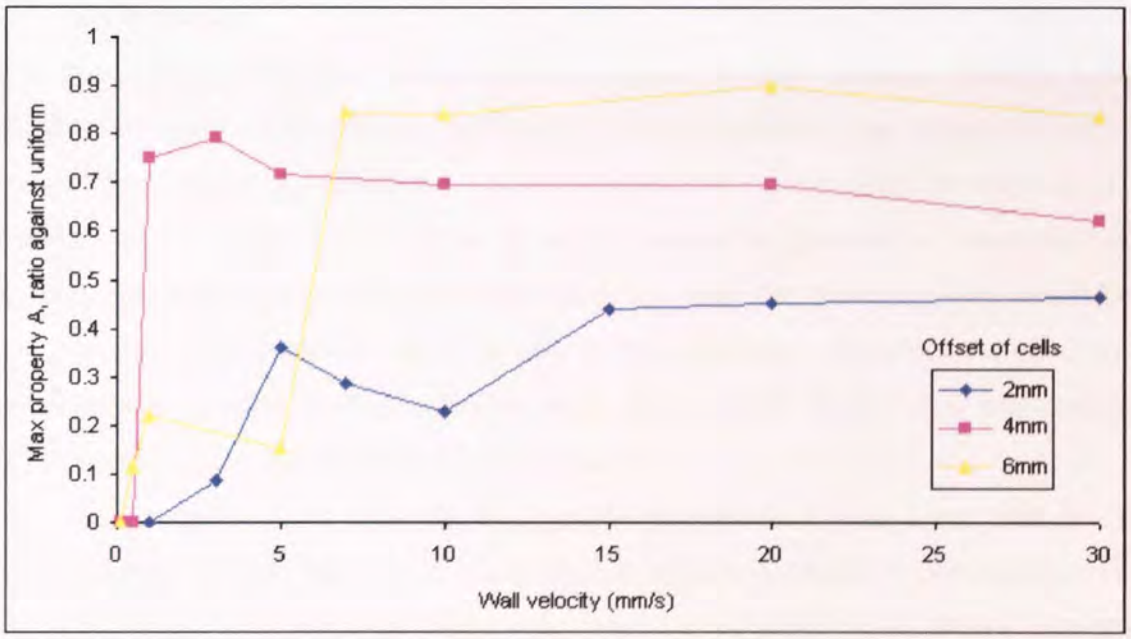

Figure 5.37. The maximum value of property A achieved, from 200 particles originating over a 0.02mm length, within the three-dimensional, geometrically periodic, throughput system, with throughput of 5mm^3/s against the velocity of the upper and lower walls, for three different offsets between cells. Property A is presented as a ratio to the average distance between particles obtained by the three different uniform distributions associate with each geometry.

Figure 5.36 shows the maximum values of property A obtained, throughout a cascade, within the domain with an offset of 4 mm, for a variety of throughput rates. Complementary to

previous systems it can be seen that the effect of increasing the throughput rate is to increase the velocity of the walls required to provide sufficient particle displacement to induce chaotic motion. One would note here, however, that the cross sectional separation achieved is not as near to that of the uniform distribution of particles as the pervious time periodic throughput system. This may suggest that there are regions of stagnation and bypassing of certain parts of the domain, probably the extremities of the offset cells.

Figure 5.37 shows the effect of the magnitude of the geometric offset of cells on the maximum value of property A throughout ranges of wall velocity. As each of the systems has a different cross sectional area, the uniform distribution of the same number of particles will produce different values. Therefore the maximum value for property A is expressed as a ratio to the respective uniform distribution average distance between particles. Thus a well-mixed system would attain a ratio of near unity and a poorly mixed system will attain a value towards zero. Figure 5.37 shows that the domain with the offset of 6mm indicates the greatest cross-sectional distance between particles. It is suggested that the larger the offset, within the range examined, the greater the area of disorder on the cross-section with respect to the uniform distribution of particles.

5.7 Conclusions.

This chapter has presented four different three-dimensional flow domains. Initially a closed cubic domain with perpendicular oscillating wall movements was examined and the transferability of property A from two- to three-dimensional systems was investigated. It was found that due to the increased number of nodes required to generate a three-dimensional mesh, and the limitations of computational hardware, that the elements were much larger which often resulted in particles stagnating near to the boundaries. To reduce the effect of this the meshes were graded to have a higher node density near to the walls and stagnating particles were detected and removed from calculations.

When using property A to quantify the particle separation it was found for the two-dimensional systems that there were distinct increases in the separation between ordered and disordered systems. This is not the case for the three-dimensional system, where even at low time periods the particles exhibit significant separation given sufficient time. This is suggested to be due to the perpendicular alternating streamline regimes of the three-dimensional system. Particles are not returned as an oscillation in three-dimensions as they are in two, instead they move further apart. The larger the time period or velocity amplitude the further they can move away from their original streamlines. However, at a low time period the particles often stay bounded with disordered regions, leaving ordered areas where no

particles pass through. Increasing the control parameter will move the system towards chaos, where the particles move randomly throughout the whole of the domain.

The time periodic domain was found to be effected only by parameters surrounding the oscillation, and not by the position of the particles as they travel through the domain, nor their throughput rate.

The wall velocity and the throughput effect both the spatial and geometric domains which are made up from repeating cells containing differing flow regimes alternating along the mixer. In these systems the wall velocity is constant and the particles come into contact with a streamline regime as they flow through the cells. The faster the wall velocity the further in any set time particles can be displaced. The slower the throughput the longer a particular particle will remain within any one streamline regime, and hence move further within it. Systems become more chaotic as the wall velocity is increased, and systems with lower throughput rates require a lower time period or wall velocity to become chaotic. This supports unequivocally that it is the displacement within alternating streamlines that is responsible for the onset of chaos.

This chapter has also shown that the property A can be used for investigating three-dimensional chaotic flow domains. Although where the alternating wall movements are perpendicular care should be taken to validate any conclusions from comparing the maximum property A over a range of control parameters by observing the particle trajectories or spread of particles pictorially. The use of property A for analysing the cross sectional view of spread of particles for throughput chaotic domains was successful. Conclusions over a range of control parameters can be drawn from the maximum value of property A. It is suggested that property A could confidently be used to quantitatively evaluate the spread of particles within a variety of systems with a more complex flow structure and geometry.

Recognising and supporting that it is the displacement of fluids within alternating streamlines that is responsible for the onset of chaos has significance for the design of industrial chaotic mixing equipment. A designer of such a mixer would need to work towards alternating the streamlines in whatever way best suits the fluid, process and budget, whilst making sure that stagnation points or bypassing does not occur. It has been shown here that the streamlines can be varied by the use of moving walls with oscillating boundaries, many small walls moving steadily, by creating alternating streamlines or repetitive geometries.

6. Investigation of a three-dimensional, time independent, mixing domain exhibiting chaotic trajectories.

6.1 Introduction.

This chapter presents a time independent, closed three-dimensional domain that exhibits chaotic motion. The system is similar to that presented by Dombre et al [96] in the respect that the flow is steady within a simple Eulerian representation but exhibits Lagrangian turbulence.

Signatures of chaos are shown to exist within the system, such as the growth of disordered regions throughout a range of operating parameters, stretching, bending and folding of a sample line of particles and sensitive dependence of initial conditions. By recording the positions of particles crossing an equidistant set of cross sectional slices and the observing and quantifying of the separation of a number of sample particles, a transitions from order to chaos is presented.

6.2 Introduction to the domain

The flow domain investigated could be considered as two cubes, each with a pair of translating walls that create a rotation, their ends placed together with ninety degree rotation, with respect to the moving walls. Each cube is of side length 10mm, the moving walls are indicated by shading in figure 6.1. Walls 1 and 3 translate in the positive z direction, whilst 2 and 4 in the negative. The wall movements are expected to cause two principle rotations in the flow, shown by the two grey cylinders in figure 6.1.

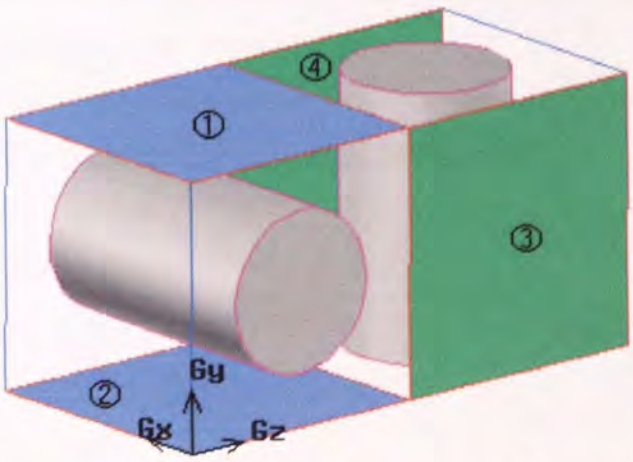

Figure 6.1. The closed three-dimensional, time-independent system. The four numbered and coloured faces indicate the moving walls and the grey cylinders represent the principle rotations that the translating walls induce.

The principle rotations within this system encourage particles to flow in a twisted figure of eight regime. Therefore for the continuation of this work, the above system will be referred to as the twisted figure of eight mixer (TF8).

The control parameter initially considered to induce chaotic motions in the TF8 is the velocity of the pairs of moving walls, and the effect of the velocity of one pair of walls with respect to the other. The velocities of the pairs of walls are presented as ratios, although it should not be considered at this stage that the ratio is the control parameter. This is discussed in more detail later in this work.

6.3 Investigation of the TF8

This chapter presents a range of time-independent cases with wall pair velocity ratios from 0.1 to 10. The velocity of one pair of walls is held constant whilst the affect of varying the velocity of the other pair, on the fluid flow regime, is considered. This is conducted for four different magnitudes of the constant velocity pair of walls.

Three methods of analysis are used to observe the effect of the differing wall pair velocities on the system and to indicate the disorder throughout the transition into chaotic motion. The first observation method, used for one constant velocity range, follows the evolution of randomly generated particles by the use of slices along the domain. The second observes the spread of particles from a small generation zone as time evolves. The third quantifies the spread of a sample of initially close particles by calculating property A.

6.3.1 Slices along the TF8

The use of slices involves the continued observation of where particle trajectories intersect an number of two-dimensional cross sections. By using this technique it is possible to observe more clearly islands of stagnation and areas of chaos.

Nineteen parallel cross sectional slices, perpendicular to the z axis, one mm apart, along the 20mm length are used to observe the trajectories, as in figure 6.2.

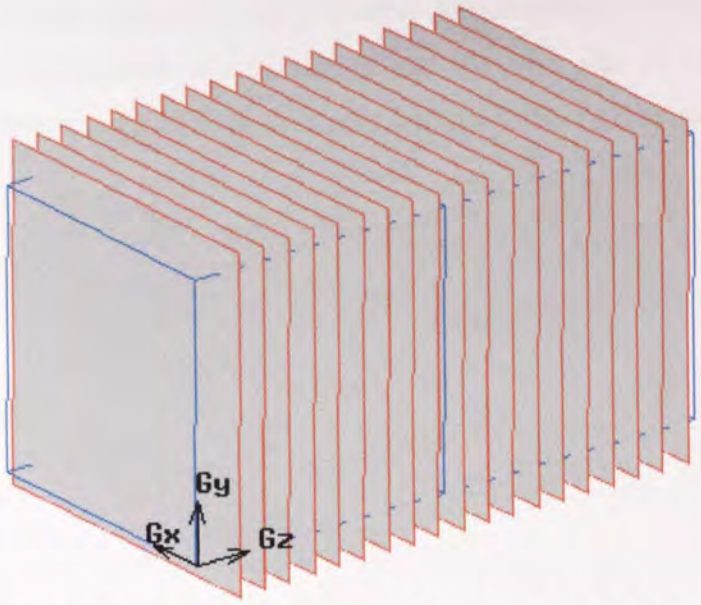

Figure 6.2. The nineteen cross sectional slices spaced 1mm apart along the TF8 mixing domain.

For each of the system velocity configurations investigated twenty-five particles are randomly produced throughout the whole domain and are allowed to evolve for one thousand seconds. Each time a particle passes through a slice the nearest trajectory co-ordinates either side are interpolated to produce a mapping of that trajectory. The interpolation is linear between the two positions either side of the slice, and is not considered to require significant optimisation as a small time step between trajectory co-ordinates of 0.1 seconds is used. The calculation of the slices and the crossing points of the particles required the creation of a specific post processing code, which can be found, annotated, in appendix D.

The results consist of a series of slices that indicate the motion of particles throughout the domain. The slices are presented in the format shown in figure 6.3, where the numbers correspond to the position, in mm, along the domain in the z direction.

1	2	3	4
5	6	7	8
9	10	11	12
13	14	15	16
17	18	19	

Figure 6.3. The format for the presentation of the slices along the TF8 mixing domain. The numbers on the slices here correspond to the position in millimetres of the slice along the z axis.

Initially five sets of system parameters are presented where one pair of walls (walls 3 and 4) are moving with a constant translation of 5mm/s. and the other pair of walls (walls 1 and 2) translate at five different velocities over the range 0 mm/s to 50mm/s (ratios of wall velocities of 0 to 10).

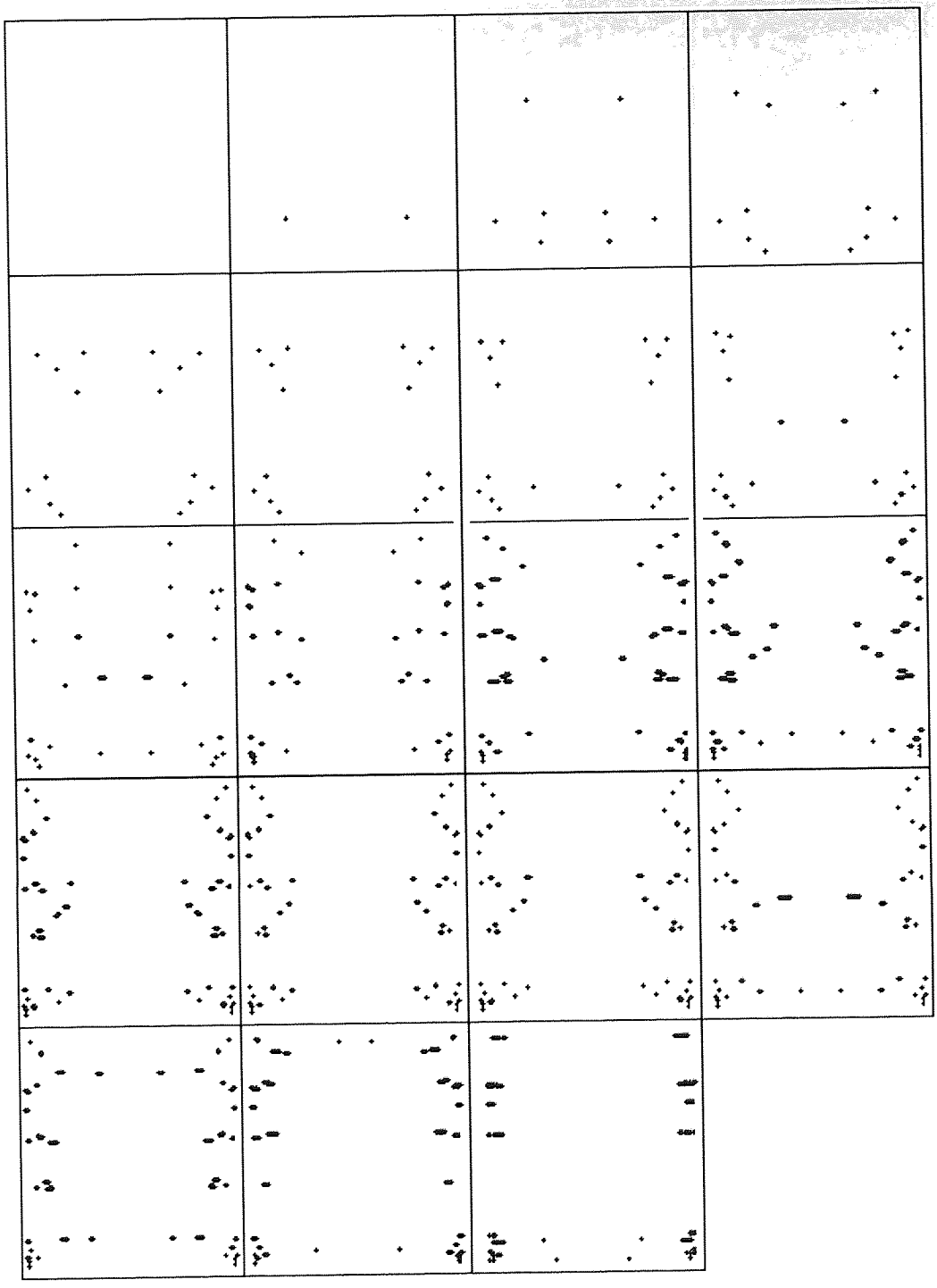

Figure 6.4. Nineteen cross sectional slices spaced every millimetre along the z-axis of the TF8 mixer showing the points of intersection of twenty-five particles evolving for one thousand seconds. Walls 3 and 4 are translating at 5mm/s, whilst walls 1 and 2 are stationary (Wall velocity ratio=0)

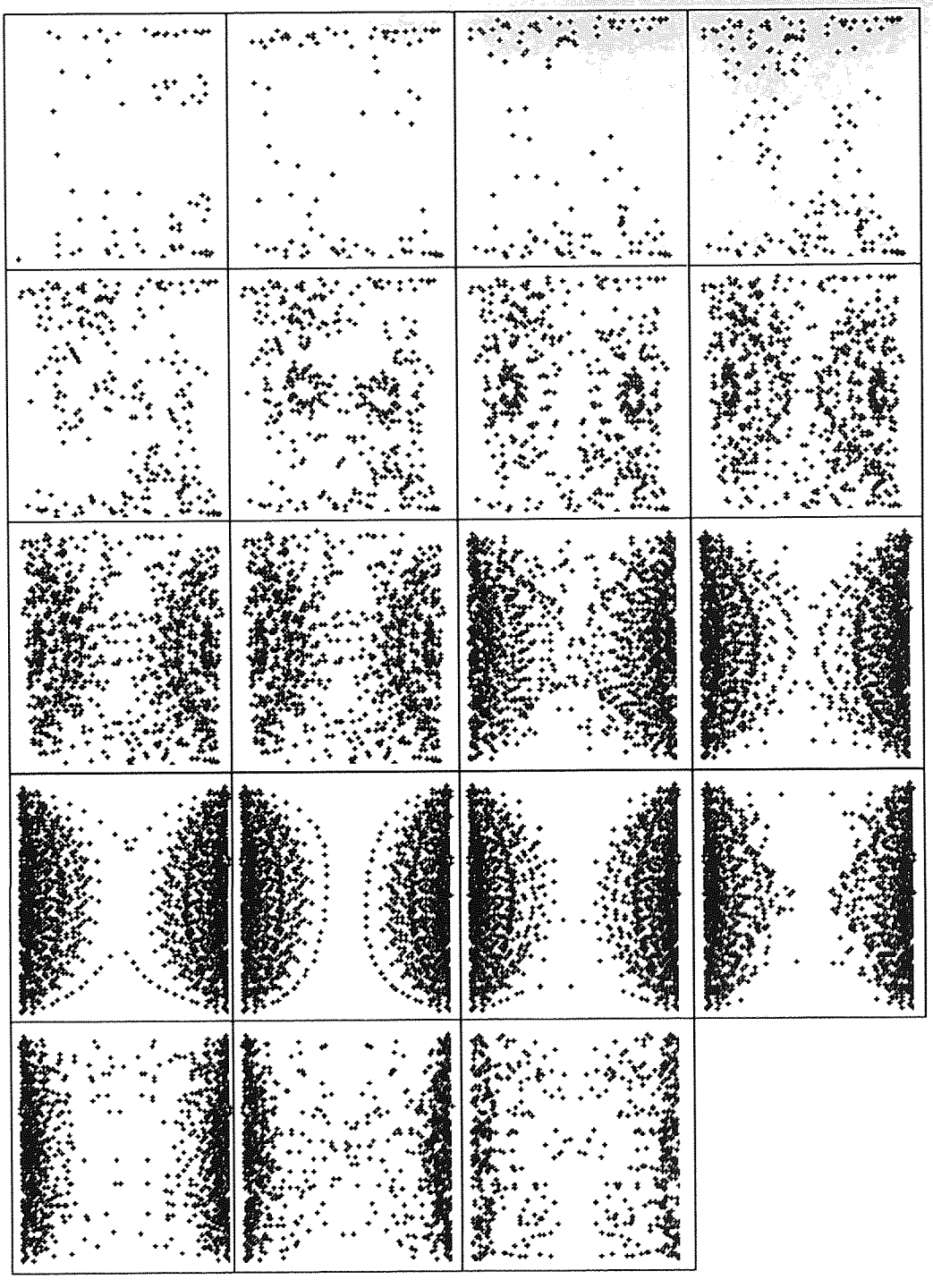

Figure 6.5. Nineteen cross sectional slices spaced every millimetre along the z-axis of the TF8 mixer showing the points of intersection of twenty-five particles evolving for one thousand seconds. Walls 3 and 4 are translating at 5mm/s, whilst walls 1 and 2 translate at 0.5mm/s (Wall velocity ratio=0.1)

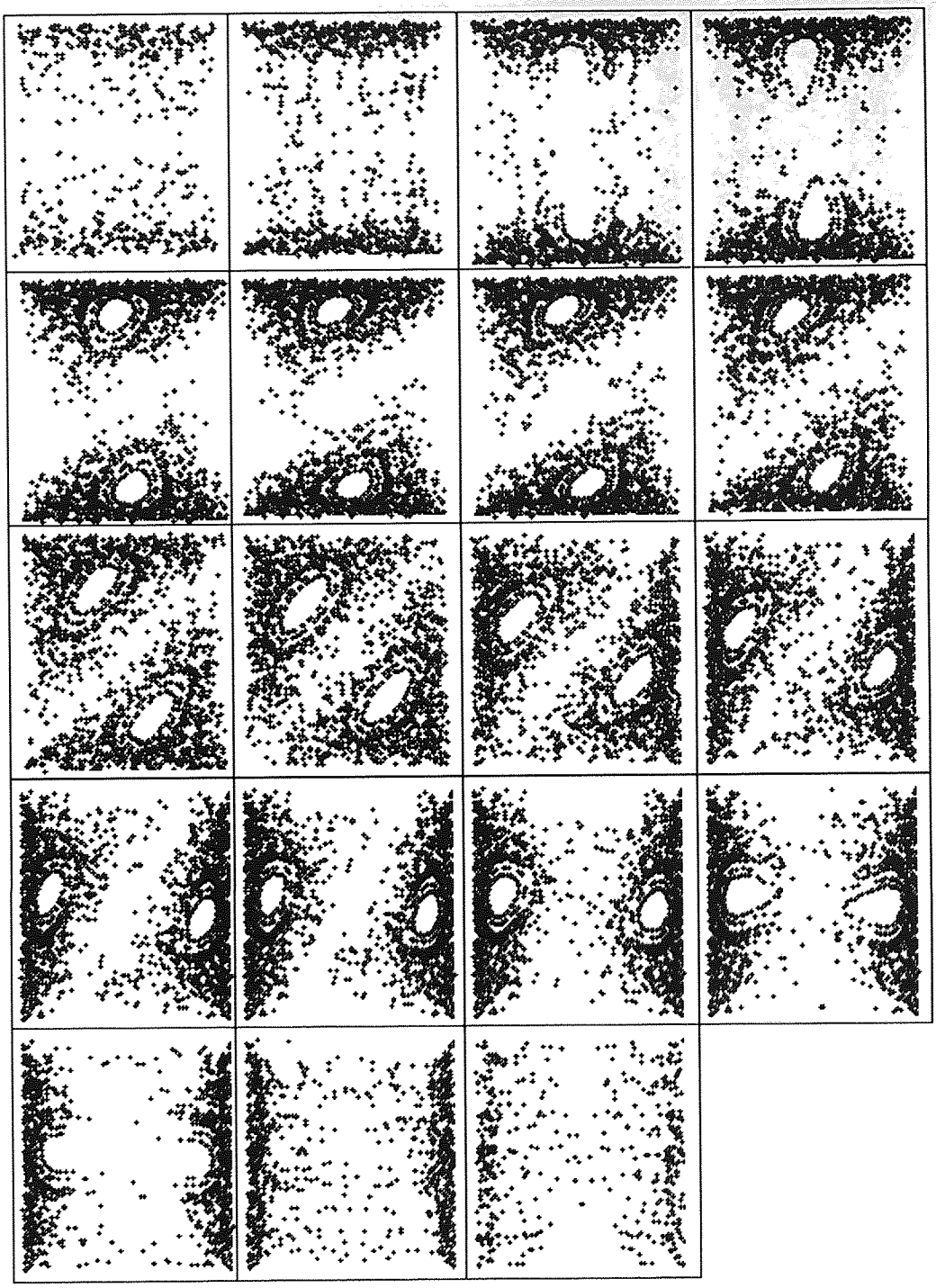

Figure 6.6. Nineteen cross sectional slices spaced every millimetre along the z-axis of the TF8 mixer showing the points of intersection of twenty-five particles evolving for one thousand seconds. Walls 3 and 4 are translating at 5mm/s, whilst walls 1 and 2 translate at 5mm/s (Wall velocity ratio=1)

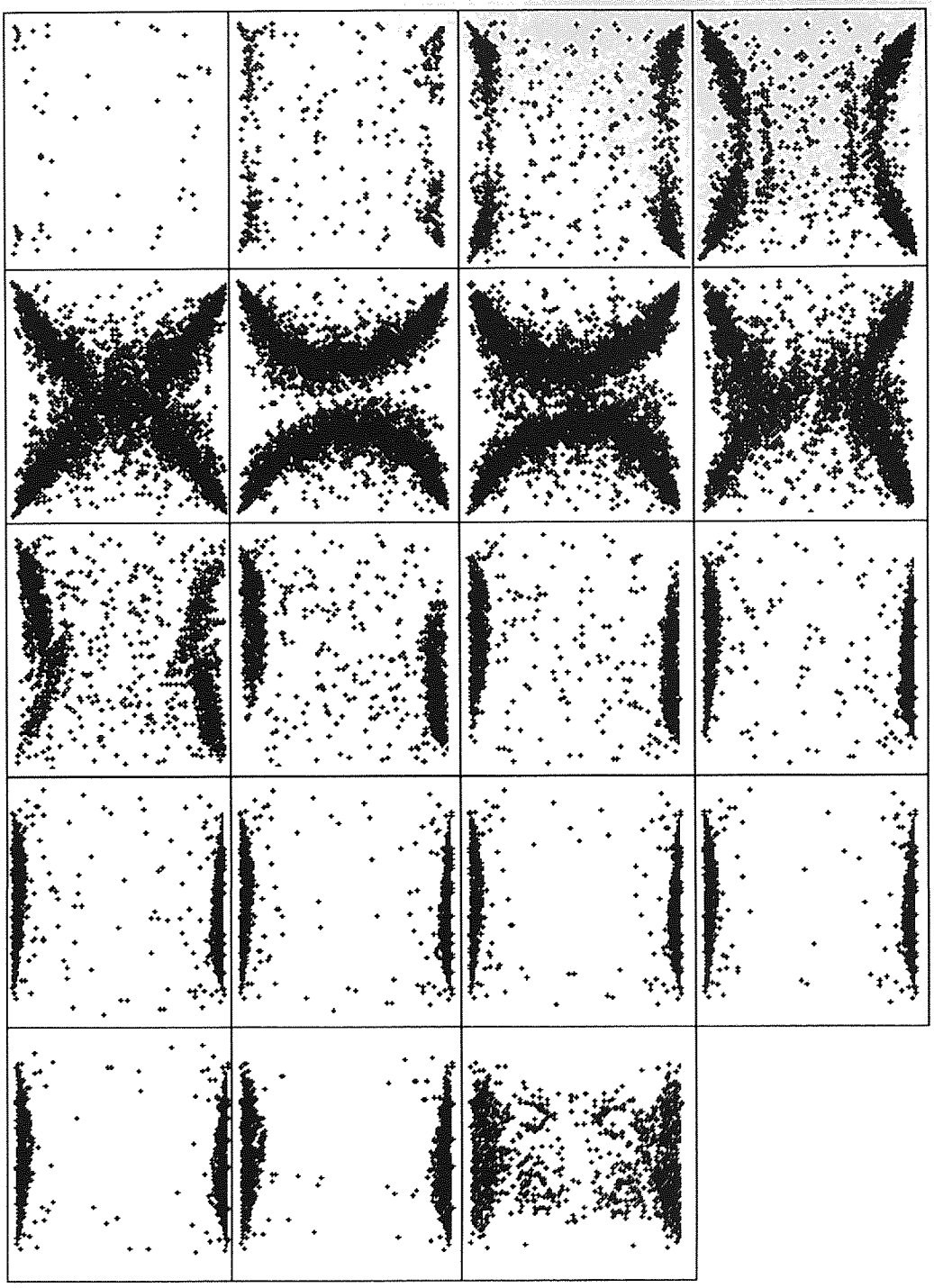

Figure 6.7. Nineteen cross sectional slices spaced every millimetre along the z-axis of the TF8 mixer showing the points of intersection of twenty-five particles evolving for one thousand seconds. Walls 3 and 4 are translating at 5mm/s, whilst walls 1 and 2 translate at 20mm/s (Wall velocity ratio=4)

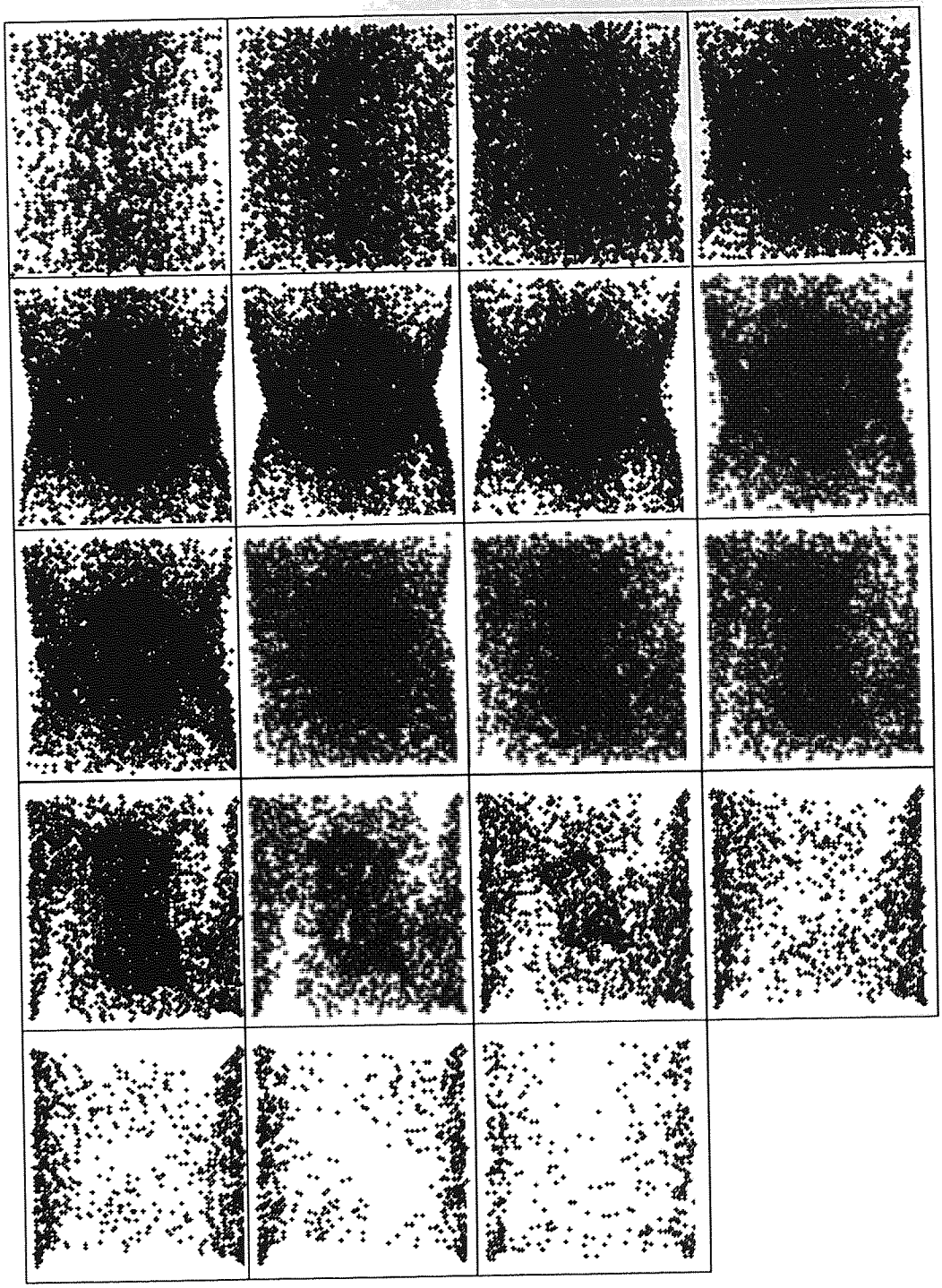

Figure 6.8. Nineteen cross sectional slices spaced every millimetre along the z-axis of the TF8 mixer showing the points of intersection of twenty-five particles evolving for one thousand seconds. Walls 3 and 4 are translating at 5mm/s, whilst walls 1 and 2 translate at 50mm/s (Wall velocity ratio=10)

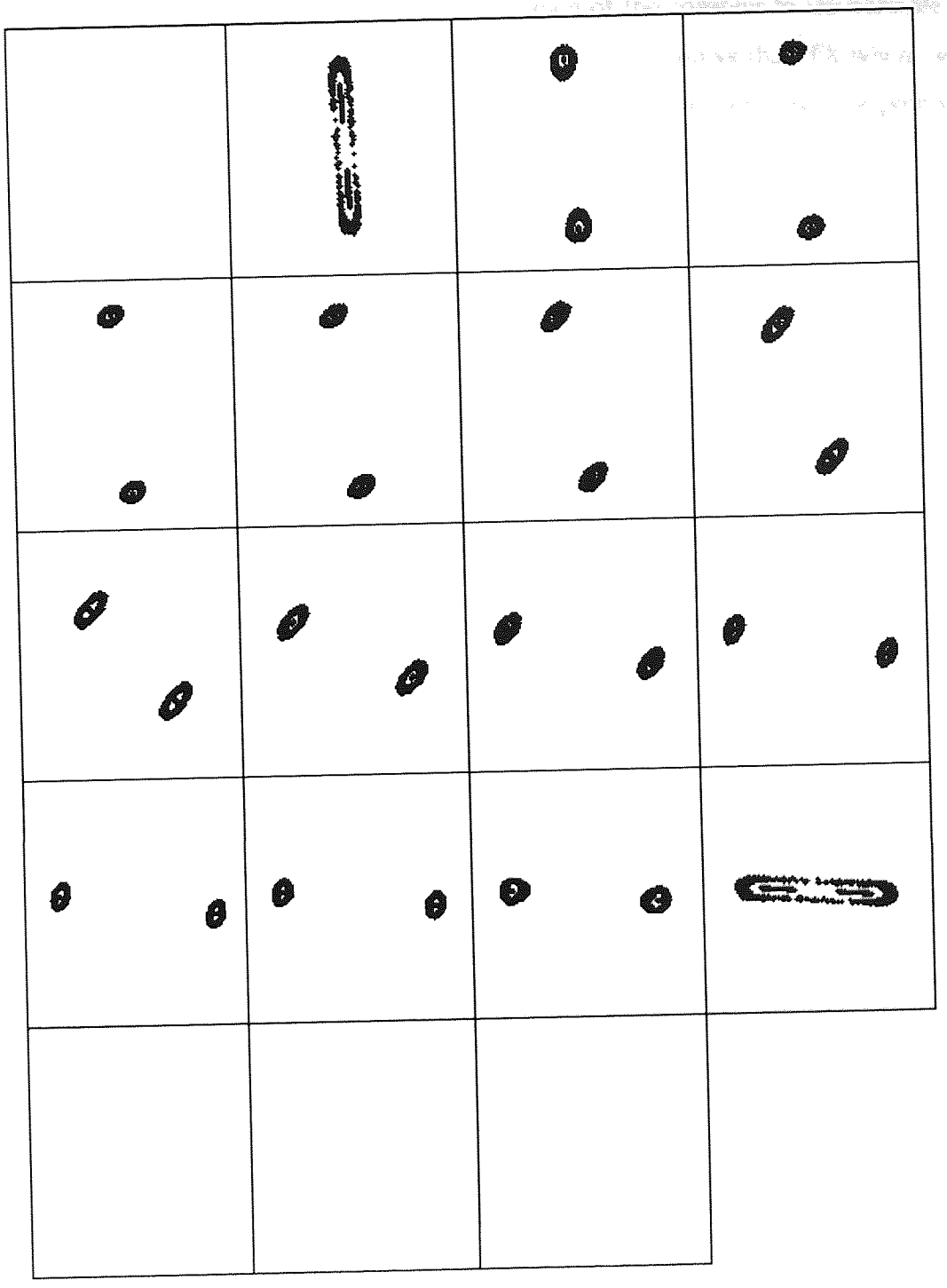

Figure 6.9. Nineteen cross sectional slices spaced every millimetre along the z-axis of the TF8 mixer showing the points of intersection of twenty-five particles originating with a tori evolving for one thousand seconds. Walls 3 and 4 are translating at 5mm/s, whilst walls 1 and 2 translate at 5mm/s (Wall velocity ratio=1)

Figures 6.4 to 6.8 show the nineteen cross sectional slices of the TF8, with the constant moving pair of walls with a velocity of 5mm/s. Ratios of the constant to the variable pair of moving walls are 0, 0.1, 1, 4 and 10 respectively. Figure 6.4 shows the TF8 where only one pair of walls is in motion (walls 3 and 4.) It can be seen that there are few points where particles have crossed the slices. This would suggest that the motion of the particles is periodic, and cross each slice at the same point.

When the system is operated with the second pair of walls in motion, with a translation velocity 0.5mm/s, it can be seen that the second principle rotation is affecting the systems order. Figure 6.5 shows that particles no longer exhibit periodic motion, and regions of disorder are evident within the flow domain. It is also possible, however, to observe ordered regions indicated by the empty spaces on the slices. Figure 6.6 shows the slices along the TF8 where all moving walls have equal velocity magnitudes. It is possible to observe symmetry within the system. The slice positioned where z=10, in the middle of the domain has symmetry across its diagonal. At low z slices there is an obvious empty region running left to right across the slice. As one observes slices from the origin along the positive z direction, it can be seen that the empty region twists, until it runs top to bottom of the slice at high z values. These empty regions correspond to the principle rotations created by the wall translations, and the rotation symmetry is due to all wall velocities being equal. It can be seen that there are significant areas of disordered flow, broken up by the twisted empty regions. It is also possible to observe secondary rotations caused by the principle rotations. These can be seen as empty islands surrounded by what appears to be invariant curves. Particles that originate and move within disordered regions cannot enter the ordered regions from tori and likewise particles within tori cannot exit. This is clearly shown in figure 6.9 where the regular region clearly is impenetrable, as the twenty-five particles that originate within the tori do not exit. Particles may be travelling around the TF8 with some periodicity giving rise to elliptic points, which is suggested by the concentric orbits of the invariant curves

When the velocity of the moving walls 1 and 2 is increased to four times of that of walls 3 and 4, it can be seen in figure 6.7 that the presence of the tori is no longer evident and the regions of disorder appear to now be primarily in the half of the domain associated with the faster pair of walls. When the system is operated with walls 3 and 4 ten times faster than walls 1 and 2 (ratio of 10) it can be seen that great disorder occurs. Here again the disordered region is mostly between the faster pair of walls, except disorder has engulfed the majority of that half and is extending into the slower moving half of the domain also.

Figures 6.4 to 6.8 show that the TF8 with one pair of walls moving produces periodic particle trajectories. If the second pair of walls is also set in motion then disorder regions appear within the ordered flow. As the velocity of one pair of walls is increased the disordered

regions within the system also increase up to the point where the majority of the TF8 domain is disordered.

It is considered that it is the velocity of the walls and the ratio of the velocities of the wall pairs, not the ratio of velocities alone, that is responsible for the transition into increased disorder. This is suggested due to if the control parameter were wall ratio alone then the TF8, when operating with a wall pair ratio of 0.1 would, with rotational symmetry, be equivalent to the ratio of 10. It can be seen however (figure 6.4 and 6.8) that the particle trajectories are significantly different and therefore it is the velocity and the ratio that affects the disorder.

6.3.2 Discussion of the separation of particles in the TF8, pictorially.

In this section the spread of 200 initially close particles is observed. Figure 6.10 shows the initial position of the small zone within which the particles originate. The particle positions are selected at random within the zone, and allowed to evolve for 1000 seconds. The position of each particle is recorded at intervals of time and shown, in figures 6.11-6.15, for the same range of wall velocities as section 6.3.1.

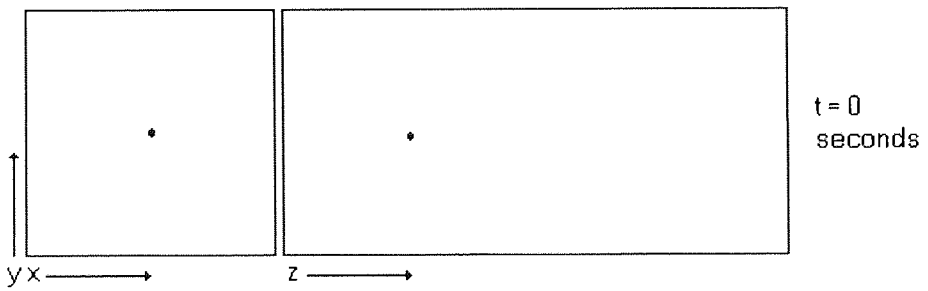

Figure 6.10. Showing the small zone where the two-hundred particles originate in the TF8 mixer.

As expected the separation of particles, where only one pair of walls is in operation, is small. After 1000 seconds in figure 6.11 it can be seen that the line of particles has stretched. Which can be attributed to laminar shear. The separation of particles in the system with a wall pair velocity ratio of 0.1, figure 6.12, is also low, however, there does appear to be the presence of some bending and folding beginning to take place at approximately 1000 seconds. The following three velocity ratios of 1, 4 and 10, in figures 6.13 - 6.15 respectively, show that bending and folding of the particle set does take place. Particles completely separate and disassociate from their original neighbours. Reaching this point is much more rapid for a wall pair ratio of 10.

As with the previous section the disorder in the system appears to be significantly increased as the ratio of the velocities of the wall pairs is increased. Once again though it is suggested that the ratio and the velocity is responsible for the onset of chaotic motions.

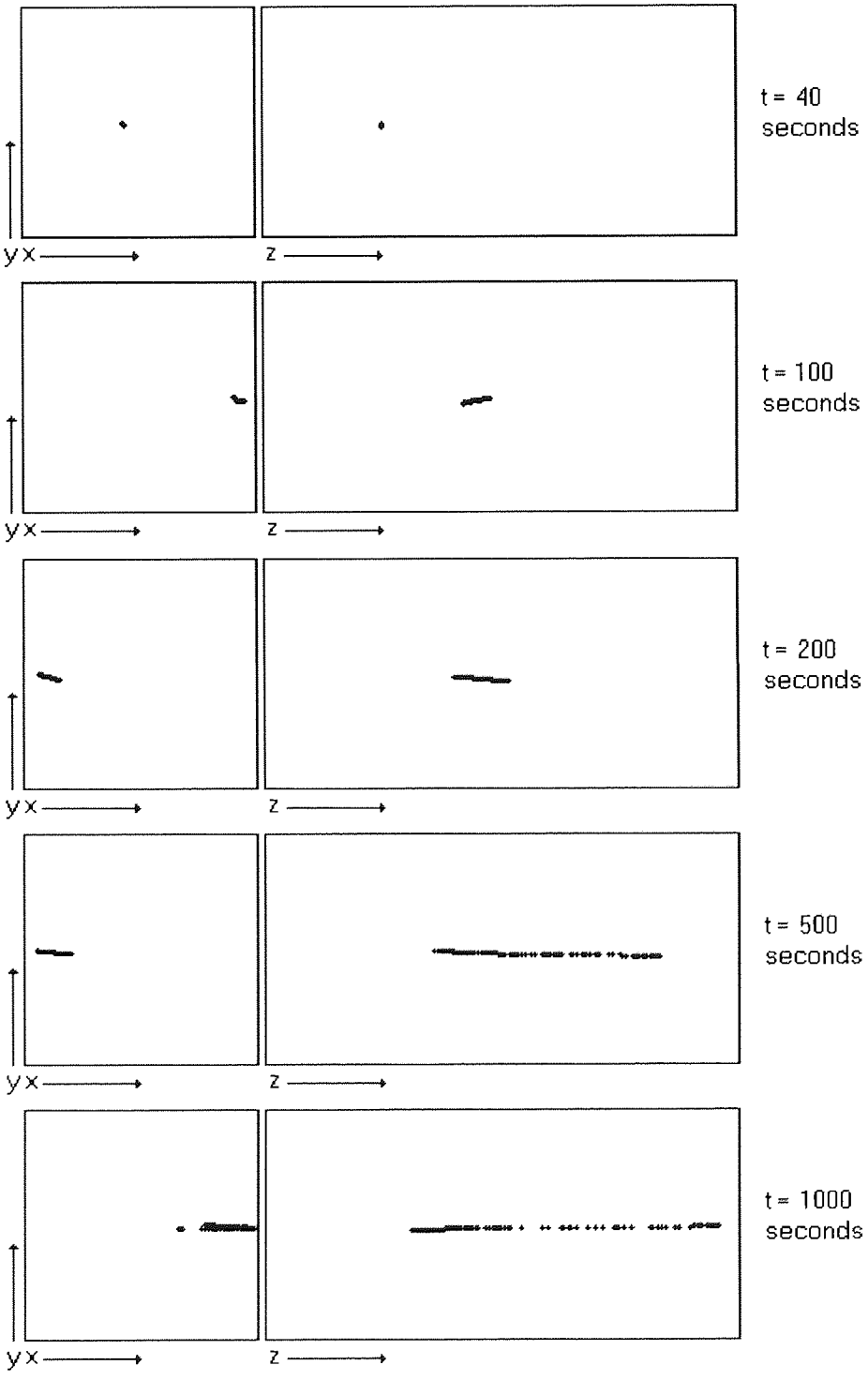

Figure 6.11. xy and yz views of the TF8 mixer showing the positions of two hundred originally close particles after varying amounts of time. Walls 3 and 4 are translating at 5mm/s, whilst walls 1 and 2 are stationary (Wall velocity ratio=0)

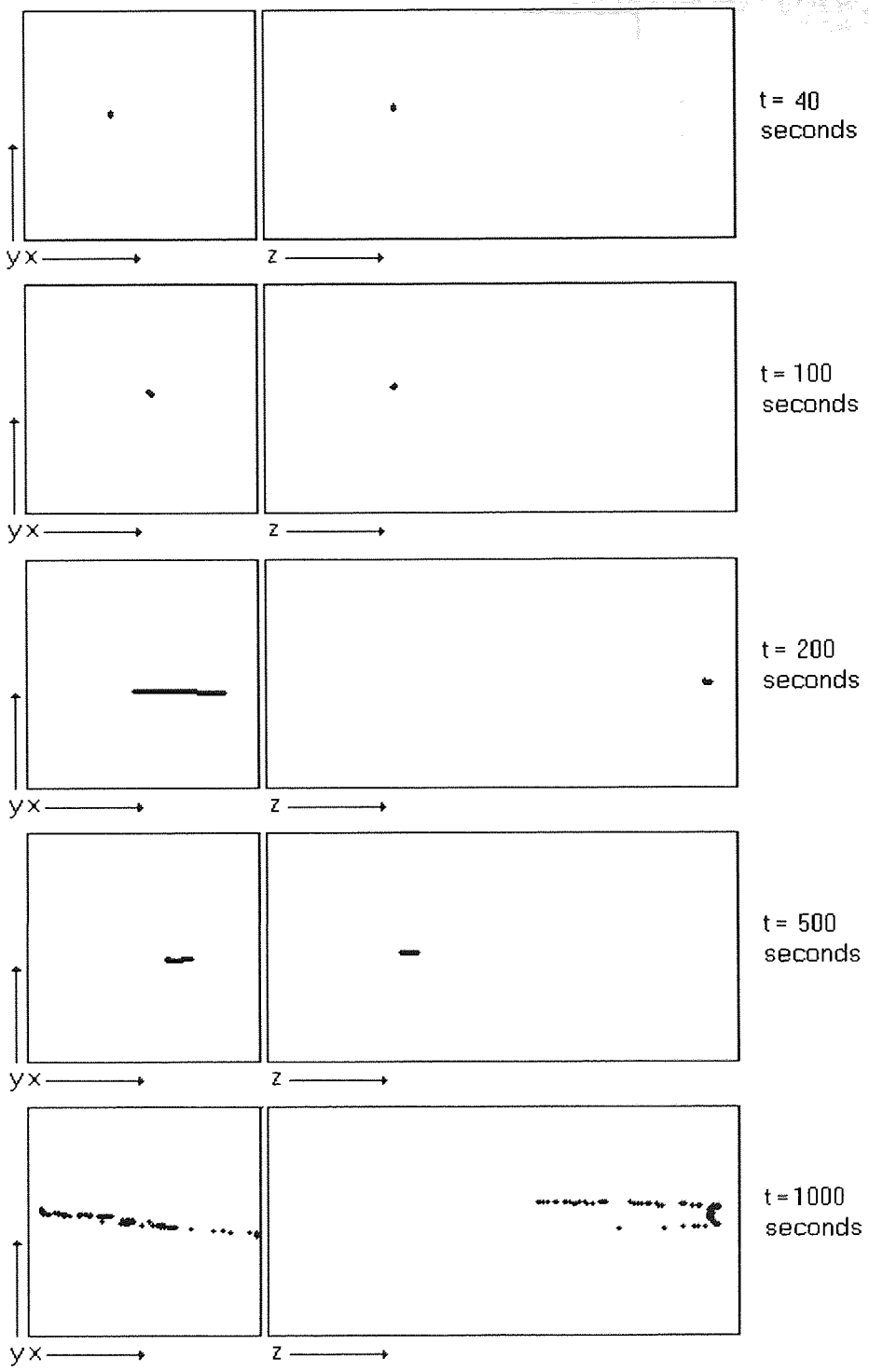

Figure 6.12. xy and yz views of the TF8 mixer showing the positions of two hundred originally close particles after varying amounts of time. Walls 3 and 4 are translating at 5mm/s, whilst walls 1 and 2 are translating at 0.5mm/s (Wall velocity ratio=0.1)

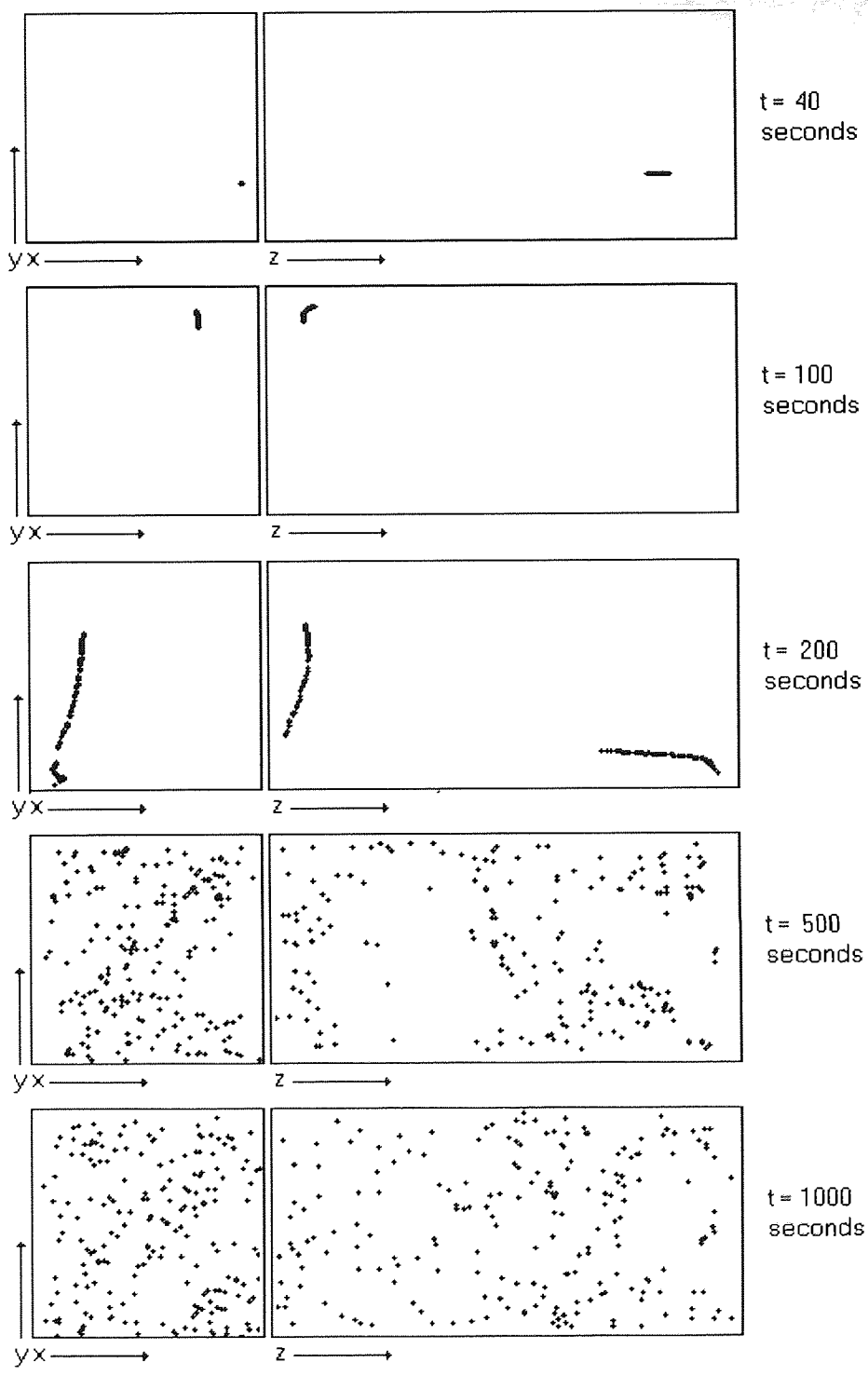

Figure 6.13. xy and yz views of the TF8 mixer showing the positions of two hundred originally close particles after varying amounts of time. Walls 3 and 4 are translating at 5mm/s, whilst walls 1 and 2 are translating at 5 mm/s (Wall velocity ratio=1)

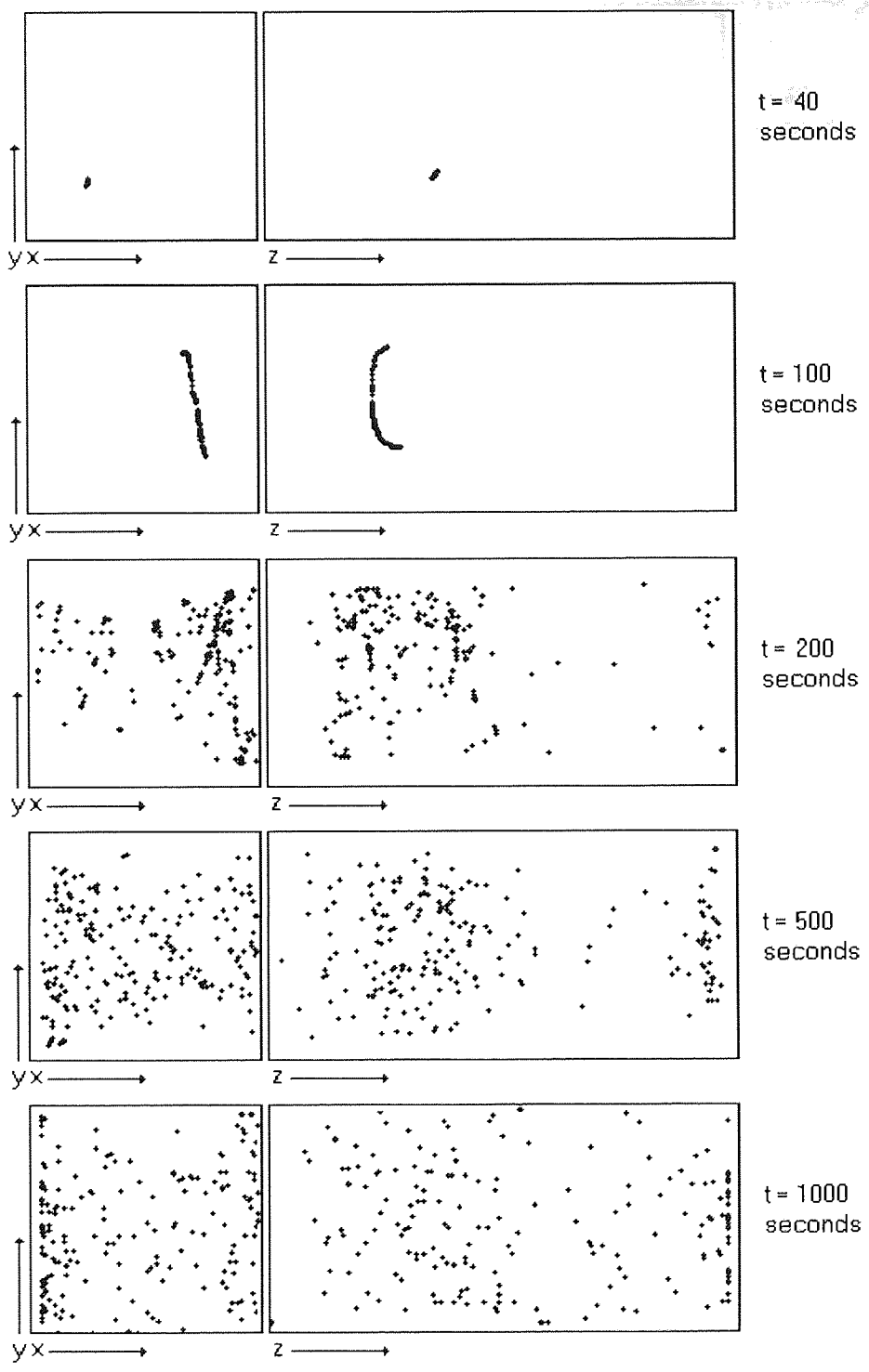

Figure 6.14. xy and yz views of the TF8 mixer showing the positions of two hundred originally close particles after varying amounts of time. Walls 3 and 4 are translating at 5mm/s, whilst walls 1 and 2 are translating at 20 mm/s (Wall velocity ratio=4)

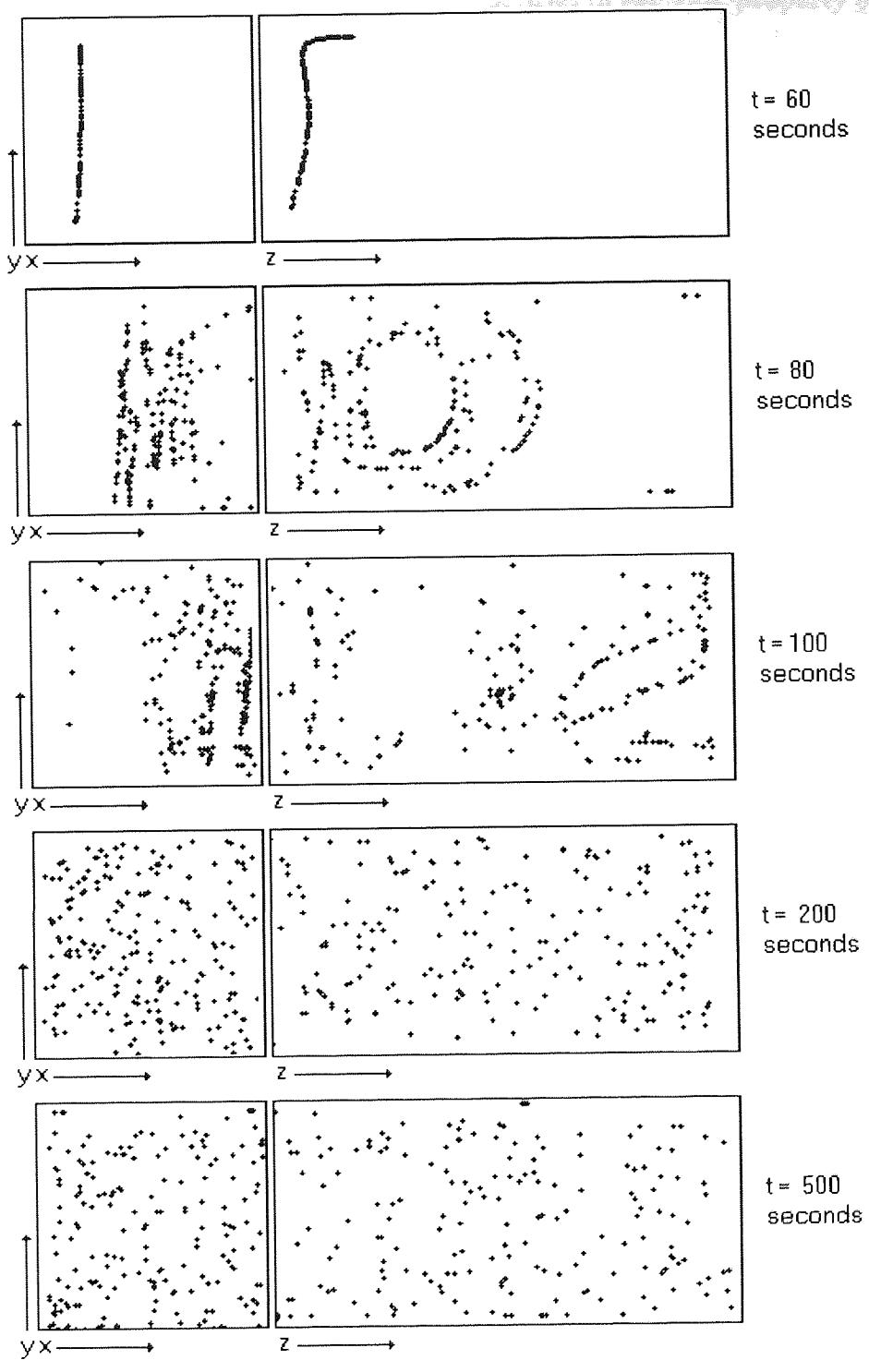

Figure 6.15. xy and yz views of the TF8 mixer showing the positions of two hundred originally close particles after varying amounts of time. Walls 3 and 4 are translating at 5mm/s, whilst walls 1 and 2 are translating at 50 mm/s (Wall velocity ratio=10)

6.3.3 Discussion of the separation of particles in the TF8, property of divergence of the distance between particles.

The separation of initially close particles can be quantified by the use of property A. Figures 6.16 –6.19 show property A against time for constant wall velocities of 0.1, 1, 5 and 10 mm/s respectively, for eight different wall velocity ratios.

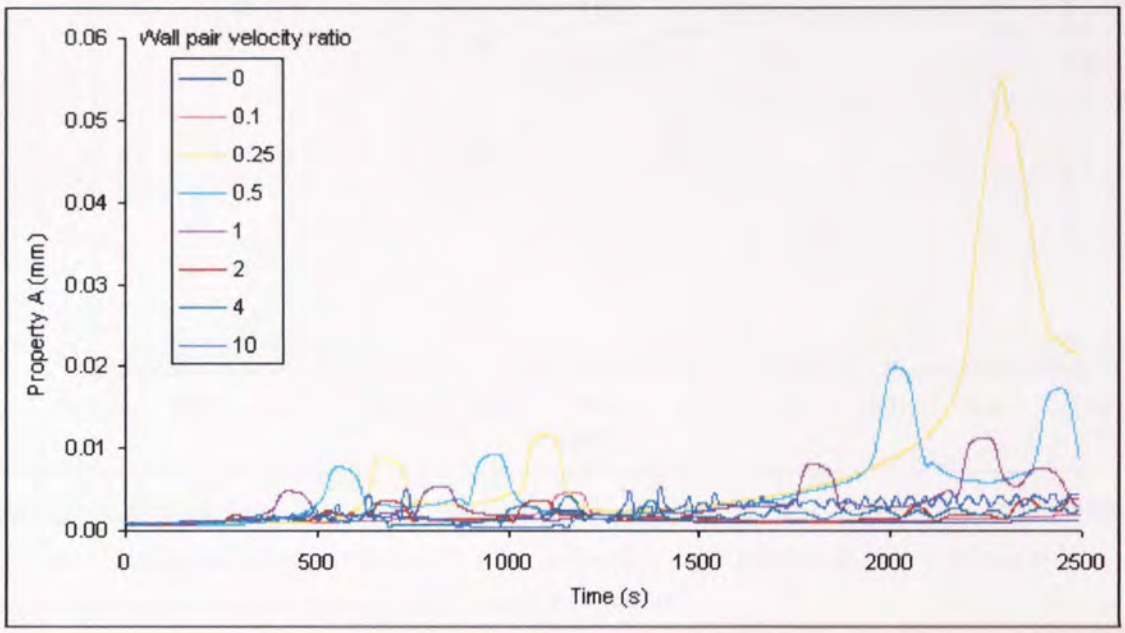

Figure 6.16. Property A calculated from 200 initially close particles within the TF8 over 2500 seconds, where walls 3 and 4 translate with a base velocity of 0.1 mm/s and walls 1 and 2 translate at various velocities corresponding to ratios between the two pairs of walls from 0 to 10.

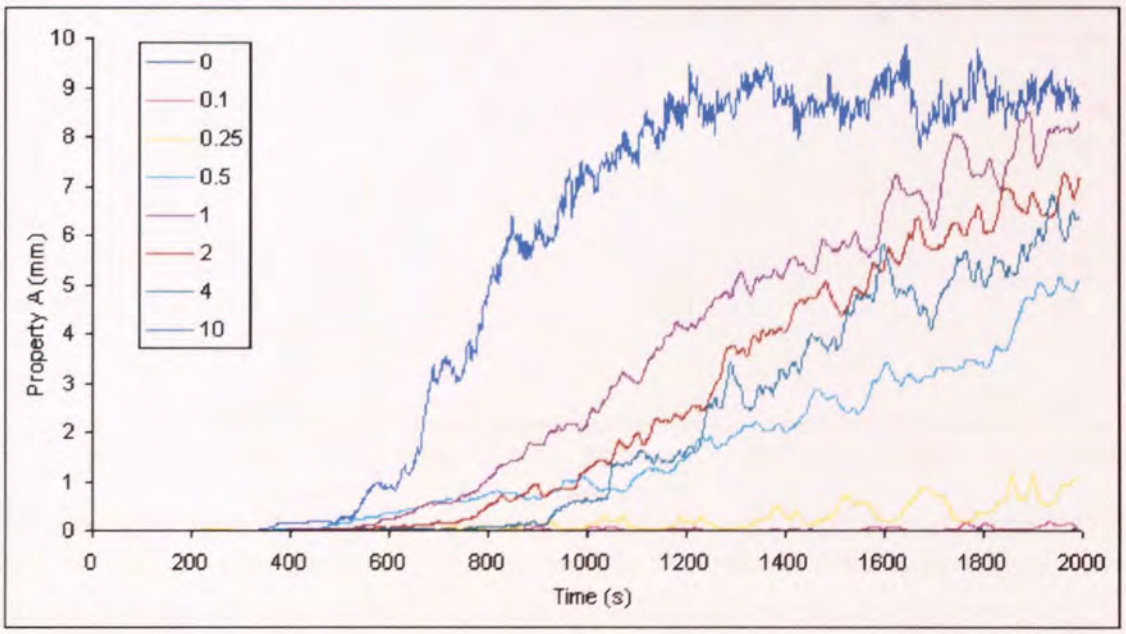

Figure 6.17. Property A calculated from 200 initially close particles within the TF8 over 2000 seconds, where walls 3 and 4 translate with a base velocity of 1 mm/s and walls 1 and 2 translate at various velocities corresponding to ratios between the two pairs of walls from 0 to 10.

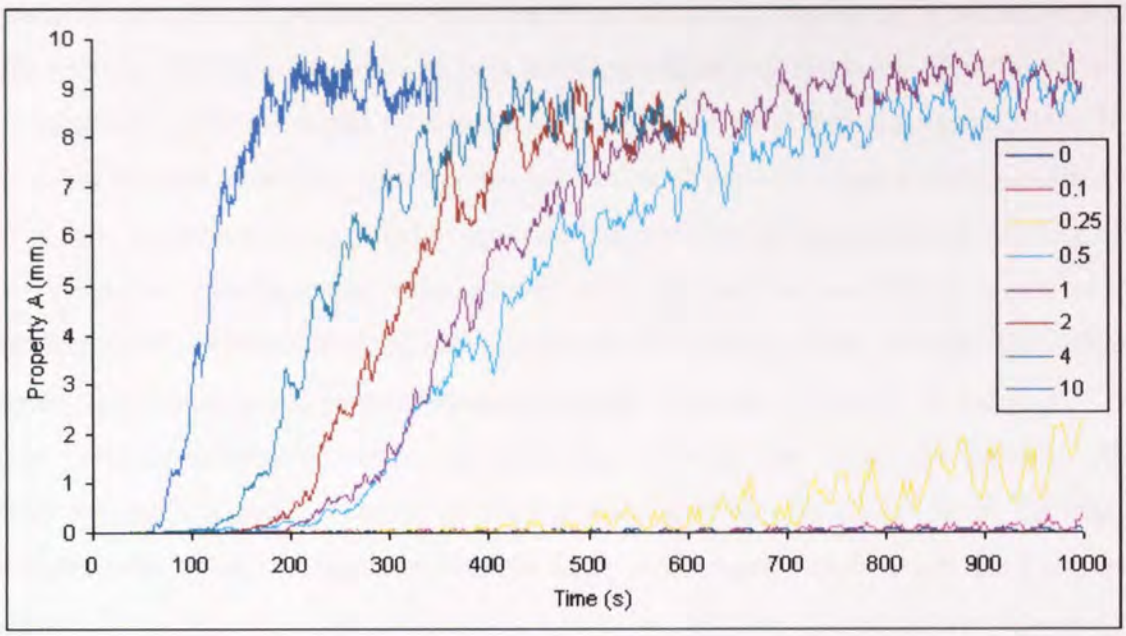

Figure 6.18. Property A calculated from 200 initially close particles within the TF8 over 1000 seconds, where walls 3 and 4 translate with a base velocity of 5 mm/s and walls 1 and 2 translate at various velocities corresponding to ratios between the two pairs of walls from 0 to 10.

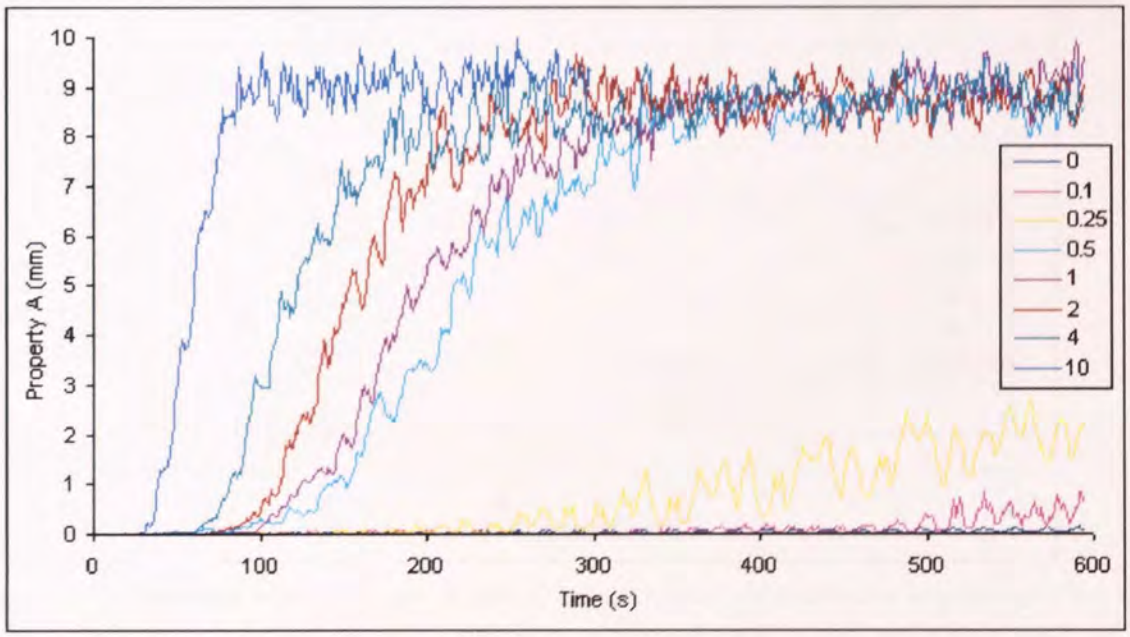

Figure 6.19. Property A calculated from 200 initially close particles within the TF8 over 600 seconds, where walls 3 and 4 translate with a base velocity of 10 mm/s and walls 1 and 2 translate at various velocities corresponding to ratios between the two pairs of walls from 0 to 10.

Figure 6.16 shows the TF8 where the base velocity of both walls 3 and 4 is 0.1mm/s. where it can clearly be seen that the particles do not significantly diverge, even where the ratio is ten. Where the base velocity is increased to 1mm/s it can be seen in figure 6.17 that when operating with a ratio of 0.5 or above some separation of particles does occur. Once again one can observe the plot of property A that has been previously shown to be characteristic of chaotic motion, rapid growth followed by a levelling off period. Figures 6.18 and 6.19, where the constant velocities are 5 and 10 mm/s respectively also exhibit characteristic plots. It can be seen that for both base velocities that the separation of particles occurs more rapidly as the velocity ratio is increased. It would be expected that the effect of increasing the velocity of the system would be to increase the distance travelled by the particles, and therefore subject them more often to the differing flow associated with the two halves of the domain. This effect of increased velocity can again be seen when comparing the plots in figure 6.18 and 6.19.

In time periodic systems the effect of increasing velocity was to reduce the time period required for chaos to occur. There is no such cascade shifting effect here. From the range of velocities tested it can be suggested that the ratio of the velocities between the two sets of walls must be sufficiently large for chaos to occur. For all base velocities investigated chaos consistently did not occur for systems with ratios of 0, 0.1 and 0.25. It could be suggested that the 'twist' in the flow is required to be sufficient enough to significantly displace particles from streamlines motions. However no comment can be made about the disorder within a system with a low wall velocity ratio with a significantly increased the wall base velocity.

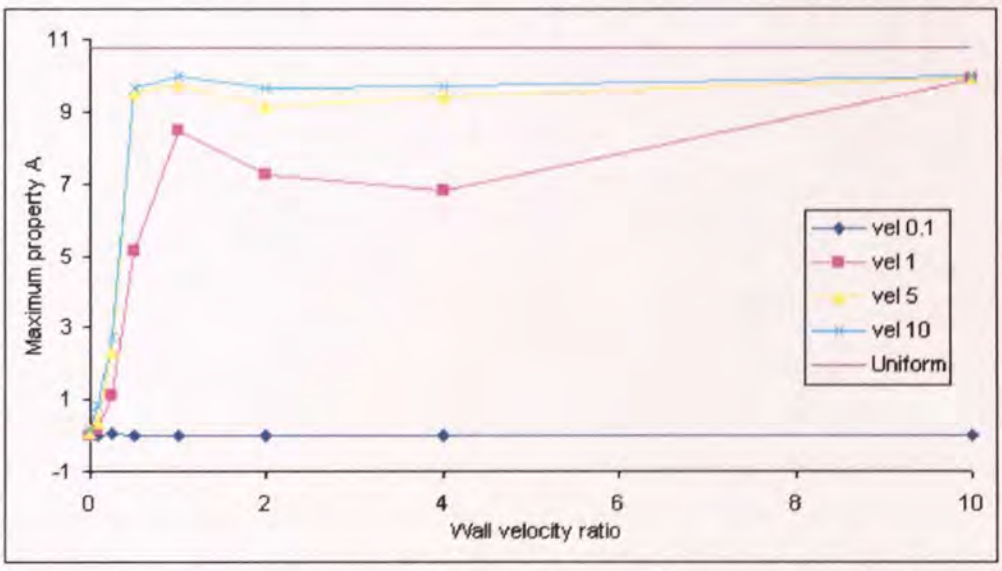

Figure 6.20. The maximum value of property A achieved in the TF8 in the times indicated in figures 6.16 to 6.19 over a range of wall pair velocity ratios, for a number of base velocities, compared to the average distance between two hundred uniformly distributed particles.

Figure 6.20 shows the maximum divergence between the particles for the systems with different constant velocities. It suggests that the as the base velocity is increased the

maximum divergence also increases. This is thought not to be the case. The low values of property A are due to the initially close particles not having sufficient time to completely separate. Figure 6.21 shows the distance between two particles originating 0.001mm apart within the TF8 with a base velocity of 0.1mm/s over a range of velocity ratios for 20,000 seconds. It can be seen that the system now displays significant divergence at ratios of 0.5 and above.

The above results would suggest that there is a required ratio between the velocities of the two pairs of walls in order for chaos to occur. If one more microscopically observed the range of ratios between 0 and 0.5 one is likely to observe a cascade of period doubling towards chaotic motion similar to that observed for time period domains.

It has also been shown that once within a chaotic regime that the effect of increasing the base velocity is to reduce the time required to significantly separate initially close particles. There is no evidence to suggest that the base velocity has any affect on the point at which chaos occurs within a range of a control parameter which is, in this case, the ratio of wall pair velocities.

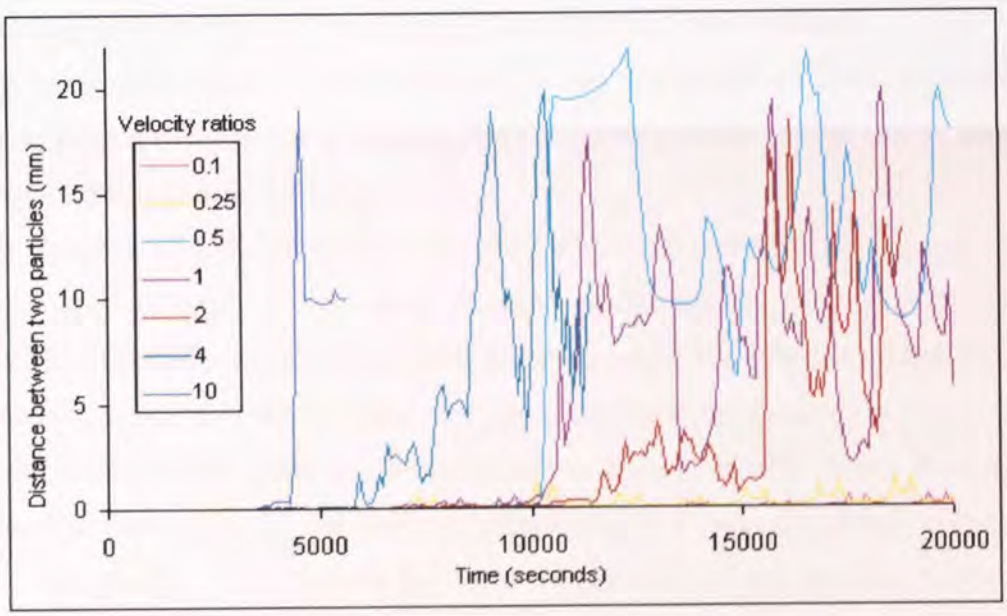

Figure 6.21. The distance between two initially close particles within the TF8 over 20,000 seconds, where walls 3 and 4 translate with a base velocity of 0.1 mm/s and walls 1 and 2 translate at various velocities corresponding to ratios between the two pairs of walls from 0 to 10.

6.4 Discussion and conclusion

Figures 6.4 to 6.9 show clearly that the separation achieved between initially close particles is likely to be dependent on their initial positions throughout the domain. The majority of the disorder in the TF8, can be observed between the faster wall pair. This can be seen when comparing the TF8 with a base velocity of 1 mm/s and a ratio of 10, with a base velocity of

10mm/s and a ratio of 0.1. These two systems are directly comparable through rotational symmetry and the only difference is that the particles observed originate within opposite halves of the TF8 domain. The particles originating within the faster half of the domain exhibit significant separation. This is noticeably different to the poor separation indicated in the same system where the particles originate within the slower half of the domain. The systems would be comparable if the particles used to calculate property A in the two systems were both from the same of either the fast or slow side.

This chapter has investigated the presence of chaotic trajectories within a time independent system. Investigating the system by the use of cross sectional slices highlighted that as the velocity ratio between the two pairs of walls increased from ratio=0 disordered regions appeared. These grew until they covered the majority of the domain, and in particular the half containing the faster pair of moving walls. Ordered regions were found within the system and the presence of a tori was evident when the wall pair velocity was equal.

The TF8 was also investigated over a range of operating parameters by observing the spread of a sample of particles originating from a small zone within the flow domain. This highlighted the presence of bending and folding of the sample line of particles became more evident and rapid as the ratio of the velocity of the wall pairs was increased.

The same spread of particles was quantified by the use of property A. It has been shown that it would be possible to observe a cascade from order into chaos by the use of property A, when supported by pictorial methods.

The control parameter considered here is the ratio of the wall pair velocities. It was found that once within a chaotic regime the effect of increasing the control parameter further was to reduce the time taken for initially close particles to separate. The effect of increasing the base velocity was to reduce the time taken by particles to separate significantly.

Due to variances in the disorder at different positions throughout the system the cascade can only represent the region of the domain within which it was generated. However it is suggested that similar trends would be found irrespective of the position of the particle generation zone.

7. Discussion, further investigation and development of property A.

7.1 Introduction.

The previous chapters have shown a variety of systems and through these presented variations in fluid movements as control parameters and boundary movements have varied.

The notable work presented is the variety of simple domains that highlight differing forms of chaotic motion. Focus has been on the understanding of the particle motion to develop and prove concepts that may aid design of future chaotic mixing domains. To make visible the effect of control parameters on the particle movements various techniques have been implemented. The most successful of these was the observation of the particle spread, both pictorially and quantitatively by the use of property A which is the average distance between particles and their initial neighbours originating from a small line.

The flow domains in this work are relatively simple and some of them are unoriginal or perhaps classic, in the case of the two-dimensional cavity, this is to aid the development of concepts of chaotic motion. Towards the latter parts of the work the domains became more complex, throughput domains for example. The affect of various control parameters in these systems was possible to conceptualise and pre-empt due to the particle movements observed within the simple two-dimensional domains.

This chapter presents a discussion of the observations, properties investigated and conclusions formulated within the previous chapters. It then goes on to suggest possible further investigation and developments of mixing domain configurations using the concepts developed concepts. Finally there is a discussion of possible developments to property A towards producing a more robust property that is capable of yielding significant amounts of information regarding the mixing quality throughout time in variety of mixing domains.

7.2 Discussion of the parameters and concepts developed throughout this work.

The aim of this work was to advance the investigation of chaotic mixing domains using commercial computational fluid dynamical tools. Commercial CFD was chosen over specific code generation due to the possibilities of easily generating complex mixing geometries and the speed at which changes could be made to examine ranges of parameters. Commercial CFD is becoming more widely used by engineers to develop a variety of process engineering units. Another aim of this work was to observe chaotic advection through widely available CFD software, and thus potentially promoting of chaotic mixing domains to more engineering designers.

This work has successfully presented cascades from ordered to chaotic motions in a variety of systems as operating parameters are varied. A number of methods for viewing disorder were adapted or established and chronologically presented with respect to their development.

The latter techniques for observing system disorder relied on the sensitive dependence of initial conditions which can be observed through the separation of initially close particles through time. This feature was observed so that it provided information that was more significant to the needs of the industrial mixing equipment design engineer, rather than the mathematician. For example, properties that suggest the quality of mixing throughout time, thus indicating residence times were favoured over properties or flow features that refer to instantaneous disorder.

The first system investigated in this work was the two-dimensional time periodic cavity with an approximated smooth boundary oscillation, similar to that presented experimentally by Leong and Ottino [48]. It was found, through observing macroscopic pictorial representations of particle trajectories, that as the time period of boundary oscillation was increased the system became more disordered, until what appeared to be chaotic motion. Increased disorder was also observed through a more microscopic observation of a trajectory passing near to a reference point within the domain. It was found that as the control parameter, the time period of boundary oscillation, was increased the particle began to oscillate around the reference point, which indicated the presence of a period doubling cascade. This work showed that chaotic motion in laminar fluids can be replicated by the use of commercial CFD. The computational tests compliment the published experimental results and it is possible to observe the change in fluid motion from order towards and into chaos.

Through observing the particle trajectories in detail throughout the early stages of the cascade it was possible to suggest why the systems disorder changes in the way that it does. It is well known that systems with alternating streamlines can exhibit chaotic motion. However no author has previously attempted to suggest why operating parameters affect the fluid motion in the way that they do. Consider a system with two alternating streamline motions that have reflective symmetry (as in the two-dimensional cavity system). The distance that a particle can travel in either streamline depends on the duration of its residence in that streamline. At a low time period (high frequency) a particle can only displace a small distance from one instantaneous streamline, before being returned by the other. Hence the particle oscillates, which may, on a macroscopic scale, appear as similar to a steady state system.

As the time period of oscillation is increased a particle will remain in one streamline for an extended period of time. This will allow it to displace more distance along that streamline, before being returned and hence the particles oscillation will increase, and may now be macroscopically visible. There becomes a point where the particle remains in one streamline

for sufficient time such that it displaces significantly so that one extreme instantaneous flow pattern will not cancel out the other to form an oscillation of the particle. The particle begins to behave stochastically. It is this rationale that forms the basis for the explanation of the effect of varying control parameters and is used to suggest more complex design concepts.

The disorder in the two-dimensional cavity system was then observed by the use of a property derived from the instantaneous mixing efficiency. Comparing the time-averaged property of the instantaneous mixing efficiency against time period of boundary oscillation produced a plot containing a peak. It was suggested that the peak corresponded to a point within the cascade associated with the onset of chaos. It was found, through observing the position of the peak in the cascade, that increasing the velocity amplitude of the moving walls affected the cascade by reducing the time period at which chaos occurs. The rationale discussed above this can be extended to explain this by; it is the amount displacement of a particle within a individual streamline that controls the onset of chaos. A particle with a higher velocity will travel further in the same time, thus it will reach the point where its displacement is not returned as an oscillation by the opposing streamline at a lower time period. This was also found to be true for the two-dimensional time periodic eccentric cylindrical system. It was also found the degree eccentricity between the inner and outer cylinders affected the disorder. When the cylinders were concentric the effect of oscillating the boundaries was to alternate the speed of particles and not the streamlines, hence no disorder occurred. When an eccentricity is imposed alternating streamlines exist and disorder can occur. It was found that as the eccentricity was increased the overall time period required to induce chaos was reduced. The particles begin to oscillate more violently as streamlines become more different, thus travelling further away from their original orbit in the same period of time.

Through using the instantaneous mixing efficiency it was possible to produce characteristic plots that exhibit peaks which indicate the onset of chaos. However the property does not represent the degree of disorder within a system throughout time, and is therefore of limited use to the design engineer. Also the fall in the property after the peak suggests order restoring. which cannot be, and is not, the case. Systems operating with time periods larger than that at the peak continue to exhibit sensitive dependence to initial conditions and are therefore within chaos. It was suggested that this drop in the value is due to, at large time periods, the system is operating for a significant time as each streamline, and consequently the instantaneous mixing efficiency is low.

For the continuation of the analysis of chaotic mixing domains a quantifiable property of the mixing was developed that provides information about the degree of disorder and the quality of mixing over time, thus being able to provide designers with significantly more information than an instantaneous property.

The property makes use of the signature of chaos, sensitive dependence to initial conditions. In the simplified weather system presented by Lorenz [5] he noted that two points within a system, that were initially close, evolved to a point where their trajectories bore absolutely no resemblance to each other. It was noted that if the points were two initially close particles of fluid in a mixing system, under chaotic conditions, they would separate to the point where their trajectories are unrelated, and hence the system would be well mixed. The property, termed property A, was generated form a small line of particles within the flow domain. Each particle was assigned their two nearest neighbours along the line. The distance between each particle and its neighbours was calculated at regular time steps. Property A is the average distance between two particles along the line, which was shown against time with its maximum value being compared over a range of operating parameters.

Property A was shown to yield consistent results throughout ranges of its generation parameters, and to produce conclusions that were consistent with previous two-dimensional analysis. Therefore it was suggested that property A be extended for use in three dimensions.

Using property A, and corroborating pictorial observations of particle trajectories, a variety of three-dimensional systems were investigated, these include time periodic, time independent, throughput and closed domains.

The inclusion of the third dimension enabled systems to operate with perpendicular motions. The first three-dimensional system to be investigated was a closed cubic domain operating with perpendicular flip-flop oscillating boundaries. Property A showed that throughout ranges of time period the cascade from order into chaos was not as visible as it was for the two-dimensional cavity system, and that the effect of increasing the velocity of the wall boundaries only appeared to hasten the separation of particles, and not shift the cascade. This was noted to be due to the alternating boundary motions not opposing each other as they were in two dimensions due to operating perpendicularly. Particles within the system will eventually separate, irrespective of the time period of velocity amplitude.

Three different three-dimensional throughput systems were investigated using property A. Due to the laminar shear, and particles moving slowly near the walls property A was calculated over the cross section perpendicular to the throughput flow to avoid misleading large values of separation. The first system, known as the time periodic domain was a long rectangular domain, with the movement of top and bottom walls oscillating in a flip-flop motion perpendicular to the flow. The following two systems were time-independent and made up from many repeating cells. The first of these, a spatially periodic domain, has two moving walls in each cell configured such that particles become incident to different, opposing streamline motions as they flow through each cell. The second, a geometrically

periodic domain, contains two exact similar streamline motions within each cell, however they are offset perpendicular to the throughput flow, so that their centres of rotation oscillate. The disorder within the fluid in the time periodic system was found to be effected only by parameters surrounding the oscillation, the time period and velocity amplitude, and not by the longitudinal position of the particles as they travel through the domain, nor their throughput rate.

The velocity of the wall translation and the throughput rate both effect the disorder of the fluid in both the spatially and geometrically periodic domains. In these systems the wall velocity is constant and the particles come into contact with differing streamline regimes as they flow through the cells. The faster the wall velocity the further in any set time particles can be displaced. The slower the throughput the longer particles will remain within any one streamline regime, and hence move further within it, before flowing into another. Systems become more chaotic as the wall velocity is increased, and systems with lower throughput rates require a lower time period to become chaotic. This supports unequivocally that it is the displacement of particles within alternating streamlines that is responsible for the onset of chaos.

The final three-dimensional system to be investigated was the twisted figure of eight mixer (TF8). This domain consists of two adjacent cubes each with two translating walls that cause a rotation within the flow. The cubes are set so that two principle rotations cause a twisted figure of eight motion that is steady within Eularian representation, but exhibits Langrangian turbulence.

The system was investigated by the use of three different methods. The first involved generating cross sectional slices along the domain and observing where a number of particles crossed these. It was found that as the ratio of the velocities within the two cubes was increased the disorder increased. The range of ratios investigated saw the destruction of ordered regions, tori and invariant curves. The second method observed the spread of a small sample of particles. Under chaotic conditions bending, stretching and folding in the fluid occurred. The final method was to quantify the spread of particles using property A. This showed that as the velocity ratio between the two cubes increased from zero chaos occurred. Once within disorder the effect of increasing the velocity ratio further was to increase the time to significantly separate the particles. It was found, however, that these results are dependent on the generation position of the particles used to calculate property A, although it was expected that a similar result be obtained from other locations within the domain.

This work has presented an explanation for why and how periodic boundary conditions effect disorder and produce chaotic motion within a laminar fluid system. Information achieved through extending this theory enables one to suggest further domains that are expected to

produce chaotic mixing. The theory is therefore a good starting point for an engineer designing chaotic mixing equipment. Some 'starting points' are discussed in section 7.3.

Chaotic mixing has been quantified by a property that yields, not only information about the overall disorder, but also indicates the time required to achieve that mixing. The property is universal and could be applied to any system, and has also been used in this work to investigate a steady state chaotic system. Unfortunately the property is limited due to its generation from a small area. If that area happens to be situated in an ordered region (such as an invariant tori) then the value returned may be spurious. In this work all conclusions from property A have been corroborated using observations of particle trajectories. Section 7.4 discusses developments of property A so that it could be used with increased confidence to yield significant amounts of design information to be considered when designing industrial chaotic mixing equipment.

7.3 Further investigation of flow domains.

The earlier chapters of this work presented two-dimensional simulations of chaotic flow domains. This enabled the development of simple concepts of particle movements and the development of qualitative and quantitative properties. These systems are ideal for the investigation of properties of the fluid, such as reaction or if one was interested in the effects of visco-elasticity on chaotic motion, for example. The variety of different physical properties and effects within a chaotic domain are almost endless, and could provide a wealth of research for the future.

This work, and especially this section, is more concerned with geometry and boundary operating parameters, and their effect on the fluid motion.

In two dimensions the design of a chaotic mixing domain requires alternating streamline motion which can be caused by the oscillation of the motion of the top and bottom walls of the cavity, and the inner and outer walls of the eccentric cylindrical system. Unfortunately in two-dimensional chaos one is limited to cross sectional approximations and closed domains, due to the unavailability of perpendicular movements. There are, however, a number of configurations that could be considered as modifications to the two systems mentioned above. These include, for a cavity system, the effect of geometric aspect ratio, non-parallel walls, rotating blades or shifting geometry within the domain, as shown in figures 7.1 – 7.4 respectively. Other authors have too recommended system configurations based on their investigations [12, 90].

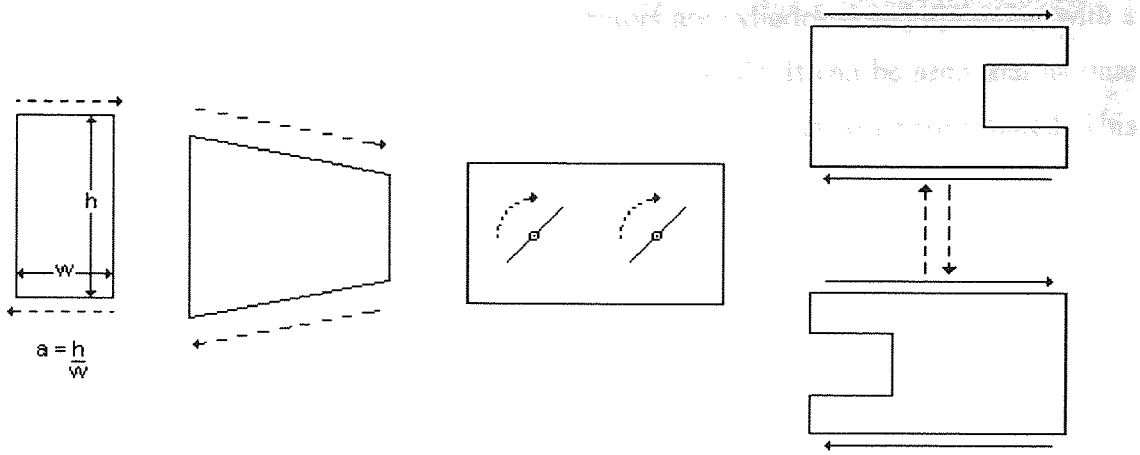

Figure 7.1. Showing the aspect ratio of a two dimensional cavity. Figure 7.2. Indicates non-parallel walls of the two-dimensional cavity. Figure 7.3. Exhibiting two rotors within the two dimensional cavity. Figure 7.4. Indicates time periodic geometry of the two dimensional cavity.

The eccentric cylindrical system could be modified to contain more inner cylinders that operate time periodically (figure 7.5), or an internal mixer containing two rotors whose oscillation oscillates time periodically as shown in figure 7.6.

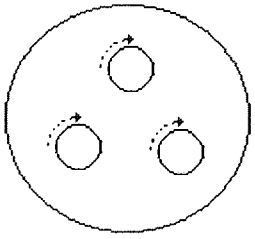

Figure 7.5. Two-dimensional time periodic eccentric cylindrical system containing three inner cylinders.

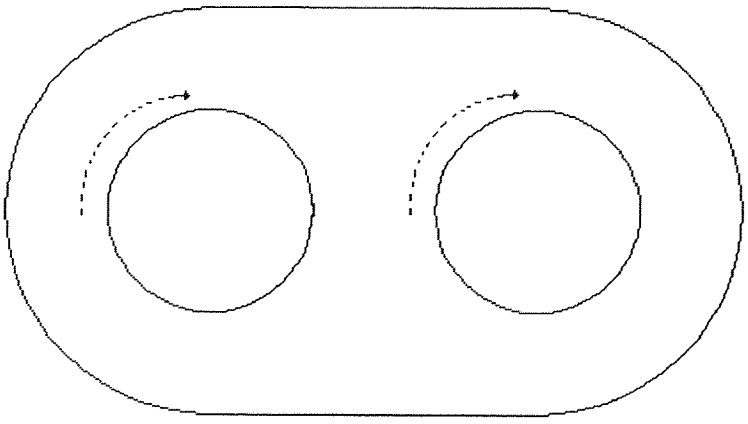

Figure 7.6. Simple representation of an internal mixer containing two time periodic rotors, represented by cylinders.

Figure 7.7 shows the spread of two hundred particles, as time evolves, in the simplified two-dimensional model of an internal mixer, where the rotors are cylindrical and operating with a velocity amplitude of 10 mm/s and a time period of 20 seconds. It can be seen that as time evolves the particles spread throughout the domain, until they appear to be well mixed. This can be quantified by the use of property A.

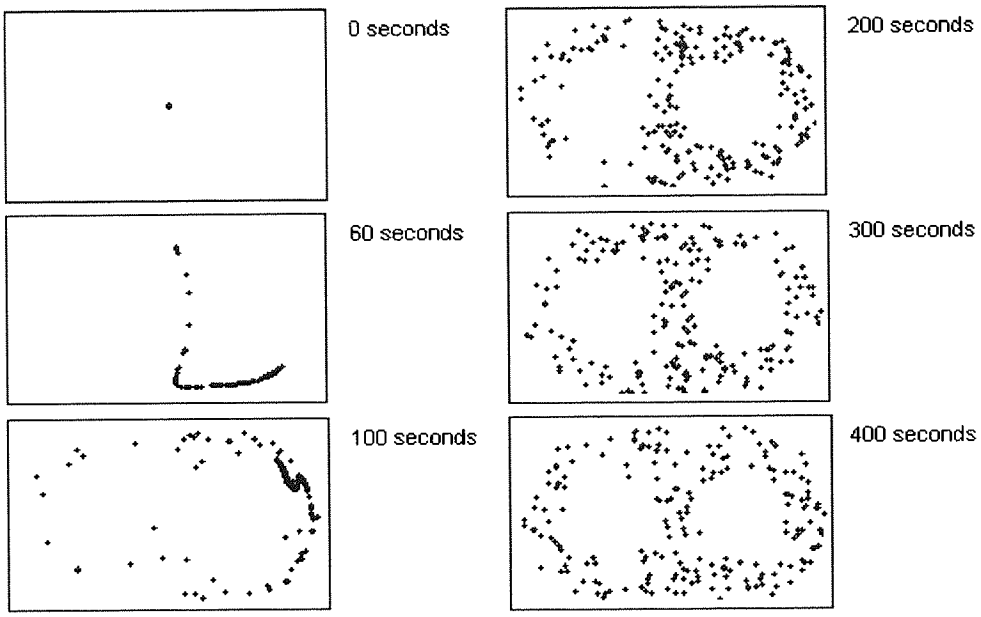

Figure 7.7. The spread of 200 particles at intervals over 400 seconds originating from a small generation zone in the two-dimensional simplified internal mixing domain, where the time period of rotor movement oscillation is 20 seconds with amplitude of 10mm/s.

Figure 7.8 shows property A against time for the system in figure 7.7. The plot is characteristic of one that has, previously in this work, been associated with chaotic motion. The figure shows a slow initial separation, followed by an exponential separation, followed by the levelling off phase associated with the particles no longer baring any resemblance to their original neighbours.

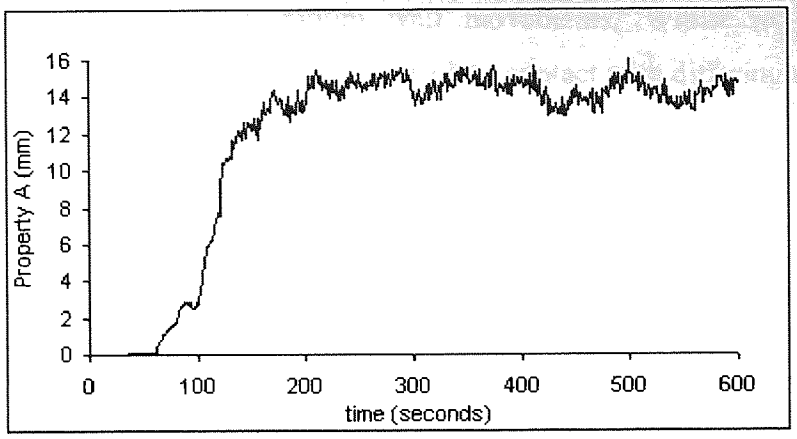

Figure 7.8. Property A against time generated from 200 particles originating from a small generation zone in the two-dimensional simplified internal mixing domain, where the time period of rotor movement oscillation is 20 seconds with amplitude of 10mm/s.

Much work has been carried out into the mixing in internal mixers [38, 102-104] although there are no notable works including time dependent boundaries. For a more realistic simulation of an internal mixer the rotors should appear more like blades, figure 7.9. This would involve time periodic geometry, and therefore require different modelling techniques. Developments in commercial CFD such as the Mesh Supposition Technique, available in Polyflow, [105] make possible this kind of model. One of the features of a real internal mixer is the curve of the rotors that induce axial motion of the fluid, figure 7.10.

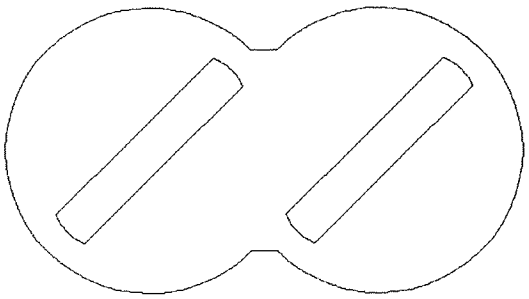

Figure 7.9. Two-dimensional internal mixer with rotor blades.

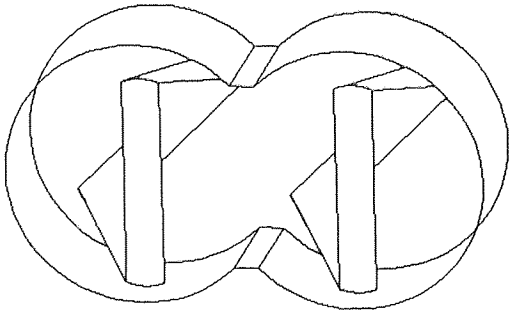

Figure 7.10. Three-dimensional internal mixer with twisted blades to induce axial mixing.

Variations and extensions in investigations of the closed cubic three-dimensional time periodic domain could be similar to those suggested for the two-dimensional cavity. This could include the periodic movement of all six faces of the cube, varying the aspect ratios, inclusion of blades, rotors or intrusions in the domain or time dependent geometry.

Chapter five presented three throughput domains that exhibit chaotic motion. Introducing the third dimension allowed the models to contain perpendicular boundary movements to the fluid flow. Each of the three systems induce chaos through the alternation of cross sectional streamlines. Particles in the time dependent system are subjected to alternating streamlines due

to oscillations between top and bottom wall movements. Whilst in the spatially and geometrically periodic systems the particles come into contact with differing streamlines as they flow through the system.

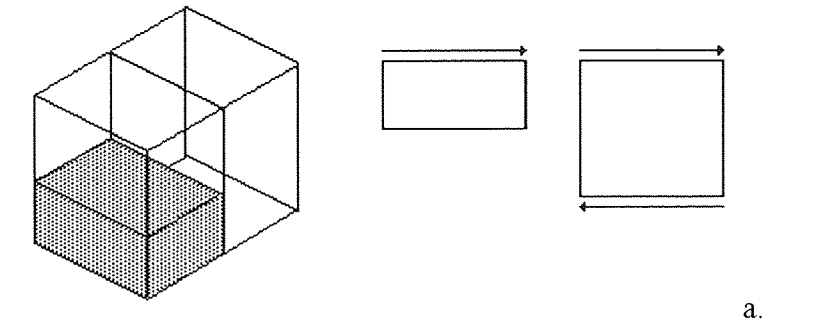

a.

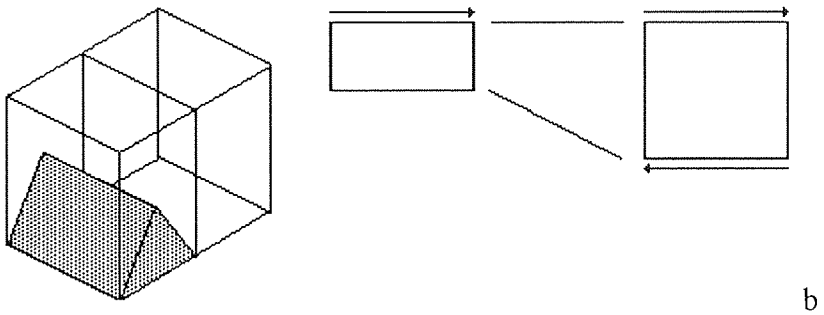

b

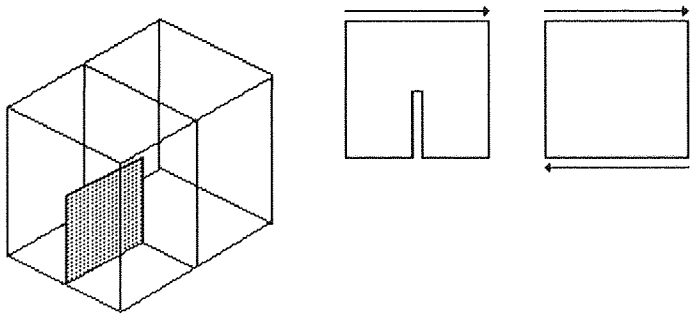

c

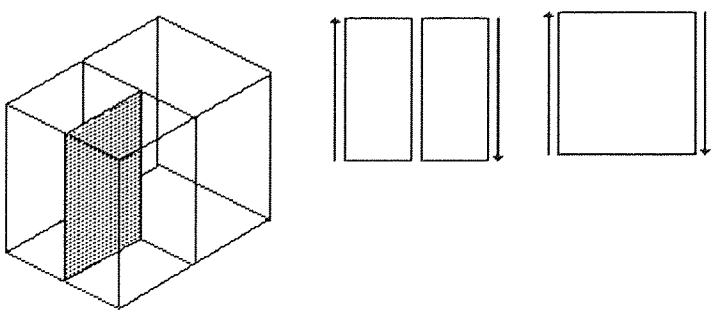

d

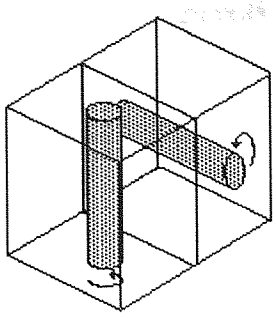

e

Figures 7.11a-e. Cells of a throughput mixer that would induce alternating streamlines, and (for figures a-d) pictorial representation of the streamlines. Figures a-d shows obstructions to the flow, a block, triangular block, a fin and a wall, respectively, whilst figure e shows stirrers along the domain, that would induce twisting flow.

The use of various inserts in a throughput duct can produce the effect of alternating streamlines. Figures 7.11a-d each represent one cell of a throughput domain that would cause a pair of alternating streamlines, and would therefore be expected to exhibit chaotic motion. Figure 7.11a shows a block placed across the width of the domain, with the top wall translating, thus producing the two streamline forms in the domain cross sections shown. It is expected however that there may be stagnation in the dips and possible bypassing of particles in the upper sections. It may then be desirable to change the shape of the block into a triangle (figure 7.11b.) although bypassing may still occur. It could be suggested that there would be an optimum distance between, and the geometry of the blocks.

If the block width were reduced so that it resembled a fin protruding from the base of the domain, with the top wall in motion, as figure 7.11c, then the particles would be subjected to the streamline motion shown. This would reduce the bypassing and stagnation of particles in the lower half of the domain. If the fin were elongated so as to stretch to the top of the domain, and the two vertical walls were to move, figure 7.11d, then the particles would be subjected to splitting streamlines. The angle of the blade, both to the vertical and the throughput flow of the fluid could be investigated for their effect on chaotic motion and subsequent mixing quality. The inclusion of stirrers along the throughput domain would subject particles to a twisting motion as they pass through the mixer (figure 7.11e.)

It is evident that there are a vast variety of different configurations within the throughput system that produce an alternation in streamline motion which is restricted only by the imagination. Other authors have also considered such domains. Ottino [99] suggests that streamlines may be altered through a wavy fin running the length of the base of a throughput duct, where the upper wall translates perpendicular to the flow.

Many domain and insert configurations have been suggested, but it is not, by far, a definitive list. One should however consider the design complexity of any inserts, rotors or blades and their obstructive effect to the flow, in terms of reducing the flow rate, increasing the pressure drop, or creation of stagnation points or bypassing. Also the effects of shear on the material being mixed may dictate the selection of any insert, rotor or blade. A polymer requiring high shear may benefit from inserted blades and closely meshing rotors [36] whereas the shear sensitive contents of a fermenter may require more gentle methods of inducing chaotic mixing [33].

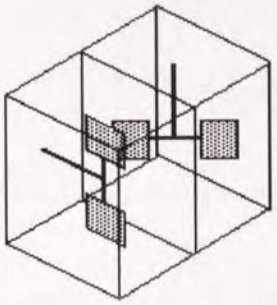

Figure 7.12. Twisted figure of eight mixer with blades on rotors.

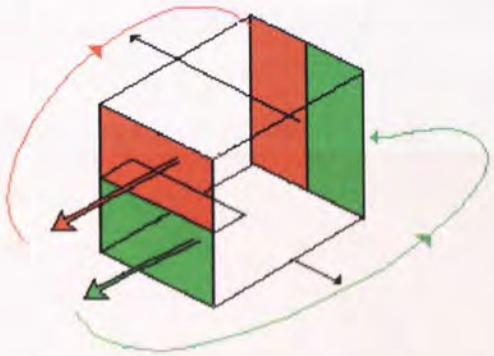

Figure 7.13. Motion of a Kenics or partitioned pipe mixer mimicked in a closed domain by the use of re-circulating flows.

Chapter six observed time independent chaotic motion in the twisted figure of eight mixer (TF8). This domain could be modified to include curved ends that may aid the rotating motion of flow, and perhaps reduce any stagnation that may exist in the corners. Also the effect of aspect ratio could be investigated. For a practical mixer, say for the mixing of cement, the twisted rotational fluid movement could be recreated by the use of two stirrers set at ninety degrees to each other (figure 7.12.) The blade design, and configuration, the power required to stir various fluids and the reduction of stagnation points could be investigated with respect to the quality and speed of mixing.

Other closed domains that make use of twisting flows are re-circulating flows. The domain in figure 7.13 mimics the motion of a Kenics mixer [43] by the use of a re-circulating flow. The

fluid exits the domain in two halves, which both twist and re-enter, again in two halves, but at ninety degrees to the exit. The continued splitting and rotating of the fluid produces significant mixing. Operating the walls periodically to the flow may increase the efficiency of the mixing.

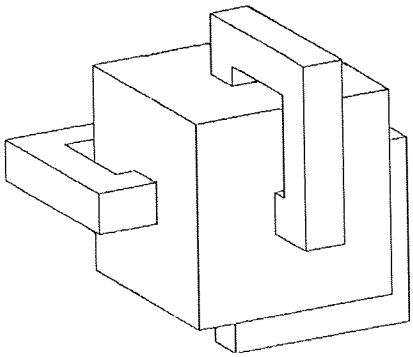

Figure 7.14. Closed time dependent re-circulating flow domain that causes chaotic mixing.

The re-circulating domain in figure 7.14 produces chaotic motion by removing fluid from the centre of three faces of the cubic mixer and pumping it back into the system through three corresponding faces at ninety degrees to the exits. Figure 7.15 shows the spread of one thousand particles as time evolves. It can be seen that the particles spread randomly throughout the domain, although there are areas where mixing is poor.

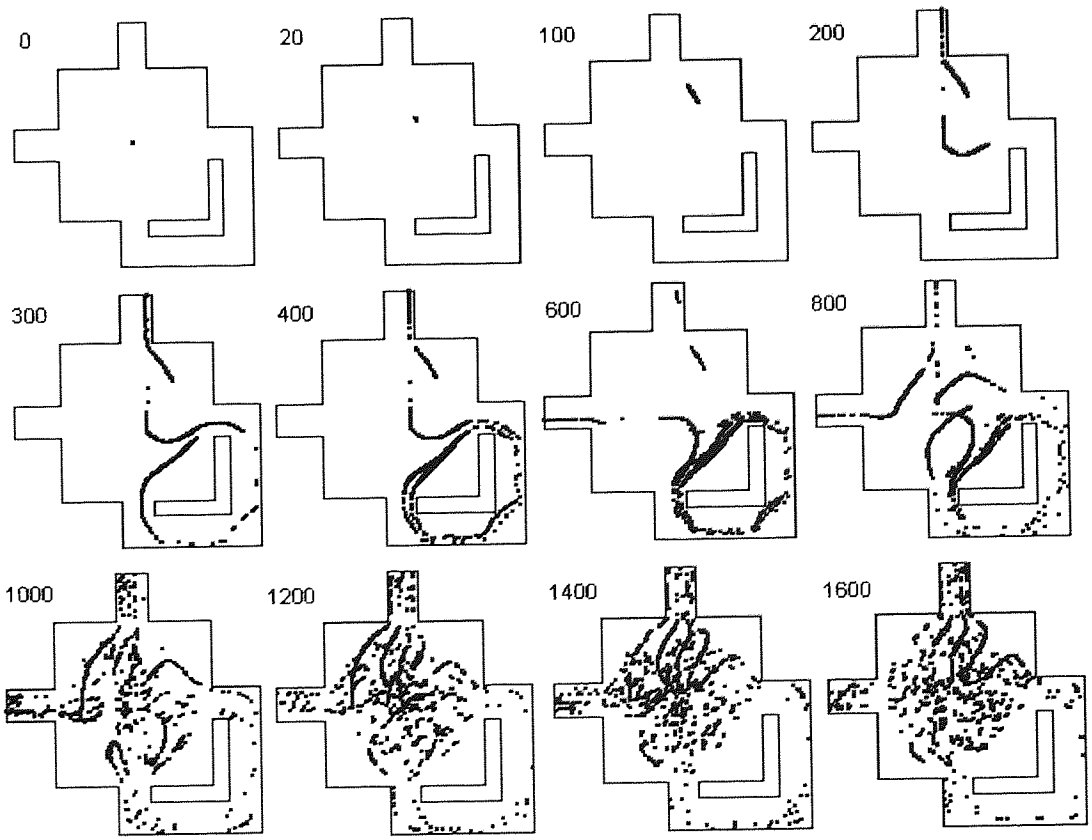

Figure 7.15. Cross sectional view of the spread of 1000 particles originating from a small generation zone in the re-circulating mixer over 1600 seconds. Each of the three re-circulation loops is operating at the same arbitrary flow rate.

The separation of the particles can be quantified by the use of property A. Figure 7.16 shows the property A against time for two hundred particles originating from a small line in the centre of the domain. The plot shows characteristic features similar to those exhibited by other chaotic systems. Initially there is low divergence, followed by a growth stage, although not as rapid as seen previously, and the beginnings of levelling off of the plot corresponding to the particles baring no resemblance to their original neighbours.

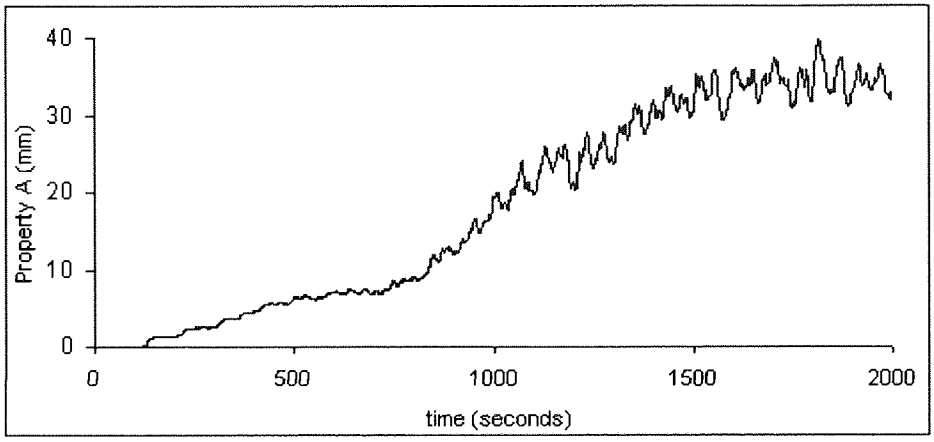

Figure 7.16. Property A against time for 200 particles originating within a small generation zone in the centre of the re-circulating mixer.

The value of property A in the disassociated region should be taken as an indication of the disorder only, as the distance between particle pair is a linear measurement. The value of property A would include the gap in the domain if one particle were in a re-circulation pipe and its original neighbour was in the centre of the domain. For systems with complex geometries being able to suggest a value for property A for a comparison uniform distribution of particles becomes difficult. A satisfactory method for suggesting such a value would need to be developed if a comparison is to be drawn between systems of vastly differing geometries.

Through using the concepts developed in the previous chapters it has been shown to be possible to suggest domains that will produce chaotic mixing. This has applications in many process industries, particularly those working with laminar fluids, such as the polymer, food, bio-chemical and pharmaceutical industries. Chaos is an effective method of achieving good mixing that can be induced in high or low shear systems. The full extent of geometries and

systems that could be mixed more efficiently using chaos has not been realised by a long way. If systems could be mixed more efficiently then there would be less need for high power consumption. Through using commercial CFD techniques to simulate innovative chaotic flows a great number of mixing processes could be radically improved.

7.4 Further development of property A.

Property A was developed to quantify the sensitive dependence to initial conditions of chaotic mixing systems in the form of particle separation. It is produced by a specific post processing code that uses the co-ordinate data of a number of originally neighbouring particles to calculate the average distance between them.

To ensure that significant separation of particles is observed property A is calculated from trajectories originating from a small zone of generation. However this may result in representation of only a small region of the flow domain. This was not considered to be significant when observing two-dimensional systems as the main point of interest is the onset of 'full' chaotic motions, and when this occurred the particles travel throughout all of the domain. Thus making the position generation zone inconsequential. This can be seen in figure 7.17. where a single particle trajectory is shown over 3000 seconds in the two-dimensional smoothly oscillating cavity system, presented in chapter two. It can be seen that the particle trajectory covers the whole of the domain with no obvious islands of ordered flow where the particle does not travel, thus the trajectory would be similar irrespective of its generation position.

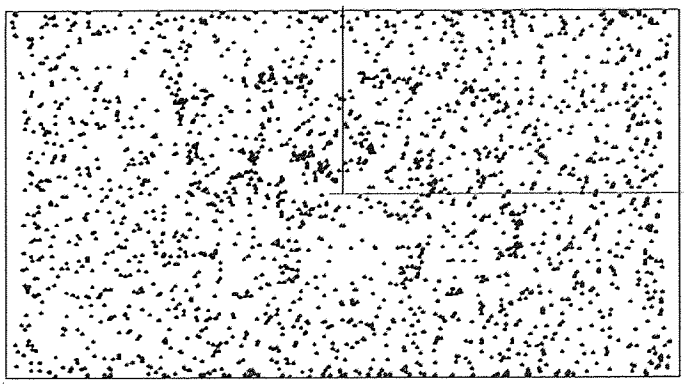

Figure 7.17. (As figure 2.6.) Time snap shots of a particle trajectory for 3000 seconds in the two-dimensional smoothly oscillating cavity where U=26.9 mm/s, T=20 seconds.

The position of the generation zone of the particles within the domain is of more significance when considering three-dimensional systems. This became evident in chapter six when investigating the TF8 mixing domain. It was recognised that there were highly chaotic regions

and islands of ordered motion present. Figure 7.18 shows the positions that particles cross a slice at the centre of the TF8 mixing domain.

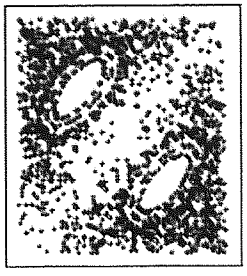

Figure 7. 18. (Taken from figure 6.6.) The cross sectional slice midway along the z-axis of the TF8 mixer showing the points of intersection of twenty-five particles originating from random positions and evolving for one thousand seconds. All walls are translating at 5mm/s.

It can clearly be seen that there are islands of order surrounded by invariant curves in seas of disorder. Consequently if the particles used to calculate property A were to originate from within the ordered island, then its value would be significantly lower than if the particles originated from with the disordered region. Due to this it was recommended in the previous chapter that the property A not be used as the sole tool for investigating the disorder within a system and all conclusions were corroborated with observations of trajectories.

It is thought that it would be useful if property A could be used more independently and account for the local deviations in mixing quality. However to achieve this property A should be extended to quantify and compare the quality of mixing at various points within a mixing system.

A mixing domain will require the superimposing of a three-dimensional grid. At each intersection of grid lines a generation zone, of specified size, containing a set number of particles will be produced, as shown, for example, in figure 7.19 for the cubic domain with a grid of 10 by 10 by 10.

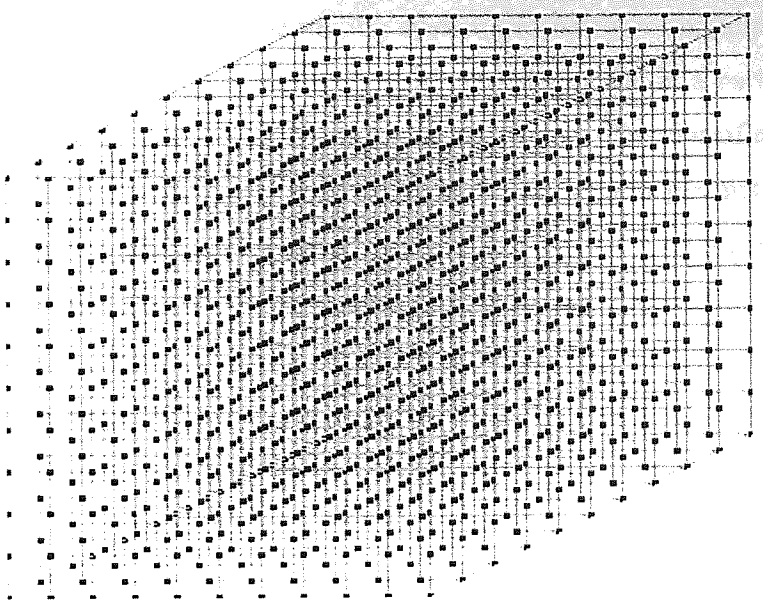

Figure 7.19. Indicating the generation zones for particles to be used to calculate property A in a cubic system with a grid of 10 by 10 by 10.

As time evolves property A can be calculated for each set of trajectories which will produce many local property A values. All of the local property A values can be averaged to give an indication of the overall mixing quality, or they can be treated using a variety of statistical techniques. Each local property A value could be individually compared to the value obtained from a uniform distribution of particles to suggest the quality of mixing from each point. If this were mapped regions of poor mixing and islands of ordered fluid motion could be highlighted. Through observing the frequency that the separation of sets of trajectories is within set ranges, corresponding to the quality of mixing, further information could be obtained about the mixing system.

	Maximum value obtained from local property A values as a percentage of the value obtained from the uniform value.										
	0-10%	10-20%	20-30%	30-40%	40-50%	50-60%	60-70%	70-80%	80-90%	90-100%	over 100%
Number of local property A within range	139	117	123	135	150	127	116	131	141	145	7

Table 7.1. Example of frequency results of the mixing obtained from 1331 local property A values compared, as a percentage, to the uniform distribution.

The example results in table 7.1 show that the mixing within this system is varied. Some of the local property A values suggest that particles are within ordered flow regimes, whilst other sets of particles exhibit significant divergence. Through observing the generation locations within in the domain that correspond to low disorder, designers would be able to

suggest where to make alterations to the mixing system geometry or operating conditions. For example if this analysis showed that a domain exhibited stagnation in a particular corner, the designer may wish to fill in that area and test the system again. The aim of an analysis of this nature would to be to optimise operating parameters and domain geometry to produce an efficient and well-mixed system. In terms of results as in table 7.1 well mixed would be when the majority of the local property A values are within the 80 to 100% of the average distance between particles obtained from the uniform distribution.

One could use the technique to investigate smaller areas of the domain. Say, for example if a stagnating section of the system was to have baffles inserted. A designer could 'zoom in' on this area by calculating the local property A over a much finer grid in a smaller area. Particles would still travel throughout the whole domain, but small flow circulation behind walls may be detected. The magnified analysis could continue until the effect of the stagnation begin observed had negligible effect on the overall process.

Through similar methods of analysing the local property A data residence times can also be optimised. By observing the local property A values by the time taken to reach a specified percentage of mixing one could optimise a throughput system to mix all of the fluid within a similar time, or for a closed domain the longest time required to mix throughout all points could be suggested. Once again the geometry and operating parameters can be manipulated to produce the desired mixing time.

The amount of information that can be yielded from the property A, when analysed in this way is potentially great and would be of significant use to the designers of industrial equipment. In order to carry out this analysis, using the commercial software, either new codes would need to be created, or the commercial codes would need to be manipulated. It would also involve the addition of a few 'do' loops to the code presented in appendix B for the post processing of the trajectory co-ordinate data.

To carry out this technique to investigate and optimise a mixing system would require a significant amount of computational time. There are many variables that would effect the time required. These include the mesh density, the number of points to generate local property A and the number of particles, the frequency at which their trajectory co-ordinates are recorded and their lifetime. These variables would have to be optimised to suggest what values would give meaningful results, however it would appear from previous optimisations that the more reliable quantitative results are obtained when the more computationally expensive range of variables are used. At present a separate data file has to be produced for each of the different zones of particle generation to produce each local property A. For the example suggested in figure 7.19 and table 7.1 this would mean 1331 separate tests. Each test, depending on the values selected for the variables, could take up to 10 hours to run on a machine that has a spec

fp [106] of 20, which amounts to about one and a half years of computational time. Personnel time could be significantly reduced by producing a code to create, run and analyse each of the 1331 data and results files automatically. Suggestions of how to reduce the computational time include manipulating the commercial source code or creating efficient specific codes that are streamlined for this purpose. Unfortunately the commercial source codes are unavailable to the author, and the creation of specific codes is not with the remit of this work. If one were to continue to use the commercial CFD software then the number of generation sites required to run could be reduced through targeting areas of specific interest.

Computers are fast becoming more powerful with processors in excess of one gigahertz being currently widely available. Although this method at present appears to be computationally expensive, it is suggested that fairly soon the computational power required will be available to make this method of detailed analysis, using commercial CFD techniques, a viable and effective alternative to physically modelling mixers. The wealth of information that is obtainable through this method of quantifying the separation of particles, using property A, will assist designers of industrial equipment in making efficient and cost effective mixing devices.

References

1 'The Larousse Encyclopedia of Mythology' (1996) Chancellor Press

2 Z. Sardar, I. Abrams. 'Introducing Chaos' (1999) Icon Books

3 I. Stewart. 'Does God Play Dice. The new mathematics of chaos' (1997) Pegnuin Group

4 J. Gleick. 'Chaos' (1997) Minerva

5 E. Lorenz. 'Deterministic Non periodic Flow' *J.Atmos. Sci* (1963) **20** p130-141

6 M. Overd and S. Generalis, 'Using CFD to investigate the flow of a viscous fluid in a cavity with oscillating boundaries,' *Intern. Polymer Processing.* (1999) **14** p128-135

7 M. Overd. POLYFLOW Users Group Meeting. Brugge (1998) Polyflow SA., Place de l'Universite 16, Louvain-la-Neuve, Belgium.

8 P. Hall, D. Papageorgiou. 'The Onset of Chaos in a Class of Naviour-Stokes solutions

9 R. Khayat. 'Onset of Taylor vortices and chaos in viscoelastic fluids' *Phys Fluids* (1995) **7** (9) p2191- 2219

10 A. Brandstater, H. Swinney. 'Strange attractors in weakly turbulent Couette-Taylor flow' *Phys Review A.* (1987) **35** (5) p2207-2220

11 P. Addison. 'Fractals and Chaos' (1997) Institute of Physics Publishing.

12 J. Ottino, 'Kinematics of Mixing: Stretching, Chaos and Transport.' (1989) Cambridge University Press.

13 P. Drazin 'Non-linear systems' (1997) Cambridge University Press

14 E. Ott ' Chaos in dynamical systems' (1993) Cambridge University Press

15 P. Glendinning. 'Stability, instability and chaos'(1999) Cambridge University Press

16 R. Devaney. 'An introduction to chaotic dynamical systems.' (1986) Benjamin/ Cumming Publishing.

17 A. Holden. 'Chaos.' (1986) Manchester University Press

18 R. Hilborn. 'Chaos and non-linear dynamics' (2000) Oxford University Press.

19 D. Jordan, P.Smith. 'Non-linear ordinary differential equations'(1988) Oxford University Press

20 H. Korsch, H. Jodl ' Chaos' (1998) Springer

21 F. Moon 'Chaotic and fractal dynamics' (1992) J. Wiley

22 P. Bryant, R. Brown, H. Abarbanel 'Lyapunov exponents from observed time series' *Phys. Review. Letters* (1990) **65** (13) p 1523-1526.

23 J. Froyland, K. Alfsen. 'Lyapunov-exponent spectra for the Lorenz model.' *Physical Review A* (1984) **29** (5) p2928-2931

24 N. Harnby, M. Edwards, A. Nienow. ' Mixing in the process industries' (1985) Butterworth

25 S. Nagata. 'Mixing, principles and applications' (1975) Wiley

26 E. Nauman, B. Buffham. 'Mixing in continuous flow systems' (1983) Wiley

27 Z. Sterbacek, P.Tausk. 'Mixing in the chemical industry.'(1965) Pergamon

28 V. Uhl, J. Gray. 'Mixing, theory and practise' (1966) Academic Press

29 J. Ulbrecht, G. Patterson. 'Mixing of liquids by mechanical agitation.' (1985) Gordon and Breach Science Publishers.

30 D. Heldman. 'Food process engineering.'(1975) Avi Publishing Company

31 P. Fryer, D. Pyle, C. Rielly. 'Chemical Engineering for the food industry.' (1996) Chapman and Hall

32 P. Doran. 'Bio-process engineering principles.' (1999) Academic Press

33 J. Bailey, D. Ollis. 'Bio-chemical engineering fundamentals.' (1987) McGraw-Hill

34 J. Agassant, P. Avenas, J. Sergent, P. Carreau. 'Polymer processing- principles and moddelling.' (1991) Hanser

35 M. Berins 'Plastics engineering handbook of the society of the plastics industry.' (1991) Van Nostrand Reinhold

36 S. Middleman. 'Fundamentals of Polymer Processing.' (1977) McGraw-Hill

37 Hold. 'Non-linear Experiemnts'

38 A. Harries. PhD Thesis. (2001) Aston University

39 Kim, Kwon. Adv. in Pol. Tech (1996). 15, p41-54

40 Kim, Kwon. Adv. in Pol. Tech (1996). 15, p55-69

41 J. Ottino, R. Chella. 'Laminar Mixing of Polymeric Liquids; A brief review of recent theoretical developments. Polymer Eng. Sci. (1983) 23 (7) p357- 379

42 Manas-Zlocower, Tadmor. 'Mixing and compounding of polymers, theory and practice.' (1994) Hanser Publications

43 T. Avalosse, T. Crochet, 'Finite element simulation of mixing2: 3D flow through a Kenics mixer' *AiChE J.* **43** (3) p588-597.

44 H. Aref. 'Stirring by chaotic advection.' *J. Fluid Mech.*(1984) **143**, p1-21

45 Aref, Balachandar. 'Chaotic advection in a Stokes flow.' *Phys. Fluids* (1986) **29** (11) p3515-3521

46 Chaiken, Chu, Tabor, Tan. 'Lagrangian turbulence and spatial complexity in a Stokes flow.' *Phys. Fluids.* (1986) **30** (3) p687-694.

47 Chien, Rising, Ottino. 'Laminar mixing and chaotic mixing in several cavity flows.' *J. Fluid Mech.* (1986) **170**, p 355-377

48 C. Leong, J. Ottino, 'Experiments on mixing due to chaotic advection in a cavity,' *J. Fluid Mech.* (1989). **209**. 463- 499.

49 Nishimura, Kunitsugu. 'Fluid mixing and mass transfer in two-dimensional cavities eith time periodic lid velocity.' *Int. J. Heat and Fluid Flow.* (1997) **18** p497-506

50 Zhang, Zumbrunnen. 'Chaotic Mixing of Two Similar Fluids in the Presence of a third Dissimilar Fluid.' *AIChE J.* (1996) **42** No. 12 p3301-3309.

51 Cerbelli, Zalc, Muzzio. 'The evolution of material lines curvature in deterministic chaotic flows.' *Chem. Eng. Sci.* (2000) **55** p 363-371.

52 M. Bryden, H. Brenner. 'Effect of laminar chaos on reaction and dispersion in eccentric annular flow.' *J. Fluid Mech.* (1996) **325** p219-237

53 M. Overd and S. Generalis, 'Investigation of the characteristics of chaotic flow domains with oscillating boundaries.' Fluid Mixing 6. (1999) p105-115

54 Swanson, Ottino. 'A comparative computational and experimental study of chaotic mixing of viscous fluids.' *J. Fluid Mech.* (1990) **213** p 227-249

55 Niederkorn, Ottino. 'Chaotic Mixing of Shear-Thinning Fluids.' *AIChE J.* (1994) **40**, No 11, p1782-1793.

56 Tjahjadi, Ottino. 'Stretching and breakup of droplets in chaotic flows.' *J. Fluid Mech.* (1991) **232** p191-219

57 Giona, Adrover, Muzzio, Cerbelli. 'The geometry of mixing in 2-d time-periodic chaotic flows.' *Chem. Eng. Sci.* (2000) **55** p 381-389

58 Clifford, Cox. 'What affects the yield of a chemical reaction in a lamellar structure?' *Fluid Mixing 6.* (1999) p93-104

59 Ling. 'Chaotic Mixing in the Enhanced Mixing Simulator.' *Poly. Eng. and Sci.*(1995) **35,** No. 11 p 929-941

60 J. Glimm, D. Saltz. 'Statistical Evolution of Chaotic Fluid Mixing.' *Phys. Rev. Letters.* (1998) **80** (4) p 712-715

61 Ghosh, Chang, Sen. 'Heat transfer enhancement due to slender re-circulation and chaotic transport between counter-rotating eccentric cylinders.' *J. Fluid Mech.* (1992) **238** p119-154.

62 Tang, Boozer. 'Design criteria of a chemical reactor bad on a chaotic flow.' *Chaos* (1999) **9** No. 1, p 183-194

63 Muzzio, Liu. 'Chemical reactions in chaotic flows.' *Chem. Eng. J.* (1996) 64 p117-127

64 W. Zukowski, M. Berezowski. 'Generation of chaotic oscillations in a system with flow reversal.' *Chem. Eng. Sci.* (2000) **55** p339-343

65 Lubbert, Lapin, Dudukovic, Devanathan. 'Chaotic flow in bubble column reactors.' *Chem. Eng. Sci.* (1995) **50** No.16, p2661-2667.

66 Liu, Muzzio, Peskin. 'Quantification of Mixing in Aperiodic Chaotic Flows.'In *Chaos Applied to Fluid Mixing.* H. Aref (ed) Pergamon (1995) p125-149.

67 Perez, Chacon, Castellanos. 'Behaviour of dynamical systems subjected to continuous and discontinuous forcing: Application to laminar chaotic mixing.' *Int. J. Bif. and Chaos* (1996) **6** p2627-2634

68 Hwu, Young, Chen. 'Chaotic Advections for Stokes Flows in Circular Cavity.' *J. Eng. Mech.* (1997) p774-782.

69 B. Kaye. 'Powder Mixing.' (1997) Chapman and Hall

70 D. Khakhar, J McCarthy, J. Gilchrist, J. Ottino. 'Chaotic mixing of granular materials in two-dimensional tumbling mixers.' *Chaos* (1999) **9** (1) p195-205

71 T. Shinbrot, A. Alexander, M. Moakher, F.Muzzio. 'Chaotic granular mixing.' Chaos (1999) 9 (3) p611-620

72 M. Abbot, D. Basco. 'Computational Fluid Dynamics. An introduction for engineers' (1997) Longman

73 H. Versteeg, W. Malalasekera. 'An introduction to Computational Fluid Dynamics.'(1996) Longman

74 C. Shaw. 'Using Computational Fluid Dynamics' (1992) Prentice Hall

75 Polyflow (http://www.polyflow.be/) Polyflow SA., Place de l'Universite 16, Louvain-la-Neuve, Belgium.

76 Fluent Europe Inc. (http://www.fluent.com/) Holmwood House, CortworthRoad, Sheffield S11 9LP.

77 AEA Technology (CFX) (http://www.aeat.co.uk/cfx/cfxapp.htm) 329 Harwell,

Didcot, Oxfordshire, OX11 0RA, United Kingdom.

78 Computational Dynamics Ltd. (http://www.cd.co.uk/) Computational Dynamics Limited, Olympic House, 317 Latimer Road, London, W10 6RA, England.

79 ICEM (http://icemcfd.com/) Berkeley, CA (Main office) 2855 Telegraph Ave., Suite 501, Berkeley, CA 94705.

80 Concentration, Heat and Momentum Ltd. (http://CHAM.co.uk) Bakery House, 40 High Street, Wimbledon Village, London. SW19 5AU, UK.

81 Amtec Engineering Inc. (INCA) (http://www.amtec.com/) P.O. Box 3633. Bellevue, WA 98009- 3633 USA.

82 ADINA R & D, Inc. (http://world.std.com/~adina/transp.html) 71 Elton Avenue, Watertown, MA 02172, USA.

83 PolyDynamics, Inc. (http://www.polydynamics.com/pdintro.htm) 1685 Main Street West, Suite 305, Hamilton, Ontario, Canada L8S 1G5

84 G. Batchelor 'Introduction to fluid dynamics.'(1967) Cambridge University Press

85 Bird, Stewart, Lightfoot. 'Transport Phenomena.' (1960) Wiley

86 R. Panton. 'Incompressible flow' (1984) Wiley

87 C. Chow. 'An introduction to fluid mechanics' (1979) Wiley

88 Gallagher, Oden, Tayler, Zienkiewicz. Finite elements in fluids – volume one.' (1975) Wiley

89 P. Anderson, O. Galaktionov, G. Peters, F. Van de Vosse, H. Meijer. 'Analysis of mixing in three-dimesional time periodic cavity flows.' *J. Fluid Mech* (1999) **386** p149-166.

90 H. Kusch, J. Ottino. 'Experiments on mixing in continuous chaotic flows.' *J. Fluid. Mech.* (1992) **236** p319-348

91 Khakar, Franjione, Ottino. 'A case syudy of chaotic mixing in deterministic flows, the partitioned pipe mixer.' *Chem Engng Sci* (1987) **42** 2909-2926

92 Mezic, Wiggins, Betz. *Chaos* (1999) **9** No.1 p173-182

93 Hobbs, Muzzio. 'The Kenics static mixer: a three-dimensional chaotic flow' *Chem. Eng. J.* (1997) **67** p153-166.

94 Jones, Thomas, Aref. 'Chaotic advection by laminar flow in a twisted pipe.' *J. Fluid Mech.* (1989) **209**, p335-357

95 Jones, Young. 'Shear dispersion and anomalous diffusion by chaotic advection.' *J. Fluid Mech.* (1994) **280,** p149-172.

96 Dombre, Frisch, Greene, Henon, Mehr, Soward. 'Chaotic streamlines in the ABC flows.' *J. Fluid Mech.* (1986) **167**, p 353-391

97 G. Fountain, D. Khakhar, J. Ottino. 'Visualisation of three-dimensional chaos.' *Science.* (1998) **281** 683-686

98 J. Cartwright, M. Feingold, O. Piro. 'Chaotic advection in three-dimensional unsteady incompressible laminar flow.' *J. Fluid Mech.* (1996) **316** p 259-284.

99 Ottino, Muzzio, Tjahjadi, Franjione, Jana, Kusch. 'Chaos, Symmetry, and Self-Similarity. Exploiting Order and Disorder in Mixing Processes.' Science (1992) **257**, p754-760.

100 Franjione, Ottino. 'Stretching in duct flows.' *Phys. Fluids A* (1991) **3**, 11, p2819-2821

101 M. Overd, S. Generalis. 'Laminar fluid chaotic mixing by time dependent and time independent boundaries in three-dimensional continuous flow.' *Intern. Polymer Processing* (2001) in press

102 M. Ghoreishy. 'A Transient Finite Element Model of Mixing of Rubber Compounds in a Banbury Mixer.' *Iranian Polymer J.* (1996) **5** (1), p.30-41

103 H. Yang, I. Manas Zloczower. '3D Flow Field Analysis of a Banbury Mixer.' *Intern. Polymer Processing* (1992) **7** (3) p195-p203

104 T. Wong, I. Manaszloczower. '2-Dimensional Dynamic Study Of The Distributive Mixing In An Internal Mixer.' *Intern Polymer Processing* (1994) **9** (1) p.3-10

105 T. Avalosse. 'Mesh Supersition Technique, short course.' Polyflow User Group Meeting 1998.

106 All Published SPECfp rates 95 Results http://www.specbench.org/osg/cpu95/results/rfp95.html

Nomenclature

D	rate of dissipation
D	deformation tensor
dX, dx	infinitesimal material length
E	initial element
E*	subsequent element
e	eccentricity
e_λ	instantaneous mixing efficiency
g	gravity
M	orientation of dX
M	Parameter derived from e_λ
m	orientation of dx
∇p	pressure force per unit volume
r	radius
T	time period
t	time
U	amplitude of oscillation
u	velocity moving boundaries
X, x	position in element
x_n, y_n	two-dimensional co-ordinates of particles
Z	distance between two particles
α	phase difference
ε_1, ε_2,	scaling factors
ξ	local co-ordinates of X in E
ξ^*	local co-ordinates of x in E*
λ	Lyapunov exponent
λ	length stretch
ρ	density
τ	viscous forces
∇	vector differential operator or divergence

Appendix A - Code for calculating property A. 2d

A.1. Overview and background to code

The file shown, in part, below an example of that used to calculate the two-dimensional property A. The code reads data from POLYFLOW mixing task results in to an array. The values in the array are processed, and the results are written to file.

The input data is in the form:

```
     0
     2      50
     0       0       1 time
     1       8       2 coordinates
       101
0.0000000E+00  0.7000000E+01  0.7047082E+01
0.1000000E+01  0.6840460E+01  0.6912227E+01
0.2000000E+01  0.6672275E+01  0.6795492E+01
0.3000000E+01  0.6495902E+01  0.6696288E+01
0.4000000E+01  0.6312931E+01  0.6614149E+01
0.5000000E+01
     →
     →
     →         0.2020900E+01  0.1367638E+01
0.9700000E+02  0.2004447E+01  0.1106611E+01
0.9800000E+02  0.1989699E+01  0.8169041E+00
0.9900000E+02  0.1977584E+01  0.4794469E+00
0.1000000E+03  0.1970328E+01  0.1027631E+00
         1
       101
0.0000000E+00  0.7000000E+01  0.7135818E+01
0.1000000E+01  0.6845441E+01  0.6997216E+01
0.2000000E+01
     →
     →
```

Details of the files construction are given at the beginning of each file. The values of interest within this code have been highlighted here with colours. The 50 denotes the number of particle trajectories in this file. The 101 indicates the number of positions recorded along the trajectory. The file then contains three columns showing the time and corresponding co-ordinates for the particles. The value 1 after the trajectory indicates whether the trajectory has had a normal or abnormal stop and will recorded a 1 or 0 respectively. This code uses this value to detect stagnation points. 101 refers again to the number of positions along a trajectory follow. This value may change for each particle when using open flow domains, and therefore has to be read before each individual trajectory.
The output data is then simply the property of divergence recorded at time step corresponding to those in the input files.

A.2.. Variables and labels.

The variables used throughout the code are described below.

Arrays

result - stores the result data (property A) for each time increment

rpart - stores the trajectory positions, with time for each particle trajectory. Particles are stored along the i, time is in the j, for example 5 particles of 1000 seconds each would produce an array of i = (3*5), j = 1000

rsort - stores the same co-ordinate data as rpart, but after being sorted to order the initial positions to their immediate neighbours on the one dimensional line

Variables

fi - filename inputted by user without the index
fo - filename to open, after the code has generated the index
ftime - value of time read from trajectory in data file
fxco, fyco - value of x and y co-ordinates respectively, read from data file
ic1, ic2, ic3, ic4 - used in generating the index number for the input file
ifc - label of the open input file, increments with the index
ifw - variable in do 44
ilamp, ilamt - used to move around rsort array
ilampp - variable in do 43
ilo, iso, irrr, isort, ilinei - used to move around rsort array
ind - number of positions of one trajectory in the data file
indam - used to read trajectories throughout code
index - variable in do 30
inum - number of files with same prefix to read
ipart - used to move around rpart array
ipnum - total number of particles in one file
ipoint - variable in do 20
ird - reads either 0 or 1, 0 value will remove trajectory as a stagnation point
irr - variable in do 39
itpnum - total number of particles
itt - variable in do 38
ra, rb, rc, re - remove unwanted values from the input data files
rdist1 - straight line distance between two particles
rdtl1 - total distance between all particles
res - =fi, used to generate the output filename
res1 - the output filename
rsmin - minimum value, used in the generation of rsort
rxl, ryl - x and y distance between two particles respectively

Numerical labels

10 - end

15 - format text input
20, 30, 33, 37, 38, 39, 42, 43, 44 - do continues
85 - output file index
87 - format output file

A.3. The code with annotation

Setting up arrays and variables

```
      real rpart(7000,7000)
      real result(1,7000)
      real rsort(7000,7000)
      character *11 fo
      character *6 fi
      character *6 res
      character *10 res1

      ic1=0
      ic2=0
      ic3=0
      ic4=0
      ipart=1
      print *,'Enter the name of the file to be read (7)'
      read (5,15) fi
      res=fi
      itpnum=0
 15   format(a)
      print *,'How many files to read?'
      read (5,*) inum
```

Increments the index of the filename (fi) to give fo, this routine enable up to 9999 files with the same filename and incremental indexes. (for example where fi = 'mixing' fo = 'mixing.0001', 'mixing.0002', etc)

```
      do 33 ifc=11, (inum+10), 1
            ic1=ic1+1
            if (ic1.eq.10) then
            ic1=0
            ic2=ic2+1
            end if
            if (ic2.eq.10) then
            ic2=0
            ic3=ic3+1
            end if
            if (ic3.eq.10) then
            ic3=0
            ic4=ic4+1
            end if
   fo=fi//'.'//char(ic4+48)//char(ic3+48)//char(ic2+48)//char(ic1+48)
      print *, fo
```

Open each file in turn, read into rpart array all trajectories.

```
      open (unit=ifc, err=10, file=fo, status='old')
      rewind ifc
      read (ifc,*) ra
      read (ifc,*) re, ipnum
      read (ifc,*) rb
      read (ifc,*) rc
      itpnum=itpnum+ipnum
      do 30 index=1, ipnum, 1
```

```
      read (ifc,*) ind
      do 20 ipoint=1, ind, 1
      read (ifc,*) ftime, fxco, fyco
      rpart (ipart,   ipoint)=ftime
      rpart (ipart+1, ipoint)=fxco
      rpart (ipart+2, ipoint)=fyco
20    continue
```

Check to ensure the end of the trajectory has been reached, if not then an error has occurred and the program is stopped

```
      read(ifc,*) ird
      if (ird.gt.1) then
      print *,'error ird gt 1'
      print *, index
      stop
      end if
      if (rpart(ipart,ind).eq.rpart(ipart,ind-1))then
      indam=ind-1
      else
      indam=ind
      end if
```

Detection of POLYFLOW recognised stagnation points, if found then alerts the user, few are expected in two-dimensional systems.

```
      if (ird.eq.0) then
      print *,'STAGNATION POINT'
      end if
      ipart=ipart+3
30    continue
      close (ifc)
      print *, 'Total number of particles=',itpnum
33    continue
```

All particle trajectories have been entered into rpart array.

```
      ilamp=1
      ilo=1
```

Sorting the particle initial positions into order with respect to the y co-ordinates. Beginning with the first particle in rpart, the initial y position is compared to that of all others. If it is the smallest then all of its trajectory is stored first in rsort. To remove it from later calculations the initial y co-ordinate is replaced by 1000000. If it is not the smallest then the next particle is observed with respect to all others. The loop continues until all trajectories have been ordered.

```
      do 39 irr=1, itpnum, 1
      iso=3
      rsmin=100000
      do 37 isort=1, itpnum, 1
      if (rpart(iso,1).lt.rsmin)then
      rsmin=rpart(iso,1)
      ilinei=iso
      end if
      iso=iso+3
37    continue
      do 38, itt=1, indam, 1
      rsort(ilo,itt)=rpart(ilinei-1,itt)
      rsort(ilo+1,itt)=rpart(ilinei,itt)
      rpart(ilinei,itt)=1000000
38    continue
```

```
      ilo=ilo+2
 39   continue
```

Calculation of the property of divergence. The calculation is carried out by observing the first two particles, at the first time step, in the array rsort (they are here immediate neighbours) and the distance between them calculated. The code then moves to the second and third particle, and repeats the distance calculation. Once the distance between all pairs of particles along the line have been calculated the summed value is stored in the results array. The code them moves to the next time increment to repeat the process. This continues until the end of the particle lifetimes.

```
      do 42, ilamt=1, indam, 1
      do 43, ilampp=1, (itpnum-1), 1
      rxl=((rsort((ilamp),ilamt))-(rsort((ilamp+2),ilamt)))**(2)
      ryl=((rsort((ilamp+1),ilamt))-(rsort((ilamp+3),ilamt)))**(2)
      rdistl=(rxl+ryl)**(0.5)
      ilamp=ilamp+2
      rdtl=rdtl+rdistl
 43   continue
      result(1,ilamt)=rdtl
      rdtl=0
      ilamp=1
 42   continue
```

Writing the results file. Results array (result) is written in one column representing the total property of divergence as time increments.

```
      res1=res//'.dal'
      open (unit=85, err=10, file=res1 ,status='new')
 87   format (e14.7)
      write (85,*) '  '
      write (85,*) 'File name ',res1
      write (85,*) '  '
      write (85,*) '  Lamellar-length'
      write (85,*) '  '
      do 44, ifw=1, indam, 1
      write (85,*) result(1,ifw)
 44   continue
      close (85)
      print *, 'File ', res1 ,' created'

 10   end
```

Appendix B - Code for calculating property A. 3d

B.1. Overview and background to code

This code presented here is used to calculate the three dimensional property A. The code is similar to that for two-dimensions as it uses the exact same technique. The codes differ in the reading of the particle trajectory data. Due to the presence of stagnation points extra routines have to be included to manage this. The code reads data from POLYFLOW mixing task results in to an array. The values in the array are processed, and the results are written to file. The input data is in the form presented in appendix A, except it contains an extra line of co-ordinates corresponding to the z axis.

As appendix A the output data is property A recorded at time steps corresponding to those in the input files. Here there is an additional line of figures indicating the number of particles remaining within the system. This is particularly important when considering the throughput domains.

B.2. Variables and labels

The variables used throughout the code are described below.

Arrays

ileft - stores the numbers of particles remaining in the domain, written in the output file

iptime - stores an index number and lifetime of all particles. Used to calculate how many particles are remaining in the system at each time step

result - stores the result data (property A) for each time increment

rpart - stores the trajectory positions, with time for each particle trajectory. Particles are stored along the i, time is in the j, for example 5 particles of 1000 seconds each would produce an array of i = (3*5), j = 1000

rsort - stores the same data as rpart, but after being sorted to order the initial positions to their immediate neighbours on the one dimensional line

Variables

fi - filename inputted by user without the index
fo - filename to open, after the code has generated the index
ftime - value of time read from trajectory in data file
fxco, fyco, fzco - value of x, y and z co-ordinates respectively, read from data file
iaaa - input from user. If value equals one the calculation will continue
ialarm - number of particles required for a test to run, input by the user each time the code is run
ic1, ic2, ic3, ic4 - used in generating the index number for the input file
iclear - to read past and ignore a line of data in the file ifc

iexit - number of particles exiting an open domain in any one time step
ifc - label of the open input file, increments with the index
ilamp, ilamt - used to move around rsort and result arrays
ilampp - variable in do 43
ilo, iso, irrr, isort, ilinei - used to move around rsort array
ind - number of positions of one trajectory in the data file
indam - used to read trajectories throughout code
index - variable in do 30
index2 - used to move around iptime array
indmax - particles mat exit or stagnate at different times, this variable sets reading of the array to the maximum value obtained
inum - number of files with same prefix to read
ipart and ipoint- used to move around rpart array
ipnum - total number of particles in one file
ipoint - variable in do 20
ird - reads either 0 or 1, 0 value will remove trajectory as a stagnation point
irr - variable in do 49
isss - variable in do 39
istag - number of stagnating particles identified by the code and removed from the tests
itpnum - total number of particles
itt - variable in do 38
ittt - variable in do 41
ivvv - variable in do 23
iw - variable in do 89
ra, rb, rc, re - remove unwanted values from the input data files
rdist1 - straight line distance between two particles
rdtl1 - total distance between all particles
res - fi, used to generate the output filename
rsmin - minimum value, used in the generation of rsort
rxl, ryl, rzl - x, y and z distance between two particles respectively

Numerical labels

10 - end
15 - format text input
29 - goto receipt missing out moving along rpart array to overwrite stagnating particle trajectories
87 - format output file
85 - output file index
20, 23, 27, 30, 37, 38, 39, 41, 42, 43, 49, 89 - do continues

B.3. The code with annotation

Setting up arrays and variables

```
real rpart(1650,3010)
real result (3010)
real rsort (1650,3010)
```

```
      integer iptime (2,3010)
      integer ileft (3010)

      character *6 fi
      character *10 res
      character *11 fo
      istag=0
      itpnum=0
      index2=0
15    format(a)
1     print *,'Enter the name of the file to be read (7)'
      read (5,15) fi
      print *,'How many files to read?'
      read (5,*) inum
      print *,'How many particles?'
      read (5,*) ialarm
     ipart=1
```

Increments the index of the filename (fi) to give fo, this routine enables up to 9999 files with the same filename and incremental indexes.

```
       do 27 ifc=11, (inum+10), 1

         ic1=ic1+1
      if (ic1.eq.10) then
      ic1=0
      ic2=ic2+1
      end if
      if (ic2.eq.10) then
      ic2=0
      ic3=ic3+1
      end if
      if (ic3.eq.10) then
      ic3=0
      ic4=ic4+1
      end if
```

Open each file in turn, read into rpart array all trajectories.

```
fo=fi//'.'//char(ic4+48)//char(ic3+48)//char(ic2+48)//char(ic1
+48)

          print*, ifc,' ', fo
          open (unit=ifc, err=10, file=fo, status='old')
          rewind ifc

      read (ifc,*) ra
      read (ifc,*) re, ipnum
      read (ifc,*) rb
      read (ifc,*) rc
        itpnum=itpnum+ipnum
             do 30 index=1, ipnum, 1
```

```
                read (ifc,*) ind

                  do 20 ipoint=1, (ind-1), 1
                        read (ifc,*) ftime, fxco, fyco, fzco
                        rpart (1,       ipoint)=ftime
                        rpart (ipart+1, ipoint)=fxco
                        rpart (ipart+2, ipoint)=fyco
                        rpart (ipart+3, ipoint)=fzco
```

Check to ensure the end of the trajectory has been reached, if not then an error has occurred and the program is stopped. Should never occur under normal circumstances and is therefore an indicator of a major failure.

```
20              continue
          read(ifc,*) iclear
              read(ifc,*) ird
               if (ird.gt.1) then
                 print *,'error ird gt 1'
                 print *, index
                 stop
               end if
```

Detection of POLYFLOW recognised stagnation points, if found then alerts the user.

```
                if (ird.eq.0) then
                   istag=istag+1
               print *,'STAGNATION POINT @ ',index+(itpnum-
ipnum)
                   goto 29
                end if
```

Goto 29 misses out moving along rpart array (ipart=ipart+3). The following particle trajectory therefore overwrites the stagnating trajectory.

Do loop to run through the particle trajectory and examine each time step with respect to the fifth previous time step. If all three co-ordinates are within a tolerance of 0.01mm then the particle is deemed to have stagnated and is removed from the calculations. A time tolerance is set, so that only particles that stagnate before 1000 seconds are removed.

```
      do 23 ivvv=6, (ind-1),1

       if((abs(((rpart(ipart+1,ivvv))-(rpart(ipart+1,ivvv-5))))
     .  lt.0.01).and.(abs(((rpart(ipart+2,ivvv))-(rpart(ipart+2,
     .  ivvv-5)))).lt.0.01.and.(abs(((rpart(ipart+3,ivvv))-
     .  (rpart(ipart+3,ivvv-5)))).lt.0.01)).and.ivvv.lt.1000)then
        istag=istag+1
        print *, 'Stagnation point!! Total particles removed.',istag
         goto 29
         end if
23    continue

                index2=index2+1
```

Occasionally POLYFLOW repeats the last time step co-ordinates, especially where the particles exit the domain. The following if command recognises and corrects this.

```
if (rpart(ipart,ind).eq.rpart(ipart,ind-1))then
      indam=ind-1
      else
      indam=ind
end if

     indam=indam-1

     if (indam.gt.indmax) then
       indmax=indam
       print *, indmax
     end if
```

Stores in an array an index number relating to a particle and its corresponding trajectory lifetime.

```
                iptime (1,index2)=index2
                iptime (2,index2)=indam

               ipart=ipart+3
29 continue
```

Do 30 until all particles in file are read.

```
30      continue
      close (ifc)
```

Do 27 until all particles in all files have been read

```
27     continue
   itpnum=itpnum-istag
```

If the number of particles stored in the rpart array is less than the number of particles that the user has specified as their minimum requirement, the program alerts the user. They are given the option of continuing with the particles that are stored or exiting to start again with more files. If more particles are stored than are required then the program uses only the specified number.

```
if (itpnum.lt.ialarm) then
print *,'You have below your desired limit of particles'
print *,'Either load more data files, or enter 1 to continue'
 read(5,*) iaaa
   if (iaaa.ne.1)then
       stop
       end if
    end if
    if (itpnum.gt.ialarm) then
 itpnum =ialarm
 end if
   print *,itpnum,' particles'
   print *,' '
```

```
      print *,'running,  please wait.....'
```

Do loop to run through the iptime array. The loop calculates the numbers of particles exiting and these remaining at each time step. This data will be included in the output file and is particularly important when investigating the throughput domains.

```
        do 39 isss=1, indmax,1
         iexit=0
         do 41 ittt=1, itpnum
         if(iptime(2,ittt).lt.isss) then
          iexit=iexit+1
       end if
41       continue
           ileft (isss)=(itpnum-iexit)
39       continue
```

The continuation of this code calculates property A. Firstly the randomly generated particles must be ordered and assigned their nearest neighbours. Secondly property A must be calculated, and finally the output file must be created and written.

```
ilamp=1
ilo=1
```

The do loop reads through all of the z co-ordinates to find the lowest one. Once it finds this it reads the x, y and z co-ordinates from rpart array into rsort array. The rpart z co-ordinate is then over written with a large value so that the second lowest particle z co-ordinate can be found. This continues until all particles have been ordered with respect to their originating z co-ordinate, and are now stored in the array next to their nearest neighbours.

```
do 49 irr=1, itpnum, 1

iso=3
```

rsmin is a generic large value to use as a starting point to rearrange particles into an ordered line.

```
rsmin=100000

do 37 isort=1, itpnum, 1
if (rpart(iso,1).lt.rsmin)then
rsmin=rpart(iso,1)
ilinei=iso
end if
iso=iso+3
37 continue

do 38, itt=1, indmax, 1
rsort(ilo,itt)=rpart(ilinei-1,itt)
rsort(ilo+1,itt)=rpart(ilinei,itt)
rsort(ilo+2,itt)=rpart(ilinei+1,itt)
rpart(ilinei,itt)=1000000
```

```
38 continue
   ilo=ilo+3

49 continue

   ipr=1
```

Calculating property A. The code calculates the linear distance between particles and their neighbours, then averages this for all of the pairs within the system.

```
    do 42, ilamt=1, indmax, 1

    do 43, ilampp=1, (itpnum-1), 1

    rxl=((rsort((ilamp),ilamt))-(rsort((ilamp+3),ilamt)))**(2)
    ryl=((rsort((ilamp+1),ilamt))-(rsort((ilamp+4),ilamt)))**(2)
    rzl=((rsort((ilamp+2),ilamt))-(rsort((ilamp+5),ilamt)))**(2)
          rdistl=(rxl+ryl+rzl)**(0.5)
    ilamp=ilamp+3
    rdtl=rdtl+rdistl

43  continue
    result(ilamt)=rdtl
    rdtl=0
    ilamp=1
42  continue
```

Creating and writing the output file (*.dal). The file is prefixed with the same name as the input file (for example if fi = 'mixing' then res = 'mixing.dal'. The value of property A is outputted for each time step.

```
102    res=fi//'.dal'
      open (unit=85, err=10, file=res ,status='new')
87     format (e14.7)
      write (85,*) 'Lamellar length'
      write (85,*) 'File ', res
      write(85,*)' '
      write(85,*)'  Lam_length  '
      write(85,*)' '

      do 89 iw=1, indmax,1
    write (85,87) result(iw)

89    continue

      close (85)

      print *, 'File ', res ,' created'

10    end
```

Appendix C – Code for calculating the positions of a number of particles a increments of time.

C.1. Overview and background.

The code below reads the data files from the POLYFLOW mixing tasks, by using a similar method to that presented in appendix A, and is not included here for simplicity.
The code produces co-ordinate data for the position of each particle for selected time increments. The output from the code is in the form of:

```
Particles          200   <-- Number of particles
System = mix__1          <-- System filename
Maximum time =     2000  <-- Maximum time of evolution
```

Time intervals taken →

0	0	0	20	20	20	40
5.00000	5.13882	5.00000	7.61625	2.15003	5.82117	9.39622
5.00000	5.06110	5.00000	7.64447	2.15233	5.96026	9.37139
5.00000	5.04059	5.00000	7.65184	2.15370	5.99640	9.36322
5.00000	5.15557	5.00000	7.61011	2.15017	5.79085	9.40050
5.00000	5.13666	5.00000	7.61703	2.15003	5.82507	9.39565
5.00000	5.15690	5.00000	7.60962	2.15019	5.78843	9.40082
5.00000	5.12797	5.00000	7.62021	2.15007	5.84073	9.39327
5.00000	5.10720	5.00000	7.62778	2.15039	5.87809	9.38716
5.00000	5.05058	5.00000	7.64825	2.15299	5.97881	9.36730
5.00000	5.09789	5.00000	7.63116	2.15065	5.89477	9.38423
5.00000	5.02867	5.00000	7.65618	2.15466	6.01743	9.35807
5.00000	5.06884	5.00000	7.64168	2.15189	5.94655	9.37428

The first three columns contain the co-ordinate data for all 200 particles at time=0 seconds. In the file shown the positions are taken every 20 seconds until the total time of 2000 seconds. The output file has been designed to enter directly into Microsoft Excel using the 'Fixed Width' function on opening.

C.2. Variables and labels.

Arrays

itime – stores the time intervals of the co-ordinate data
rplt – stores the co-ordinates for the output
rpart – stores the trajectory positions, with time for each particle trajectory.

Variables

fi – filename inputted by user without the index.
ic – variable in do 50
im – variable in do 73
ima – move around rpart array
imap - move around rpart array
indmax – maximum time
ipfile – label for the output file
iplott – identifies the interval to be observed
iti – to print intervals
itim – move around itime array

itpnum - total number of particles
iwr - variable in do 87
ix - to print co-ordinate data
res - the output filename

Numerical labels

10 - end.
50, 73, 87 - do continues.
101 - format output file.
102 - format output file.

C.3. The code with annotation

Setting up variables

```
      iplott=0
      ima=1
      ipfile=66
```

Create the output results file.

```
      res=fi//'.plt'
      print *, res
      open (unit=ipfile, err=10, file=res, status='new')
```

Write the headers of the output results file.

```
      write (ipfile,*) 'Particles ',itpnum
      write (ipfile,*) 'System = ',file
      write (ipfile,*) 'Maximum time = ',indmax
      write (ipfile,*) ' '
```

Loop through all time intervals until a designated time for taking the co-ordinate positions.

```
      do 50 ic=1, indmax,1
      if(iplott.eq.20.or.iplott.eq.0) then
      iplott=0
      imap=2
```

For the designated time intervals take co-ordinates from array rpart and sort them into co-ordinates corresponding to time intervals in array rplt.

```
      do 73, im=1, itpnum, 1
      rplt (ima,im)=rpart(imap, ic)
      rplt (ima+1,im)=rpart(imap+1, ic)
      rplt (ima+2,im)=rpart(imap+2, ic)
      imap=imap+3
 73   continue
```

Write time interval into itime array

```
      itime (itim)=(ic-1)
      itime (itim+1)=(ic-1)
      itime (itim+2)=(ic-1)
      itim=itim+3
      ima=ima+3
      end if
```

```
      iplott=iplott+1
 50   continue
      print *, itim
```

Write the time intervals and co-ordinate data into the result file.

```
      write (ipfile,102) (itime (iti), iti=1,itim-1)
      do 87, iwr=1, itpnum, 1
 101  format(1000(f9.5,1x))
 102  format(1000(i5,5x))
      write (ipfile,101) (rplt (ix,iwr), ix=1,ima-1)
 87   continue
      close (ipfile)
      print*,'file made'
 10   end
```

Appendix D - Code for calculating the positions of the particle trajectories intersecting the slices in TF8 mixer.

D.1. Overview and background

The input data and method for transferring data from file to array is identical to that presented in appendix B, and similar to appendix A. Therefore the corresponding section of this code has been omitted.

This code uses the co-ordinate data of particle trajectories created in a POLYFLOW mixing task to calculate where the individual particle trajectories cross a number of slices placed at increments along the flow domain. The output data is then the cross sectional co-ordinates on the corresponding slices along the flow domain in the z direction.

D.2. Variables and labels

Arrays

rslice - array for storing co-ordinate data on each slice
rpart - stores the trajectory positions, with time for each particle trajectory.

Variables

fi - output filename prefix
iarri, iarrj - used to move around rslice array
iarrjm - records the maximum number of co-ordinates and is used to ensure that the output file is long enough for all of the data
inslic - total number of slices, calculated from rzmax, rzmin and rdslic
iparti - variable in do 97
ipfile - associated with the label for the output file
irunp, irunt - used to move around rpart array
islice - variable in do 99
itimax - maximum lifetime of all particles
itpnum - total number of particles
iwrite - variable in do 90
ix - variable used in writing output to file
rdslic - user inputted distance between slices
res - output filename
rspos - position of the object slice
rxrat1, ryrat1 - ($x_1 - x_2$) and ($y_1 - y_2$) respectively
rxrat2, ryrat2 - ($z_1 - z_2$)
rxrat, ryrat - (rxrat1/rxrat2) and (ryrat1/ryrat2) respectively
rxmul, rymul - ($z_{slice} - z_1$)
rxintc, ryintc - (rxrat * rxmul) and (ryrat * rymul)
rzmax - user inputted maximum z value for slices
rzmin - user inputted minimum z value for slices

Numerical labels

10 - end
89 - format output file
92, 94 - goto receipt
90, 97, 98, 99 - do continues

D.3. The code with annotation

Open output file

```
ipfile=66
res=fi//'.sli'
print *, res
open (unit=ipfile, err=10, file=res, status='new')
write (ipfile,*) 'Particles ',itpnum
write (ipfile,*) 'System  ',fi
write (ipfile,*) 'Maximum time  ',itimax
write (ipfile,*) ' '
```

User required to enter parameters for the generation of the slices along the domain. The inputted information will be used to calculate the number and positions of the slices.

```
print *, 'Enter Z min'
read (5,*) rzmin
print *, 'Enter Z max'
read (5,*) rzmax
print *, 'Enter the distance between slices in Z direction'
read (5,*) rdslic
print *, ' '
print *, 'Origin assumed to be at zero'
print *, ' '

inslic=((rzmax-rzmin)/rdslic)-1
print *, 'Total number of slices = ',inslic

iarrj=2
iarri=1
```

The code generates each slice in turn. It then searches through every particle trajectory to find a time step at which a particle has crossed the object slice. If that occurs the positions either side of the slice are linearly extrapolated to find the point that corresponds to the trajectory crossing the slice, this is stored in an array. After every particle trajectory has been searched the next slice is generated and the process repeated.

```
do 99 islice=1, inslic, 1

print *,'slice ',islice

rspos=rspos+rdslic

irunp=1
```

```
      do 97 iparti=1, itpnum,1

      irunp=irunp+3

      do 98 irunt=1, itimax, 1

      if ((rpart(irunp,irunt).le.rspos).and.
     .      (rpart(irunp,irunt+1).ge.rspos)) then
      goto 94
      end if

      if ((rpart(irunp,irunt).ge.rspos).and.
     .      (rpart(irunp,irunt+1).le.rspos)) then
      goto 94
      end if

      goto 92
 94   continue
```

The linear interpolation is carried out on both the x and y co-ordinate independently with respect to the position of the object slice on the z axis. The following example shows how the code works.

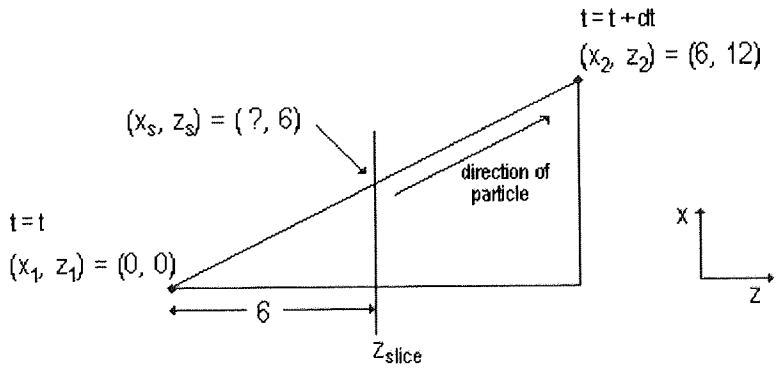

$rxrat1 = (x_1 - x_2) = (0 - 6)$

$rxrat2 = (z_1 - z_2) = (0 - 12)$

$rxrat = (rxrat1/rxrat2) = ((x_1 - x_2)/(z_1 - z_2)) = (-6 / -12) = 0.5$

$rxmul = (z_s - z_1) = (6 - 0) = 6$

$rxintc = x_1 + (rxrat * rxmul) = (((x_1 - x_2)/(z_1 - z_2)) * (z_s - z_1))$

$= 0 + 0.5 * 6 = 3$

Where the slice is at 6 from x_1 in the example above the position that the trajectory (linearly) crosses the slice is at an x co-ordinate of 3. The exact same calculation is carried out for the y co-ordinate to find the cross sectional co-ordinates the trajectory crosses the object slice.

```
      rxrat1=(rpart((irunp-2),(irunt)))-(rpart((irunp-2),(irunt+1)))
```

```
      rxrat2=(rpart((irunp),(irunt)))-(rpart((irunp),(irunt+1)))
      rxrat= rxrat1/rxrat2

      rxmul=rspos-(rpart((irunp),(irunt)))

      rxintc=(rpart((irunp-2),(irunt))) + (rxrat*rxmul)


      ryrat1=(rpart((irunp-1),(irunt)))-(rpart((irunp-1),(irunt+1)))
      ryrat2=(rpart((irunp),(irunt)))-(rpart((irunp),(irunt+1)))
      ryrat= ryrat1/ryrat2

      rymul=rspos-(rpart((irunp),(irunt)))

      ryintc=(rpart((irunp-1),(irunt))) + (ryrat*rymul)


      iarrj=iarrj+1

      rslice (iarri, 1) = islice
      rslice (iarri+1, 1) = islice
      rslice (iarri, iarrj) =rxintc
      rslice (iarri+1, iarrj) =ryintc

   92 continue

   98 continue

   97 continue

      iarri=iarri+2

      if (iarrj.gt.iarrjm) then
      iarrjm=iarrj
      end if

      iarrj=1
   99 continue
```

Create the output file from rslice array

```
   89 format (1000 (f7.4,1x))
      do 90 iwrite=1, iarrjm, 1
      write (ipfile, 89) (rslice (ix, iwrite), ix=1,(inslic*2))
   90 continue

      close (ipfile)
      print*,'file made'
   10 end
```

The following table shows a section of a sample file of output data. 100 particles with a life span of 200 seconds were used in the example. The x and y co-ordinates crossing five different slices in the z direction are shown here. This data could be inserted into a graphing package to view the results, typically in this work Microsoft Excel was used for this purpose.

Particles 100
System mix005
Maximum time 200

1	1	2	2	3	3	4	4	5	5
3.0924	4.6903	5.5438	6.3464	4.6531	8.7543	3.2777	7.3950	4.4346	6.5926
1.9676	0.0340	1.9654	0.0304	1.9635	0.0294	1.9623	0.0291	1.9615	0.0291
2.9300	5.0105	5.5000	6.4178	4.6857	8.7202	3.3099	7.4325	4.4445	6.6396
1.3468	0.0329	1.3443	0.0290	1.3427	0.0281	1.3418	0.0279	1.3414	0.0278
2.8898	5.0939	5.4906	6.4359	4.6863	8.7122	3.3192	7.4406	4.4480	6.6503
1.0764	0.0275	1.0743	0.0233	1.0731	0.0227	1.0726	0.0225	1.0723	0.0225
2.8814	5.1118	5.4887	6.4398	4.6862	8.7105	3.3212	7.4422	4.4488	6.6525
0.9951	0.0265	0.9930	0.0234	0.9919	0.0229	0.9914	0.0227	0.9912	0.0227
3.1521	4.5796	5.5620	6.3213	4.6278	8.7676	3.2674	7.3772	4.4327	6.5738
2.1247	0.0394	2.1223	0.0341	2.1202	0.0330	2.1187	0.0326	2.1177	0.0326
3.0381	4.7947	5.5284	6.3700	4.6696	8.7425	3.2879	7.4093	4.4372	6.6091
1.7982	0.0494	1.7947	0.0440	1.7921	0.0426	1.7904	0.0422	1.7893	0.0421
2.8258	5.2317	5.4769	6.4653	4.6826	8.6996	3.3348	7.4520	4.4543	6.6669
3.0823	4.7095	5.5408	6.3508	4.6566	8.7521	3.2795	7.3977	4.4350	6.5957